THE UNIVERSITY OF HULL

THE ROLE OF *N*-LINKED GLYCOSYLATION AND SIALYLATION IN REGULATING HUMAN PROTEINASE-ACTIVATED RECEPTOR 1 & 4 EXPRESSION AND SIGNALLING

Being a Thesis Submitted for the Degree of Doctor of Philosophy

In the Department of Cardiovascular Respiratory Medicine, University of Hull

By

Yu Pei Xiao (B.Sc, M.Sc)

(April, 2008)

ABSTRACT

Proteinase-activated receptors (PARs) are a novel family of G-protein coupled receptors (GPCRs) that mediate many of the diverse biological effects of proteinases on target cells. *N*-linked glycosylation is a common post-translational modification in the GPCR superfamily that enables the cell to regulate protein function without recourse to the genome. Previous pharmacological studies have found that activation of $hPAR_2$ by mast cell tryptase can be regulated by receptor N-terminal glycosylation. However, the role of *N*-linked glycosylation in regulating the expression and function of other PARs is not known.

We assessed the role of *N*-linked glycosylation and sialylation in regulating cell surface expression and proteinase activation/disarming of $hPAR_1$. Wild-type $hPAR_1$ and a panel of glycosylation-deficient mutant receptors were permanently expressed in the Kirsten virus sarcoma transformed rat kidney epithelial (KNRK) cell line. Western blot analysis revealed that $hPAR_1$ is a heavily glycosylated and sialylated receptor and *N*-linked glycosylation occurs at all five consensus sites of $hPAR_1$ in KNRK cells, namely, Asn^{35}, Asn^{62}, Asn^{75}, Asn^{250}, and Asn^{259}. Flow cytometry and confocal microscopy analysis revealed that removal of *N*-linked glycosylation sequons at these positions blocked $hPAR_1$ cell surface expression to varying degrees, and indicated that glycosylation at all sites is required for optimal cell surface expression of $hPAR_1$. Removal of all glycosylation sequons resulted in near total retention of the receptor within the cytosol. Calcium signalling assays revealed that (with the exception of N62QN75Q) no significant changes in receptor sensitivity to thrombin, trypsin and TFLLR-NH_2 were observed for the glycosylation mutant receptors when compared to wt-$hPAR_1$. Interestingly, N62QN75Q displayed significantly reduced sensitivity to trypsin, but not thrombin and TFLLR-NH_2 compared to wt-$hPAR_1$. Further experiments revealed that $hPAR_1$N62QN75Q was strikingly more susceptible to be disarmed by trypsin, thermolysin, proteinase 3 and elastase but not cathepsin G.

We next assessed $hPAR_4$ which has a putative *N*-linked glycosylation site in close proximity to the putative cleavage/activation site. Western blot analysis revealed that $hPAR_4$ is *N*-linked glycosylated, and is also heavily sialylated. Flow cytometry and confocal microscopy analysis revealed that glycosylation and sialylation are required but not essential for $hPAR_4$ receptor cell surface expression. Intracellular calcium signaling experiments showed that wt-$hPAR_4$ triggers a robust calcium signal following treatment with either the PAR_4-AP AYPGQV-NH_2 (100 μM) or thrombin (5 nM). However, $hPAR_4$(N20Q) failed to signal to either AYPGQV-NH_2 or thrombin at the same concentrations. In addition, sialylation appeared to have no significant effect on calcium signalling. MAPK signalling experiments indicated that the glycosylation mutant $hPAR_4$(N20Q) triggered the ERK pathway, whilst wt-$hPAR_4$ mainly triggered the p38 pathway. This is the first demonstration of *N*-linked glycosylation of a GPCR regulating signalling in this way.

In summary, this thesis has highlighted the importance of *N*-linked glycosylation and sialylation in regulating $hPAR_1$ and $hPAR_4$ expression and signalling. More specifically we have shown that *N*-linked glycosylation of PARs plays a vital role in regulating the susceptibility to proteinase disarming of the receptor and the signalling pathway triggered by the receptor.

TABLE OF CONTENTS

LIST OF TABLES

LIST OF FIGURES

LIST OF ABBREVIATIONS

AP	Agonist peptide
amp	Ampicillin
bp(s)	base-pair(s)
β-ME	β-mercaptoethanol
BMK-1	Big MAP Kinase-1
BSA	Bovine Serum Albumin
CAB	Calcium assay buffer
cAMP	Cyclic adenosine monophosphate
cDNA	Complementary DNA
CG	cathepsin G
CHO	Chinese Hamster Ovary Cells
CIP	calf-intestine phosphatase
DEPC	Diethylpyrocarbonate
dil^n	dilution
DMEM	Dulbecco's modified eagle's medium
DNA	Deoxyribonulceic Acid
dNTP(s)	deoxynucleotide tri-phosphate(s)
EC_{50}	Concentration of agonist required to elicit 50% of maximal response
ECL	Extracellular loop
EDTA	Ethylenediaminetetraacetic acid
ELA	elastase
ERK1/2	Extracellular Signal Regulated Kinases ½ (also p44/42)

eYFP	enhanced yellow fluorescent protein
FACS	Fluorescence Activated Cell Sorting
FCS	Fœtal Calf Serum (heat inactivated)
FITC	Fluorescein isothiocyanate
FW	Formula Weight
GABA	Gamma-aminobutyric acid
G418	Geneticin
GPCR	G Protein-Coupled Receptor
GRK	G Protein-coupled receptor Kinases
HEL	Human embryonic leukemia cell
hPAR	Human proteinase activated receptor
Inc.	Incubate
IL-*	Interleukin-*
Kb	kilo-base
KCl	Potassium Chloride
KNRK	Kirsten murine sarcoma virus-transformed Rat Kidney epithelial cells
LB	Luria Bertani
M	Molar
MACS	Magnetic Activated Cell Sorting
MAPK	Mitogen Activated Protein Kinase
MCP	Monocyte Chemotactic Protein
MCS	Multiple Cloning Site
MEM	Minimal Essential Media
mRNA	Messenger RNA
MW	Molecular Weight

NEB	New England Biosciences
Neu5Ac	N-acetylneuraminic acid
NTP	Nucleotide tri-phosphate
OD	Optical Density
OST	oligosaccharyltransferase
PAR	Proteinase Activated Receptor
PBS	Phosphate Buffer Saline
PCR	Polymerase Chain Reaction
PKC	Protein Kinase C
PLC	PhosphoLipase C
PNGaseF	N-Glycosidase F
PR3	proteinase 3
PVDF	Polyvinylidene fluoride
RT	Room Temperature
RNA	Ribonucleic Acid
RTase	Reverse Transcriptase
RT-PCR	Reverse Transcription PCR
SD	Standard Deviation
SDS-PAGE	Sodium dodecyl sulphate polyacrylamide gel electrophoresis
SEM	Standard Error of the Mean
STI	Soya Bean Trypsin Inhibitor
TAE	Tris acetate/disodium EDTA
temp	Temperature
TL	Tethered ligand
TNF	Tumour necrosis factor

UV	Ultra-violet

UNITS OF MEASUREMENT

A	amps
Ci	Curie
Da	Daltons
g	Grams
h	Hour
l	Litres
M	Molar
min	minutes
mol	moles
^{o}C	Degrees Celsius
secs	Seconds
u/µl	units per µl (enzyme concentration)
V	Volts
~	Approximately
%	percent
[X]	Concentration of X

MULIPLES OF UNITS

k	kilo	10^{3}
c	centi	10^{-2}
m	milli	10^{-3}
µ	micro	10^{-6}
n	nano	10^{-9}

GLUTAMIC ACID and ASPARTIC ACID ABBREVIATIONS

Symbol	3-letter code	Full name
A	Ala	Alanine
C	Cys	Cysteine
D	Asp	Aspartic
E	Glu	Glutamic
F	Phe	Phenylalanine
G	Gly	Glycine
H	His	Histidine
I	Ile	Isoleucine
K	Lys	Lysine
L	Leu	Leucine
M	Met	Methionine
N	Asn	Asparagine
P	Pro	Proline
Q	Gln	Glutamine
R	Arg	Arginine
S	Ser	Serine
T	Thr	Threonine
V	Val	Valine
W	Trp	Tryptophan
X	Xxx	Unknown/Any
Y	Tyr	Tyrosine

ACKNOWLEDGEMENTS

This research took place within the Biomedical Research Lab of the University of Hull. Funding the studentship and research was supplied by Prof. A. H. Morice.

My sincere thanks to Dr. S. J. Compton and Prof. A. H. Morice for their friendly and patient guidance, encouragement and advices over the past three years. Many thanks especially to Dr. Laura Sadofsky, Dr. Rithwik Ramachandran and Dr. Andrew Botham for their help with various techniques when I first started work in the lab and further assistance around the lab. Many thanks to Dr. Xu and Dr. Neil for their help with proof reading. I would also like to thank everyone in the Division of Cardiovascular & Respiratory Studies at Castle Hill for help with various things over the past three years.

This thesis is dedicated to my parents,

Mr. En Mu Xiao and Mrs. Yun Zhen Teng

DECLARATION

I hereby declare that the thesis entitled " The Role of *N*-linked Glycosylation and Sialylation in Regulating Human Proteinase-Activated Receptor 1 & 4 Expression and Signalling" has not been submitted for a degree, diploma or any other qualification at any other university. This thesis is the result of my own work and does not include any work that is the outcome of collaboration.

Yu Pei Xiao

PUBLICATIONS

Articles

Yu-Pei Xiao, Alyn H Morice and Steven J Compton. (2008) The role of *N*-linked glycosylation in regulating human proteinase-activated receptor-1($hPAR_1$) cell surface expression and signal transduction. (Manuscript in preparation).

Ramachandran, R., Sadofsky, L. R., **Xiao, Y**., Botham, A.M., Cowan, M., Morice, A. H. and Compton, S. J. (2007) Inflammatory Mediators Modulate Thrombin and Cathepsin-G Signaling in Human Bronchial Fibroblasts by Inducing Expression of Proteinase-Activated Receptor-4. *Am J Physiol-Lung Cell*, 292(3),L788-98.

Mahmoud Saifeddine, Michelle L. Seymour, **Yu-Pei Xiao**, Steven J. Compton, Steeve Houle, Rithwik Ramachandran, Wallace K. MacNaughton, Serge Simonet, Christine Vayssettes-Courchay, Tony J. Verbeuren, and Morley D. Hollenberg. (2007) Proteinase-activated receptor-2 activating peptides: distinct canine coronary artery receptor systems. *Am J Physiol Heart Circ Physiol* 293: H3279-H3289.

Conference abstracts

Y. Xiao, A. H. Morice and S. J. Compton. (2007) *N*-linked glycosylation regulates proteinase activation and disarming of human proteinase-activated receptor-1 ($hPAR_1$). LifeSciences2007 abstract

Y. Xiao, A. H. Morice and S. J. Compton. (2007) *N*-linked glycosylation regulates human proteinase-activated receptor-1($hPAR_1$) cell surface expression and disarming by neutrophil proteinases & thermolysin. HYMS research conference

Y. Xiao, A. H. Morice and S. J. Compton. (2004) The role of *N*-linked glycosylation in regulation of proteinase-activated receptor 1, 3 & 4 expression and function. HYMS research conference

1. GENERAL INTRODUCTION

1.1 G-PROTEIN COUPLED RECEPTORS

1.1.1 The superfamily of G-protein coupled receptors

Cell surface receptors serve as communication channels between cells and their surroundings, enabling an organism to distinguish environmental changes and react accordingly in order to survive. The largest family of cell surface receptors is termed G-protein coupled receptor (GPCR). All GPCRs have a structure of seven hydrophobic transmembrane helices including three extracellular loops, three cytosolic loops, an extracellular N-terminal domain and a cytosolic C-terminal tail (Gether, 2000; Drake *et al.*, 2006; Oldham & Hamm, 2008). Ligand binding to the extracellular ligand binding site results in the coupling of a GPCR to a trimeric signal-transducing G protein complex, and this consequently activates different downstream molecules resulting in the generation of an intracellular second messenger and coupling to intracellular effector systems (Cabrera-Vera *et al.*, 2003; Wettschureck & Offermanns, 2005).

Several classification systems have been applied to organize this superfamily according to the ligand structure, sequence homology, and receptor function. One of the most widely used systems categorises GPCRs into class A-F by Kolakowski on the basis of their structural homology, functional similarity, and genetic characteristics (Kolakowski, 1994; Gether, 2000). Human GPCRs have been grouped into classes A-C. There is a high amino acid homology between members of the same subfamily, but little or no sequence similarity is observed between subfamilies.

Class A, the rhodopsin-like family, represents the largest subgroup of GPCRs and includes receptors for many neuropeptides, most neurotransmitters (such as dopamine and serotonin) and glycoprotein hormones (Oldham & Hamm, 2008). This family is characterised structurally by a short extracellular N-terminal tail, several highly

conserved amino acids and a disulphide bridge that connects the first and second extracellular loops and a potentially palmitoylated cysteine in the carboxy-terminal tail causing formation of a putative fourth intracellular loop (Gether, 2000; Oldham & Hamm, 2008). A typical example of this group is the rhodopsin receptor (Oldham & Hamm, 2008).

Class B, the secretin-like family, is characterised by a relatively long N-terminal domain containing several cysteines which form a network of disulphide bridges (potentially within the receptor or with adjacent receptors) (Gether, 2000; Oldham & Hamm, 2008). Similar to class A, receptors in this class contain a disulfide bridge connecting extracellular loop (ECL) 2 and 3 (Gether, 2000). However, class B lacks the palmitoylation site and contains conserved amino acids specific to this group (Gether, 2000). The class B consists of calcitonin, glucagon, and vasointestinal peptide receptors.

Class C, the metabotropic glutamate family, is characterised by a very short and highly conserved third intracellular loop, and a very long extracellular tail (~600 amino acid) which contain the ligand-binding site and a long carboxyl tail (Gether, 2000). The class C receptors do not have any of the key features characterizing class A and B receptors (Gether, 2000). Metabotropic glutamate, GABA and taste receptors are amongst the members of Class C GPCRs.

Classes D, E and F represent fungal pheromone receptors, cAMP receptors, and Frizzled/Smoothened receptors respectively.

1.1.2 G proteins and the role in GPCR signalling paradigm

Guanine nucleotide binding proteins (G proteins) are a family of heterotrimeric proteins that transduce extracellular signals received by a GPCR to intracellular effectors (Oldham & Hamm, 2008). Moreover, membrane-associated G proteins are vital in

determining the specificity and temporal characteristics of the cellular responses to signals (Hamm, 1998).

G proteins are made up of three subunits: α, β, and γ-subunits (Hamm, 1998; Cabrera-Vera *et al.*, 2003; Oldham & Hamm, 2008). According to current knowledge, at least 16 genes encode for mammalian G protein α-subunits, 5 genes encode for β-subunits, and 12 genes encode for γ-subunits (Downes & Gautam, 1999; Cabrera-Vera *et al.*, 2003; Oldham & Hamm, 2008).

Gα-subunits contain two domains: a GTPase domain involved in binding and hydrolyzing GTP and a unique helical domain that buries the GTP in the core of the protein (Oldham & Hamm, 2008). The GTPase domain contains the site for the binding of guanine-nucleotides, guanosine diphosphate (GDP) and guanosine triphosphate (GTP) and exhibits intrinsic GTPase activity (Cabrera-Vera *et al.*, 2003). The helical domain may play a role in directing specificity of receptor- and effector-G protein coupling (Cabrera-Vera *et al.*, 2003). Classically, G proteins are divided into four families $G\alpha_{i/o}$, $G\alpha_{s}$, $G\alpha_{q/11}$, and $G\alpha_{12/13}$, based on Gα-subunits sequence homology, gene structure, and regulation of specific effectors (Cabrera-Vera *et al.*, 2003; Oldham & Hamm, 2008).

The Gβ and Gγ subunits form a tightly linked functional dimmer (βγ-complex), and it is not dissociable except by denaturation (Hamm, 1998). The βγ-complex binds to a hydrophobic pocket present in Gα-GDP, and also the βγ-complex freed from the α-subunits is known to regulate various effectors (Cabrera-Vera *et al.*, 2003; Wettschureck & Offermanns, 2005).

In the inactive heterotrimeric state, GDP is bound to the Gα-subunit**.** The interaction of ligand with its cell surface receptor causes conformational changes of the receptor domains leading to association of GPCRs with G proteins (Cabrera-Vera *et al.*, 2003). G proteins are activated by receptor-catalyzed guanine nucleotide exchange resulting in

GTP binding to α subunit, and GTP binding leads to dissociation of Gα-GTP from Gβγ-complex and from the receptor. After the Gα-GTP has dissociated from the Gßγ-dimer, Gα then directly interacts with effector proteins to continue the signaling cascade (Cabrera-Vera *et al.*, 2003). Both Gα-subunit and Gβγ-complex are able to regulate downstream cellular effectors including phospholipases, adenylyl cyclase, and ion channels (Cabrera-Vera *et al.*, 2003; Oldham & Hamm, 2008). Termination of the response occurs when GTP is hydrolysed to GDP, which inactivates α subunit and drives reassociation of the heterotrimer (Hamm, 1998; Cabrera-Vera *et al.*, 2003).

GPCR signalling is one of the most complex paradigms amongst cell surface receptors, determined by the large number of subtypes identified for each G protein subunits. In addition, most GPCRs are able to activate more than one G protein subtype, thus one single GPCR is able to functionally couple to more than one subtype of G protein resulting in the activation of several signal transduction cascades (Wettschureck & Offermanns, 2005).

1.2 PROTEINASE-ACTIVATED RECEPTORS

Proteinase activated receptors (PARs) are a group of class A GPCR (rhodopsin family) and play important roles in hemostasis and thrombosis, as well as in inflammatory and proliferative responses triggered by tissue injury (Macfarlane *et al.*, 2001; Traynelis & Trejo, 2007). PARs have seven transmembrane domains, three intracellular loops and three extracellular loops, an extracellular N-terminus and an intracellular C-terminal tail (Macfarlane *et al.*, 2001; Hollenberg & Compton, 2002) (Figure 1.1). PARs are characterised by their unique mechanism of activation (Vu *et al.*, 1991a; Macfarlane *et al.*, 2001; Hollenberg & Compton, 2002). Unlike most other GPCRs, which require exogenous agonist binding to specific sites on the receptor, PARs are a unique class of GPCRs carrying their own ligand, which remain cryptic until unmasked by proteolytic cleavage. Rather than being activated through a conventional ligand-binding process, PARs can be stimulated by serine proteases through cleavage of the receptor N-terminal extracellular domain, which releases a new amino terminus sequence that acts as a tethered ligand (TL) by binding intramolecularly to the receptor to trigger transmembrane signaling (Figure 1.2) (Macfarlane *et al.*, 2001; Cirino & Vergnolle, 2006). Interestingly, short synthetic peptides, based on the proteolytically revealed tethered ligand sequences, are capable of binding to PARs and mimic the actions of agonistic proteinases (Vu *et al.*, 1991a; Nystedt *et al.*, 1995; Hollenberg, 2005a). There are four PARs encoded in the mammalian genome, namely PAR_1, PAR_2, PAR_3, and PAR_4 respectively (O'Brien *et al.*, 2001; Traynelis & Trejo, 2007).

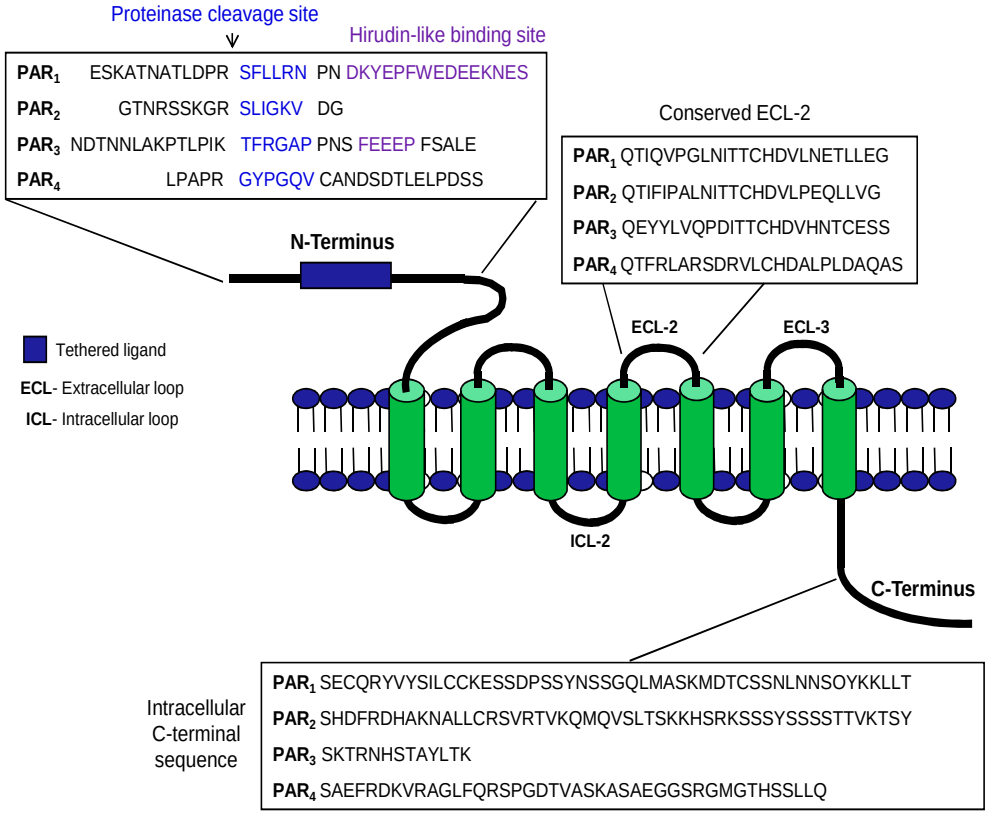

Figure 1.1 Classical PAR structural features. The proteinase cleaves and activates PAR at the specific site (*black arrow*), unmasking a cryptic N-terminal sequence "tethered ligand" of the receptor (*blue*). Hirudin-like binding domain sequences for PAR_1 and PAR_3 are presented in *purple*. [Adapted from (Steinhoff *et al.*, 2005)]

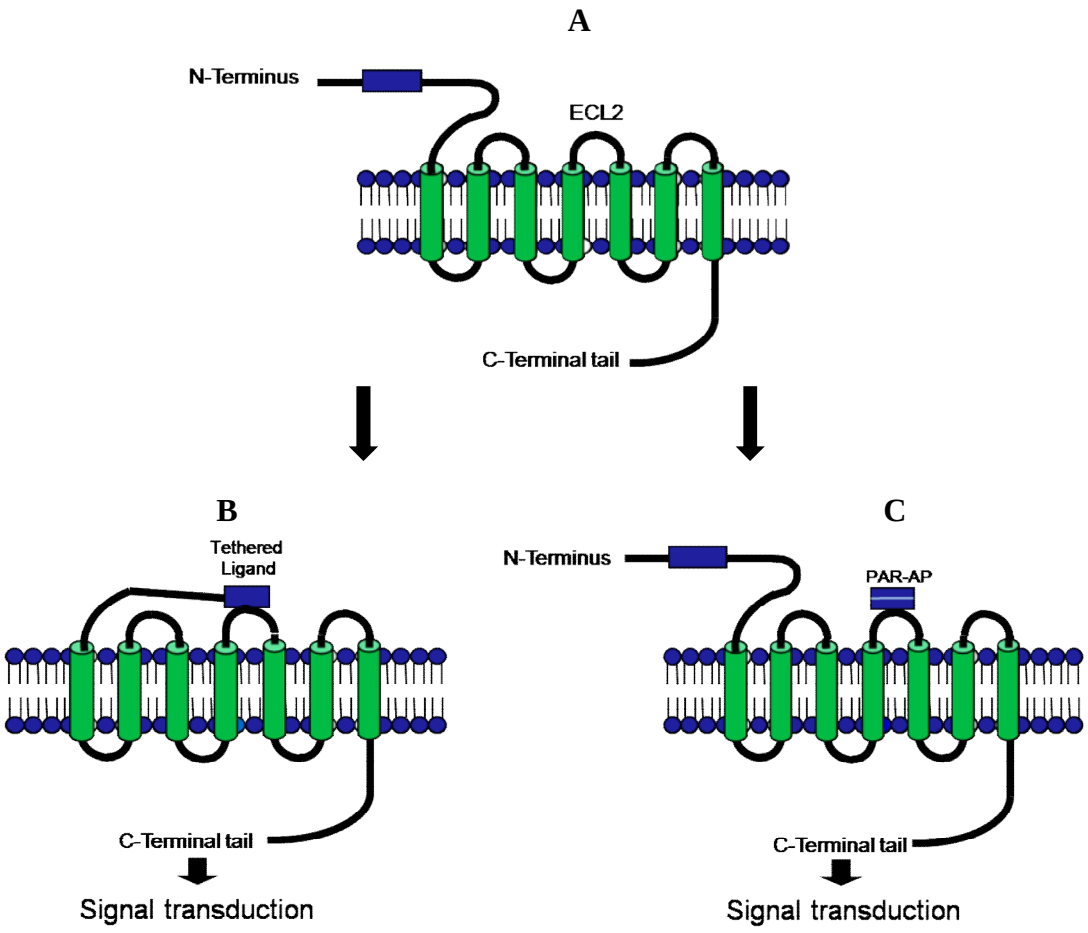

Figure 1.2 Mechanism of PAR activation. (A) and (B) illustrate the receptor activation by proteolysis cleavage. (C) shows the binding of an activating peptide to the receptor. [Adapted from (Hollenberg & Compton, 2002; Ossovskaya & Bunnett, 2004)]

1.2.1 Discovery of the PAR family

The searches for a thrombin receptor led to the discovery of the first proteinase-activated receptor (PAR_1); PAR_1 was initially cloned by two laboratories using RNA derived from thrombin-responsive cells of human and hamsters in oocytes from *Xenopus* (Rasmussen *et al.*, 1991; Vu *et al.*, 1991a). In contrast to PAR_1, PAR_2 was identified serendipitously through screening a mouse genomic library using degenerate primers to the second and sixth transmembrane domains of the bovine neurokinin 2 receptor, and later the authors further reported the cloning of PAR_2 (Nystedt *et al.*, 1994; Nystedt *et al.*, 1995a; Nystedt *et al.*, 1995b; Ossovskaya & Bunnett, 2004). In addition, $hPAR_2$ was also cloned by another group shortly afterwards (Bohm *et al.*, 1996). PAR_3 was identified as a second thrombin receptor when gene ablation studies showed that platelets from the PAR_1 knockout mice remained responsive to thrombin, whereas responses to PAR_1-AP (agonist peptide) were not detectable (Connolly *et al.*, 1996). Subsequently a rat PAR_3 was first cloned out using degenerate primers to conserved domains of PAR_1 and PAR_2 to screen RNA from rat platelets and then employed the sequence obtained to identify $hPAR_3$ and $mPAR_3$ cDNA clones from commercially available cDNA libraries through PCR and hybridisation assays (Ishihara *et al.*, 1997). The fourth family member PAR_4 was identified by two different laboratories independently through DNA sequence database searches using conserved domains of the other three previously cloned PARs, both groups identified expressed sequence tags (ESTs) with considerable homology to the known PARs (Xu *et al.*, 1998; Kahn *et al.*, 1998b). There may be genes for additional PAR family members, but so far none have been identified (O'Brien *et al.*, 2001).

To date the genes encoding four family members have been identified in humans and mice: in humans PAR_1, PAR_2 and PAR_3 are tightly clustered at chromosome 5q13,

while PAR_4 is located separately at 19p12 (Xu *et al.*, 1998; Kahn *et al.*, 1998a); in mice PAR_1, PAR_2 and PAR_3 are in a cluster that maps to 13d2 and PAR_4 is located at 8b3(Kahn *et al.*, 1998a). The PAR_1 gene encodes a 425 amino acid and 430 amino acid protein in humans and mice respectively (Vu *et al.*, 1991a). $hPAR_2$ encodes a protein of 397 residues with the typical characteristics of a GPCR and with ~30% amino acid identity to human PAR_1 (Nystedt *et al.*, 1994; Ossovskaya & Bunnett, 2004). $hPAR_3$ is revealed to be made up of 374 amino acids and shares ~28% sequence homology to human PAR_1 and PAR_2 (Ishihara *et al.*, 1997; Ossovskaya & Bunnett, 2004). The $hPAR_4$ cDNA sequence encodes a 385 amino acid protein and is ~33% homologous to the other human PARs, but with some distinct differences in the amino and carboxy-terminal domains (Xu *et al.*, 1998; Ossovskaya & Bunnett, 2004). PAR_1, PAR_3 and PAR_4 are thrombin receptors. PAR_2 was activated by trypsin, mast cell tryptase and factor Xa but not thrombin (Steinhoff *et al.*, 2005).

1.2.2 PAR activation

Unlike other GPCRs, PARs have a distinct mode of activation. It is well known that most GPCRs agonists are small hydrophilic molecules, which are soluble in the extracellular fluid (Dery *et al.*, 1998). These agonists can activate their respective receptors by binding reversibly to extracellular and transmembrane domains of the receptor to initiate the cellular responses (Wettschureck & Offermanns, 2005). On the other hand, PARs can be regarded as GPCRs carrying their own ligand. In the presence of an activating protease (i.e. thrombin for PAR_1, PAR_3 and PAR_4; trypsin for PAR_2) the N-terminal peptide bond of the intact receptor is cleaved at a specific point unmasking a new N-terminus of the TL sequence, which subsequently binds to the conserved regions in the ECL2 of the cleaved receptor causing receptor activation and

initiating signal transduction (Figure 1.1, Figure 1.2 (A) and (B)) (Hollenberg & Compton, 2002; Traynelis & Trejo, 2007). The resulting N-terminal fragment of the receptor has no known function (Macfarlane *et al.*, 2001; Hollenberg & Compton, 2002; Ossovskaya & Bunnett, 2004).

PAR activation was ascribed exclusively to the family of serine proteases (i.e. thrombin and trypsin). However, recent findings have shown that enzymes of the coagulation system, trypsin of pancreatic and extrapancreatic origin and mast cell tryptase may also be the activating proteases for PARs (Macfarlane *et al.*, 2001; Sokolova & Reiser, 2007). Thrombin activates PAR_1, PAR_3 and PAR_4, but not PAR_2 (Cirino & Vergnolle, 2006). Trypsin activates PAR_1, PAR_2 and PAR_4. The coagulation factors Xa and VIIa when complexed with tissue factor can activate both PAR_2 and PAR_1, whereas factor Xa alone can activate PAR_1 and PAR_2 (Cirino & Vergnolle, 2006). The activated protein C (APC) has been shown to activate PAR_1 and PAR_2 (Hirano, 2007). In addition, plasmin and cathepsin G can activate PAR_1 and PAR_4 (Hirano, 2007). Although PAR_2 was originally believed to be a receptor activated by trypsin and mast cell tryptase (Nystedt *et al.*, 1994; Molino *et al.*, 1997a), a number of endogenous and exogenous proteinases such as kallikreins and mite allergens are now known to stimulate PAR_2 as well (Ossovskaya & Bunnett, 2004; Hollenberg, 2005a; Oikonomopoulou *et al.*, 2006a; Oikonomopoulou *et al.*, 2006b). Apart from proteases, PARs can also be activated by short synthetic peptides (5-6 amino acids), derived from the proteolytically revealed tethered ligand (Vu *et al.*, 1991a; Scarborough *et al.*, 1992) (Figure 1.2 (A) and (C)). This was first described for PAR_1, and a series of structure-activity studies identified several high-affinity peptide agonists or antagonists (McIntosh *et al.*, 2007). A similar strategy has been employed and the peptide tools for other PARs were also reported. To date, the PAR activating peptides (PAR-APs) are available for PAR_1, PAR_2 and PAR_4,

but some of them may have cross-reactivity between receptors and species (Blackhart *et al.*, 1996; Hollenberg *et al.*, 1997; McIntosh *et al.*, 2007). However there is no specific activating peptide for PAR_3 (Hansen *et al.*, 2004; Kaufmann *et al.*, 2005; McIntosh *et al.*, 2007).

1.2.2.1 PAR_1

The activation mechanism of PAR_1 has been well established. The extracellular N-terminus domain of PAR_1 contains a thrombin cleavage recognition and cleavage site ($LDPR^{41}\downarrow S^{42}FLLRN$, where $\downarrow$ denotes cleavage) and immediately downstream is situated a highly acidic region reminiscent of the leech anticoagulant hirudin ($D^{51}KYEPFWEDEE$) which can bind to an anion binding site on thrombin and could serve to temporarily concentrate thrombin at the receptor surface (Vu *et al.*, 1991a; Ossovskaya & Bunnett, 2004). Vu *et al.* also demonstrated the importance of the cleavage recognition sequence by domain swap experiments where replacement of the LDPR with the sequence DDDK, the recognition site for the protease enterokinase, abolished thrombin responses and made the receptor susceptible to enterokinase activation (Vu *et al.*, 1991b). In addition deletion of the hirudin like domain (residues 51-63) dramatically reduced the potency of thrombin activation of PAR_1 (Vu *et al.*, 1991b). A later study suggested that the receptor's hirudin like domain induces a conformational change in thrombin's active moiety to effect receptor activation (Ishii *et al.*, 1995). Thus, it was proposed that thrombin interacts with PAR_1 through the sequence LDPR and DKYEPFWEDEE and cleaves the receptor at the $LDPR^{41}\downarrow S^{42}$ site to activate the receptor (Ossovskaya & Bunnett, 2004). Previous studies ultilizing domain swap experiments in xenopus PAR_1 and $hPAR_1$ have revealed a critical role for the ECL2 in conferring TL binding specificity (Gerszten *et al.*, 1994; Lerner *et al.*, 1996)

and further experiments identified the region encompassing residues 259-262 and to a lesser extent residues 82-90 as conferring the $hPAR_1$ TL recognition specificity (Nanevicz *et al.*, 1995; Nanevicz *et al.*, 1996). Therefore, the interaction between the TL and ECL2 was critical for signalling.

The activating peptide for PAR_1 (PAR_1-AP) ranging from 5-14 amino acids in length was derived from the PAR_1 tethered ligand sequence in different species. The activating peptide for $hPAR_1$ was shown to be SFLLRN, but this peptide is not specific for $hPAR_1$ as it displayed cross-reactivity with $hPAR_2$ (Blackhart *et al.*, 1996). Substitution of the first serine residue with a threonine, similar to the *xenopus* TL, giving the AP TFLLRN-NH_2 made it highly specific to PAR_1 (Hollenberg *et al.*, 1997). It is interesting to note that PAR_1-AP generally show lower potency than thrombin in activating the receptor. One previous study showed that the deletion of residues 68-93 of PAR_1 completely abolished PAR_1 AP-induced responses, but not that of thrombin, thus the author suggested that APs might interact with different or additional sites on PAR_1 (Blackhart *et al.*, 2000).

1.2.2.2 PAR_2

The N-terminus extracellular domain of PAR_2 consists of 46 residues and contains a putative trypsin cleavage recognition sequence ($SKGR^{34}\downarrow S^{35}LIGKV$) (Ossovskaya & Bunnett, 2004). Mutation of the cleavage site prevents trypsin cleavage and activation of PAR_2 (Ossovskaya & Bunnett, 2004). PAR_2-AP corresponding to the TL domain (SLIGKV) directly activates PAR_2 without the requirement for hydrolysis by trypsin (Ossovskaya & Bunnett, 2004; McIntosh *et al.*, 2007). An *N*-linked glycosylation site is present in the N-terminus of PAR_2 and regulates signalling by tryptase but not trypsin or PAR_2-AP (Compton *et al.*, 2002b), which indicates a role of post-translational

modification in conferring protease specificity to the receptor. Interestingly, the TL domain of signalling-defective cleaved PAR_1 can transactivate PAR_2 in human endothelial cells, but this mechanism is less efficient than intramolecular activation of the same receptor (Arora *et al.*, 2007).

1.2.2.3 PAR_3

The N-terminus extracellular domain of PAR_3 contains a putative thrombin cleavage site ($LPIK^{38}\downarrow T^{39}FRGAP$), and a hirudin-like site (FEEFP) that is distal to the thrombin cleavage site (Ossovskaya & Bunnett, 2004). Mutation of the thrombin cleavage site prevents thrombin cleavage and activation of PAR_3 (Ossovskaya & Bunnett, 2004). In addition, PAR_3 is efficiently cleaved by thrombin but does not appear to signal on its own (Arora *et al.*, 2007). However, in distinct contrast to PAR_1, PAR_2 and PAR_4, N-terminal TL derived peptides for PAR_3 do not activate PAR_3 (Ossovskaya & Bunnett, 2004; McIntosh *et al.*, 2007).

1.2.2.4 PAR_4

By utilising site-directed mutagenesis, the N-terminal cleavage site of PAR_4 ($R^{47}\downarrow G^{48}YPGQV$) was confirmed to be cleaved by both trypsin and thrombin with an EC_{50} of 5 nM for both agonists (Xu *et al.*, 1998). Mutation of the cleavage site prevents activation of PAR_4 by thrombin and trypsin, but not by the synthetic peptide; thus this confirms the importance of proteolytic cleavage for receptor activation (Ossovskaya & Bunnett, 2004). Interestingly, there is crosstalk between different PARs (Arora *et al.*, 2007). No specific thrombin binding sites are seen on PAR_4, and thrombin activates PAR_4 with a potency that is 50-fold less than for activation of PAR_1 (Ossovskaya & Bunnett, 2004). PAR_1 and PAR_4 are the functional thrombin receptors in human

platelets, whereas PAR_3 and PAR_4 together mediate thrombin signalling in mouse platelets (Arora *et al.*, 2007). The neutrophil granular protease cathepsin G can also activate PAR_4 resulting in platelet aggregation and Ca^{2+} signalling in fibroblasts transfected with PAR_4 (Sambrano *et al.*, 2000). FXa and trypsinogen IV were also shown to activate PAR_4 (Camerer *et al.*, 2000; Cottrell *et al.*, 2004). Similar to PAR_1, PAR_4 was shown to be activated by synthetic activating peptides derived from the proteolytically revealed TL sequence GYPGQV, albeit with a relatively low potency (EC_{50} = 100 μM) (Xu *et al.*, 1998; McIntosh *et al.*, 2007). Later another synthetic peptide GYPGKF was generated from $mPAR_4$ (Kahn *et al.*, 1998b). Recently, AYPGKF which has an alanine in place of the glycine was found to possess over 10-fold greater potency than GYPGKF (Faruqi *et al.*, 2000).

1.2.3 PAR signalling

Once activated, PARs undergo conformational changes that facilitate coupling to heterotrimeric G proteins, and lead to the activation of phosphoinositide 3 kinase, phospholipase C isoforms, small G protein Rho, an increase of cytosolic Ca^{2+} concentration and activation of mitogen-activated protein kinase (MAPK) cascades that finally lead to various cellular responses (Sokolova & Reiser, 2007). The signalling events triggered by PAR activation are unique for cell types and PAR subtypes (Sokolova & Reiser, 2007). Linkage of a PAR to a particular signalling pathway depends largely on the interactions formed by the receptor C-terminal and G-proteins.

1.2.3.1 PAR_1

A considerable amount of work has been done to investigate the signalling of PAR_1, considerably more than that of the other three PARs. PAR_1 is shown to couple with

multiple G-proteins, and interactions with $G\alpha_{q/11}$, $G\alpha_{i/o}$ and $G\alpha_{12/13}$ subtypes (Macfarlane *et al.*, 2001) leading to intracellular Ca^{2+} mobilization, activation of MAPK, RhoGEF-mediated Rho and Rac signalling and other effectors to promotes diverse cellular responses (Traynelis & Trejo, 2007). In addition, lipid enzyme and protein kinases have also been implicated as part of the PAR_1 signalling paradigm. Coupling of PAR_1 to $G\alpha_{q/11}$ leads to PLC-induced phosphoinositide hydrolysis producing IP3 and diacylglycerol (DAG) as well as subsequent calcium mobilization, protein kinase C (PKC) and MAP kinases activation (Arora *et al.*, 2007). This represents the major PAR_1 signalling pathway in platelet activation (Offermanns *et al.*, 1997). The interaction between PAR_1 and a $G\alpha_{q/11}$ was also reported in astrocytes (Wang *et al.*, 2002) and indicated in astrocytoma cells (LaMorte *et al.*, 1993). In addition PAR_1 signalling through $G\alpha_{q/11}$ was shown through the use of G-protein specific antibodies which inhibited PAR_1 mediated calcium signalling in CCL-39 fibroblast cells (Baffy *et al.*, 1994) and through co-immunoprecipitation of $G\alpha_{q/11}$ with PAR_1 (Ogino *et al.*, 1996). The PAR_1 interaction with $G\alpha_i$ has been revealed in multiple cell systems including HEL cells (Brass *et al.*, 1991), osteosarcoma cells (Babich *et al.*, 1990), vascular smooth muscle cells (Kanthou *et al.*, 1996), fibroblasts (Hung *et al.*, 1992a), platelets (Kim *et al.*, 2002), astrocytes (Wang *et al.*, 2002) and endothelial cells (Vanhauwe *et al.*, 2002). Hung *et al.* reported that the coupling of PAR_1 to $G\alpha_i$ resulted in cAMP inhibition (Hung *et al.*, 1992b). In addition, Voss *et al.* reported that PAR_1 couples to $G\alpha_{i/o}$ in human platelets and activates phosoinositide-3 kinase (PI3K) regulating platelet aggregation (Voss *et al.*, 2007). PAR_1 also couples to $G\alpha_{12/13}$ and it was shown from the studies on thrombin stimulated platelets (Offermanns *et al.*, 1994) and astocytoma cells (Aragay *et al.*, 1995; Post *et al.*, 1996). $G\alpha_{12/13}$ binds RhoGEFs, which activate small G-proteins such as Rho (Arora *et al.*, 2007).

1.2.3.2 PAR_2

Compared to PAR_1, considerably less is known about PAR_2-mediated signaling. Numerous studies show that PAR_2 activation leads to increased second messenger responses suggesting the coupling of PAR_2 to $G_{q/11}$, $G\alpha_{i/o}$ and perhaps $G_{12/13}$ (Traynelis & Trejo, 2007). After the activation PAR_2 binds to arrestin and then internalized, and the interaction of the internalized PAR_2 with arrestin is thought to sustain ERK-1/2 signalling in the cytoplasm independently of G-protein activation (Arora *et al.*, 2007).

1.2.3.3 PAR_3 and PAR_4

PAR_4 was reported to couple to $G\alpha_{q/11}$ and $G\alpha_{12/13}$ but not $G\alpha_{i/o}$, at least in fibroblasts (Arora *et al.*, 2007). However, PAR_3 has not been shown to signal through G proteins so far (Arora *et al.*, 2007; Traynelis & Trejo, 2007).

Apart from signalling through intracellular Ca^{2+} mobilization, it is now known that PARs are associated with MAP Kinases cascade activation to modulate cell growth and differentiation (Hur & Kim, 2002). To date, five distinct subfamilies of MAP kinase have been reported in the mammalian, namely extracellular signal-regulated kinase (ERK)-1 and 2, c-Jun amino-terminal kinases (JNKs), p38 MAP kinase, ERK-3/4, and ERK-5 or big MAP kinase-1 (BMK-1) (Pearson *et al.*, 2001).

ERK-1/2: ERK-1/2 are also known as the classical mitogen kinases and represent the first and best studied cascade amongst all MAPK (Pearson *et al.*, 2001). ERK-1/2 are proteins of 42 and 44 kDa respectively. The ERK pathway is well-known for its role as the key regulator for cell survival and proliferation (Kohno & Pouyssegur, 2003).

p38 MAP kinase: p38 isoforms, the second mammalian stress-activated MAP kinase subfamily, are strongly activated by physical and chemical stress stimuli, UV radiation,

and cytokines for example TNFα and IL-1, but minimally affected by mitogenic stimuli (Chen *et al.*, 2001). Signalling through p38 is linked to cell differentiation and apoptosis. PAR_4 signalling has been reported to activate calcium signalling in different cell system (Kahn *et al.*, 1998; Xu *et al.*, 1998; Camerer *et al.*, 2002) and MAPK signalling in vascular smooth muscle cells (Bretschneider *et al.*, 2001). A previous study reported that PAR_4 were involved in Src dependant p38 phosphorylation and activation of ERK and PLC in cardiomyocytes derived from PAR_1 knockout mice (Sabri *et al.*, 2003). A recent study has also reported PAR_4 activation via the p38 MAPK pathway in endothelial cells (Fujiwara *et al.*, 2005). Chapter 5 of this thesis will focus mainly on ERK-1/2 and p38 MAP kinase.

1.2.4 Termination of PAR signalling

In theory, while PARs are activated, the resulting TL remains bound to the receptor, the activation state of the PAR therefore would be expected to elicit a continuous signalling event and would be irreversible. However, this does not appear to be the case. PAR mediated responses are seen to be transient in nature with rapid desensitization and receptor internalisation that tightly regulates PAR signalling (Macfarlane *et al.*, 2001; Hollenberg & Compton, 2002; Sokolova & Reiser, 2007). Various studies have reported that sequences within the intracellular receptor domains, especially the C-terminal tail, regulate receptor desensitisation and internalisation (Macfarlane *et al.*, 2001; Hollenberg & Compton, 2002; Trejo, 2003). Desensitization of activated GPCR signalling responses are initiated by G protein-coupled receptor kinases (GRKs) (Krupnick & Benovic, 1998; Moore *et al.*, 2007) and/or Protein Kinase C (PKC) (Krupnick & Benovic, 1998). The GRKs or PKCs bind to, and rapidly phosphorylate the receptor typically within the C-terminal domain (Krupnick & Benovic, 1998). The

phosphorylated receptor then attracts β-arrestin binding resulting in uncoupling the receptor from the G-protein and also blocking of further G protein-initiated signalling (Lohse *et al.*, 1990; Attramadal *et al.*, 1992). Arrestins also interact with clathrin and the clathrin adaptor protein-2 (AP2) to facilicate GPCR internalization (Traynelis & Trejo, 2007). Once desensitised the receptors are internalised and directed to lysosomes for degradation. So far, receptor desensitisation and internalisation mechanisms have been best studied for PAR_1 and to a lesser extent for PAR_2 and PAR_4, with almost nothing known about PAR_3.

1.2.5 Physiological roles of PARs and diseases

The tissue distribution of the four PAR family members have been studied by a number of approaches intensively and are mostly complete for PAR_1 and PAR_2, however, the expression patterns of PAR_3 and PAR_4 are less well characterized, and rely mainly upon analyses of mRNA expression (O'Brien *et al.*, 2001).

PAR_1 distribution in the different organ systems is quite astounding. To date, PAR_1 has been detected in a variety of tissues including platelets; endothelial cells; fibroblasts; monocytes; T cells positive for CD 8, CD 16, and either CD 56 or CD 57; natural killer (NK) cells; CD 34^+ hematopoietic progenitor cells; dental pulp cells; smooth muscle cells (SMC); epithelial cells; neurons; glial cells; mast cells; and certain tumor cell lines (Steinhoff *et al.*, 2005).

PAR_2 has been widely expressed in brain, lia (DRG), eye, airway, heart, GI tract, pancreas, the colon, kidney, bladder, liver, prostate, ovary, testes, and skin, and is found in various cell types such as keratinocytes, epithelial cells, endothelial cells, SMC, osteoblasts, as well as immune cells such as T cells, neutrophils, mast cells, or eosinophils (Steinhoff *et al.*, 2005; McIntosh *et al.*, 2007). Investigations of PAR_2

functionality in these various systems are still ongoing; however the unique tissue distribution of PAR_2 suggests a possible role in disease states, particularly those in relation to inflammation and immunity (McIntosh *et al.,* 2007). For example, PAR_2 is upregulated during inflammation and activation of PAR_2 leads to chronic inflammation and arthritis (McIntosh *et al.,* 2007). So far, PAR_1 and PAR_2 appear as potential new therapeutic targets for the treatment of chronic inflammation. In addition, further studies have documented a role for PAR_2 in tissue oedema (Vergnolle, 1999), granulocyte infiltration (Vergnolle, 1999; Cenac *et al.,* 2002), vascular permeability (Kawabata *et al.*, 1998), and vessel relaxation (Glusa *et al.*, 1997).

PAR_3 has been detected in human bone marrow, heart, brain, placenta, liver, pancreas, thymus, small intestine, stomach, lymph nodes, and trachea, although the cell types remain to be identified (Steinhoff *et al.,* 2005). In mouse, PAR_3 is found to be expressed in megakaryocytes and platelets, among other cell types (Steinhoff *et al.,* 2005). However, no expression of the receptor on human platelets was observed, which differs from that observed with the murine receptor. Interestingly, Ishihara *et al.* reported that there is species specific variation in PAR_3 function (Ishihara *et al.,* 1997).

PAR_4 has been identified and cloned from human, mouse and rat tissues: $hPAR_4$ (human PAR_4) is widely expressed in brain, testes, placenta, lung, liver, pancreas, thyroid, skeletal muscle, and small intestine (Steinhoff *et al.,* 2005). PAR_4 mRNA has also been detected in human platelets (Xu *et al.*, 1998). $rPAR_4$ (rat PAR_4) is expressed in esophagus, stomach, duodenum, jejunum, distal colon, spleen, and brain (Steinhoff *et al.,* 2005).

Since the discovery of PARs, a wide range of physiological and pathophysiological events have been attributed to PAR mediated cellular effects. The specifics of their involvement in these processes however still remain unclear. PARs are present in many

cell types, with partially overlapping tissue expression patterns. The complex interplay between PARs, multiple proteinases, proteinase inhibitors and other molecules (i.e. glycosylation) that may be present in different organ systems, and under different pathological conditions, make the understanding of PAR mediated events a complex exercise (Hollenberg, 1996; Ossovskaya & Bunnett, 2004; Steinhoff *et al.*, 2005). However, the main interesting and of particular importance to this study is $hPAR_1$ and $hPAR_4$. Thus, a more extensive discussion of these thrombin receptors in the relationship with diseases will be informed as followed.

1.2.5.1 Cardiovascular system

PAR_1 (Vu *et al.*, 1991a; McNamara *et al.*, 1993; D'Andrea *et al.*, 1998), PAR_3 (Bretschneider *et al.*, 2003) (Schmidt *et al.*, 1998) and PAR_4 (Bretschneider *et al.*, 2001; Fujiwara *et al.*, 2005) are expressed by multiple cells in the cardiovascular and circulatory system, including the circulating cells as well as the vascular endothelial and smooth muscle cells. Human platelets express PAR_1 and PAR_4 (Kahn *et al.*, 1999) while murine platelets express PAR_3 and PAR_4 (Kahn *et al.*, 1998b).

It is now known that thrombin influences cellular behaviour via PAR_1, PAR_3 or PAR_4. Previous studies reported that thrombin is a major stimulator of platelets resulting in a cascade of effects culminating in platelet aggregation both *in vivo* and *in vitro* (Hung *et al.*, 1992b). Both PAR_1 and PAR_4 were found to be co-expressed in human platelets, however, the action of thrombin in causing platelet aggregation has been shown to be predominantly mediated by PAR_1 (Kahn *et al.*, 1999). The fact that PAR_1-blocking antibodies inhibited human platelet activation at low concentrations of thrombin but not high (Brass *et al.*, 1992; Hung *et al.*, 1992b) suggested that although PAR_1 is important in platelet aggregation it is not the only receptor involved. Indeed, PAR_4 was found to

have much lower affinity for thrombin compared to that of PAR_1 and only responds to high concentrations of thrombin. PAR_4 has been implicated in maintaining the sustained effect of thrombin, thereby contributing to the late phase of platelet aggregation (Covic *et al.*, 2000). In mouse, PAR_3 instead of PAR_1 plays an important role in platelet aggregation (Ishihara *et al.*, 1997). Similar to PAR_1 in humans, PAR_3 blocking antibodies were reported to block mouse platelet activation at low concentrations of thrombin but not high (Ishihara *et al.*, 1998). In addition, PAR_3 knockout mice showed reduced platelet aggregation at low concentrations of thrombin, but not high (Kahn *et al.*, 1998). Therefore PAR_3 is essential for low concentrations of thrombin induced platelet activation, but rely on PAR_4 as a second receptor for platelet aggregation at high thrombin concentrations (Kahn *et al.*, 1999). In addition, it has also been suggested that PAR_4 may be involved in responding to proteinases other than thrombin, and $hPAR_4$ activation by the neutrophil proteinase cathepsin G has been revealed (Sambrano *et al.*, 2000).

In vasculature, PAR_1 activation causes endothelium-dependent nitric oxide mediated vasorelaxtion in vessels isolated from various species including the human pulmonary artery (Hamilton *et al.*, 2001), porcine coronary artery (Hamilton & Cocks, 2000), rat aorta (Magazine *et al.*, 1996), internal mammary arteries (Ballerio *et al.*, 2007), as well as in a few smaller vessels such as the human and porcine intramyocardial arteries (Hamilton *et al.*, 2002). Recently PAR_4 has been reported to induce nitric oxide (NO) production in vascular endothelial cells, denoting a possible role in mediating vasodilation (Momota *et al.*, 2006).

PAR_1 and PAR_4 have been implicated in mediating vascular inflammatory responses as the increased expression of proteinases from inflammatory cells and the coagulation cascade might serve to activate these receptors. Activation of PAR_1 through intraplantar

injection of PAR_1-AP in rat paw caused oedema and the authors suggested that this effect was partly due to PAR_1 mediated plasma extravasation to tissue (Vergnolle *et al.*, 1999). The involvement of PAR_4 in inflammatory responses was also revealed through observations *in-vivo* that thrombin and PAR_4-AP, but not PAR_1-AP induced leukocyte rolling in rat mesenteric venules (Vergnolle *et al.*, 2002). In addition PAR_4 activation has also been implicated in vascular smooth muscle proliferation (Bretschneider *et al.*, 2001).

1.2.5.2 Respiratory system

PAR expression is detectable throughout the respiratory system and all evidence gathered thus far point towards critical roles in pulmonary physiology and pathology. So far PAR_1 has been identified expressed on numerous airway associated cell lines including pulmonary fibroblasts (Trejo *et al.*, 1996; Chambers *et al.*, 1998) and epithelial cells (Asokananthan *et al.*, 2002a), endothelial cells (D'Andrea *et al.*, 1998; Kataoka *et al.*, 2003) as well as smooth muscle cells (Lan *et al.*, 2000; Walker *et al.*, 2005). Signalling through PARs is also aided in part by the expression of a large number of potential PAR agonists in the airways including trypsin (Cocks *et al.*, 1999), mast cell tryptase (Molino *et al.*, 1997), neutrophil proteinases (Uehara *et al.*, 2003), and allergens (Asokananthan *et al.*, 2002b). PAR_4 expression appears to be limited to respiratory epithelial (Shimizu *et al.*, 2000; Asokananthan *et al.*, 2002a), endothelial (Kataoka *et al.*, 2003) and smooth muscle cells (Lan *et al.*, 2000). Additionally all PARs are shown on airway epithelial and smooth muscles cells by immunohistochemical staining using receptor specific antibodies (Knight *et al.*, 2001).

An important function of PARs in the respiratory system involves mediation of airway tone through regulating contraction or relaxation of smooth muscle cells (Lan *et al.*,

2002). The mitogenic property of thrombin is exemplified via activation of PAR_1 on human airway smooth muscle cells (Tran & Stewart, 2003; Walker *et al.*, 2005). Work further supporting the importance of PAR_1 in the pulmonary fibrotic response has been carried out in rats using bleomycin-induced pulmonary fibrosis (Howell *et al.*, 2001; Howell *et al.*, 2002). PAR_1 expression is significantly increased in a bleomycin induced model of pulmonary fibrosis, and use of thrombin inhibitors reduced CTGF gene expression and collagen accumulation (Howell *et al.*, 2001; Howell *et al.*, 2002). Activation of PAR_1 in human airway epithelial cells by Pen C13, an immunodominant mold allergen, was shown to result in IL-8 production, indicating an important role in the pathogenesis of this form of asthma (Chiu *et al.*, 2007).

1.2.5.3 Gastrointestinal system

PARs, expressed in a wide variety of cells in the gastrointestinal tract with a weak detection in the stomach, but strong expression in the colon and the small intestine, are considered as an "emergency" mechanism highly relevant into the contex of innate immunity (Vergnolle, 2008). It is well established that PAR_1 has been located on endothelial cells (Vergnolle *et al.*, 2004), epithelial cells (Buresi *et al.*, 2001; Buresi *et al.*, 2002), smooth muscle cells (Kawabata *et al.*, 2004), myofibroblasts (Seymour *et al.*, 2003) and on enteric neurons (Corvera *et al.*, 1997). PAR_4 is highly expressed in the small intestine and the colon with expression indicated on gastric smooth muscle cells (Hollenberg *et al.*, 1999) and epithelial cells (Mule *et al.*, 2004).

Of all the body systems, the gastrointestinal tract is the most exposed to proteinases. Thus, expression and function of PARs may be especially relevant in the gastrointestinal system. To date, PAR_1 has been shown to mediate ion transport, electrolyte secretion, intestinal motility, increased permeability, apoptosis, contraction of longitudinal muscle

and in contrast, relaxation of colonic circular muscle (Saifeddine *et al.*, 1996; Corvera *et al.*, 1999; Buresi *et al.*, 2002; Mule *et al.*, 2002; Vergnolle, 2005). In addition, PAR_1 is also involved in maintenance of mucosal integrity and/or pathogenesis of mucosal inflammation/injury throughout the GI tract including the oesophagus (Ossovskaya & Bunnett, 2004). PAR_1 may play dual roles in the development of intestinal inflammation as they are pro- and anti- inflammatory. PAR_4 is involved in relaxing pre-contracted rat oesophagus, in contrary to PAR_1 which causes further contraction (Kawabata *et al.*, 2000a). Furthermore, PAR_4 does not appear to play significant roles in GI exocrine secretion. Unlike PAR_2, PAR_1 and PAR_4 are not involved in the regulation of salivary or pancreatic exocrine secretion (Nguyen *et al.*, 1999; Kawabata *et al.*, 2000b; Kawabata *et al.*, 2000c). It is known that PAR_1, PAR_2 and PAR_4 are all expressed on intestinal smooth muscle and the activation of these receptors can alter the gastrointestinal motility (Vergnolle, 2005). Recently, Lee *et al.* reported that PAR_1 and PAR_2 but not PAR_4 activation causes contraction in the human and guinea-pig gallbladders and may play important roles in the control of gallbladder motility (Lee & Huang, 2007). The authors suggested that PAR_1 or PAR_2 agonists may be of potential therapeutic value in gallstone disease (Lee & Huang, 2007).

1.2.5.4 Renal system

In normal human kidney tissue PAR_1 has been shown to be present in endothelial, mesangial and epithelial cells (Grandaliano *et al.*, 2000) and primary human renal carcinoma cells (Kaufmann *et al.*, 2002). It was reported that in fibrin associated kidney diseases such as crescentic glomerular nephritis and thrombotic microangiopathy there was a reduced cellular PAR_1 expression within the glomerular lesions (Xu *et al.*, 1995). Later, PAR_1 activation was shown to result in enhanced glomerular crescent formation,

T cell and macrophage infiltration, fibrin deposition, and elevated serum creatinine in a murine model of crescentic glomerular nephritis (Cunningham *et al.*, 2000), which clearly highlighting the involvement of PAR_1 in the pathogenesis of crescentic glomerular nephritis. In addition, PAR_1 has also been shown to play a role in renal haemodynamics (Gui *et al.*, 2003).

1.2.5.5 Nervous system

PAR_1 expression has further been revealed in human astrocytoma cells (Grishina *et al.*, 2005) and peripheral nervous system cells (Noorbakhsh *et al.*, 2003). PAR_4 expression has also been reported in human astrocytes (Kaufmann *et al.*, 2000). Both PAR_1 and PAR_4 are reported to be activated by thrombin in human astrocytomas, contributing to the excitability and survival of the cells (Kaufman & Fuchs, 2000). Activation of PAR_1 leads to morphological changes and proliferation in neurons and astrocytes (Noorbakhsh *et al.*, 2003; Nicole *et al.*, 2005). A later study reported that the activation of PAR_1 also involved in the astrocyte proliferation disorder (Nicole *et al.*, 2005). The activation of PAR_1 by thrombin was also shown to protect neuronal cell and astrocytes from hypoglycaemia or oxidative stress induced cell death (Vaughan *et al.*, 1995). More recently PAR_1 has also been shown to play a role in HIV associated neurodegenerative disorders (Boven *et al.*, 2003; Ishida *et al.*, 2006). Ishida *et al.* also reported that PAR_1 is up-regulated in Parkinson disease effected brain tissue (Ishida *et al.*, 2006), and further provides a thrombin mediated protective pre-conditioning against Parkinson disease related behavioural deficits (Cannon *et al.*, 2006). Olianas *et al.* reported that PAR_1 is also expressed in rat olfactory neurons and addition of the thrombin resulted in a rapid neurite retraction suggesting a role of PAR_1 in neuritogenesis (Olianas *et al.*, 2007).

1.2.5.6 Immune system

PAR expression has been revealed on many immune cells. It is well established that activation of PARs can influence monocyte motility and chemotaxis, modulate pleiotropic cytokine responses, contribute to mononuclear cell proliferation, and induce apoptosis in various immune cells (Steinhoff *et al.*, 2005). Expression of PAR_1 has been detected on macrophages and monocytes (Colognato *et al.*, 2003) as well as mast cells (D'Andrea *et al.*, 2000). In addition, T cells (Mari *et al.*, 1996) and Jurkat-T leukemic cells (Bar-Shavit *et al.*, 2002) have been shown to illicit responses to low-levels of thrombin suggesting these cells may express PAR_1. Expression of PAR_4 has been reported on leukocytes (Vergnolle *et al.*, 2002). Thrombin mediated PAR activation in the immune system are primarily concerned with chemotaxis and the release of cytokines from inflammatory cell lines.

PAR_1 has a role in neurogenic inflammation, for example intraplantar injection of PAR_1 agonists causes oedema of rat paw through the release of substance P from peripheral afferent neurons (de Garavilla *et al.*, 2001). In addition PAR_1 has been implicated in hyperalgesia (Asfaha *et al.*, 2002). Previous studies have demonstrated that PAR_1 can play both anti-flammatory and proinflammatory roles in different models of inflammatory bowel disease (Shpacovitch *et al.*, 2007). PAR_4 and PAR_2 play important roles in modulation of leukocyte motility *in vivo* (Shpacovitch et al., 2007). PAR_4 has been shown to have a proinflammatory role in rat raw oedema, and the underlying mechanism appears to be non-neurogenic possibly through neutrophil recruitment activation and the kallikreinkinin system (Hollenberg *et al.*, 2004; Houle *et al.*, 2005). To date, *in vitro* studies have reported that the effects of PAR activation on human innate immune cells are mainly associated with activation of PAR_1 or $PAR_{2;}$ and very little is known about the potential role of PAR_4 in mediating inflammation *in vivo*

(Shpacovitch et al., 2007). The activation of PAR affects the main functions of innate immune cells, such as motility, adhesion, and secretion of inflammatory mediators (Shpacovitch *et al.*, 2007). Therefore, PARs may serve as ideal therapeutic targets for inflammatory, infections, or autoimmune diseases (Shpacovitch *et al.*, 2007).

1.2.5.7 Others

Coagulant proteases and PARs have been implicated in several types of malignant cancer (Arora *et al.*, 2007). PAR_1 is reported to be a potential oncogene, for example it is associated with metastasis and invasion in breast carcinoma xenograft (Boire *et al.*, 2005). In addition, activation of PAR_1 induced proliferation of colon cancer cells implicate that PAR_1 should be considered as grown factors and potential actors of mitogenic and metastatic evens (Darmoul *et al.*, 2003; Vergnolle, 2005).

1.3 PROTEINASES RELATED TO PAR SIGNALLING

The term *proteinase* is used as a synonym word for *endopeptidase*. *Peptidases* comprise of two groups of enzymes *endopeptidases* and *exopeptidases*. The name *peptidase* was first proposed by the International Union of Biochemistry and Molecular Biology (IUBMB) (1984) to describe the same group of enzymes that catalyse the hydrolysis of covalent peptidic bonds, and the widely used term *protease* is synonymous with *peptidase*.

Proteinases can be classified into four distinct classes by the biochemical catalytic mechanisms: Serine proteinases, metalloproteinases, cysteine proteinases, and aspartic proteinases (Owen & Campbell, 1999). Serine proteinases and metalloproteinases are most active at neutral pH and play major roles in degradation of extracellular proteins; however, the aspartic and cysteine proteinases have acidic pH optima and play a vital role in intracellular protein digestion within the lysosomes (Owen & Campbell, 1999).

Serine proteinases are the largest class of mammalian proteinases and are also the main focus of this project. Serine proteinases have a catalytically essential serine residue at the active site. Their activity depends on three residues Asp102, His57, and Ser195 (chymotrypsinogen numbering), which form the catalytic triad and are essential in the catalytic process (Owen & Campbell, 1999). In addition to their role in protein degradation, certain serine proteinases can also signal directly to cells by cleaving PARs. The best example of this is thrombin, a serine proteinase generated by the coagulation cascade, which has direct PAR_1-mediated effects on platelets, endothelial cells, immune cells, fibroblasts, myocytes, astrocytes and neurons (Schmidlin & Bunnett, 2001).

A number of mechanisms have been proposed as to how proteinases are capable of modulating various cellular responses. Proteinases have been shown to act as signalling molecules that are able to send specific signals to cells through the activation of PARs

(Schmidlin & Bunnett, 2001; Traynelis & Trejo, 2007). It has been hypothesized that PARs may be activated and attenuated by more than one proteinase. Any proteinase that cleaves the correct peptide bond within the N-terminus of a PAR may be able to expose the tethered ligand domain that binds onto the extracellular loop II of the receptor to initiate signalling (O'Brien *et al.*, 2001). Conversely, proteinases can also disarm the PARs by amputating the tethered ligand domain from the receptor (O'Brien *et al.*, 2001). For example, PAR_1 can be activated by thrombin but disarmed by neutrophil proteinases such as cathepsin G (Molino *et al.*, 1995), elastase and proteinase 3 (Renesto *et al.*, 1997). Proteinases can also selectively activate one PAR, whilst selectively disarming another; or will activate/disarm the same receptor depending on the proteinase concentration. An example of this is the ability of cathepsin G to simultaneously disarm PAR_1 and activate PAR_4 on human platelets (Sambrano *et al.*, 2000).

The physiological and pathophysiological processes resulting from proteinase mediated signalling events are therefore a product of that proteinase's effect on all the PARs expressed in the particular tissue environment where it is present.

1.3.1 Thrombin

The name thrombin derives from 'thrombus' as it plays a key role in the blood coagulation. Thrombin is synonymous with *factor IIa* which is the last protease capable of producing a thrombus or blood clot in the coagulation cascade (Barrett *et al.*, 1998; Coughlin, 2000). Its other alternative name is fibrinogenase as thrombin cleaves fibrinogen to yield fibrin monomers (the fibrous matrix of blood clots). Thrombin is derived from its proenzyme or zymogen form (prothrombin or coagulation factor II) through cleavage by factor Xa in the presence of the cofactor Va, Ca^{2+} and a

phospholipid surface (Krishnaswamy *et al.*, 1993). Thrombin was identified as a trypsin-like member of the chymotrypsin family of serine proteases produced at sites of vessel injury or tissue damage. Therefore the structure and catalytic mechanism of thrombin is similar to trypsin, it has a positively charged amino acid at the P1 position of the scissile bond (nomenclature of Schechter and Berger, where substrate residues are numbered from the scissile P1–P1' bond toward the N- and C-termini, respectively) (Schechter & Berger, 1967; Huntington, 2005).

Thrombin has been the target of intense study since its discovery in the 19th century (Huntington, 2005). Many studies demonstrated that thrombin has diverse effects on cells (Barrett *et al.*, 1998). It is now clear that thrombin *(i)* is a major player in the early steps of blood coagulation, *(ii)* is a significant contributor to the 'thrombin burst' through positive feedback mechanisms, *(iii)* functions to stabilize clots and participates in attenuating its own procoagulant activity (Mann *et al.*, 2003; Huntington, 2005). Furthermore, one of the most important actions of thrombin is that it cleaves and activates protease-activated receptors (PARs) 1, 3 and 4 (Ofosu, 2003). Thrombin cleaves $hPAR_1$ between Arg41 and Ser42 to expose tethered ligand SFLLRN and initiate signalling; $hPAR_3$ also contains the thrombin binding sites; however, $hPAR_4$ lacks such sites and thus responds only to higher concentration of thrombin (Schmidlin & Bunnett, 2001).

1.3.2 Trypsin

Trypsin is often referred to as a proteolytic enzyme or proteinase, which is produced in the pancreas in an inactive form, trypsinogen (Barrett *et al.*, 1998; Dery *et al.*, 1998; Paszcuk *et al.*, 2008). Trypsinogen is secreted by exocrine cells of the pancreas and released into the lumen of the small intestine (Vergnolle, 2008). From there, it is then transported to the duodenum, where it catalyses the digestion of proteins to polypeptides and amino acids, and it is an essential food-digestive enzyme (Hirota *et al.*, 2006; Paszcuk *et al.*, 2008).

Classically, trypsin is one of three principal digestive proteinases, the other two being pepsin and chymotrypsin. Trypsin is remarkably similar in chemical composition and in structure to chymotrypsin. Both enzymes also appear to have similar mechanisms of action; residues of histidine and serine are found in the active sites of both (Barrett *et al.*, 1998). The chief difference between these two molecules seems to be in their specificity, that is, each is active only against the peptide bonds in proteins that have carboxyl groups donated by certain amino acids. For trypsin these amino acids are arginine and lysine, for chymotrypsin they are tyrosine, phenylalanine, tryptophan, methionine, and leucine (Barrett *et al.*, 1998). Trypsin can be inactivated or inhibited by a number of specific or non-specific protease inhibitors, many of them belonging to the serpine family (Barrett *et al.*, 1998; Hirota *et al.*, 2006). Soya bean trypsin inhibitor (STI) is the most widely used trypsin inhibitor in biotechnological applications. Chemists have made good use of this fact. For instance, trypsin is used *(i)* in biotechnological applications, especially in the cultivation of mammalian cells, *(ii)* as a protein degrading enzyme in the processing of non-trypsin sensitive biopolymers, *(iii)* in formalin-fixed, paraffin-embedded immunohistochemical procedures (Barrett *et al.*, 1998). In humans, trypsin is associated with many disorders, for example *(i)* imbalances in regulation of

trypsin cause imbalances in insulin, *(ii)* imbalances in other regions of the body of trypsin and trypsin-like proteins are thought to play a role in emphysema, asthma, arthritis, skin disorders, and cancerous tumour growth (Ossovskaya & Bunnett, 2004; Arora *et al.*, 2007; McIntosh *et al.*, 2007).

In addition, proteases such as thrombin and trypsin are known to activate PARs, and thereby exert cellular effects such as platelet aggregation, endothelium-dependent relaxation and myometrial contraction (Dery *et al.*, 1998; Hamilton *et al.*, 1999; Nakayama *et al.*, 2001; Shintani *et al.*, 2001). PAR_1, PAR_2 and PAR_4 can be activated by trypsin (Dery *et al.*, 1998; Cocks & Moffatt, 2000; Macfarlane *et al.*, 2001). However since trypsin cleaves at three different points in the PAR_1 N-terminus (41-42, and preferentially 70-71 and 82-83) (Nakayama *et al.*, 2004) at low concentrations (< 40 nM) it will disarm PAR_1, whereas higher concentrations will activate the receptor (Kawabata *et al.*, 1999). Interestingly, the activation of PAR_1 by trypsin appears cell-type-specific. One study reported that PAR_1 was cleaved and disabled by trypsin on platelets (Ofosu *et al.*, 1998). Furthermore, trypsin has also been reported to disarm PAR_1 in endothelial cells (Nakayama *et al.*, 2003; Nakayama *et al.*, 2004). This differential activation/disarming indicate that perhaps there exist other factors influencing trypsin activation or disarming of PAR_1.

1.3.3 Thermolysin

Thermolysin, the prototype of the M4 family of zinc metalloproteases, is a 34.6 kDa proteolytic enzyme secreted by the gram-positive thermophilic bacterial *Bacillus thermoproteolyticus* (Endo, 1962; De Kreij A, 2000). Thermolysin cleaves peptides and proteins at the N-terminal side of the hydrophobic residues leucine (Leu), isoleucine (Ile), phenylalanine (Phe) and valine (Val) (Barrett *et al.*, 1998).

Thermolysin is widely used in protein chemistry as a nonspecific protease to obtain sequence or conformational data (Barrett *et al.*, 1998). Recently, lots of studies reported that this M4 family comprises of several proteases generated by bacteria involved in lung pathology. Molla *et al.* reported that thermolysin is an inflammatory bacterial protease which increases vascular permeability (Molla *et al.*, 1987). Dery *et al.* reported that in insect SF9 cells thermolysin cleaves PAR_1 within the tethered ligand domain (SFLLR) at Phe^{43}-Leu^{44} and Leu^{44}-Leu^{45}, suggesting that thermolysin terminates signalling by destroying the PAR_1 tethered ligand (Dery *et al.*, 1998). In addition, thermolysin is reported to disarm PAR_1 and PAR_2 in porcine coronary endothelial cells (Hamilton *et al.*, 1999). Furthermore, thermolysin has shown different sensitivity towards activating or disarming PAR_2 in different human epithelial cell types (Ubl *et al.*, 2002).

1.3.4 Neutrophil serine proteases

Recruitment of neutrophils to the site of inflammation is essential for host defence against infection (Pham, 2006). For example neutrophils can migrate from blood vessel lumen into the lung interstitium and airway lumen during infection and inflammation, and **t**hey play an important role in host defence against infection, but may also cause tissue injury (Hiemstra *et al.*, 1998; Wiedow & Meyer-Hoffert, 2005). Neutrophil granulocytes are generated in the bone marrow, and then circulate to the bloodstream (Savill *et al.*, 1989; Hiemstra *et al.*, 1998). They adhere to the endothelium and migrate to the infected site where they engulf and degrade microorganisms using a combination of oxidative and non-oxidative mechanisms (Faurschou & Borregaard, 2003; Pham, 2006). Neutrophils contain at least four types of granules including azurophil granules, specific granules, gelatinase granules and secretory granules (Pham, 2006). The

azurophil granules, also called primary granules, are defined by their high content of myeloperoxidase (MPO), bactericidal permeability-increasing protein, defensins and a family of structurally related serine proteases – neutrophil elastase, cathepsin G, and proteinase 3 in high concentration around 1pg enzyme per cell (Wiedow *et al.*, 1996; Pham, 2006). Once released, neutrophil serine proteases potentially are fully activated because they can function optimally in a neutral environment

1.3.4.1 Elastase

Polymorphonuclear leukocyte elastase or neutrophil elastase was first identified in 1968 by Janoff & Scherer (Janoff & Scherer, 1968). The term elastase (ELA) describes an enzyme capable of the proteolytic release of soluble peptides from insoluble elastin, and such activity is essential for defining a proteinase as an elastase (Janoff & Scherer, 1968). ELA is a 30 kDa glycoprotein, containing 20% of neutral sugars with only a small amount of sialic acid. ELA belongs to the chymotrypsin family of serine proteinases, and it is formed of a single polypeptide chain of 218 amino acid residues and four disulfide bridges (Barrett *et al.*, 1998). ELA is highly cationic, with a strongly basic isoelectric point (pH 10–11), and it cleaves bonds that are carboxyterminal to small hydrophobic residues (particularly bonds having valine at the P1 position) (Owen & Campbell, 1999).

1.3.4.2 Cathepsin G

The name cathepsin G (CG) was given by Starkey & Barrett in 1976 (Starkey & Barrett, 1976). CG is a typical chymotrypsin family member, and it is a 28.5 kDa cationic serine proteinase that shares 37% sequence homology with ELA (Barrett *et al.*, 1998). It consists of a 235-residue polypeptide chain that has one potential *N*-linked

glycosylation site and three disulfides (Salvesen *et al.*, 1987). It has a chymotrypsin-like catalytic activity, in that it preferentially cleaves peptide bonds that are carboxy-terminal to bulky aliphatic or aromatic residues (particularly bonds having phenylalanine at the P1 position). Interestingly, a recent study reported that CG activity can be inhibited by lactoferrin (He *et al.*, 2003).

1.3.4.3 Proteinase 3

Proteinase 3 (PR3), also termed p29b or myeloblastin, is a neutral serine proteinase mainly stored in the azurophilic granules of neutrophils and the granules of monocytes (Baggiolini *et al.*, 1978; Kao *et al.*, 1988; Bories *et al.*, 1989; Rao *et al.*, 1991a). PR3 was originally identified by Baggiolini *et al.* as an α-naphthyl acetate esterase present in azurophilic granules of human PMNL (Baggiolini *et al.*, 1978). In 1990 Campanelli and colleagues reported that a ~29 kDa gene product termed p29b generated from human bone marrow, and subsequently named it as proteinase 3 (Campanelli *et al.*, 1990). The authors also pointed out that PR3 is more abundant in neutrophils than elastase and has a similar proteolytic profile and specific activity (Campanelli *et al.*, 1990). One year later, Rao *et al.* reported that the molecular mass of PR3 is 26.8 kDa (Rao *et al.*, 1991a). PR3 is a cationic serine proteinase that consists of 222 amino acids plus two carbohydrate chains at *N*-linked glycosylation sites (Barrett *et al.*, 1998). PR3 shows extensive N-terminal sequence similarity to proteinases of the trypsin superfamily with strongest homology to human ELA and CG (Kao *et al.*, 1988; Rao *et al.*, 1991a). Moreover, there is a striking homology between the amino acid sequence of the putative activation site of PR3 and that of ELA (Rao *et al.*, 1991a). Thus, this proteinase has an elastaste-like specificity for small aliphatic residues (Ala, Val, Ser, Met) at the P1 and P1’ sites, especially PR3 prefers either alanine or valine at the P1 site (Rao *et al.*,

1991a). PR3 was originally described as a protein that hydrolyzes elastin (a major structural protein of the lung) with an efficiency equivalent to that of ELA (Kao *et al.*, 1988). Recently, it has been shown that PR3 exhibits various biological functions including enhancement of TNF-α and IL-1β release from human monocytic cell lines (Coeshott *et al.*, 1999), production of IL-8 and monocyte chemoattractant protein-1 (MCP-1) by human endothelial cells (Berger *et al.*, 1996). PR3 also participates in the killing of microorganisms (Campanelli *et al.*, 1990). PR3 is a major target antigen of anti-neutrophil cytoplasmic antibodies in Wegener's granulomatosis (van der Geld *et al.*, 2001). PR3 can also cause extensive tissue damage and emphysema after intratracheal instillation into hamsters (Rao *et al.*, 1991a).

1.3.4.4 Neutrophil serine proteinases and PARs

PAR_1 has been reported to be disarmed by neutrophil proteinases such as cathepsin G, elastase and proteinase 3 (Renesto *et al.*, 1997). However, cathepsin G was also reported to activate murine fibroblasts transfected with $hPAR_1$ (Shpacovitch *et al.*, 2007). In addition, elastase and cathepsin G have both been shown to inactivate PAR_2 by cleaving amino terminal domains distinct from the activation site, rendering the receptors unresponsive to the activating proteinases in both transfected cells and bronchial fibroblasts (Dulon *et al.*, 2003; Ramachandran *et al.*, 2007). Despite the suggestions that cathepsin G and proteinase 3 disarm PAR_2, they were also reported to activate PAR_2 in human gingival fibroblasts (Loew *et al.*, 2000; Shpacovitch *et al.*, 2007). Cathepsin G has also been shown to abolish signalling by thrombin in PAR_3 transfected cells (Cumashi *et al.*, 2001). Cathepsin G is reported to activate PAR_4 in receptor-transfected fibroblasts, PAR_4-expressing oocytes, and human platelets (Shpacovitch *et al.*, 2007). One possible explanation for such contradictory results could

be due to variations in PAR glycosylation and the subsequent availability of different receptor cleavage sites (Loew *et al.*, 2000; Shpacovitch *et al.*, 2007). Thus further investigation is required to address the complexities of cathepsin G, proteinase 3 and elastase in PAR signalling.

1.3.5 Plasmin

Plasminogen is the zymogen of the serine protease plasmin, and it is synthesized in the liver and present at micromolar concentrations in human plasma and extracellular fluids (Barrett *et al.*, 1998; Judex & Mueller, 2005). The mature human plasminogen consists of 791 amino acid resides in a single polypeptide chain, and plasmin is a two-chain serine protease (Barrett *et al.*, 1998). Plasmin cleaves its substrates at lysine and arginine residues, with specificity similar to that of thrombin (Barrett *et al.*, 1998). Most of the enzymatic activities of plasmin can also be catalyzed to some degree by other closely related enzymes, such as trypsin, or enzymes of the coagulation or fibrinolysis systems (Barrett *et al.*, 1998).

Plasmin is one of the important enzymes present in blood, and it degrades many blood plasma proteins, such as fibrin clots (Barrett *et al.*, 1998; Judex & Mueller, 2005). Plasmin plays a key role in blood clot lysis, and its major physiological substrates are fibrinogen and fibrin (Barrett *et al.*, 1998). Deficiency in plasmin may lead to thrombosis, as clots are not degraded adequately. The plasmin system plays many important roles in physiology and pathophysiology. Apart from clot lysis, plasmin has also been implicated in fibrinolysis, wound healing, adipose tissue development, and tumor invasion and metastasis (Judex & Mueller, 2005).

Interestingly, plasmin can activate/disarm PARs. For example, plasmin was reported to activate PAR_1 in fibroblasts and induce the PAR-mediated transcription of motility

factors (Pendurthi *et al.*, 2002). However, Kuliopulos *et al.* showed that plasmin has a low affinity for the traditional thrombin cleavage site on PAR_1 and a higher affinity for a cleavage site that is further downstream; in effect, plasmin is more likely to make PAR_1 refractory to further thrombin stimulation than to stimulate calcium mobilization (Kuliopulos *et al.*, 1999). In addition, plasmin was also reported to be capable of inducing platelet activation through activation of PAR_4 (Quinton *et al.*, 2004).

1.3.6 Tryptase

Initially a trypsin-like protease was detected in mast cells by Glenner & Cohen (1960) using histochemical substrates, and this protease was subsequently named as tryptase by Lagunoff & Benditt (1963) (Barrett *et al.*, 1998). The name tryptase is now almost exclusively used to refer to mast cell serine proteases with trypsin-like specificities. Mast cell tryptase is mainly stored in the dense cytoplasmic granules of mast cells and accounts for 23% of the total cellular protein of human mast cells (Schwartz *et al.*, 1981). The release of tryptase from the secretory granules is a characteristic feature of mast cell degranulation. One previous study reported that tryptase is a tetrameric neutral serine protease with a molecular weight of approximately 130 kDa, and the genes encoding mast cell tryptase are located on the short arm of chromosome 16 (Payne & Kam, 2004). In addition tryptase was reported to be highly heterogeneous in size, charge and activity, for example, tryptase purified from lung and skin with different molecular masses ranging from 29 to 40 kDa (Peng *et al.*, 2003). The authors suggested that the variable degrees of glycosylation of tryptase in different tissue may be a major contributor to the size and charge heterogeneity (Peng *et al.*, 2003).

Mast cell tryptase has become a useful marker for mast cell activation. It is well known that mast cells play a central role in inflammatory and immediate allergic reactions in

airways, and tryptase is a pathological mediator of numerous allergic and inflammatory conditions (such as asthma, rhinitis) (Berger *et al.*, 2003; Bradding *et al.*, 2006; Sokolova & Reiser, 2007). Interestingly, mast cells have also been implicated as having pivotal roles in arthritis, and tryptase was reported to stimulate histamine release from synovial cells (He *et al.*, 2001). In addition, a recent finding suggested that tryptase stimulates IL-8-dependent neutrophil chemotactic activity from endothelial cells and could be important in stimulating leucocyte accumulation following mast cell activation (Compton *et al.*, 2000b). Several previous studies suggested that the tryptase inhibitors would be suitable as a novel treatment for arthritis, bronchial asthma and other inflammatory and allergic conditions of the airways (He *et al.*, 2001; Sheth *et al.*, 2003; He *et al.*, 2004).

Interestingly, tryptase activation of PAR_2 has been demonstrated in a variety of cell types including cultured HUVEC (Human Umbilical Vein Endothelial Cells), rat colonic myocytes, keratinocytes and guinea-pig myenteric neurons, human airway smooth muscle cells (Corvera *et al.*, 1997; Molino *et al.*, 1997a; Schechter *et al.*, 1998; Berger *et al.*, 2001). However, some reports (Molino *et al.*, 1997a; Schechter *et al.*, 1998; Corvera *et al.*, 1999; Alm *et al.*, 2000), but not others (Corvera *et al.*, 1997; Steinhoff *et al.*, 2000), have indicated that tryptase appears to behave as a partial agonist compared to trypsin for activating PAR_2, implying that PAR_2 activation by tryptase may be influenced by other factors. Furthermore, one recent study also reported that glycosylation of PAR_2 could provide novel mechanisms for regulating receptor activation by tryptase and possibly other proteases (Compton *et al.*, 2001).

1.3.7 Chymase

The name chymase was first proposed by Lagunoff & Benditt (1963) to denote an enzyme similar to pancreatic chymotrypsin, previously detected in mast cells (Barrett *et al.*, 1998). In more recent usage, the term chymase refers to a group of chymotryptic serine proteases expressed in mast cell secretory granules (Barrett *et al.*, 1998). Chymase is a monomeric serine protease with a molecular weight of 30 kDa and is found exclusively in the MC_{TC} subpopulation of mast cells (Barrett *et al.*, 1998). This protease is stored in the same granules as tryptase and is either bound to heparin or chondroitin E (Barrett *et al.*, 1998). Human chymase exists in at least two distinct but similar forms, and the differences in affinity for heparin and distribution in skin, heart, and other tissues could have important consequences for enzyme function (McEuen *et al.*, 1998). Chymase can be inhibited by the circulating serine protease inhibitors such as α_1-antichymotrypsin, α_1-proteinase inhibitor and α_2-macroglobulin (Schechter et al., 1989). Inhibitors of chymase can be potent mast cell stabilizers, particularly in the skin (He *et al.*, 1999). A previous study reported that chymase could contribute to increases in microvascular permeability following mast cell degranulation in allergic disease (He & Walls, 1998a). In addition, counting chymase-positive (MC_{TC}-type) mast cells in tumor stroma was suggested to be a good prognosis predictor for LBACs (localized bronchioloalveolar carcinomas), especially Noguchi type-C tumors (Nagata *et al.*, 2003). Chymases can activate angiotensin I and II and thus are involved in hypertension and atherosclerosis (Caughey, 2007). Chymase was reported to disarm PAR_1 in dermal fibroblasts (Schechter *et al.*, 1998). Chymase might also modulate cell function via other PARs, but direct evidence for this is still lacking (Shpacovitch *et al.*, 2007).

1.4 POST-TRANSLATIONAL MODIFICATIONS OF PARs

Post-translational modification means the chemical modification of a protein after its translation. There are a number of different post-translational modifications including glycosylation, phosphorylation, methylation and acylation. Among these one of the most common post-translational modifications that many GPCRs are known to undergo is glycosylation (He *et al.*, 2002). It is well known that GPCR contain at least one site of glycosylation in the *N*-terminal domain, although some exceptions exist (A_2 adenosine receptor lacks *N*-terminal sites but has glycosylation sites in ECL2) (Wheatley & Hawtin, 1999). Glycosylation is the process which involves the addition of saccharides to proteins or lipids, and the majority of proteins synthesized in the rough endoplasmic reticulum undergo glycosylation (Kornfeld & Kornfeld, 1985b). This process is the first of four principal modification steps in the synthesis of membrane proteins and secretory proteins. Characteristically, glycosylation can occur via *N*, or *O* linkages: *N*-linked glycosylation to the amide nitrogen of asparagine side chains and *O*-linked glycosylation to the hydroxy oxygen of serine and threonine side chains. *N*-linked glycosylation is extremely common and nearly two-thirds of the sequences stored in SWISS-PROT contain the potential *N*-glycosylation consensus sequon, Asn-X-Ser/Thr (where X can be any amino acid except proline) (Apweiler *et al.*, 1999) and are therefore potentially glycosylated. However, *O*-linked glycosylation, unlike *N*-linked glycosylation, appears to have no consensus sequence (Apweiler *et al.*, 1999). Since N-linked glycosylation of GPCR is the focus of this thesis, we will focus on this in the following sections.

1.4.1 *N*-linked glycosylation

N-linked glycosylation, which adds oligosaccharides to the nitrogen in the side-chain amide of asparagines residues (Opdenakker et al., 1993; Wheatley & Hawtin, 1999), requires the asparagines in a consensus sequence of Asn-X-Ser/Thr, where X can be any amino acid except proline, although not all asparagines possessing the glycosylation sequon are glycosylated in a given protein (Kornfeld & Kornfeld, 1985b; Wheatley & Hawtin, 1999). In addition, the Asn-X-Thr/Ser acceptor site must be correctly orientated and accessible for glycosylation to occur (Wheatley & Hawtin, 1999). Furthermore, not all consensus sites are actually glycosylated as the oligosaccharide is trimmed and elaborated during moving through the endoplasmic reticulum (ER) and the Golgi apparatus (Wheatley & Hawtin, 1999).

1.4.1.1 Diverse *N*-linked glycans have a common core structure

Oligosaccharides exist in three categories termed high-mannose, complex and hybrid (Wheatley & Hawtin, 1999). In mature glycoproteins *N*-linked glycan moieties are structurally diverse. However, when initially added in the ER to growing nascent polypeptides, these glycans share a common core structure which is homogeneous and relatively simple (Figure 1.3) (Helenius & Aebi, 2001). This core oligosaccharide (core glycan) remains fairly consistent among eukaryotes and consists of three glucoses, nine mannoses and two *N*-acetyl-glucosamines ($Glc_3Man_9GlcNAc_2$-) (Figure 1.4) (Helenius & Aebi, 2001, 2004).

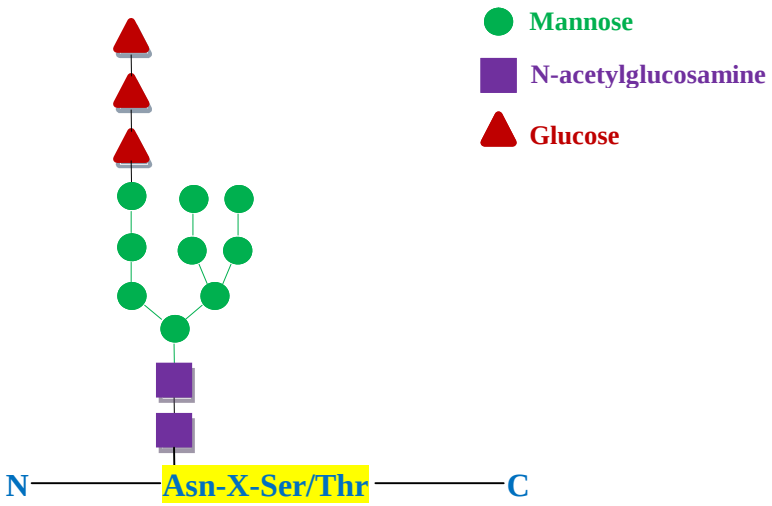

Figure 1.3 *N*-linked core oligosaccharide. The core glycan ($Glc_3Man_9GlcNAc_2$-) has 14 saccharides: 3 glucoses (*red triangles*), 9 mannoses (*green circles*), and 2 N-acetylglucosamines (*purple square*). *N*-linked glycans are added to nascent proteins in the lumen of the rough ER as "core oligosaccharides" that have the structure shown. These are bound to the polypeptide chain through an N-glycosidic bond with the side chain of an asparagine that is part of the Asn-X-Ser/Thr consensus sequence.

1.4.1.2 The biosynthesis of *N*-linked glycans in ER

Classically, the biosynthesis of *N*-linked glycosylation begins with transferring the core glycan from the lipid carrier onto the nascent protein by oligosaccharyltransferase in the ER (Wheatley & Hawtin, 1999) (Figure 1.3, 1.4).

Firstly, biosynthesis of the core glycan, which occurs on both sides of the ER membrane, starts by addition of monosaccharides to a lipid carrier (dolichol-pyrophosphate) by monosaccharyltransferases (Helenius & Aebi, 2001). Seven sugars are first added to the dolichol pyrophosphate lipid carrier by specific glycosyltransferases on the cytosolic

surface (Burda *et al.*, 1999). Once the seven sugar chain has been added to dolichol pyrophosphate, the chain is then translocated to the lumen side of the ER by heptasaccharide flippase enzymes (Helenius & Aebi, 2002) (Figure 1.4). Whether facing the lumen or the cytosol, each individual glycosyltransferase displays strong preference towards a single oligosaccharide substrate (Burda *et al.*, 1999). Tunicamycin can inhibit this first step of the pathway by inhibiting the transfer of *N*-acetylglucosamine to dolichol pyrophosphate thereby effectively blocking the whole *N*-glycosylation process (Tkacz & Lampen, 1975; Elbein, 1984). Therefore, tunicamycin is often applied to prevent *N*-glycosylation of recombinant receptors expressed by cells in culture (Wheatley & Hawtin, 1999).

The next step is the addition of the remaining seven oligosaccharides, the last being the addition of a terminal α-1,2 linked glucose residue which acts as an indicator for efficient recognition by the oligosaccharyltransferase (OST) (Figure 1.4) (Burda & Aebi, 1998; Helenius & Aebi, 2004). It is known that OST scans the emerging polypeptide for glycosylation sequons (Asn-X-Ser/Thr) and attaches the completed core oligosaccharide from the dolichylpyrophosphate carrier to a growing nascent polypeptide chain, which is coupled through an N-glycosidic bond to the side chain nitrogen of the Asn residue (Helenius & Aebi, 2004). The transfer of a glycan to the side chain of the Asn requires formation of a loop in the polypeptide so that the hydroxyl groups of Ser or Thr can contact the Asn amide and render it more nucleophilic (Helenius & Aebi, 2004). This explains why the middle residue X in the sequon cannot be a proline; proline prevents the folding of the growing peptide into a loop thus preventing the third amino acid in the sequon (serine or threonine) contacting the asparagines to cause it to become more hydrophilic and thus more reactive (Helenius & Aebi, 2004). Several factors can control the attachment of oligosaccharides to potential glycosylation sites, including the number

and location of potential glycosylation sites in the protein, and the cell specific expression of glycotransferases, which enzymatically modify the glycan chains once they are attached to the protein core (Opdenakker *et al.*, 1993; Harduin-Lepers *et al.*, 2001).

Immediately after coupling to the polypeptide chain, the last two terminal glucose residues are removed by glycosydases I and II (Helenius & Aebi, 2001). The removal of glucose serves as a quality control for proper folding of these glycoproteins and their readiness for transit to the Golgi apparatus (Hebert *et al.*, 2005). After the correctly folded protein is generated and the final glucose residue removed, a series of mannosidases then start to cleave one or all of the α1,2 bound mannoses (Kornfeld & Kornfeld, 1985a).

1.4.1.3 The processing of *N*-linked glycans in the Golgi complex

After the glycoprotein moves to the Golgi complex, the glycan chains undergo further trimming of mannoses before further extension of the glycan branches in the lumenal side of Golgi, and subsequently development of the diversity of glycans begins (Figure 1.4) (Hossler *et al.*, 2007). The Golgi apparatus consists of stacks of membranous compartments including cis, medial, trans, and TGN (trans-Golgi network) cisternae, interestingly these cisternae are not biochemically homogeneous (Hossler *et al.*, 2007). After the glycoprotein enters the *cis* golgi lumen it proceeds through the golgi apparatus passing through the *medial* golgi and into the *trans* golgi. While these secretory glycoproteins travel through these Golgi compartments the glycan extension reactions are catalyzed by varying compositions of glycosylation enzymes in each compartment. For example, on its journey the addition of sugars to the different positions of that extending glycan is catalyzed by a number of different glycosyltransferases, ea’ch

adding a particular monosaccharide through a specific glycosidic bond (Kornfeld & Kornfeld, 1985b; Hossler *et al.*, 2007). The Golgi contains a diverse range of glycosyltransferases, which can add a wide range of saccharide moieties to the developing *N*-linked glycan. Thus *N*-linked glycan microheterogeneity arises through enzyme processing in the Golgi apparatus (Hossler *et al.*, 2007). Furthermore, these intermediate glycans along the biosynthetic pathway in the Golgi have more than one available reaction site, either on the same or different sugar moieties, for receiving a monosaccharide (Hossler *et al.*, 2007). Most glycans consist of bi-antennary structures, however tri-antennary and tetra antennary occur often, and five or more branches do occur. The final addition of a galactose and sialic acid residue to the terminal sugar of each branch occurs in the *trans* golgi and the reactions are catalysed by galactosyltransferase and sialyltransferase respectively (Figure 1.4).

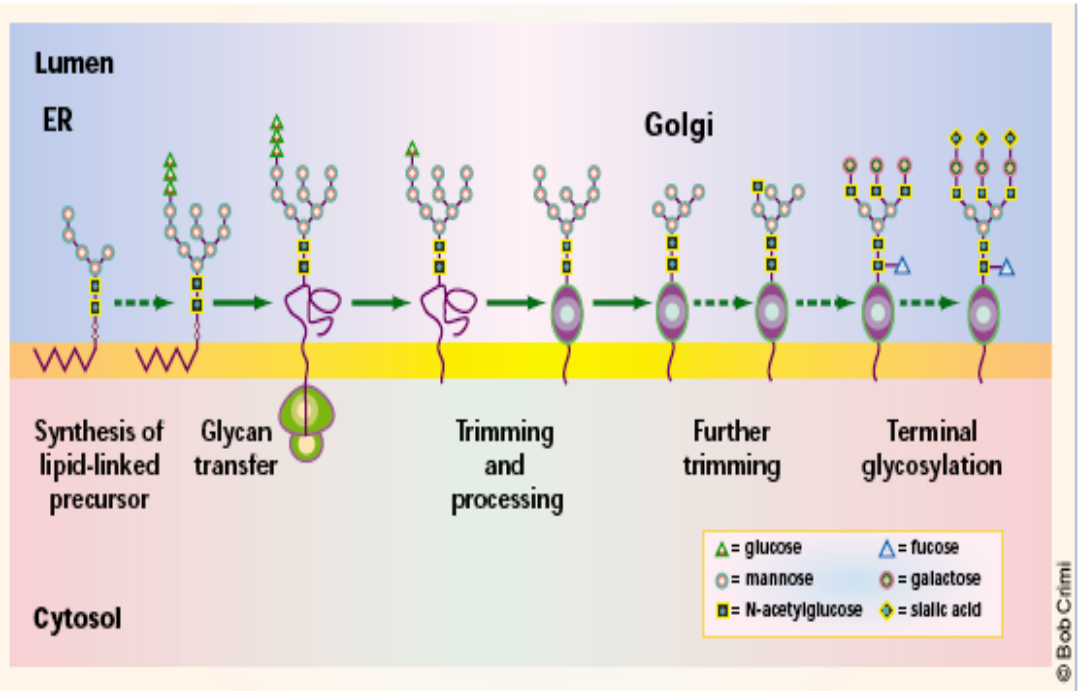

Figure 1.4 Biosynthesis of the *N*-linked glycan. Synthesis starts by the addition of sugars onto dolichylphosphate (in the cytosol), which is then flipped over into the lumen of the endoplasmic reticulum (ER), and then the core glycan ($Glc_3Man_9GlcNAc_2$-) is generated. The glycan is then transferred to the nascent, growing polypeptide. Sugars are trimmed off, and the polypeptide is then correctly folded before being moved to the Golgi complex. The glycoprotein goes through a series of further modifications, ending with the capping of the oligosaccharide branches with sialic acid and fucose in the Golgi. (Helenius & Aebi, 2001)

1.4.2 Sialic Acid

The term sialic acid encompasses a large family of acidic 9-carbon sugars, which are typically located at the terminal positions of a variety of glycoconjugates (Lehmann *et al.*, 2006). One member of this family, *N*-acetylneuraminic acid (Neu5Ac), is the form that is most commonly found in mammalian glycoconjugates, which is a nine-carbon sugar acid formed by condensation of pyruvate with *N*-acetylmannosamine (Drickamer, 2006). In the nucleus, Neu5Ac are converted to CMP-Neu5Ac by CMP-Neu5Ac synthetase, and then transported to the *trans* golgi where it becomes a substrate for the sialyltransferases, and subsequently attached to the terminal oligosaccharide chain of glycoproteins (Munster-Kuhnel *et al.*, 2004). These residues are most typically linked via α(2-3) and α(2-6) to galactose (or lactose), as well as α(2-8) and α(2-9) linkages in homopolymers of Neu5Ac (polysialic acid) (Angata & Fukuda, 2003; Ressa & Linhardt, 2004).

Sialic acids of cell surface glycoproteins and glycolipids play a pivotal role in the structure and function of animal tissues. Sialic acid has been implicated in a number of disease states including cystic fibrosis and tumours (Kube *et al.*, 2001; Malykh *et al.*, 2001). In addition, many pathological microbes employ sialic acids to promote infection. For example, some viruses can utilize hemagglutinin (a sialic acid binding lectin) or neuraminidase (an enzyme that cleaves sialic acid) to gain entry into a cell promoting infection (Ressa & Linhardt, 2004).

The pattern of cell surface sialylation is species and tissue-specific, is highly regulated during embryonic development, and changes with stages of differentiation. A mutant Pro5 cell line derived from Chinese Hamster Ovary cell (CHO) has been developed; this mutant cell line, Lec2 (ATCC Number: CRL-1736), is deficient in CMP-sialic acid transport and therefore glycoproteins synthesised in this cell line are not sialylidated.

This cell line is therefore a useful tool to determine whether sialic acid is important in glycoprotein function or trafficking (Compton *et al.*, 2002b). Indeed, Compton *et al.* reported that $hPAR_2$ *N*-linked glycosylation and sialylation regulates receptor expression and/or signalling (Compton *et al.*, 2002b). Another useful tool for studying the effect of sialic acid on proteins is the enzyme neuraminidase. Neuraminidase is a carbohydrase or glycosidase enzyme which was first discovered in the influenza virus, and it cleaves the terminal sialic acid residues from glycoconjugates (Gottschalk, 1958).

1.4.3 *N*-linked glycosylation and glycoprotein

The importance of *N*-linked glycosylation for expression and function has been studied for many GPCRs, however, the role of the *N*-glycosylation is somewhat variable. In general, *N*-linked glycosylation is believed to play a major role in facilitating protein folding, protein stability and protection from proteolysis, intracellular trafficking, secretion, and cell surface expression (Opdenakker *et al.*, 1993; Helenius, 1994). In addition, glycosylation may be important for maintaining a protein's correct conformation, enzymatic acitivity, and other structural functions (Opdenakker *et al.*, 1993; Imperiali & Rickert, 1995).

It is becoming apparent that *N*-linked glycans play a wide variety of roles during protein folding both *in vitro* and *in vivo*. Newly synthesised proteins begin folding immediately upon entry to the ER. By binding to the chaperone proteins, the glycoproteins cannot be prematurely exported from the ER, and are allowed to complete their correct folding process (Hammond *et al.*, 1994; Ellgaard & Helenius, 2003). If proteins are still misfolded after glycans are added, they are not allowed to leave the ER, instead they are degraded (Ellgaard & Helenius, 2003). Current understanding suggests that the presence of a glycan can induce rigidity in a protein structure possibly by restricting freedom of

mobility of the peptide chain (Ellgaard & Helenius, 2003). The high incidence of glycosylation occurring at crucial locations on the protein could provide evidence in favour of a role for *N*-linked glycosylation in protein folding (Petrescu *et al.*, 2004).

1.4.4 *N*-linked glycosylation and PARs

It is now clear that $hPAR_1$ contains a total of five potential *N*-linked glycosylation sequons (Figure 1.5 (A), Table 1.1)(Compton, 2003). Two sequons are located within ECL2 ($N^{250}I^{251}T^{252}$, $N^{259}E^{260}T^{261}$) and three are located on the receptor N-terminus ($N^{35}A^{36}T^{37}$, $N^{62}E^{63}S^{64}$, $N^{75}K^{76}S^{77}$). Interestingly, ($N^{35}A^{36}T^{37}$) is located at the N-terminal of the cleavage/activation site ($LDPR^{41}/S^{42}FLLR$) and the remaining two ($N^{62}E^{63}S^{64}$, $N^{75}K^{76}S^{77}$) are at the C-terminal of the cleavage-activation site. $hPAR_2$ possesses two glycosylated *N*-linked glycosylation sequons (Figure 1.5 (B), Table 1.1)(Compton, 2003): one lies on the receptor N-terminus ($N^{30}R^{31}S^{32}$) which is very close to the putative cleavage/activation site, and the second one is located on ECL2 ($N^{222}I^{223}T^{224}$). The glycosylation status of either $hPAR_3$ or $hPAR_4$ had not been previously addressed when this thesis project started. According to the derived amino acid sequence analysis $hPAR_3$ possesses three putative *N*-linked glycosylation sequons: two on the receptor N-terminus ($N^{25}D^{26}T^{27}$ and $N^{82}A^{83}T^{84}$), the former being located near the putative cleavage/activation site. The third *N*-linked glycosylation sequon lies on ECL3 ($N^{331}N^{332}T^{333}$) (Figure 1.5 (C), Table 1.1) (Compton, 2003). $hPAR_4$ only possesses one putative *N*-linked glycosylation site, located on the receptor N-terminus ($N^{56}D^{57}S^{58}$) and within the putative cleavage/activation site (Compton, 2003). (Figure 1.5 (D), Table 1.1).

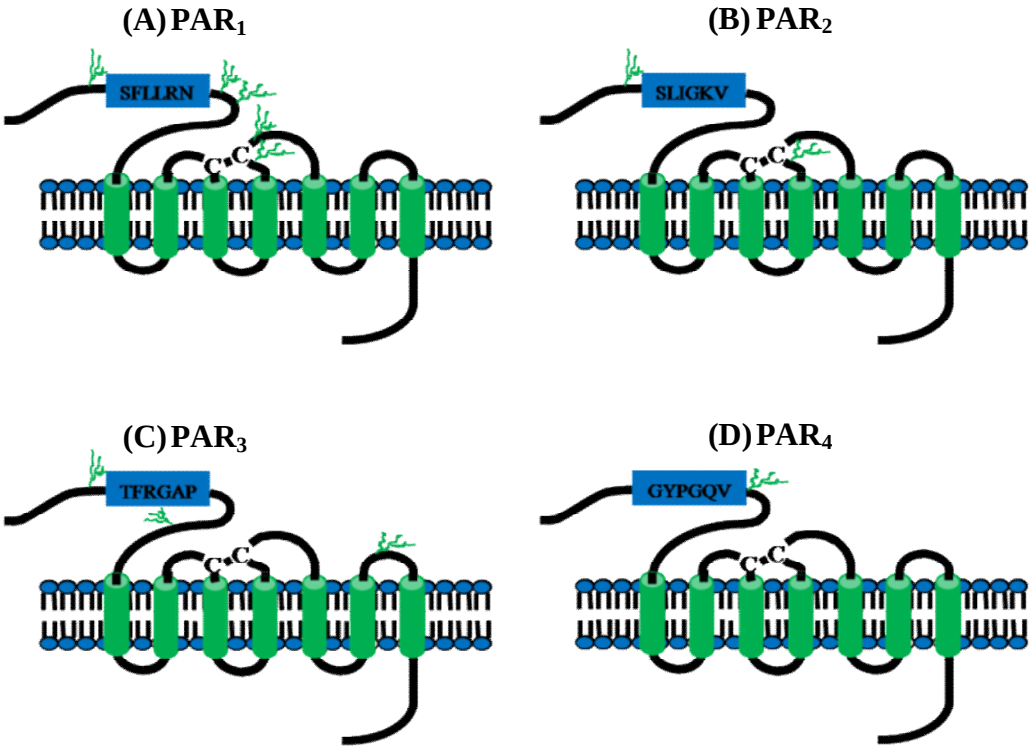

Figure 1.5 Representative models of the *N*-linked glycosylation in PARs. (A) PAR_1, (B) PAR_2, (C) PAR_3, and (D) PAR_4 indicating the approximate location of putative *N*-linked glycosylation sites for each PAR. [Adapted from (Compton, 2003)]

	PAR_1	**PAR_2**	**PAR_3**	**PAR_4**
N-terminus	$N^{35}A^{36}T^{37}$	$N^{30}R^{31}S^{32}$	$N^{25}D^{26}T^{27}$	$N^{56}D^{57}S^{58}$
	$N^{62}E^{63}S^{64}$		$N^{82}A^{83}T^{84}$	
	$N^{75}K^{76}S^{77}$			
ECL1	–	–	–	–
ECL2	$N^{250}I^{251}T^{252}$	$N^{222}I^{223}T^{224}$	–	–
	$N^{259}E^{260}T^{261}$			
ECL3	–	–	$N^{331}N^{332}T^{333}$	–

Table 1.1 Putative *N*-linked glycosylation sequons and their amino acid position in PARs. Single letter is used for amino acids. ECL, extracellular loop. [Adapted from (Compton, 2003)]

The importance of *N*-linked glycosylation for receptor expression and function has been studied for many GPCRs. Most of the GPCRs have relatively short extracellular amino-terminals with one or more putative glycosylation sequons, but the role of *N*-glycosylation is somewhat variable. Some studies using site-directed mutagenesis or treatment with tunicamycin have revealed that impaired glycosylation does (Rands *et al.*, 1990; Goke *et al.*, 1994; Kaushal *et al.*, 1994; Davidson *et al.*, 1995; Garcia Rodriguez *et al.*, 1995; Couvineau *et al.*, 1996; Ray *et al.*, 1998; Walsh *et al.*, 1998; Ho *et al.*, 1999; Jayadev *et al.*, 1999; Pang *et al.*, 1999; Nagayama *et al.*, 2000) or does not (van Koppen & Nathanson, 1990; Fukushima *et al.*, 1995; Unson *et al.*, 1995; Bisello *et al.*, 1996; Innamorati *et al.*, 1996; Kimura *et al.*, 1997) affect receptor expression and/or function.

Given that PARs are members of GPCRs and activated by a novel proteolytic mechanism, glycosylation may also play a critical role in PAR expression and function. Each PAR possesses a different number of putative *N*-linked glycosylation sites implying that there is potentially differential glycosylation across the PAR family (Compton, 2003). Interestingly, each of the four PAR family members has one putative *N*-linked glycosylation site in their N-terminus, which is close to the putative cleavage/activation site. Placing a negatively charged oligosaccharide chain in this region of the receptor may be critical for proteinase recognition and receptor signaling. Indeed, this has been shown to be true for PAR_2 (Compton *et al.*, 2002b). Previous pharmacological studies found that activation of $hPAR_2$ by mast cell tryptase can be regulated by receptor N-terminal glycosylation (Compton *et al.*, 2002b). Compton *et al.* showed that tryptase activation of PAR_2 could be unmasked in cells that were initially unresponsive cells by: 1) pretreating the cells with the sialidase, neuraminidase, 2) pretreating the cells with tunicamycin, and 3) expressing a mutant PAR_2 receptor ($hPAR_2N30A$) devoid of the N-terminal *N*-linked glycosylation site (Compton *et al.*,

2001; Compton *et al.*, 2002b). These results pointed to a role for *N*-linked glycosylation on the receptor N-terminus, but more specifically, sialylation, in regulating tryptase activation of PAR_2 (Compton *et al.*, 2002b).

However the role of *N*-linked glycosylation in regulating PAR_1 and PAR_4 cell surface expression and function has not yet been determined. One previous study reported that pharmacological inhibition of glycosylation caused a marked reduction in PAR_1 cell surface expression in human T-lymphoblastoid cells (Vouret-Craviari *et al.*, 1995). The specific glycosylation sites, which mediate this function, are unknown and the importance of these sites in regulating proteinase signalling and cell surface expression remain unknown. Therefore, a systematic study is required to explore the role of each glycosylation site in regulating $hPAR_1$ and $hPAR_4$ cell surface expression and receptor function.

1.5 HYPOTHESIS OF THIS PROJECT

The major hypothesis of this study is that ***"N-linked glycosylation and sialylation may regulate $hPAR_1$ and $hPAR_4$ cell surface expression and signalling."***

1.6 AIMS

In order to test this hypothesis the specific aims of this study were to determine:

1) The role of *N*-linked glycosylation and sialylation in regulating $hPAR_1$ cell surface expression and signalling.

2) Whether *N*-linked glycosylation regulates proteinase disarming of $hPAR_1$.

3) The role of *N*-linked glycosylation and sialylation in regulating $hPAR_4$ cell surface expression and signalling.

2. MATERIALS AND GENERAL METHODS

The methods described in this chapter are those which are common to all chapters. Techniques which were specific to an individual chapter are described in full in the methods section of that particular chapter.

2.1 MATERIALS AND REAGENTS

Dulbecco's modified Eagle's medium (DMEM), sodium pyruvate, antibiotic-antimycotic (penicillin G sodium, streptomycin sulfate, and amphotericin B), heat inactivated foetal calf serum (FCS), trypsin EDTA, enzyme-free cell dissociation buffer, geneticin (G418), Opti-MEM media and Lipofectamine 2000, dNTPs and Oligo$(dT)_{12\text{-}18}$ primer, Accuprime DNA polymerase were all purchased from Invitrogen (Life Technologies Inc. Paisley, UK). Primers were designed "in-house" and purchased from MWG-biotech (Ebersberg, Germany) and Sigma-Genosys (Pampisford, Cambridgeshire, UK). PCR purification kits, Gel extraction kits, RNeasy RNA isolation kits, Omniscript RT-PCR kits, and plasmid isolation kits were all bought from Qiagen (Crawley, West Sussex, UK). Taq DNA polymerase was obtained from New England Biolabs (Hitchin, Herfordshire, UK). XL1-Blue supercompetent cells and the QuikChange® site-directed mutagenesis kit were purchased from Stratagene® Europe (Amsterdam, NL). The rapid DNA ligation kit was bought from Roche (Lewes, East Sussex, UK). All restriction enzymes were purchased from New England Biolabs (Hitchin, Hertfordshire, UK). Fluo-3 acetoxymethyl ester was purchased from Cambridge Biolabs (Cambridge, UK). All PAR-APs were synthesized by the Peptide Synthesis Facility, University of Calgary, Alberta, Canada or purchased from Peptides International (Kentucky, USA). Enhanced yellow florescent protein (eYFP) was obtained from BD Biosciences (Alto, USA). The murine anti-HA.11 monoclonal antibody was obtained from Covance, UK. The

ProFound HA.11 immunoprecipitation Kit, Restore^{TM} Western Blot Stripping Buffer, M-Per mammalian protein extraction reagent were purchased from PIERCE (PIERCE, Cheshire, UK). The enhanced chemiluminescence (ECL) western blotting detection reagents and analysis system and anti-murine horseradish peroxidase conjugated secondary antibody were obtained from Amersham Biosciences, Buckinghamshire, UK. The polyvinylidene fluoride (PVDF) transfer membrane was bought from Amersham Pharmacia Biotech. AF1 regent was purchased from CITIFLUOR (CITIFLUOR, London, UK).

All other chemicals and reagents were purchased from Sigma-Aldrich (Poole, Dorset, UK) unless otherwise stated.

2.2 PCR

2.2.1 Polymerase Chain Reaction

Polymerase Chain Reaction (PCR) amplification and the detection of target genes were performed by using 1 µl of sample cDNA and the specific oligonucleotide primers. Water blanks were included in all assays to ensure that there was no genomic DNA contamination in the reagents. Each PCR was carried out in a total volume of 50 µl and consisted of 2 µg of sample cDNA, 5 µl of 10x PCR running buffer, 0.2 mM dNTPs, 1 U of Taq polymerase, 20 pmol forward primers and 20 pmol reverse primers, and DEPC water. The PCR reactions were cycled on a Primus96 thermocycler (MWG biotech) (Table 2.1). The PCR samples were analysed by electrophoretic separation on a 1.3% agarose gel at 160 V for 30 min and visualised by ethidium bromide under ultraviolet light.

Process	Temperature	Time	Number of Cycles
Initial denaturation	95°C	2 min	1 cycle
DNA denaturation	94°C	30 sec	25-35 cycles
Primer annealing to DNA	50°C-60°C	30 sec	
Template extension	72°C	60-90 sec	
Final extension	72 °C	10 min	1 cycle

Table 2.1 Cycle conditions for PCR reaction.

2.2.2 Site-directed mutagenesis

Site-directed mutagenesis to create the glycosylation-defective cDNA constructs was performed by using a QuikChange^{TM} site-directed mutagenesis kit (Stratagene) according to the manufacturer's instructions. Briefly, a pair of complementary primers with 25-45 bases long was designed for each mutagenesis, and the mutation to change asparagine to glutamine was placed in the middle of the primers. The primer also had a minimum GC content of 40% and started and finished with a G or a C. The reaction was amplified using *Pfu* DNA polymerase (2.5 U/ μl) and parental cDNA with these primers for 16 cycles in a DNA thermal cycler (Techne-Techgene FTGENE2D), and run as per the stragene Quick Change site-directed mutagenesis kit instructions (Table 2.2, 2.3). In order to remove the parental cDNA, 1 μl of *DpnI* restriction enzyme (10 U/μl) was applied to each sample. The samples were then incubated at 37^{o}C for 1 h before the bacterial transformation.

Reagent	Volume
10X reaction buffer	5.0 µl
dNTPs mix	1.0 µl
oligonucleotide primer # 1	1.0 µl (125 ng)
oligonucleotide primer # 2	1.0 µl (125 ng)
***Pfu Turbo* DNA polymerase**	1.0 µl (2.5 U)
cDNA template	1.0 µl (50 ng)
DEPC H_2O	40 µl

Table 2.2 The reagents used for site-directed mutagenesis PCR.

Segment	Cycles	Temperature	Time
1	1	95°C	30 sec
2	16	95°C	30 sec
		55°C	1 min
		68°C	2 min/kb of plasmid length

Table 2.3 The cycling parameters for site-directed mutagenesis PCR.

2.3 Ligation

After being generated by PCR amplification, the cDNA was then subcloned into the expressing vector by using the rapid ligation kit. The generation of the construct was confirmed by DNA sequencing analysis (MWG). Briefly, the ligation reaction contained 10 µl of 2 x ligation buffer, 1 µl of linearised vector (with the engineered restriction sites cleaved), 6 µl of cDNA (with the engineered restriction sites cleaved), 1 µl of DNA ligase and 2 µl of DEPC water to make a final volume of 20 µl. The reaction was incubated at RT for 5 min. For the negative control, an identical reaction was set up with the of DEPC water in place of the cDNA.

2.4 Bacterial transformation

The bacterial transformations were carried out as per standard transformation protocol provided by Promega. For each transformation, 50 μl of competent *E.coli* cells (XL1-Blue) were prepared by being thawed on ice (4ºC), and then added with 1.7 μl of 10% β-Mercaptoethanol (β-ME). Cells were then gently agitated by tapping the tube every two minutes for a total of 10 min. 7 μl of sample vector DNA was then added to the β-ME treated *E.coli*, swirled and incubated on ice for 30 min. An extra transformation using 30 ng of pcDNA3.1 (-) was carried out as a control. The cells were then heat shocked at 42^{o}C for 45 seconds before placing back onto ice for a further two minutes. 500 μl of LB broth (pre-heated to 42^{o}C) was then added to the cells before incubation at 37^{o}C, with shaking at 200 rpm for 60 min. Transformants were then selected via plating 250 μl of transformation reaction mixture onto LB agar plates containing ampicillin (100 μg/ml) and incubated at 37^{o}C overnight along with the transformation control.

Single colonies from the transformed *E.coli* master plate were randomly picked and incubated with 5 ml of LB broth media containing ampicillin (100 μg/ml) in a shaking incubator at 37°C overnight to allow the colonies to grow. The transformed *E.coli* master plates were stored at 4°C.

2.5 Isolation of plasmid from transformed colonies

Plasmid DNA was extracted from the expanded colonies using a QIAgen Miniprep Kit as per the manufacturer's instructions. In order to check if individual purified plasmids contained the insert sequence, a restriction digest reaction was performed. The restriction digest reaction was carried out by incubating 5 μl of the plasmid DNA, 2 μl of 10× buffer (NEB), 2 μl of BSA (100 μg/ml), 10 μl of DEPC water, 0.5 μl of restriction enzyme A and 0.5 μl of restriction enzyme B at a temperature appropriate for the restriction enzymes used. Following the restriction digest each sample was run on a 1.3% agarose gel in order to identify colonies that possessed the insert. The DNA concentration and purity were then assessed using a Genequant spectrophotometer and an aliquot of sample was sent to MWG Biotech for insert sequencing using a T7 primer.

2.6 Preparation of expressing cell lines

2.6.1 Cell culture

Kirsten virus sarcoma transformed rat kidney epithelial cells (KNRK, American Tissue Type Culture Collection, Bethesda, MD, U.S.A.) were cultured routinely in DMEM complete growth medium (containing DMEM with 10% (v/v) FCS, 2 mM L-glutamine and 1% penicillin/streptomycin, 100 μM sodium pyruvate). The CHO fibroblast cell lines, Pro5 and Lec2 (American Tissue Type Culture Collection, Bethesda, MD, U.S.A) were grown in α-MEM complete growth medium (containing α-MEM with 10% (v/v) FCS, 2 mM L-glutamine and 1% penicillin/streptomycin, 100 μM sodium pyruvate). All cell lines were incubated at 37°C in a humidified atmosphere containing 5% CO_2 and 95% air. The cultures were supplemented approximately every 48 h with fresh growth medium.

2.6.2 Cell harvesting

To detach the cells from the flask, all media was aspirated from the flask and the cells were washed in 5 ml PBS. 5 ml cell dissociation buffer (non-enzymatic) was applied to the flask and incubated at 37°C for 3 min until the cells were detached. A light microscope was used to inspect for complete cell detachment. Fresh medium (5 ml) was added as soon as the cells had detached. The cell suspension was collected and centrifuged for approximately 5 min at 3000 g in a sterilized tube. The supernatant was discarded before the cell pellet was resuspended in 5 ml of fresh complete medium.

2.6.3 Transfection

Heterologous expression of receptor was carried out by using the LipofectAMINE® method, according to the manufacturer's protocol (Invitrogen).

Firstly, cells in 65 mm Petri dishes were grown to 50-70% confluence. Then 4 ml of Opti-Mem medium was applied to the cells after the normal growth medium had been removed. Secondly, two Falcon 5 ml polystyrene round bottom tubes (labelled ‘1’ and ‘2’) were prepared, and 1ml of Opti-Mem medium was added into each tube. 5 µg receptor expression vector was added into tube 1, and 20 µl lipofectAMINE was added into tube 2. After incubation in RT for 15 min, the contents of tube 2 were poured directly into the tube 1. The mixture was then vortexed for 4 sec and incubated for 15 min in RT. Finally, the mixture was applied to the cells after the 4 ml Opti-Mem medium had been discarded. Following 24 h incubation, the mixture medium was removed and 5 ml fresh complete growth medium was added. The cells were then incubated for a further 24 h before being grown in selection medium (G418 0.6 mg/ml, containing fresh complete growth medium) for 2 weeks.

2.6.4 Single cell cloning

In order to obtain a cell line with optimum receptor expression, a single cell cloning procedure was carried out. Briefly, the transfected cells were counted using a haemocytometer and then diluted into 5 cells per ml in the selection medium, and then 200 μl of this diluted suspension was plated into each well of a 96 well plate. Once colonies of cells became visible in the wells (normally after 2 weeks), only the cells that contained one visible colony were selected and transferred to 25 cm^2 flasks containing 5 ml of selection medium. These cells were left growing to reach confluence before intracellular calcium signalling (See Method: 2.7) measurements and FACS (See Method: 2.8) were performed in order to identify cells expressing functional receptor. Once a clone had been identified, this clone was taken through a second and third round of single cell cloning to ensure that the final set of clones were derived from a single cell.

2.6.5 Storage of frozen cell lines

The clone showing the highest level of receptor cell surface expression above control was selected as the expressing clone for all future analysis and passaged up into larger flasks before being frozen down in FCS with 10% DMSO in liquid nitrogen creating cell stocks.

2.7 Intracellular calcium mobilisation assay

Calcium signalling was performed using methods based on those by Compton *et al* (Compton *et al.*, 2000a). Cells at desired confluence were washed and harvested with PBS (without calcium or magnesium). Cells were pelleted and resuspended in 1 ml of normal culture medium containing 0.25 mM sulphinpyrazone and 25 μg of Fluo-3 AM

in DMF (N,N-Dimethylformamide). The cells were then incubated at room temperature for 25 min whilst gently shaking, to allow the fluorescent probe to be taken up by the cells. The cells were then washed by centrifugation to remove excess Fluo-3 AM and resuspended in calcium assay buffer (CAB) (20 mM HEPES, 150 mM NaCl, 3 mM KCl, 10 mM Glucose, 250 μM Sulphinpyrazone, 280 mM calcium chloride, pH 7.4). The cell suspension was then aliquoted in 100 μl amounts into Ca^{2+} assay cuvettes prepared containing a magnetic flea and 940 μl of CAB. Increases in intracellular calcium levels were measured at room temperature using a fluorospectrometer (Photon Technology International). The fluorospectrometer was set to emit an excitation wavelength of 480 nm and record light emitted with a wavelength of 530 nm. Each cuvette contained 2 ml of suspended cells in CAB and a small magnetic flea to keep the cells suspended and mix any reagents added. Concentration-effect curves were constructed for each test agonist by adding increasing concentrations of the agonist to separate cell-containing cuvettes in half log increments. The increase in fluorescence measured at 530 nm was expressed as a percentage of the maximum fluorescence signal after the addition of 2 μM calcium ionophore (A23187).

2.8 Flow cytometry analysis

Harvested cells from T25 flasks were resuspended in 300 μl of ice-cold PBS (1×). Primary antibody (e.g. ATAP-2 antibody [1 in 1000=1 μg/ml] for PAR_1) was then added, and the samples incubated on ice for 60 min with gentle swirling at 15 min intervals. 1 ml of ice-cold PBS (1x) was then added to each sample before centrifugation at 3000 g for 5 min at 4^{o}C. The supernatant was then disposed of, and cell pellets were resuspended in 300 μl of ice-cold PBS (1x). Secondary antibody (e.g. fluorescein isothiocyanate (FITC) labelled goat anti-mouse IgG [1 in 100=0.1 μg/ml])

was applied to each sample and then incubated on ice for 45 min, swirling at 15 min intervals. Following a final wash in ice cold PBS, cells were resuspended in 300 µl of PBS and analysed on a Beckton Dickinson flow cytometer. Untransfected KNRK parent cells and pcDNA3.1 expressing KNRK cells (EV) were employed as a control.

2.9 Confocal microscopy analysis

Cells were plated onto a 65 mm diameter Petri dish containing coverslips and grown in geneticin selection medium to reach the desired confluence. The cells were rinsed twice with PBS, fixed for 15 min at RT with freshly prepared 3% formaldehyde in PBS, and washed twice with PBS again. The cells were then permeabilized with PBS containing 0.2% triton X-100 for 10 min at RT, and washed again. For the staining of nuclear DNA, Propidium Iodide Solution (1:3000) was applied to the cells for 1 min. Finally, the coverslips were washed with PBS and mounted in a drop of anti-fade AF1 reagent and fixed to slides. The cells were visualised by a Nikon Eclipse (TE2000-E) microscope with a BioRad Radiance 2100 scanning system and lasers.

2.10 Whole cell extracts and immunoprecipitation

Cells were seeded into 25 cm^2 culture flasks and allowed to reach over 90% confluence. Cells were then harvested, pelleted by centrifugation at 2,500 x *g* for 5 min and lysed by adding 500 µl M-PER Reagent before shaking the mixture gently at RT for 10 min. Cell debris was removed by centrifugation at 13200 *g* for 20 min at 4 °C.

HA11 tagged PARs were immunoprecipitated using a ProFound HA11 immunoprecipitation kit as per the manufacturer's protocol.

2.11 Western blot analysis

Proteins were separated in 10% SDS polyacrylamide gels (Table 2.4), and the gel was run in a vertical gel electrophoresis unit in electrode buffer consisting of 29 mM tris base, 192 mM glycine and 0.1% (w/v) SDS. Enough electrode buffer was poured into the central buffer well so that the buffer was levelled with the top of the gels, and the remaining buffer was poured into the outer buffer dam ensuring that the bottom of the gels were submerged in buffer. Precision Plus Protein^{TM} Dual color standards (BIO-RAD) were used as size markers on the gels. Electrophoresis was carried out at 40 mA for approximately 3 h at RT, or until the blue dye had run to the bottom of the gel.

Stacking Gel	10% SDS polyacrylamide gel
5.5% Acrylamide	10% Acrylamide
12.6% Stacking gel buffer 0.5 M tris HCl pH 6.8	25% Resolving gel buffer 1.5 M tris HCl pH 8.8
0.1% SDS	0.1% SDS
0.06% Amonia persulphate	0.05% Amonia persulphate
0.14% TEMED	0.05% TEMED
Deionised water	Deionised water

Table 2.4 Chemicals used for preparation of the SDS polyacrylamide gel.

The proteins on the gel were electrotransferred to a polyvinylidene fluoride (PVDF) transfer membrane (Amersham Pharmacia Biotech) by using an electro transfer module in a Scie-Plus modular electrophoresis system. Briefly, the gel was placed on the top of a membrane, sandwiched in a cassette. Cassettes were placed in a BioRad Transblot cell containing western transfer buffer (29 mM Tris, 192 mM glycine, 20% methanol). Transfer of the proteins to the hybridization membrane was carried out at 40 mA for one and half hours at RT. Membranes were then incubated with 4% non-fat powdered milk in PBS containing 0.1% Tween-20 for 1 h at RT to block the non-specific binding. Membranes were washed briefly in PBS/0.1% Tween-20, and then incubated with the

primary antibody (in PBS/0.1% Tween-20 containing 2% non-fat milk) at 4°C overnight. Following 4 washes with PBS/0.1% Tween-20 for 15 min, membranes were incubated with peroxidase-conjugated anti-mouse secondary antibody (1:4000) diluted in 2% non-fat powdered milk (in PBS/0.1% Tween-20) for 1 h at RT. Membranes were then washed for 1 h with 4 changes of wash buffer (PBS/0.1%Tween-20).

Developing was achieved by using an enhanced chemiluminescence solution (ECL western blotting detection reagents and analysis system, Amersham Biosciences) according to manufacturer's instructions. Briefly, ECL reagents A and B mixture were applied to the protein binding surface and incubated at RT for 1 min. Excess reagent was then removed and the membrane photographed using a UVP Laboratory Products Epichem II Darkroom setup to measure chemiluminescence. Bands were visualized using Lab Works Image Acquisition & Analysis software. Pictures were taken every 5 min for 20 min, and the picture depicting bands most clearly was chosen.

2.12 Calculations and statistical analysis

Calculations were carried out using Microsoft Excel, and graphs were produced using Prism Graphpad Version 4. Statistical tests were carried out depending on the specifics of the datasets to be compared. When a comparison of two cell lines subjected to the same treatment were compared, and a paired student's t test was adopted. When comparison of a group of cell lines subjected to the same treatment was performed the one-way ANOVA (Tukey's Multiple Comparison Test) was applied where significant differences were indicated. In order to assess the changes over a period of time using a specific treatment or to assess a change over a concentration range between two different cell lines two-way ANOVA tables were adopted.

3.1 Introduction

$hPAR_1$ contains a total of five predicted sites for *N*-linked glycosylation, three sequons are located on the receptor N-terminus ($N^{35}A^{36}T^{37}$, $N^{62}E^{63}S^{64}$, and $N^{75}K^{76}S^{77}$) and two are located within extracellular loop 2 (ECL2; $N^{250}I^{251}T^{254}$, and $N^{259}E^{260}T^{261}$) (Figure 3.1.1) (Compton, 2003). Two previous studies have shown by western blot analysis that the MW of $hPAR_1$, expressed in HEK293 or COS cells, ranges from approximately 34–100 kDa (Vouret-Craviari *et al.*, 1995; Kuliopulos *et al.*, 1999). Furthermore, deglycosylation of $hPAR_1$ with N-glycosidase F (PNGaseF) decreased the molecular mass of $hPAR_1$ to approximately 36–43 kDa, which is similar to the predicted MW of $hPAR_1$ calculated on the basis of the amino acid sequence alone (Vouret-Craviari *et al.*, 1995). These findings are in agreement with Kuliopulos *et al*. who observed that $hPAR_1$ expressed in yeast (glycosylation of proteins does not occur in yeast) migrates as a protein with a molecular mass comparable to that of N-glycosidase-F-treated PAR_1 expressed in mammalian cells (Kuliopulos *et al.*, 1999). These results indicate that the additional mass of the mature receptor may be due to glycosylation and that most, if not all, of the glycosylation is *N*-linked.

Interestingly, there appears to be cell-type specific *N*-linked glycosylation of PAR_1, as PAR_1 expressed in platelets migrates as a homogenous species with an apparent MW of 75 kDa, in contrast with PAR_1 expressed in HEL and COS cells, where the receptor is heterogeneously glycosylated, resulting in receptor species ranging in apparent MW from 34–100 kDa (Kuliopulos *et al.*, 1999). In addition Bolton *et al*. also reported that $hPAR_1$ expressed in human eosinophils migrates at approximately 80kDa (Bolton *et al.*, 2003). In contrast, Brass and colleagues found that PAR_1 expressed in platelets, HEL

cells, CHRF-288 cells, and HUVECS migrated as a single species with an apparent MW of 66 kDa (Brass *et al.*, 1992).

Importantly, a preliminary report has demonstrated that tunicamycin dramatically reduces the cell surface expression of $hPAR_1$ in T lymphoblastoid cells (Tordai *et al.*, 1995). Thus, glycosylation may play an important role in the cell surface expression of PAR_1, although this has not been proved directly. In addition, one of the early functional studies demonstrated that thrombin activation and plasmin inactivation of $hPAR_1$ are little affected by receptor glycosylation (Kuliopulos *et al.*, 1999). Nevertheless, a detailed molecular study investigating the role of glycosylation in regulating receptor expression and signalling has yet to be performed. Therefore, this chapter explores the role of glycosylation and sialylation in regulating $hPAR_1$ cell surface expression and receptor signalling.

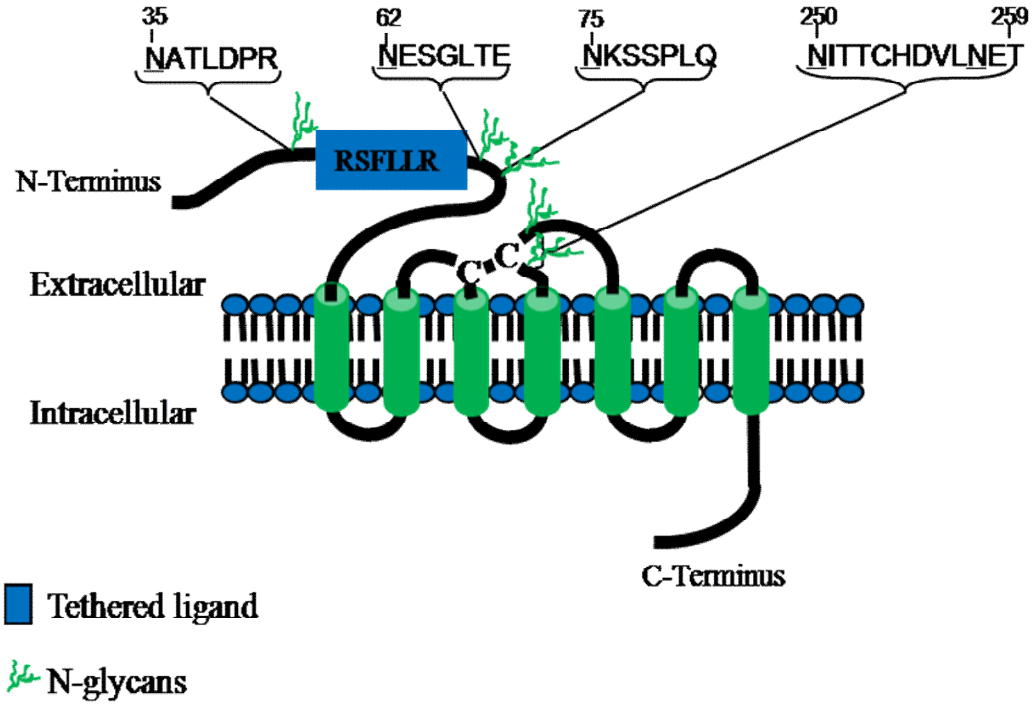

Figure 3.1.1 Representative model of hPAR$_1$ displaying the potential *N*-linked glycosylation sequons. hPAR$_1$ contains five potential *N*-linked glycosylation sequons. Three sequons are located on the receptor N-terminus ($N^{35}A^{36}T^{37}$, $N^{62}E^{63}S^{64}$, $N^{75}K^{76}S^{77}$) and two are located within extracellular loop 2 (ECL2; $N^{250}I^{251}T^{254}$, $N^{259}E^{260}T^{261}$). Of the sequons at the N-terminus, one ($N^{35}A^{36}T^{37}$) is located N-terminal of the cleavage/activation site (R^{41}/S^{42}FLLR) and the remaining two ($N^{62}E^{63}S^{64}$, $N^{75}K^{76}S^{77}$) are located downstream of the cleavage/activation site. The disulphide bridge is shown by the two cysteines (C-C). Amino acid numbering is for hPAR$_1$. [Adapted from (Compton, 2003)]

3.2 Materials and Methods

3.2.1 Materials

Wt-hPAR$_1$ (POMC-M1-hPAR$_1$-HA.11 in pcDNA3.1) and the hPAR$_1$-eYFP cDNA (**Appendix D**) were supplied by Dr. S. J. Compton. Anti-PAR$_1$ ATAP-2 monoclonal antibody was purchased from Zymed Laboratories Inc. (San Francisco, USA). M2 antibody was bought from Sigma-Aldrich (Poole, Dorset, UK)

3.2.2 Generation of Glycosylation-deficient hPAR$_1$/hPAR$_1$eYFP Constructs and Permanently Expressing Cell Lines

Initially the hPAR$_1$-eYFP cDNA was digested and ligated into pcDNA3.1. Briefly, the restriction digest reaction was carried out by incubating 15 µl of hPAR$_1$-eYFP cDNA, 2 µl of 10×buffer (2), 2 µl of BSA (100 µg/ml), 0.5 µl of *Xho*I (2000 U/µl) and 0.5 µl of *Bam*HI (2000 U/µl) at 37°C overnight. After gel purification, the *Xho*I-hPAR$_1$-HA.11-eYFP-*Bam*HI cDNA was ligated between the *Xho*I and the *Bam*HI site of the pcDNA3.1 vector to generate the wt-hPAR$_1$E (POMC-M1-hPAR$_1$-HA.11-eYFP in pcDNA3.1). *E.Coli* are transformed by the delivery of the ligation DNA sample, subsequently amplified, screened and purified as described in chapter 2 sections 2.4 and 2.5.

The oligonucleotides listed in Table 3.2.1 were designed to replace the asparagine (N) residues at positions Asn^{35}, Asn^{62}, Asn^{75}, Asn^{250}, and Asn^{259} with glutamine (Q) residues. All site-directed mutants listed in Table 3.2.3 were generated using the QuickChange® site-directed mutagenesis kit which was carried out as described in chapter 2 section 2.2.2. Single-site mutants were first constructed (Table 3.2.3). In order to elucidate the cumulative effects of a lack of glycosylation at multiple sites, four

receptors with multiple glycosylation mutations (N62QN75Q, N35QN62QN75Q, N250QN259Q, and N35-259Q) were constructed. The N62QN75Q mutant cDNA was generated using two rounds of site-directed mutagenesis PCR: the first with N75Q mutagenic primers, the second with N62Q mutagenic primers. N250QN259Q cDNA contruct was also generated by two rounds of site-directed mutagenesis PCR: the first with N250Q mutagenic primers and the second with N259Q mutagenic primers. N35QN62QN75Q cDNA construct was generated by employing a third round of site-directed mutagenesis PCR on the N62QN75Q cDNA construct using the N35Q mutagenic primers. N35-259Q cDNA construct was generated on N35QN62QN75Q cDNA by employing another two rounds of site-directed mutagenesis PCR: the first with N250Q mutagenic primers, the second with N259Q mutagenic primers. The same principle was also applied to all the $hPAR_1$eYFP ($hPAR_1$E) glycosylation-deficient mutants listed in Table 3.2.3 except for the $hPAR_1$N35-259QeYFP (N35-259QE) mutant.

N35-259Q$hPAR_1$-HA.11-eYFP cDNA was constructed by attaching eYFP to the end of N35-259Q$hPAR_1$-HA.11 using overlapping PCR as described in chapter 2 section 2.2.1. The primers used in the PCR reactions are listed in Table 3.2.2. Briefly, the N35-259Q$hPAR_1$-HA.11 segment was generated from N35-259Q$hPAR_1$-HA.11 in pcDNA3.1 using the T7 forward primer and the HA.11 reverse primer by PCR, which amplified through 17 cycles of denaturation at 95°C for 15 sec, annealing at 50°C for 30 sec, and extension for 1 min and 30 sec at 68°C. HA.11-eYFP was amplified from pEYFP vector (Clontech) using a HA.11-eYFP forward primer and a *Bam*HI-eYFP reverse primer. Finally, HA.11-eYFP was fused to the end of $hPAR_1$N35-259Q-HA.11 to generate N35-259Q$hPAR_1$-HA.11-eYFP cDNA using T7 forward primer and *Bam*HI-eYFP reverse primer by overlapping PCR. The conditions for the overlapping

PCR were as follows: 15 sec at 95°C, 30 sec at 50°C, and 2 min 30 sec at 68°C for 17 cycles. A restriction digest reaction was performed to N35-259QhPAR_1-HA.11-eYFP cDNA in order to ligate it into pcDNA3.1. Briefly, the restriction digest reaction was carried out by incubating 15 μl of N35-259QhPAR_1-HA.11-eYFP PCR sample, 2 μl of 10×buffer (2), 2 μl of BSA (100 μg/ml), 0.5 μl of *Xho*I (2000 U/μl) and 0.5 μl of *Bam*HI (2000 U/μl) at 37°C overnight. After gel purification, the digested construct was ligated between the *Xho*I and the *Bam*HI site of the pcDNA3.1 vector. The N35-259QhPAR_1-HA.11-eYFP in pcDNA3.1 was subsequently amplified and purified as described in chapter 2 sections 2.4, 2.5, and then sequenced by MWG to confirm the engineered mutations.

All the permanently expressing wild-type and mutant PAR_1/PAR_1eYFP receptor cell lines were generated and cultured as described in chapter 2 section 2.6. The clones showing the highest level of expression were selected by 1) calcium signalling assay using PAR_1-AP TFLLR-NH_2 (100 μM) as agonist and 2) FACS analysis using anti-PAR_1 ATAP-2 monoclonal antibody. KNRK cells at 90%-100% confluence and CHO cells at 40% confluence were used for all of the following experiments.

Primer	Sequences	
N35Q	5’ GGG ATC TAA GGT GGC TTG TGT TGC TTT TGA TTC	3’
	5’ GAA TCA AAA GCA ACA CAA GCC ACC TTA GAT CCC	3’
N62Q	5’ GT TAA CCC ACT TTC TTG TTT CTC CTC ATC C	3’
	5’ G GAT GAG GAG AAA CAA GAA AGT GGG TTA AC	3’
N75Q	5’ G AGG ACT GCT TTT TTG GAT GGA GAC TAA ATC	3’
	5’ GA TTA GTC TCC ATC CAA AAA AGC AGT CCT C	3’
N250Q	5’ CA GGT AGT GAT TTG GAG CCC GGG CAC	3’
	5’ GTG CCC GGG CTC CAA ATC ACT ACC TG	3’
N259Q	5’ GAG CAG GGT TTC TTG GAG CAC ATC ATG	3’
	5’ CAT GAT GTG CTC CAA GAA ACC CTG CTC	3’

Table 3.2.1 The oligonucleotides used in the site-directed mutagenesis for the generation of the $hPAR_1$ glycosylation-deficient mutants.

Primer	Sequences
T7 forward	5’ TAA TAC GAC TCA CTA TAG GG 3’
HA.11 Reverse	5’ GGC ATA ATC GGG AAC ATC ATA GGG 3’
HA.11-eYFP forward	5’ CCC TAT GAT GTT CCC GAT TAT GCC ATG GTG AGC AAG GGC 3’
BamHI-eYFP reverse	5’ GGG CCC GGA TCC TTA CTT GTA CAG CTC GTC CAT 3’

Table 3.2.2 Primers used in PCR for generation of $hPAR_1$(N35-259Q)eYFP cDNA.
$hPAR_1$(N35-259Q)eYFP: XhoI-POMC-M1-$hPAR_1$N35QN62QN75QN250QN259Q-HA.11-eYFP-*Bam*HI.

$hPAR_1$ mutant KNRK cell line	**Consensus sequence(s) disrupted**
$hPAR_1$(N35Q)	Asn-35
$hPAR_1$(N62Q)	Asn-62
$hPAR_1$(N75Q)	Asn-75
$hPAR_1$(N250Q)	Asn-250
$hPAR_1$(N259Q)	Asn-259
$hPAR_1$(N62QN75Q)	Asn-62 and Asn-75
$hPAR_1$(N35QN62QN75Q)	Asn-35, Asn-62 and Asn-75
$hPAR_1$(N250QN259Q)	Asn-250 and Asn-259
$hPAR_1$(N35-259Q)	Asn-35, Asn-62, Asn-75, Asn-250 and Asn-259
$hPAR_1$(N62Q)eYFP	Asn-62
$hPAR_1$(N62QN75Q)eYFP	Asn-62 and Asn-75
$hPAR_1$(N35QN62QN75Q)eYFP	Asn-35, Asn-62 and Asn-75
$hPAR_1$(N250QN259Q)eYFP	Asn-250 and Asn-259
$hPAR_1$(N35-259Q)eYFP	Asn-35, Asn-62, Asn-75, Asn-250 and Asn-259

Table 3.2.3 Table showing the PAR_1/PAR_1eYFP glycosylation-deficient mutant KNRK cells generated for this study. The mutants were named with an N followed by a number relating to the relative position of the potential glycosylation site and a Q.

3.2.3 Flow Cytometry Analysis

Flow cytometry analysis (FACS) was performed as described in chapter 2 section 2.8 in order to compare the differences in cell surface expression between wild type and glycosylation-deficient mutant hPAR$_1$ cell lines. The anti-PAR$_1$ ATAP-2 monoclonal antibody [1 µg/ml] was used as the primary antibody. FITC labelled goat anti-mouse IgG [0.1 µg/ml] was applied as the secondary antibody. The data was expressed as the median fluorescence of positive minus the median fluorescence of the EV (pcDNA3.1 transfected KNRK) cells.

To ensure any functional differences in responses detected between wt-hPAR$_1$ and glycosylation-deficient mutant hPAR$_1$ cell lines were due to the glycosylation mutation, FACS analysis for matching cell surface expression between glycosylation-deficient mutant hPAR$_1$ and wt-hPAR$_1$ in different time point (day 1, day2, day 3, day 4, day 5, day6) was performed. The following protocol was carried out using KNRK cells stably expressing wt-hPAR$_1$ and hPAR$_1$ glycosylation-deficient mutant receptors. Control EV cells at ~90% confluence in a T75 were also used to establish baseline. Briefly, each cell line was grown in a T75 flask until ~100% confluent. The wt-hPAR$_1$ cells were split equally into 5 T75 flasks, and hPAR$_1$ glycosylation-deficient mutant cells were split equally into 3 T75 flasks. FACS analysis was subsequently carried out as described above.

3.2.4 Confocal Microscopy Analysis

For the wt-hPAR$_1$eYFP and mutant cell lines, the light emitted by the eYFP (530 nm) fused to the receptor was used to assess receptor expression. Confocal microscopy analysis was performed as described in chapter 2 section 2.9.

3.2.5 Western Blot Analysis

3.2.5.1 Crude Membrane Preparation

Cells were seeded into 175 cm^2 flasks and grown until over 90% confluent. The cells were washed with ice-cold PBS and then incubated for 30 sec in ice-cold deionised water before 8 ml of ice-cold membrane buffer (tris base 5 mM, EDTA 0.5 mM, leupeptin 1 µg/ml, soybean trypsin inhibitor (STI) 1 µg/ml and orthovanadate 1 mM, pH 7.5) was applied to the cells. The swollen cells were harvested using a cell scraper and transferred to a 15 ml pre-chilled centrifuge tube before incubation on ice for 30 min with vortexing every 10 min. The cell suspension was then centrifuged at 500 g for 10 min at 4°C. The supernatant was transferred to 1.5 ml centrifuged tubes and the pellet containing the nuclear fraction was discarded. The supernatant was centrifuged at 13,200 g for 45 min at 4°C. The supernatant was discarded and the pellet was resuspended in 100 µl of membrane buffer. Crude membrane preparations were stored at -80°C until required.

3.2.5.2 Generation of Whole Cell Lysates with Laemmli's Sample Buffer

Cells were seeded into 25 cm^2 culture flasks and allowed to reach over 90% confluence. Cells were then harvested, pelleted by centrifugation at 2,500 g for 5 min and lysed by adding 500 µl Laemmli's sample buffer [2% SDS, 10% glycerol, 50mM Tris-HCl (pH 6.8), 5 mM EDTA, 0.008% bromophenol blue, 0.5% β-Mercaptotheanol]. The cell lysates were then transferred into 1.5 ml Eppendorf tubes and centrifuged at 13,200 g for 10 min at 4°C. The supernatants were then recovered and samples were boiled for 5 min before being resolved on a 10% SDS gel.

3.2.5.3 Immunoprecipitation

Immunoprecipitation of wt-hPAR$_1$ and wt-hPAR$_1$eYFP from KNRK, Pro5 and Lec2 cells and glycosylation-deficient mutants of hPAR$_1$ from KNRK cells via the HA.11 epitope tag was carried out as described in chapter 2 section 2.10.

3.2.5.4 Western Blot Analysis

Protein samples were separated on a 10% SDS/PAGE gel before transferring to Hybond C PVDF membrane. The membrane was incubated primarily with the murine anti-HA.11 monoclonal antibody [1 μg/ml] in PBS (0.1% Tween-20), 2% non-fat milk at 4^{o}C overnight. The membrane was then incubated with goat anti-mouse HRP [0.25 μg/ml] in PBS (0.1% Tween-20), 2% non-fat milk for 60 min at RT before analysis by using the ECL detection system. Blots were then stripped at RT for 20 min in Western Blot Stripping Buffer (PIERCE), and then incubated with the anti-eYFP antibody [0.5 μg/ml] in PBS (0.1% Tween-20), 2% non-fat milk at 4^{o}C overnight. Preliminary experiments confirmed that the stripping agent had removed the majority of the primary and secondary antibody (data not shown). After incubating with goat anti-mouse HRP [0.25 μg/ml] in PBS (0.1% Tween-20), 2% non-fat milk for 60 min at RT, and the receptor was visualized by using the ECL detection system as described in chapter 2 section 2.11.

3.2.5.5 Optimisation

A secondary antibody titration was performed in order to maximise protein visualisation and eliminate non-specific antibody binding. In addition, primary antibodies *(i)* anti-HA.11 monoclonal antibody (1:500, 1:1000, 1:2000, and 1:4000), *(ii)* eYFP antibody

(1:2000), *(iii)* ATAP-2 antibody (1:1000), and *(iiii)* M2 antibody (1:1000) were applied in order to produce the best visualisation.

3.2.6 Calcium Signalling Assay

Calcium signalling studies were performed based on the methods described in chapter 2 section 2.7. Briefly, cells were loaded with the calcium binding probe Fluo-3 and increases in intracellular calcium were detected using a fluorospectrometer with an excitation wavelength of 480 nm and a detector set to measure at a wavelength of 530 nm. Concentration-effect curves were constructed for TFLLR-NH_2, thrombin and trypsin by adding increasing concentrations of the agonist to separate cell containing cuvettes in half log increments.

Example pattern:

1	Ca^{2+} ionophore (A23187)	2 μM
2	Agonist	300 xM
3	Agonist	100 xM
4	Agonist	30 xM
5	Agonist	10 xM
6	Agonist	3 xM
7	Agonist	1 xM
8	Ca^{2+} ionophore (A23187)	2 μM
9	Agonist	1 xM
10	Agonist	3 xM
11	Agonist	10 xM
12	Agonist	30 xM
13	Agonist	100 xM

14	Agonist	300 xM
15	Ca^{2+} ionophore (A23187)	2 μM

"x" is either nanomolar, micromolar or millimolar.

Responses were calculated for each cuvette by subtracting the baseline fluorescence for the cuvette (prior to agonist addition) from the cuvettes peak fluorescence (post addition of agonist). The average for each agonist concentration was then expressed as a percentage of the A23187 mean response (maximum obtainable response) and plotted versus agonist concentration, using Prism Graphpad 4, to give the agonist concentration effect curve.

3.3 Results

3.3.1 *N*-linked Glycosylation Regulates hPAR$_1$ Cell Surface Expression

Cell surface expression of the wt and mutant receptor cell lines were analysed by flow cytometry analysis and confocal microscopy. FACS analysis demonstrated that removing any of the glycosylation sequons resulted in a significant decrease ($p<0.001$) in receptor cell surface expression (Figure 3.3.1). The N35Q mutant displayed the greatest cell surface expression [percentage relative to wt-hPAR$_1$ ± SEM: 55 ± 4 % (n=3)] compared to the other mutant cell lines. The single mutation cell line N250Q displayed the lowest expression [percentage relative to wt-hPAR$_1$ ± SEM: 10.5 ± 0.7 % (n=3) respectively] when compared to the other single mutants N35Q, N62Q, N75Q and N259Q [percentage relative to wt-hPAR$_1$ ± SEM: 55 ± 4 %; 26 ± 3 %; 13 ± 1.5 % and 26 ± 3 % (n=3) respectively]. Mutating both glycosylation sequons on ECL2 (N250QN259Q) resulted in near total loss of cell surface expression [percentage relative to wt-hPAR$_1$ ± S.E.M: 6±1 % (n=3)]. In contrast removing all glycosylation sequons on the N-terminus (N35QN62QN75Q) still resulted in nearly 50% cell surface expression compared to wt-hPAR$_1$ expression [percentage relative to wt-hPAR$_1$ ± SEM: 44.7 ± 1 % (n=3)]. Removing all glycosylation sequons (N35Q-259Q) resulted in a receptor that was expressed at a similar level to the N250QN259Q mutant [percentage relative to wt-hPAR$_1$ ± SEM: 6 ± 1 % (n=3)].

Confocal microscopy was performed to determine whether the loss of cell surface expression of mutant receptors resulted in the increased retention of receptor within the cytosol (Figure 3.3.2). Analysis of eYFP tagged hPAR$_1$ localisation in permeabilized cells by confocal microscopy demonstrated that all hPAR$_1$E types (wt-hPAR$_1$eYFP and glycosylation-deficient mutant hPAR$_1$eYFP) with the exception of N35-259QhPAR$_1$E were expressed on the cell surface, however, different levels of membrane localisation

and cytosolic retention were observed (Figure 3.3.2). There was no detectable fluorescence (eYFP signalling) observed in EV cells (pcDNA3.1-KNRK) (Figure 3.3.2 (A)). Wt-hPAR_1E displayed strong cell membrane expression with little receptor observed in the cytoplasm (Figure 3.3.2 (B)). Removal of sequon Asn^{35} in the receptor N-terminus resulted in the appearance of receptor within the cytosol (Figure 3.3.2 (C)). Removal of both sequons after the tethered ligand of PAR_1 resulted in a large amount of receptor being found in the cytosol (Figure 3.3.2 (D)). The relative intensity of the membrane localisation appeared to be reduced significantly in the N250QN259QhPAR_1E and N35-259QhPAR_1E mutants when compared with wt-hPAR_1E (Compare Figure (E) & (F) with (B)). The N35-259QhPAR_1E mutant showed a dramatic lost of cell surface expression with the highest level of receptor cytosolic retention (Figure 3.3.2 (F)).

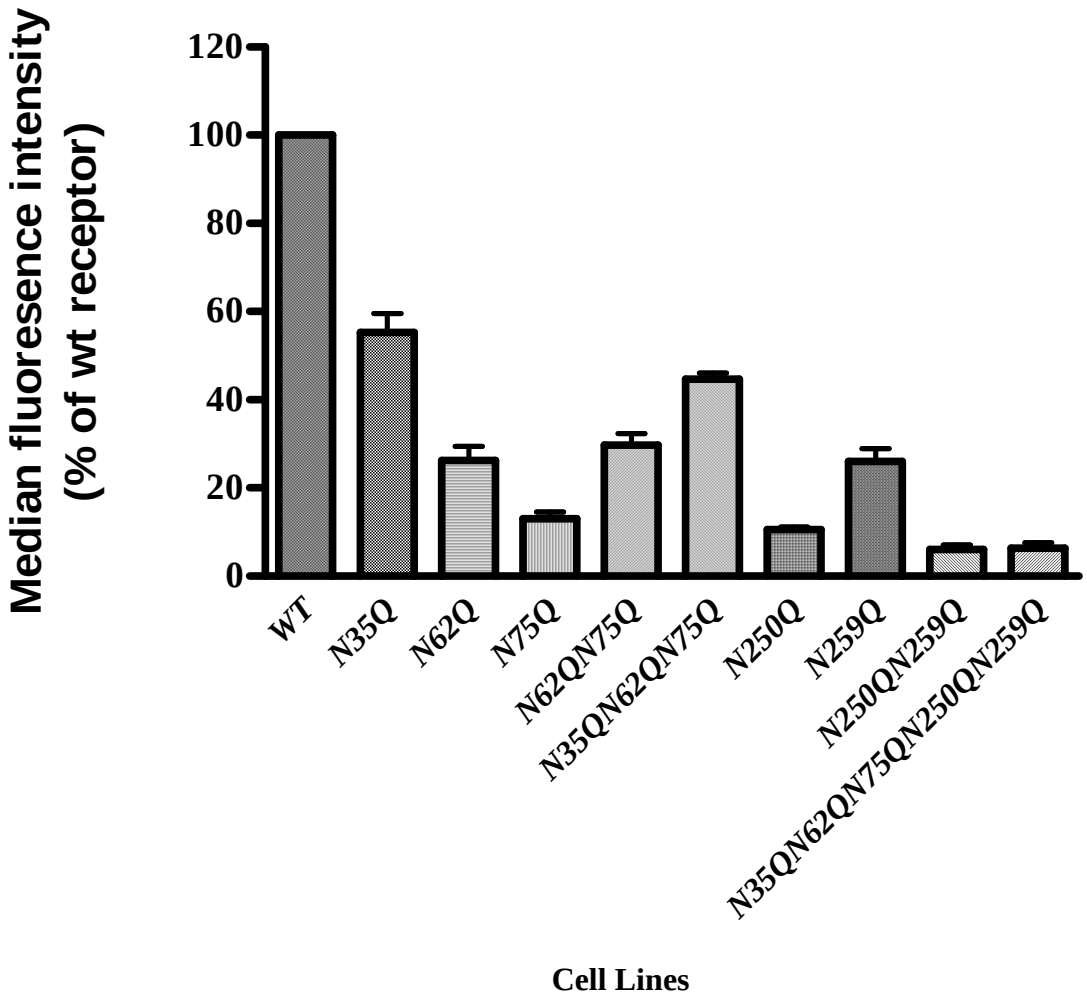

Figure 3.3.1 Cell-surface expression of the wt-hPAR$_1$ and glycosylation-deficient mutant hPAR$_1$ receptor cell lines. Cells at approx 90% confluence were harvested and incubated with the ATAP-2 antibody before incubation with an anti-mouse FITC-conjugated antibody. Cell surface expression was assessed by FACS analysis. Results are expressed as a percentage of the median fluorescence obtained with wt-hPAR$_1$ cells. The bars represent mean ± SEM of measurements for three independent experiments. The overall comparsion showed that there were significant differences between 10 groups ($p<0.0001$). Tukey's Multiple Comparison Test indicated that the cell-surface expression of all the mutant receptors were significant different from wt-hPAR$_1$ ($p<0.001$).

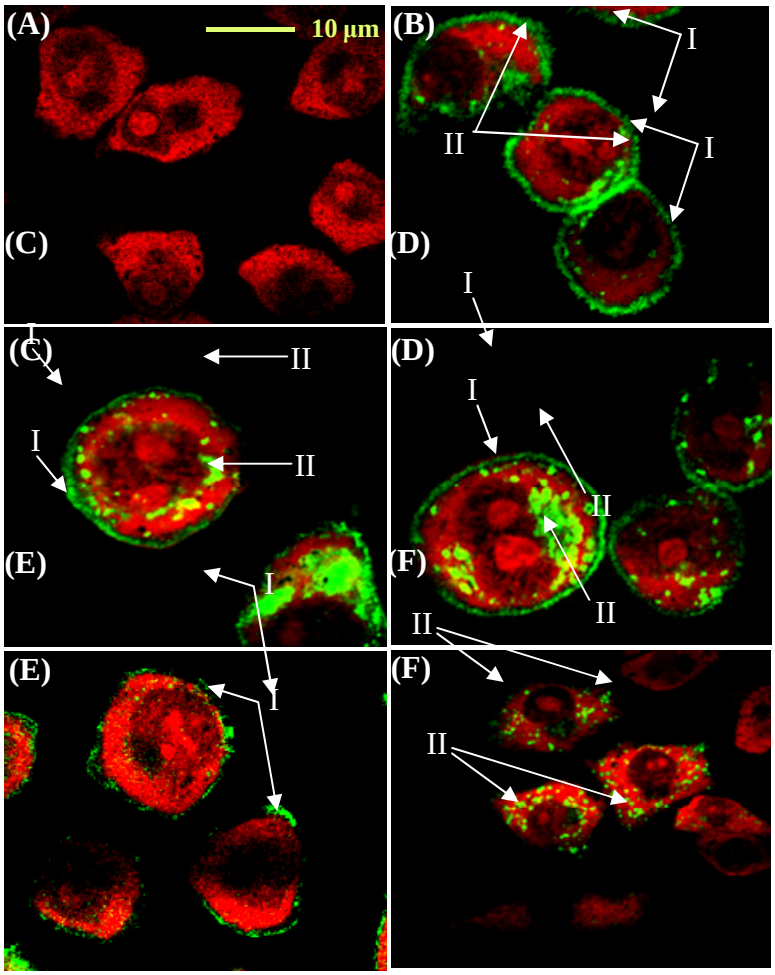

Figure 3.3.2 Confocal microscopy for wt-hPAR$_1$eYFP and glycosylation-deficient mutants in KNRK cells. Confocal microscopy images were produced by growing eYFP tagged PAR$_1$ expressing KNRK cells on coverslips before fixing and permeabilising. Cells were stained with propidium iodide prior to visualising. eYFP is visualised here in green and propidium iodide in red. **I:** cell surface expression, **II:** internal receptor expression. **(A):** EV, **(B):** wt-hPAR$_1$E, **(C):** N35QhPAR$_1$E, **(D):** N62QN75QhPAR$_1$E, **(E):** N250N259QhPAR$_1$E, **(F)**: N35-259QhPAR$_1$E. The images are representative for four independent experiments.

3.3.2 hPAR$_1$ is an *N*-linked Glycosylated Receptor

Obtaining western blot data for the hPAR$_1$ glycosylation mutants proved extremely troublesome and a considerable amount of time was expended attempting to obtain successful western blots, this is discussed in detail within the discussion.

Western blot analysis of membrane preparations was performed for wild-type and glycosylation-deficient mutant PAR$_1$. We were unsuccessful in obtaining western blot data for non-eYFP tagged wt-PAR$_1$ and glycosylation mutants regardless of which method we employed to prepare the protein sample (data not shown, please refer to discussion for detailed information), even though our positive control (PAR$_2$) worked well. We suspected that the HA.11 epitope tag may have been proteolytically removed, so we fused eYFP to the C-terminal tail of PAR$_1$, and performed western blot analysis on whole cell lysates (Figure 3.3.3).

Western blot analysis of whole cell lysates (Laemmli's sample buffer) of wt-hPAR$_1$E and non-glycosylation N35-259QhPAR$_1$E KNRK transfected cells was performed with the use of the eYFP antibody or the monoclonal HA.11 antibody (Figure 3.3.3). Wt-hPAR$_1$E migrated as multiple bands from approx ~25 kDa up to ~220 kDa, with the majority of the receptor being observed from ~75 kDa to ~220 kDa. A number of minor bands that may represent either eYFP protein or proteolytic degradation products of hPAR$_1$ were routinely observed in the 25-37 kDa range. There was only one band at ~31 kDa observed for the non-glycosylated mutant N35-259QhPAR$_1$E. In EV cells, no bands were detected, confirming the specificity of the antibody used.

Western blot analysis of immunoprecipitated wild-type and glycosylation-deficient mutant PAR$_1$ in KNRK via HA.11 epitope was performed in order to establish the degree of glycosylation associated with each glycosylation sequon within the receptor Figure 3.3.4 shows that all of the glycosylation-deficient mutant receptors displayed

different degrees of loss in molecular mass. No bands were detected in EV transfected KNKR cells (Figure 3.3.4 (A)). The molecular mass of N62QhPAR$_1$E ranged from ~37 kDa to ~250 kDa, with the majority of the receptor being observed from ~75 kDa to ~220 kDa (Figure 3.3.4 C). This is a similar pattern to that of WT-hPAR$_1$E (Figure 3.3.4 B). N62QN75QhPAR$_1$E migrated from 37-120 kDa, with the majority of the receptor being observed from ~75 kDa to ~120 kDa (Figure 3.3.4 D). N35QN62QN75QhPAR$_1$E migrated with a molecular mass at 37-200 kDa, with the majority of the receptor being observed from ~70 kDa to ~200 kDa (Figure 3.3.4 E). Only one band migrated at ~37 kDa for both N250QN259Q hPAR$_1$E (Figure 3.3.4 F) and N35-259QhPAR$_1$E (Figure 3.3.4 G). A number of minor bands that may represent either eYFP protein or proteolytic degradation products of hPAR$_1$ were routinely observed around the ~37 kDa.

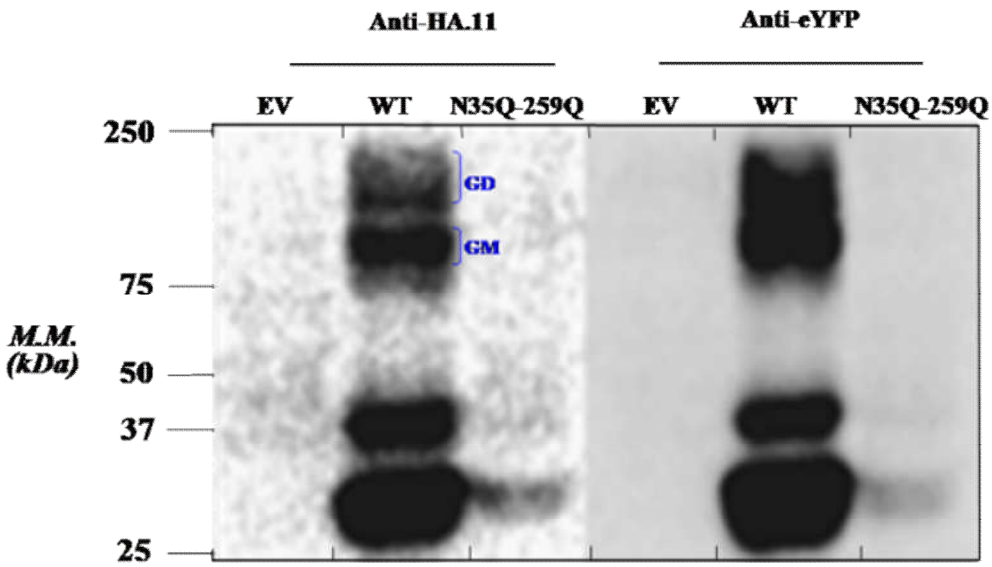

Figure 3.3.3 Western blot analysis for PAR_1. Wt-hPAR_1E and non-glycosylated mutant N35-259QhPAR_1E KNRK transfected cells whole cell lysates were separated by 10% SDS/PAGE, and Western blot analysis was conducted with the use of the eYFP antibody and the monoclonal HA.11 antibody. GD indicates glycosylated dimer; GM, glycosylated monomer. Results are representative of three separate experiments.

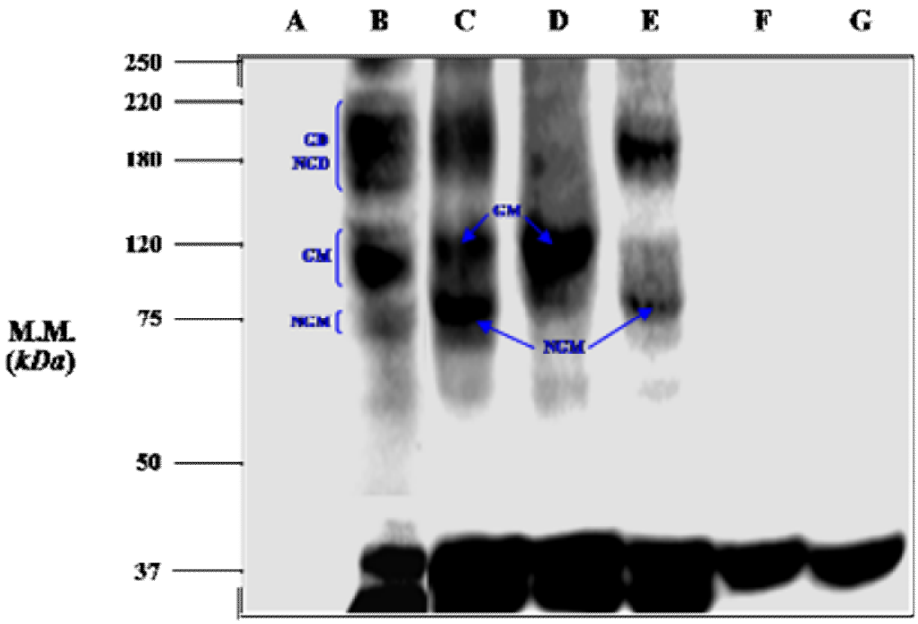

Figure 3.3.4 Blot for wt-hPAR$_1$E and glycosylation-deficient mutant hPAR$_1$E. Immunoprecipitates from KNRK cell lines expressing HA.11-tagged hPAR$_1$ ablated of the potential *N*-linked glycosylation sequons were analysed by SDS/PAGE (10% gel) and immunoblotted using HA.11 monoclonal antibody. **(A):** EV, **(B):** WT-hPAR$_1$E, **(C):** N62QhPAR$_1$E, **(D):** N62QN75QhPAR$_1$E, **(E):** N35QN62QN75QhPAR$_1$E, **(F):** N250N259QhPAR$_1$E, **(G):** N35-259QhPAR$_1$E. GD indicates glycosylated dimmer; NGD, nonglycosylated dimmer; GM, glycosylated monomer; NGM, nonglycosylated or minimally glycosylated monomer. M.M., molecular mass. Results are representative of three separate experiments.

3.3.3 Pharmacological Characterization of $hPAR_1$

To investigate whether glycosylation at individual asparagine residues had a role in $hPAR_1$ function, in terms of calcium signalling, we constructed concentration-effect curves for the selective PAR_1-AP TFLLR-NH_2, thrombin and trypsin for wt-$hPAR_1$ and the glycosylation mutant receptors. EC_{50} values of wt-$hPAR_1$ and mutant receptors for the different agonists are displayed in Table 3.3.5. The greatest shift in EC_{50} was observed for N62QN75QhPAR_1 where TFLLR-NH_2, thrombin and trypsin all displayed a greater EC_{50} value. Concentration effect curves for N35QhPAR_1 shown in Figure 3.3.6. N35Q hPAR_1 concentration effect curves were compared with wt-$hPAR_1$ (day 4) since they displayed similar cell surface expression ($p>0.05$) (Figure 3.3.6 (A)). TFLLR-NH_2 displayed negligible difference ($p>0.05$) in activating N35QhPAR_1 when compared with wt-$hPAR_1$ (day4) and inducing calcium signalling from 3 µM to 100 µM (Figure 3.3.6 (B)). For wt-$hPAR_1$ (day4) and N35QhPAR_1 thrombin stimulated a calcium response from 0.05 nM to 5 nM. The maximal response to thrombin was higher for wt than for N35Q (approx. 45 ± 2 % of A23187 and 30 ± 1.5 % of A23187 respectively) (Figure 3.3.6 (C)). Trypsin displayed signaficant differences ($p<0.05$) in activating N35QhPAR_1 when compared with wt-$hPAR_1$ (day4) and inducing calcium signalling from 3 nM to 316 nM (Figure 3.3.6 (D)). For N62QhPAR_1 (Figure 3.3.7), N75QhPAR_1 (Figure 3.3.8) and N259QhPAR_1 (Figure 3.3.9), no observable changes in receptor function were observed for TFLLR-NH_2, thrombin or trypsin when compared with their matched wt-$hPAR_1$ cell line. The cell surface expression level of N250QhPAR_1 mutant was below 10% compared to that of wt-$hPAR_1$, however, there was still a detectable calcium signal to TFLLR-NH_2 (100 µM) or thrombin (5 nM) (data not shown).

For the double mutant N62QN75QhPAR$_1$ significant differences in responsiveness to agonists were observed (Figure 3.3.10). N62QN75QhPAR$_1$ concentration effect curves were compared with wt-hPAR$_1$ (day 5) since they displayed similar cell surface expression ($p>0.05$) (Figure 3.3.10 (A)). TFLLR-NH$_2$ displayed a slight rightward shift in activating N62QN75QhPAR$_1$ compared with wt-hPAR$_1$ (day 5), stimulating a calcium signal at 3-100 µM for WT-hPAR$_1$ and 10-100 µM for N62QN75QhPAR$_1$ respectively, but achieved the same maximum response of 42 ± 1.5 % of A23187 at 100 µM in both cell lines (Figure 3.3.10 (B)). For N62QN75QhPAR$_1$ and wt-hPAR$_1$ (day 5), thrombin induced a calcium signal from 0.05 nM to 5 nM (Figure 3.3.10 (C)). However, the magnitude of the responses to thrombin in N62QN75QhPAR$_1$ was smaller than those obtained for wt-hPAR$_1$ (25 ± 2.5 % of A23187 and 35 ± 2 % of A23187 respectively). The EC$_{50}$ value for thrombin in N62QN75QhPAR$_1$ was 0.4 nM and for wt-hPAR$_1$ (day 5) was 0.1 nM. Interestingly, the N62QN75QhPAR$_1$ displayed reduced sensitivity towards trypsin compared to wt-hPAR$_1$ (day5), and the maximal response achieved was only 14% of A23187 compared to 32 ± 3 % of A23187 for the wt-hPAR$_1$ (day 5) (Figure 3.3.10 (D)). In addition, the EC$_{50}$ value for trypsin in N62QN75QhPAR$_1$ was greater than wt-hPAR$_1$ (day 5) (42 nM and 26 nM respectively). Finally, challenging non-glycosylated N35-259QhPAR$_1$ cells with either TFLLR-NH$_2$ (100 µM) or thrombin (5nM) resulted in small but detectable increases in calcium signalling, and subsequent treatment with A23187 (2 µM) resulted in a robust calcium response (Figure 3.3.11).

Cell lines	EC_{50}		
	TFLLR-NH_2 (µM)	**Thrombin (nM)**	**Trypsin (nM)**
WT (day4)	17	0.14	33
N35Q	16	0.2	43
WT (day5)	22	0.1	26
N62QN75Q	52	0.4	42
N259Q	16	0.1	90
WT (day6)	27	0.2	39
N62Q	29	0.4	43
N75Q	31	0.2	41

Table 3.3.5 EC_{50} values for wt and glycosylation-deficient mutant $hPAR_1$ KNRK cells and their respective matching wt-$hPAR_1$ agonist concentration effect curves.

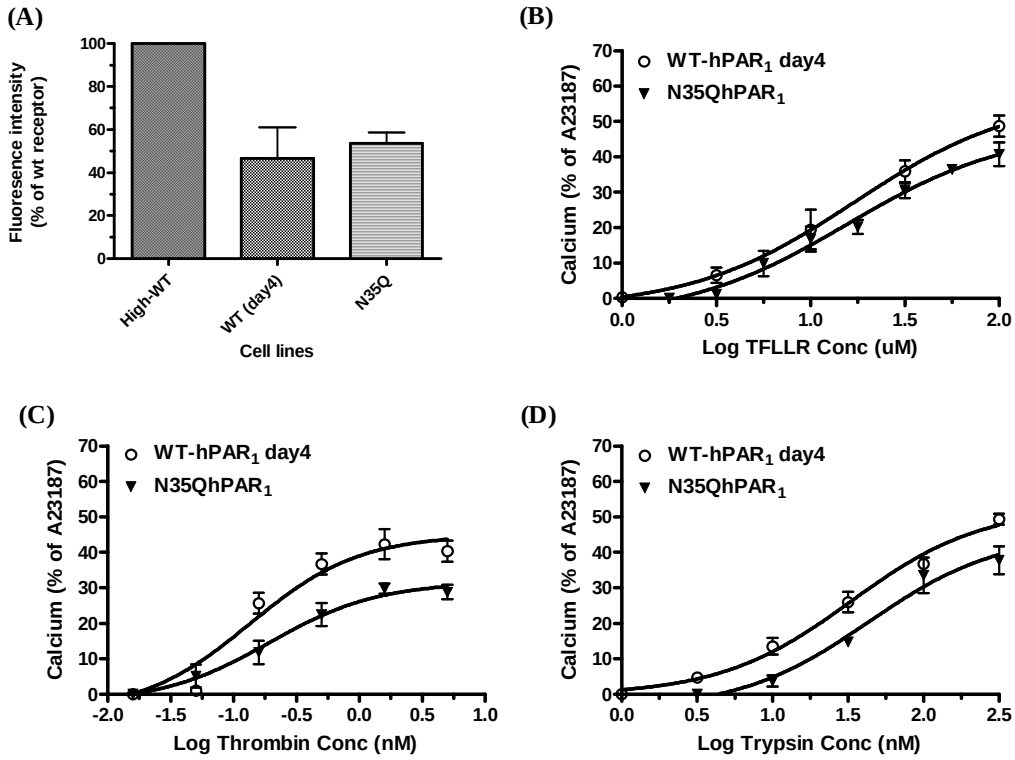

Figure 3.3.6 Cell surface expression and calcium signalling analysis of wt-hPAR$_1$ and N35Q. (A) Comparison of wt-hPAR$_1$ (KNRK-wt-hPAR$_1$ cell line: High-WT, WT (day 4)) and N35Q cell-surface expression. Cells at approx 90% confluence were harvested and incubated with the ATAP2 antibody before incubation with an anti-mouse FITC-conjugated antibody. Cell surface expression was assessed by FACS analysis. Results are expressed as a percentage of the median fluorescence obtained with High-wt-hPAR$_1$ cells. The bars represent mean ± SEM of measurements for three independent experiments. **(B)**, **(C)**, and **(D)** Calcium signalling assay for wt-hPAR$_1$ and glycosylation mutant N35Q in response to thrombin, trypsin, and TFLLR-NH$_2$. Results are expressed as the ± SEM of at least four independent experiments.

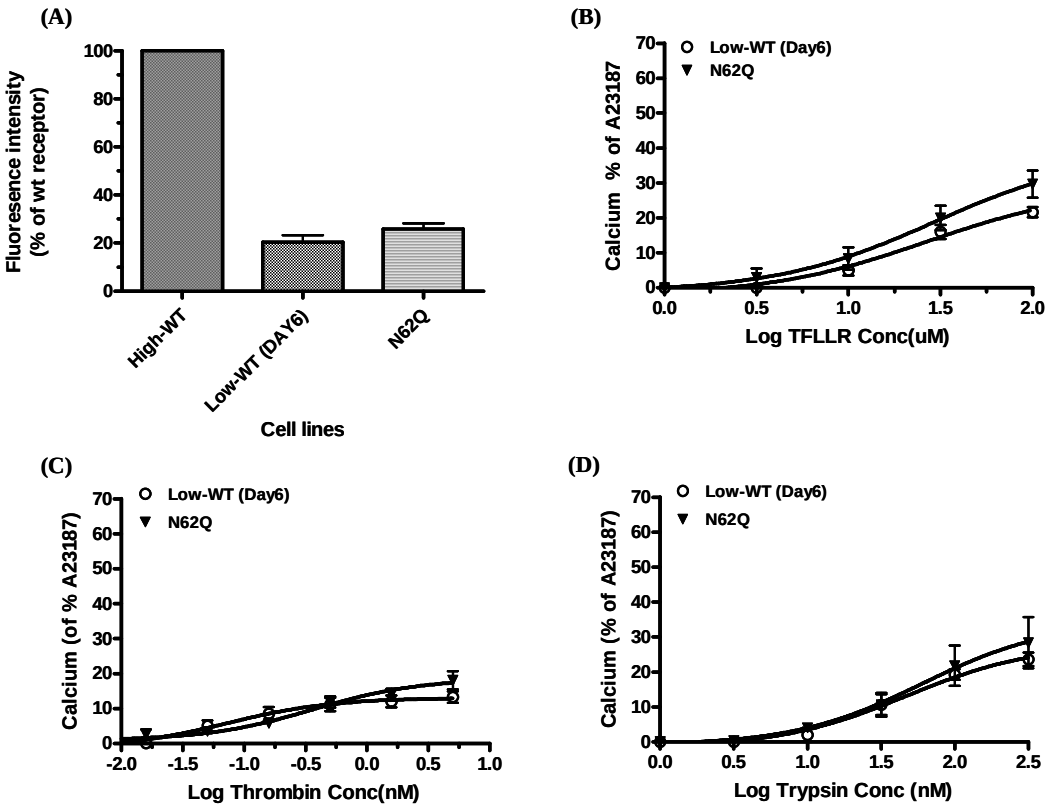

Figure 3.3.7 Cell surface expression and calcium signalling analysis of Low-WT (WT day 6) and N62Q. (A) Comparison of KNRK-wt-hPAR$_1$ (Low-WT, WT day 6) and glycosylation-deficient mutant N62Q cell-surface expression. Cells at approx 90% confluence were harvested and incubated with the ATAP2 antibody before incubation with an anti-mouse FITC-conjugated antibody. Cell surface expression was assessed by FACS analysis. Results are expressed as a percentage of the median fluorescence obtained with High-wt-hPAR$_1$ cells. The bars represent mean ± SEM of measurements for three independent experiments. **(B)**, **(C)**, and **(D)** Calcium signalling in the Low-WT and glycosylation mutant N62Q in response to PAR$_1$-AP (TFLLR-NH$_2$), thrombin and trypsin. Results are expressed as the means ± SEM of at least three independent experiments.

.

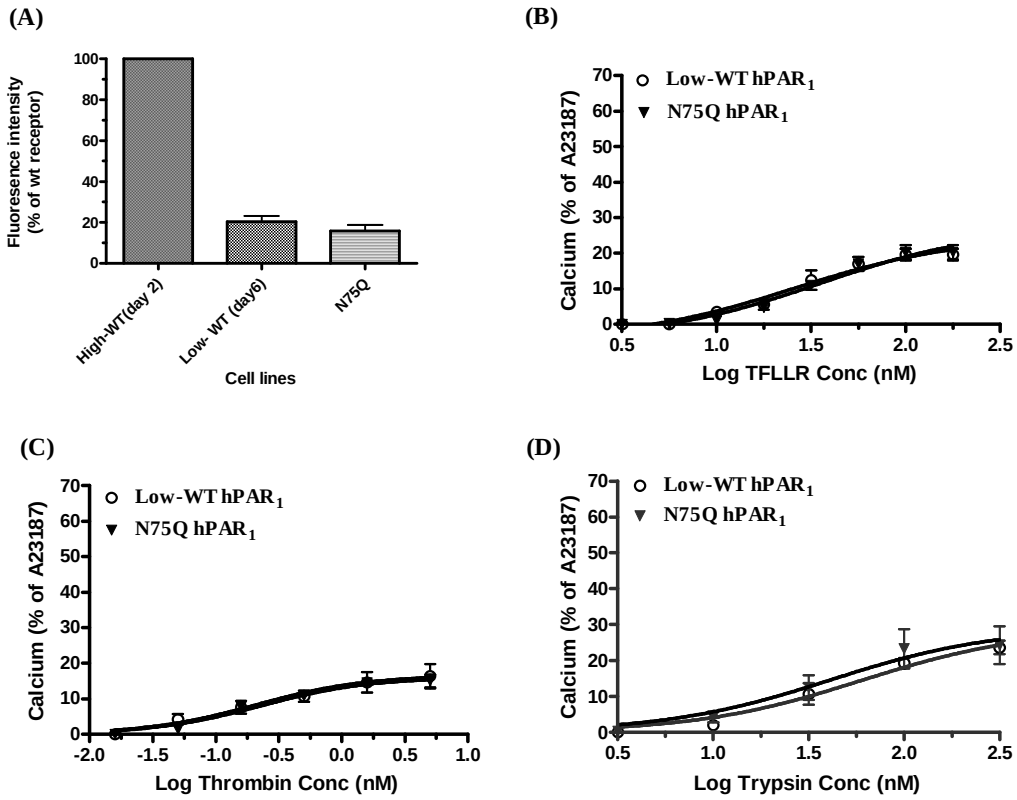

Figure 3.3.8 Cell surface expression and calcium signalling analysis of Low-WT (day 6) and N75Q. (A) Comparison of KNRK-wt-hPAR$_1$ (Low-WT, WT day 6) and glycosylation-deficient mutant N75Q cell-surface expression. Cells at approx 90% confluence were harvested and incubated with the ATAP-2 antibody before incubation with an anti-mouse FITC-conjugated antibody. Cell surface expression was assessed by FACS analysis. Results are expressed as a percentage of the median fluorescence obtained with High-wt-hPAR$_1$ cells. The bars represent mean ± SEM of measurements for three independent experiments. **(B)**, **(C)**, and **(D)** Calcium signalling in the Low-WT and glycosylation mutant N75Q in response to PAR$_1$-AP (TFLLR-NH$_2$), thrombin and trypsin. Results are expressed as the mean ± SEM of at least four independent experiments.

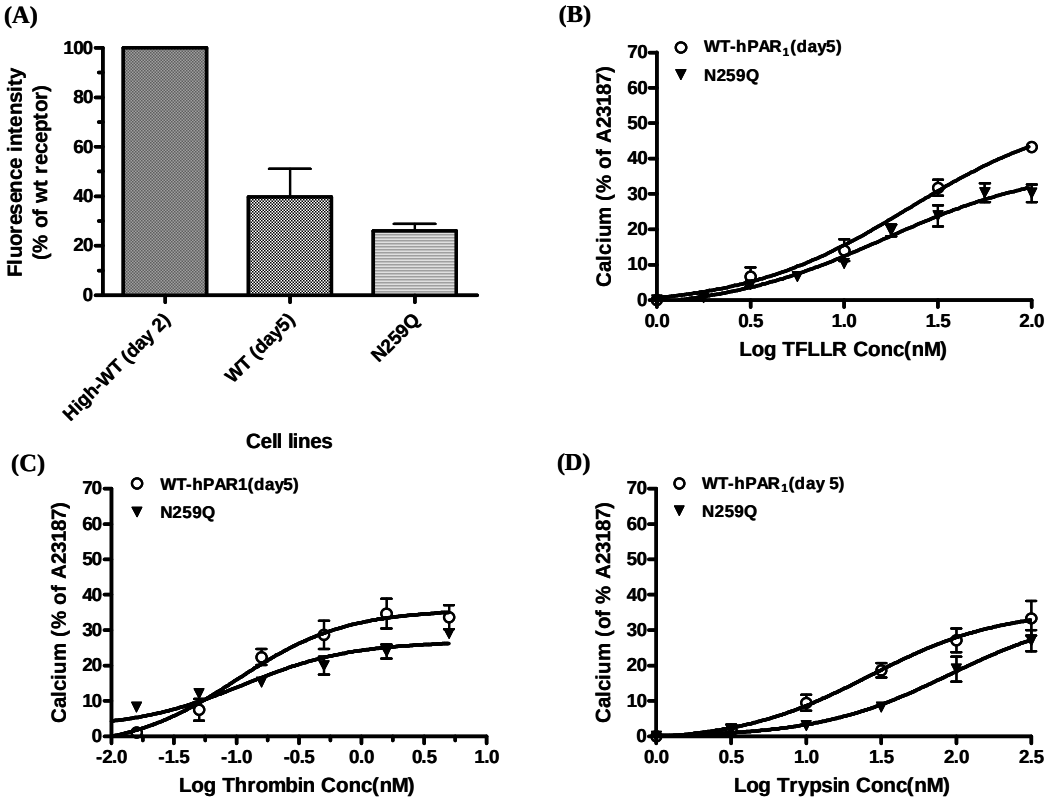

Figure 3.3.9 Cell surface expression and calcium signalling analysis of WT (day 5) and N259Q. (A) Comparison of KNRK-wt-hPAR$_1$ (WT day 5) and glycosylation-deficient mutant N259Q cell-surface expression. Cells at approx 90% confluence were harvested and incubated with the ATAP2 antibody before incubation with an anti-mouse FITC-conjugated antibody. Cell surface expression was assessed by FACS analysis. Results are expressed as a percentage of the median fluorescence obtained with High-wt-hPAR$_1$ cells. The bars represent mean ± SEM of measurements for three independent experiments. **(B)**, **(C)**, **(D)** Calcium signalling in the WT (day 5) and glycosylation mutant N259Q in response to PAR$_1$-AP (TFLLR-NH$_2$), thrombin and trypsin. Results are expressed as the means ± SEM of at least four independent experiments.

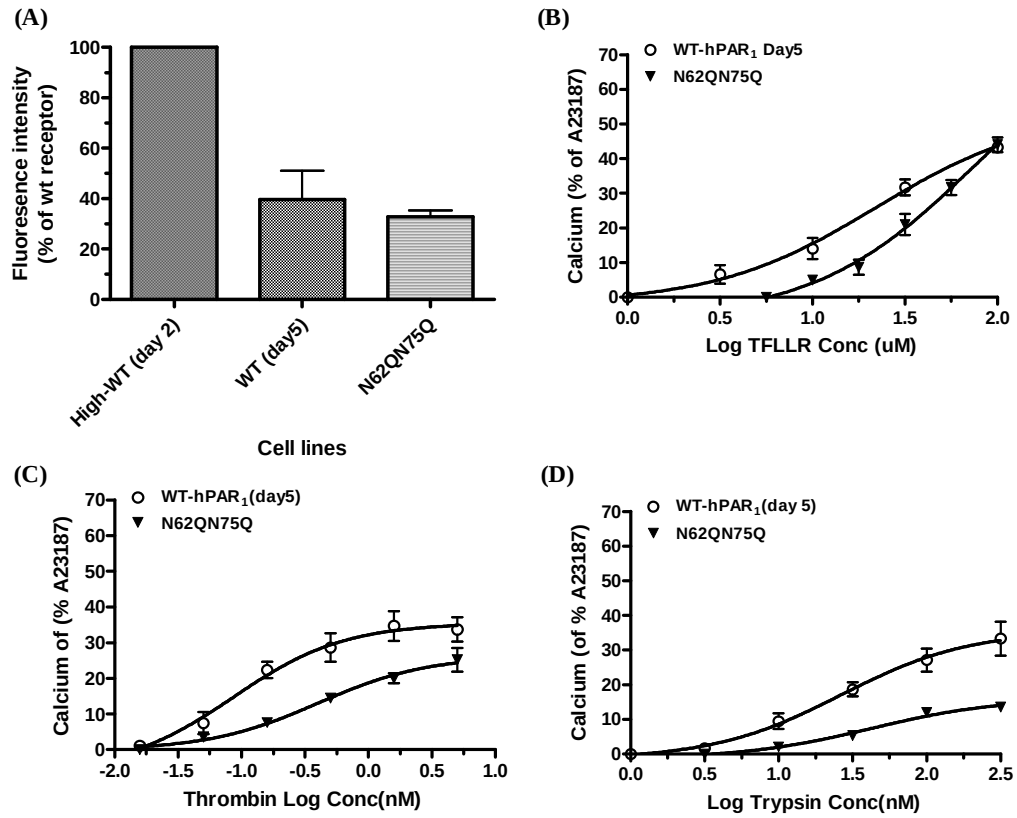

Figure 3.3.10 Cell surface expression and calcium signalling analysis of WT (day 5) and N62QN75Q. (A) Comparison of KNRK-wt-hPAR$_1$ (WT day 5) and glycosylation-deficient mutant N62QN75Q cell-surface expression. Cells at approx 90% confluence were harvested and incubated with the ATAP-2 antibody before incubation with an anti-mouse FITC-conjugated antibody. Cell surface expression was assessed by FACS analysis. Results are expressed as a percentage of the median fluorescence obtained with High-wt-hPAR$_1$ cells. The bars represent mean ± SEM of measurements for three independent experiments. **(B)**, **(C)**, **(D)** Calcium signalling in the WT (day 5) and glycosylation mutant N62QN75Q in response to PAR$_1$-AP (TFLLR-NH$_2$), thrombin and trypsin. Results are expressed as the means ± SEM of at least four independent experiments.

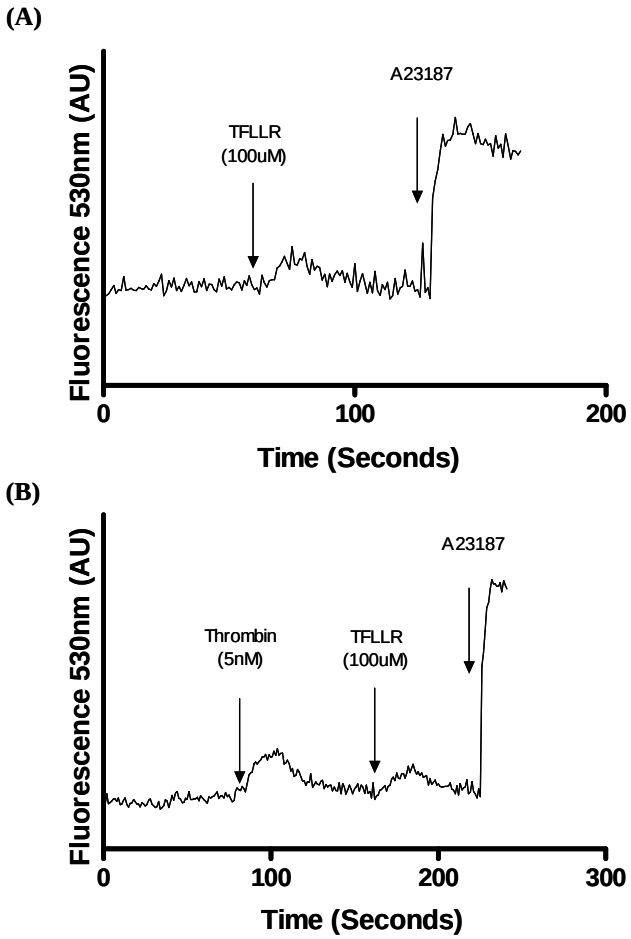

Figure 3.3.11 N35-259QhPAR$_1$E calcium signalling. (A) N35-259QhPAR$_1$E (KNRK-hPAR$_1$N35-259QeYFP) responses to PAR$_1$-AP TFLLR-NH$_2$ and A23187. **(B)** N35-259QhPAR$_1$E responses to thrombin, PAR$_1$-AP TFLLR-NH$_2$ and A23187. An increase in fluorescence (E_{530}) monitored by fluorescence spectrophotometry is indicative of calcium mobilization. Cells were loaded with Fluo-3 (22 μM) prior to incubation for 25 minutes at RT. Functional hPAR$_1$ activity was assessed by treating cells with the hPAR$_1$-AP TFLLR-NH$_2$ (100 μM) and thrombin (5 nM). Cell loading/viability was assessed by addition of A23187 (calcium ionophore, 2 μM). Arrows indicate when test agonists were added. Data shown is representative of three independent experiments.

3.3.4 The Role of Sialylation in Regulating PAR_1 Expression

To assess the role of sialylation in regulating PAR_1 expression and function, we transfected Pro5 and Lec2 cells with wt-hPAR_1E. The latter cells are unable to attach sialic acid to any of its glycoproteins (Compton *et al.*, 2002b). Receptor expression was assessed by flow cytometry and confocal microscopy. Flow cytometry data showed that both wt-hPAR_1E transfected Pro5 (Figure 3.3.12 (A)) and Lec2 (Figure 3.3.12 (B)) cells show significant rightward shift in fluorescence when compared to control CHO cells. Receptor global expression levels between hPAR_1E transfected Pro5 and Lec2 cells demonstrate that the cell lines displayed similar receptor expression (Figure 3.3.12 (C)). Confocal images of wt-hPAR_1E permanently expressed in Pro5 and Lec2 cells are shown in Figure 3.3.13. In Pro5 cells PAR_1 was seen to be distributed throughout the cell in what are assumed to be vesicles in the cytoplasm. PAR_1 was also visible at the cell membrane in Pro5 cells (Figure 3.3.13 (A), (B) and (C)). In Lec2 cells PAR_1 localisation was different with larger vesicles of receptor observed. Less membrane expression was apparent compared to Pro5 PAR_1 (Figure 3.3.13 (D), (E) and (F)).

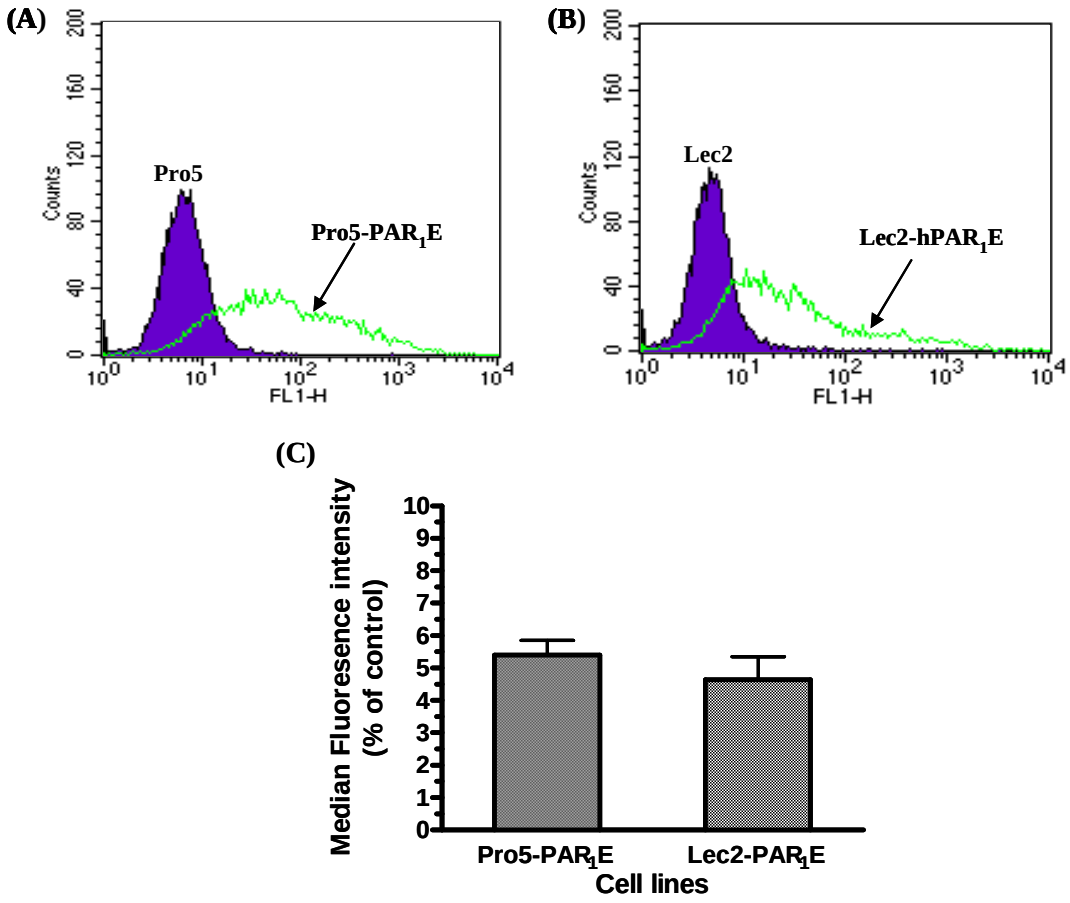

Figure 3.3.12 Flow cytometry analysis for wt-hPAR$_1$eYFP in CHO cell lines.

Flow cytometry analysis for **(A):** Pro5 and Pro5-PAR$_1$E; **(B):** Lec2 and Lec2-PAR$_1$E. **(C):** Bar graph showing relative receptor expression between Pro5-PAR$_1$E and Lec2-PAR$_1$E cell lines. Cells were washed in PBS, and 10,000 cells were analyzed for fluorescence (FL1-H) by flow cytometry. The results are representative of three separate experiments.

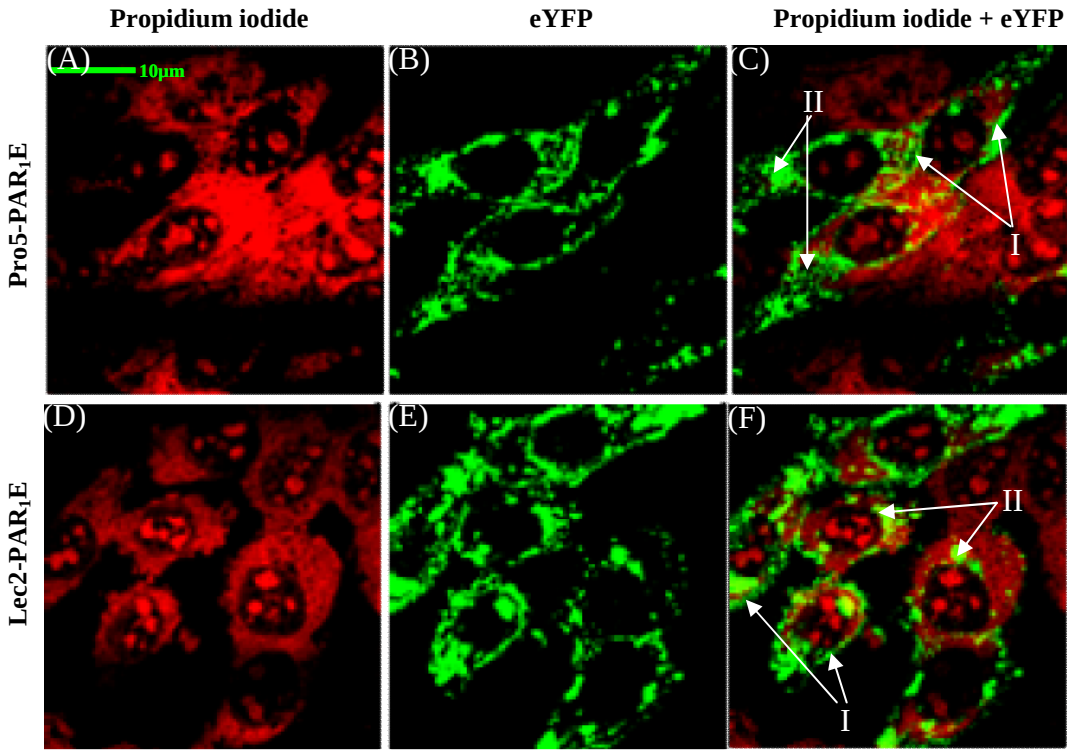

Figure 3.3.13 Confocal microscopy for wt-hPAR$_1$eYFP in CHO cells. Confocal microscopy images of Pro5-PAR$_1$E (**(A)**, **(B)** and **(C)**) and Lec2-PAR$_1$E (**(D)**, **(E)** and **(F)**) were produced by growing cells on coverslips before fixing and permeabilising. Cells were stained with propidium iodide prior to visualising. eYFP is visualised here in green and propidium iodide in red. **I:** cell surface expression, **II:** internal receptor expression. The results are representative of three separate experiments.

3.3.5 $hPAR_1$ is a Sialylated Receptor

To determine the contribution of sialic acid to the molecular mass of $hPAR_{1,}$ we performed western blot analysis for Pro5-PAR_1E alongside the Lec2-PAR_1E (Figure 3.3.14). No bands were detected in the non-transfected Lec2 and Pro5 whole cell lysates. Pro5-PAR_1E migrated as multiple bands ranging from 25-197 kDa, with the majority of the receptor being observed between approx. 75-197 kDa. Two bands were routinely observed between the 25-37 kDa range in both of Pro5-PAR_1E and Lec2-PAR_1E. The molecular mass of Lec2-PAR_1E ranged from ~25 kDa to ~150 kDa (including two bands observed between 25-37 kDa range, and another 2 clear bands observed approx. at ~70 kDa and ~150 kDa).

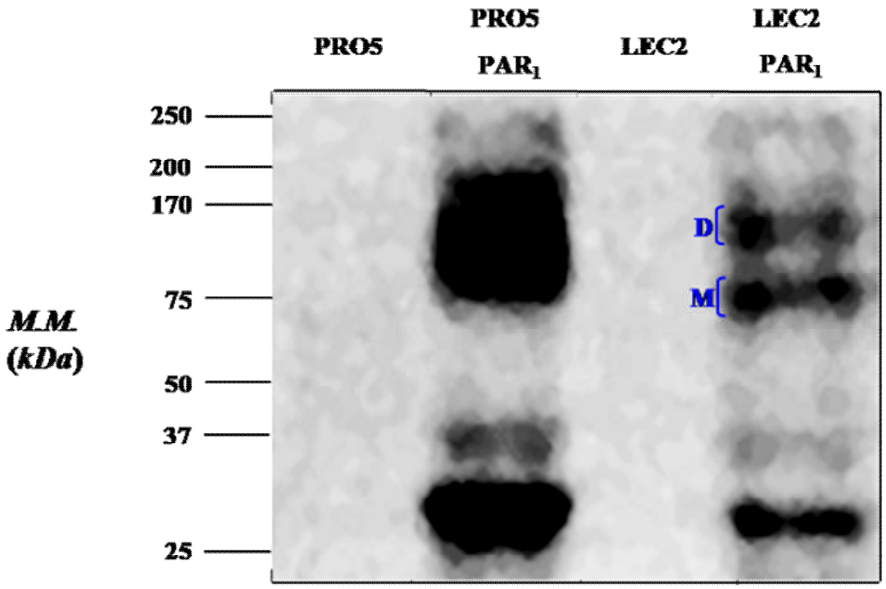

Figure 3.3.14 Western blot analysis of Pro5-PAR$_1$E and Lec2-PAR$_1$E. Protein samples were immunoprecipitated by HA11 immunoprecipitation and were analysed by SDS/PAGE (10% gel) and immunoblotted using a monoclonal HA.11 antibody. PRO5-PAR1, PAR$_1$ protein from Pro5-PAR$_1$E cells; LEC2-PAR$_1$, PAR$_1$ protein from Lec2-PAR$_1$E cells; PRO5, protein sample from non-transfected Pro5 cells; LEC2, protein sample from non-transfected Lec2 cells; M indicated nonglycosylated or minimally glycosylated monomer; D, PAR$_1$ dimer. M.M., molecular mass.

3.3.6 The Effect of Sialylation in Regulating PAR_1 Function

For the Pro5 cell line, TFLLR-NH_2 induced a calcium signal from 1 µM to 100 µM with an EC_{50} value of 8.5 µM (Figure 3.3.15 (A)). For Lec2 cells TFLLR-NH_2 induced a calcium signal from 10 µM to 100 µM with an EC_{50} value of 35 µM. The maximal response achieved for TFLLR-NH_2 was 44 ± 6 % of A23187 for Pro5, and 18 ± 1 % of A23187 for Lec2 cells (Figure 3.3.15 (A)).

The TFLLR-NH_2 concentration-effect curve (Figure 3.3.15 (B)) for Pro5-PAR_1E and Lec2-PAR_1E showed that the TFLLR-NH_2 initiated a calcium signal from 1 µM to 100 µM and 3 µM to 100 µM with an EC_{50} value of 1.5 µM and 9.8 µM respectively. The maximum response achieved was 47 ± 1 % of A23187 for Pro5-PAR_1E and 26 ± 2 % of A23187 for Lec2-PAR_1E.

For the Pro5 cell line, thrombin stimulated a calcium signal from 0.05 nM to 5 nM with a maximal response 42 ± 1.7 % of A23187 (Figure 3.3.15 (C)). For Lec2 cells thrombin stimulated a calcium signal from 0.15 nM to 5 nM with a maximal response approx. 27 ± 2 % of A23187 (Figure 3.3.15 (C)). The EC_{50} value for thrombin was 0.05 nM for Pro5 cells and 0.11 nM for Lec2 cells.

For the Pro5-PAR_1E cell line, thrombin stimulated a calcium signal from 0.05 nM to 5 nM with a maximal response approx. 50 ± 6.4 % of A23187 for Pro5-PAR_1E (Figure 3.3.15 (D)). For Lec2-PAR_1E thrombin stimulated a calcium signal from 0.15 nM to 5 nM with a maximal response approx. 26 ± 1.5 % of A23187 respectively (Figure 3.3.15 (D)). The EC_{50} value for thrombin is 0.05 nM for Pro5-PAR_1E cells and 0.12 nM for Lec2-PAR_1E.

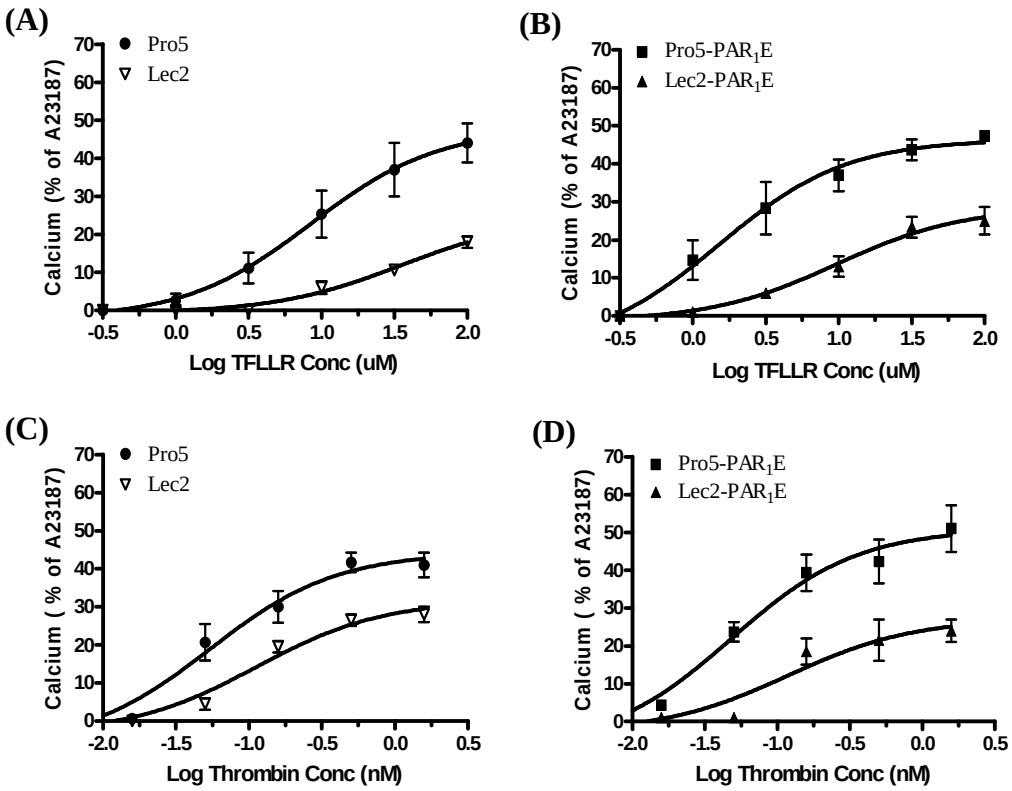

Figure 3.3.15 $hPAR_1$ agonist concentration-effect curves in untransfected and PAR_1 transfected Pro5 and Lec2 cells. (A) TFLLR-NH_2 concentration effect curves for Pro5 and Lec2 cells; **(B)** TFLLR-NH_2 concentration effect curves for Pro5-PAR_1E and Lec2-PAR_1E cells. **(C)** Thrombin concentration effect curves for Pro5 and Lec2 cells; **(D)** Thrombin concentration effect curves for Pro5-PAR_1E and Lec2-PAR_1E cells. The results are expressed as the mean ± SEM of three separate experiments each performed in duplicate.

3.4 Discussion

In this study, we adopted molecular and biochemical approaches to elucidate the roles of *N*-linked glycosylation on the function and expression of $hPAR_1$. Our data suggests that $hPAR_1$ is a heavily glycosylated receptor and that *N*-linked glycosylation probably occurs at all five consensus sites of $hPAR_1$ in KNRK cells, namely, Asn^{35}, Asn^{62}, Asn^{75}, Asn^{250}, and Asn^{259}. Removing *N*-linked glycosylation sequons at these positions blocked $hPAR_1$ cell surface expression to varying degrees, and indicated that glycosylation at all sites is required for optimal cell surface expression of $hPAR_1$. With the exception of N62QN75Q no significant changes in receptor sensitivity to thrombin, trypsin and TFLLR-NH_2 were observed when assessed by calcium signalling. Interestingly, N62QN75Q displayed significantly reduced sensitivity to trypsin, but not thrombin and TFLLR-NH_2.

We first utilised FACS and confocal microscopy to assess the expression level and the cellular distribution of wt-$hPAR_1$ and the glycosylation-deficient mutants cell lines. Disrupting the glycosylation sites by mutagenesis, individually and in combination, allowed us to probe the function of glycosylation at each locus and within each extracellular domain. In order to select the highest expression clone for each mutant, we performed over two separate transfections for each mutant. Of the mutants that possessed single site mutations within the N-terminus, N75Q displayed the lowest level of cell surface expression when compared to N35Q and N62Q. However, FACS and confocal microscopy data also revealed that there were still high levels of cell surface expression of $hPAR_1$ when removing all glycosylation sequons after the tethered ligand (N62QN75Q) or removing all glycosylation sequons on the N-terminus (N35QN62QN75Q). Therefore, the decrease in the cell surface expression of N75Q is

not due to removing glycosylation. In addition, N250Q displayed the lowest level of cell surface expression of $hPAR_1$ among all the single glycosylation mutants. Furthermore, FACS data also indicated that removing all glycosylation sequons on ECL2 resulted in similar levels of receptor expression to the mutant where all glycosylation sequons had been deleted. Interestingly, Compton's PAR_2 glycosylation study also reported similar results (Compton *et al.*, 2002b). Thus, we conclude that *N*-linked glycosylation in the N-terminus of $hPAR_1$ facilitates, but is not essential for, cell surface expression of $hPAR_1$. Moreover, *N*-linked glycosylation on ECL2 of $hPAR_1$, especially Asn^{250}, may play an important role in cell surface expression of the receptor. However ECL2 is extremely sensitive to mutations and a previous study has demonstrated that mutating residues in and around the glycosylation sequon in ECL2 of PAR_2 probably alters receptor structure and that function is compromised (Compton *et al.*, 2002b). Thus, it is hard to determine whether this lack of receptor cell surface expression is a result of loss of glycosylation at the Asn^{250} site leading to improper folding and hence retention at the ER or golgi apparatus. In that case it would appear that glycosylation at multiple sites on $hPAR_1$ plays an important role in regulating its cell surface expression. The effect of *N*-linked glycosylation was also reported to facilitate cell surface expression in other receptors, for example, Shen *et al.* also reported that the total mass of *N*-linked glycosylations is critical for the efficient folding and optimal expression of functional folate receptor α and β (FR-α and FR-β) (Shen *et al.*, 1997). Fan *et al.* also demonstrated that *N*-linked glycosylation is required for normal expression of the human calcium receptor (hCaR) at the cell surface (Fan *et al.*, 1997). Furthermore, another study reported that at least three specific sites of *N*-linked glycosylation in hCaR is critical for cell surface expression (Ray *et al.*, 1998).

We initially attempted to visualize HA.11 tagged $hPAR_1$ by western blot analysis of membrane preparations using the anti-HA.11 monoclonal antibody. However, it was not possible to identify the receptor clearly due to the multiple bands in non-transfected, as well as receptor-transfected preparations. Therefore, we optimized the experimental conditions by changing the secondary antibody dilution from *1 in 1000* to *1 in 4000*. However, we were unable to detect PAR_1 protein, even when cells from up to four 175 cm^2 flasks were used. Confocal microscopy analysis indicated that the receptors, especially glycosylation-deficient mutants, were not only expressed on the plasma membrane but also in the cytosol. We then collected the whole cell lysates by using Laemmli's sample buffer or sample buffer from PIERCE; however, there was still little or no staining. We then hypothesised that *(i)* HA.11 antibody may not be the best antibody to visualise the receptor properly although the specificity of the antibody was well demonstrated by Compton *et al* (Compton *et al.*, 2002b), or *(ii)* there might be not enough receptors in the whole cell lysates. We then performed western blot analysis with *(i)* ATAP-2 antibody, and *(ii)* M2 antibody since these antibodies recognise epitopes on the receptor N-terminus compared to HA.11, which is on the receptor C-terminus. However, the ATAP-2 antibody, and the M2 antibody even following immunoprecipitation using the M2 antibody all failed to generate any meaningful data. We then attempted to immunoprecipitate PAR_1 using the HA.11 immunoprecipitation kit. In addition, we prepared HA.11 epitope-tagged wt-$hPAR_2$ sample along with HA.11 epitope-tagged wt-$hPAR_1$. Wt-$hPAR_2$ was clearly identified but not the $hPAR_1$, thus we concluded that the HA.11 epitope of wt-$hPAR_1$ might be amputated from the receptor, thereby disabling the ability of the HA.11 antibody to recognise PAR_1.

In separate experiments (Chapter 5) we had successfully detected $hPAR_4$eYFP in KNRK cells by western blotting. We thus, hypothesised that fusing eYFP to the tail of

hPAR$_1$ may aid us in isolating the receptor because the presence of the eYFP protein may sterically hinder any proteolytic activity that may have been removing the HA.11 tag. Indeed the wt-hPAR$_1$-eYFP (wt-hPAR$_1$E) was successfully identified by western blot analysis. We first collected the whole cell lysates by using Laemmli's sample buffer, the wt-hPAR$_1$E can be identified clearly by the anti-eYFP antibody or anti-HA.11 monoclonal antibody. However, in the non-glycosylation mutant N35-259QhPAR$_1$E sample lane, only one single band could be visualised which was also observed in the same position in the wt-hPAR$_1$E lane. Also the density of this band was very faint when compared with the wt-hPAR$_1$E band and might be due to low levels of N35-259QhPAR$_1$E protein, Indeed FACS and confocal microscopy data showed that this non-glcosylation mutant N35-259QhPAR$_1$E receptor can be seen mainly in the cytosol with very low levels of fluorescence signal. Finally, we prepared eYFP tagged wt and glycosylation mutant samples using immunoprecipitations of the receptor whole cell lysates via HA.11 epitope tag.

It is well known that the molecular mass of wt-hPAR$_1$, based on its amino acid sequence, is predicted to be approximately ~47 kDa and the molecular mass of eYFP protein is ~31 kDa. Therefore, our PAR$_1$ fused with eYFP protein should migrate around the 70-80 kDa range. We proposed that in the wt-hPAR$_1$E the band around ~75 kDa may represent an unglycosylated monomer of PAR$_1$; the bands around 80-130 kDa may represent a glycosylated monomer of PAR$_1$; and the bands around 150-220 kDa may represent glycosylated and unglycosylated dimers of PAR$_1$. When removing all three glycosylation sites (Asn^{35}, Asn^{62}, Asn^{75}) in the N-terminus of the receptor, the banding pattern changed: the bands around ~180 kDa may still represent the glycosylated dimer of PAR$_1$; and the band at ~75 kDa may represent an unglycosylated monomer of PAR$_1$. When removing glycosylation sites Asn^{62} and Asn^{75}, the bands

around ~120 kDa may represent a glycosylated monomer of PAR_1. It is known that *N*-linked glycosylation has been shown to be important for normal protein folding and stability. One previous study indicated that some *N*-glycans of Hepatitis C virus (HCV) envelope glycoproteins play a major role in protein folding (Goffard *et al.*, 2005). Mochizuki *et al.* reported that at least two *N*-linked glycans are required for the bile salt export pump *(*Bsep) protein stability, intracellular trafficking, and function in the apical membrane in MDCK II cells (Mochizuki *et al.*, 2007). We also observed from the western blots that removal of *N*-linked glycosylation from the ECL2 (Asn^{250}, Asn^{259}) or removal of all *N*-linked glycosylation from the receptor resulted in only a single band being visualised which is also observed routinely in the same position from the rest $hPAR_1E$. This may represent either eYFP protein or proteolytic degradation products of $hPAR_1$. Taken together these results indicated removal of glycosylation from the ECL2 may result in incorrect folding of receptors and probable degradation. We therefore suggest that *N*-glycosylation of PAR_1, especially glycosylation sites from the ECL2 of PAR_1 (Asn^{250} and Asn^{259}), plays an important role in receptor stability. Overall, these data established that *N*-linked glycosylation has an important role in PAR_1 expression, and/or stability of the receptor, at the plasma membrane. However, further studies are needed to clarify the precise role of *N*-linked glycosylation in the above-mentioned glycoprotein biosynthetic processes.

In order to establish the role of glycosylation in regulating receptor function, agonist concentration effect curves were produced for all the glycosylation-deficient $hPAR_1$ cell lines and their respective wt-$hPAR_1$ cell line to evaluate the coupling of the mutant receptors to calcium. No significant change in receptor function was observed for all mutant cell lines compared with wt cells that demonstrate a comparable cell-surface expression. Therefore PAR_1 coupling to calcium signalling appears not to be affected by

a lack of glycosylation on the receptor. Even the N35-N259Q mutant receptor still displayed a detectable calcium signal towards TFLLR-NH_2 and thrombin thus adding strength to this conclusion. Interestingly, the selective and significant decrease in potency of trypsin towards N62QN75Q suggested that this proteinase may be disarming this receptor to a greater degree to that of wt-hPAR_1 and this is explored in greater detail in the next chapter.

We finally assessed whether PAR_1 is sialylated and the role that sialylation may play in regulating PAR_1 expression and function. We expressed the wt-hPAR_1E in Pro5 and Lec2 cells. The Pro5 cell line is the parent clone for the Lec2 cell line. The Lec2 cell line displays a substantial loss in an ability to attach sialic acid to the terminal positions on oligosaccharides. FACS and confocal imaging data revealed that removing sialylation appeared to lower the expression of PAR_1. Indeed, Pro5 and Lec2 cells constitutively express PAR_1 and the agonist concentration effect curves for Lec2 cells displayed lower maximal obtainable signals. However, we did not assess PAR_1 expression on Pro5 and Lec2 cells, but one would assume that transcription and translation of PAR_1 within these cloned cell lines would be similar. Thus meaningful data was not readily obtained from these experiments. Western blot analysis of wt-PAR_1E in Lec2 cells had a molecular mass that was up to ~47 kDa lower than that observed for wt-PAR_1E expressed in the Pro5 cells. Presumably this significant loss of ~47 kDa is due to the loss of receptor-associated sialic acid, and we can therefore conclude that PAR_1 in CHO cells, at least, is a heavily sialylated receptor.

In summary, we show that PAR_1 is heavily glycosylated and sialylated and that this glycosylation regulates cell surface expression but not coupling to calcium.

4.1 Introduction

PAR_1 can be activated and attenuated by more than one proteinase (Molino *et al.*, 1995; O'Brien *et al.*, 2001). Any proteinase that cleaves the correct peptide bond within the N-terminus of PAR_1 may be able to expose the tethered ligand and then initiate intracellular signaling to provoke a cellular response, for example, thrombin cleaves PAR_1 between Arg^{41} and Ser^{42} to expose a new N-terminal tethered ligand domain (Figure 4.1.1) (Vu *et al.*, 1991a; Dery *et al.*, 1998; O'Brien *et al.*, 2001). Conversely, proteinases can also disarm these receptors by proteolytically removing the tethered ligand domain altogether from the receptor (e.g., cathepsin G cleaves $hPAR_1$ between Phe^{55} and Trp^{56} removing the tethered ligand domain) (Molino *et al.*, 1995; O'Brien *et al.*, 2001). Such disarmed receptors remain at the cell surface and are no longer available for activation by their respective activating proteinases, but can be activated by PAR_1-AP TFLLR-NH_2 (Nakayama *et al.*, 2003).

In addition to thrombin, $hPAR_1$ can also be activated by trypsin (Vu *et al.*, 1991a; Vouret-Craviari *et al.*, 1995; Loew *et al.*, 2000; Macfarlane *et al.*, 2001), granzyme A (Suidan *et al.*, 1994), factor Xa (Molino *et al.*, 1997b), and elastase (Suzuki *et al.*, 2005). On the other hand, PAR_1 signalling to thrombin can be abolished by prior exposure of cells to trypsin (Loew *et al.*, 2000; Nakayama *et al.*, 2003), chymase (Schechter *et al.*, 1998), thermolysin (Chen *et al.*, 1996; Dery *et al.*, 1998; Ubl *et al.*, 2000), cathepsin G (Molino *et al.*, 1995; Renesto *et al.*, 1997), elastase (Renesto *et al.*, 1997) and proteinase 3 (Renesto *et al.*, 1997). Interestingly, some of these proteinases can cleave PAR_1 both at the activation site and at other disabling sites. For example, trypsin has been found to both activate and disarm PAR_1 in different cell types (Dery *et al.*, 1998; Kawabata *et al.*, 1999; Loew *et al.*, 2000; Macfarlane *et al.*, 2001; Nakayama *et al.*, 2003; Nakayama *et al.*, 2004). Plasmin has been reported to be able to activate and

disarm PAR_1 (Vouret-Craviari *et al.*, 1995; Kimura *et al.*, 1996; Parry *et al.*, 1996; Pendurthi *et al.*, 2002). Cathepsin G has been reported to activate murine fibroblasts transfected with $hPAR_1$, but not PAR_1 naturally expressed by human platelets (Sambrano *et al.*, 2000; Shpacovitch *et al.*, 2007). Elastase has also been reported to activate and disarm PAR_1 in a number of different cell systems (Renesto *et al.*, 1997; Loew *et al.*, 2000; Suzuki *et al.*, 2005).

PAR_1, downstream of the tethered ligand, possesses two *N*-linked glycosylation sequons Asn^{62} and Asn^{75} which are located along the N-terminus in a domain where disarming proteinases may target. Previously work demonstrated that elastase, cathepsin G and proteinase 3 target specific sites which are close proximally to these glycosylation sequons (Figure 4.1.1) (Molino *et al.*, 1995; Renesto *et al.*, 1997). We hypothesize that glycosylation at Asn^{62} and Asn^{75} may regulate proteinases disarming of PAR_1. Therefore, the aims of this chapter were: 1) to assess the ability of a number of proteinases to disarm the wt and glycosylation deficient $hPAR_1$, and 2) to determine which sequon is important for proteinase disarming.

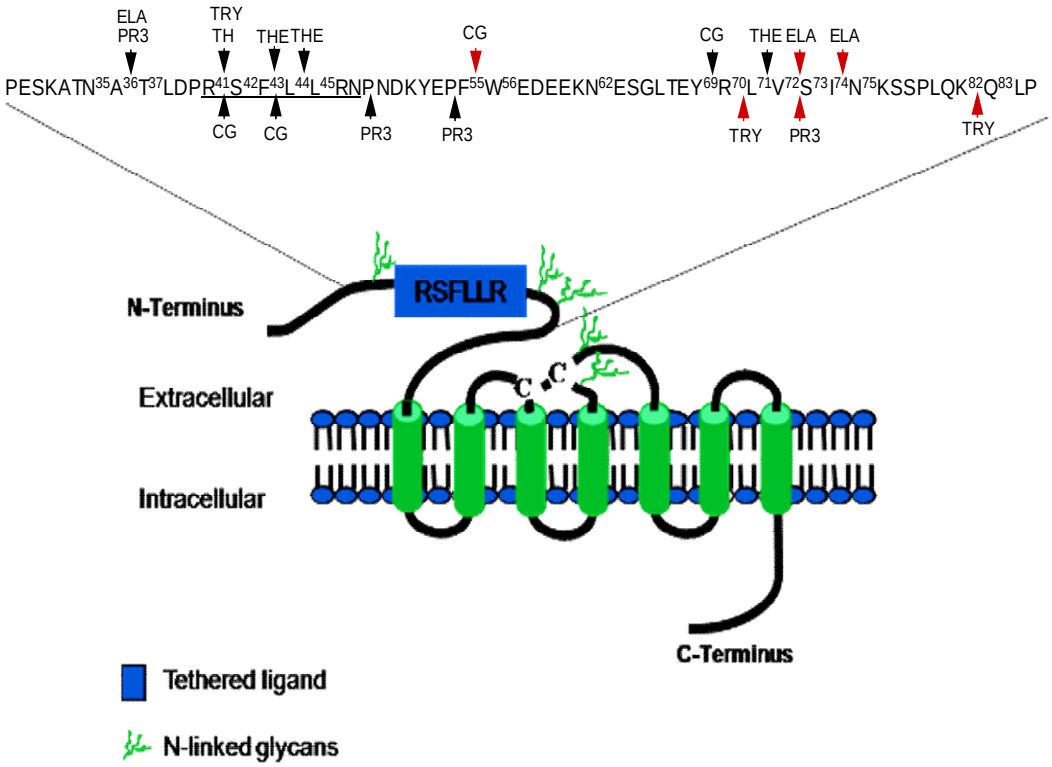

Figure 4.1.1 Potential cleavage sites of the extracellular N-terminus of hPAR$_1$ by proteinases. The red arrows indicate the preferential cleavage site for each proteinase. TH, thrombin; TRY, trypsin; THE, thermolysin; PR3, proteinase 3; CG, cathepsin G; ELA, elastase. [Adapted from (Molino *et al.*, 1995; Renesto *et al.*, 1997; Loew *et al.*, 2000; Sokolova & Reiser, 2007)].

4.2 Materials and Methods

4.2.1 Materials

Thermolysin and neuraminidase were supplied by Calbiochem, UK. Human leukocyte elastase and cathepsin-G were purchased from Elastin Products (Elastin Products Company, Inc. Missouri, USA). Proteinase 3 was obtained from Athens Research & Technology (Athens Research & Technology, Inc. Athens, Greece).

4.2.2 Generation of N62QN75QeYFP Cell Lines with Cathepsin G and Proteinase 3 Cleavage Sites Individually Removed

Site-directed mutagenesis was performed on N62QN75QeYFP (POMC-M1-$hPAR_1$(N62QN75Q)-HA.11-eYFP in pcDNA3.1) cDNA as described in chapter 2 section 2.2.2. Briefly, alanine mutations were created at amino acid positions F^{55} and W^{56} for the CG mutant (POMC-M1- $hPAR_1$N62QN75QF55AW56A-HA.11-eYFP in pcDNA3.1) or V^{72} and S^{73} for the PR3 mutant (POMC-M1-$hPAR_1$N62QN75QV72AS73A-HA.11-eYFP in pcDNA3.1) to generate $A^{55}A^{56}$ or $A^{72}A^{73}$ respectively (Figure 4.1.1). The primer sets are listed in Table 4.2.1. The resulting cDNA constructs were subsequently amplified, screened and purified as described in chapter 2 sections 2.4 and 2.5, and then sequenced to confirm the engineered mutations by MWG biotech (Milton Keynes, UK) using the MWG T7 primer. The permanently receptor expressing cell lines (in KRNK cells) were generated and cultured as described in chapter 2 section 2.6. The cell line showing the highest level of expression above control EV cells screened by FACS analysis was selected for all future experiments.

Primers	Sequences
V72AS73A	5’ GAATACAGATTAGCCGCCATCCAAAAAAGC 3’ 5’ GCTTTTTTGGATGGCGGCTAATCTGTATTC 3’
F55AW56A	5’ TAAATATGAACCAGCAGCGGAGGATGAGGAG 3’ 5’ CTCCTCATCCTCCGCTGCTGGTTCATATTTA 3’

Table 4.2.1 The oligonucleotides used for site-directed mutagenesis to generate the $hPAR_1$ CG mutant and the PR3 mutant.

4.2.3 Calcium Signalling Assay

The calcium signalling assay was performed as described in chapter 2 section 2.7. Functional receptor activity was assessed by challenging cells with the PAR_1-AP TFLLR-NH_2 (100 µM) and thrombin (5 nM).

To assess whether a test proteinase was amputating the tethered ligand from the receptor (disarming), cells were first challenged by addition of the test proteinase. Successful amputation of the tethered ligand was then monitored by a subsequent application of thrombin (5 nM), and finally followed by the addition of the PAR_1-AP TFLLR-NH_2 (100 µM). The calcium signal in response to the PAR_1 agonist proteinase will be ablated if the tethered ligand has been removed from the receptor by the test proteinase. To demonstrate that the disarmed PAR_1 is still functional and present at the cell surface, the PAR_1-AP TFLLR-NH_2 is applied. A calcium signal triggered by the PAR_1-AP is indicative of a functional PAR_1 at the cell surface, which is unresponsive to the PAR_1 agonist proteinase.

4.3 Results

4.3.1 Removal of *N*-linked glycosylation Asn^{62} and Asn^{75} from $hPAR_1$ enhances the ability of trypsin to disarm the receptor

Having found that trypsin shows reduced activity towards $hPAR_1$(N62QN75Q) by the calcium assay in Chapter 3, we then explored the ability of trypsin to disarm wt-$hPAR_1$ day5, $hPAR_1$(N62QN75Q), $hPAR_1$(N62Q) and $hPAR_1$(N75Q).

Figure 4.3.1 shows the TFLLR-NH_2 (100 µM) responses following trypsin (3, 10, 30, 100, 300 nM) and then thrombin (5 nM) challenge in wt-$hPAR_1$ and its glycosylation mutant $hPAR_1$(N62QN75Q) cells (ie. trypsin then thrombin and then TFLLR-NH_2). For wt-$hPAR_1$ the TFLLR-NH_2 responses remained same after challenging the cells with trypsin from 3-300 nM (Figure 4.3.1). Challenging the $hPAR_1$(N62QN75Q) cells with 3 nM trypsin followed by 5 nM thrombin, and then 100 µM TFLLR-NH_2, triggered a calcium signal that was similar to that seen for wt-$hPAR_1$ cells (Figure 4.3.1). However, a robust increase in the magnitude of TFLLR-NH_2 triggered calcium signal was observed after challenging the $hPAR_1$(N62QN75Q) cells with 300 nM trypsin, which was over 4-fold greater than that observed for wt-$hPAR_1$ cells ($p<0.05$) (Figure 4.3.1).

We next assessed whether glycosylation at Asn^{62} or Asn^{75} is responsible for regulating trypsin disarming of $hPAR_1$ (Figure 4.3.2). Challenging $hPAR_1$(N62Q) cells with 5 nM thrombin (TH) or 100 µM TFLLR-NH_2 (TF) resulted in a calcium response of 61.4 ± 6.7 % of A23187 and 62 ± 6.9 % of A23187 respectively (Figure 4.3.2 (A)). Challenging $hPAR_1$(N62Q) cells with 100 nM trypsin (TRY) resulted in an observable calcium signal (32 ± 8 % of A23187) (Figure 4.3.2 (A)). Addition of TH following TRY addition resulted in a marked reduction ($p< 0.001$) in the calcium response to TH compared with the response obtained with TH added alone (7.8 ± 1 % of A23187 *vs.* 61.4 ± 6.7 % of A23187) (Figure 4.3.2 (A)). Addition of TF following the addition of

TRY and TH resulted in a response that was slightly increased ($p>0.05$) in magnitude compared to the response obtained to TF following just TH addition (17.5 ± 3.6 % of A23187 *vs.* 9 ± 3 % of A23187), but was significantly reduced ($p< 0.001$) compared with the response of TF added alone (17.5 ± 3.6 % of A23187 *vs.* 62 ± 6.9 % of A23187) (Figure 4.3.2 (A)).

Challenging $hPAR_1$(N75Q) cells with TRY only resulted in a response 8 ± 1 % of A23187 (Figure 4.3.2 (B)). Challenging $hPAR_1$(N75Q) cells with TF or TH alone resulted in a calcium response of 27 ± 2 % of A23187 and 12 ± 0.7 % of A23187 respectively (Figure 4.3.2 (B)). Addition of TF following TH addition resulted in a calcium response 12 ± 1.7 % of A23187 (Figure 4.3.2 (B)). Addition of TH following addition of TRY resulted in no calcium response (Figure 4.3.2 (B)). Finally, challenging the cells with TF following TRY and TH addition triggered a calcium response 21 ± 2.7 % of A23187, which was of comparable ($p>0.05$) magnitude to the response obtained with TF alone (Figure 4.3.2 (B)).

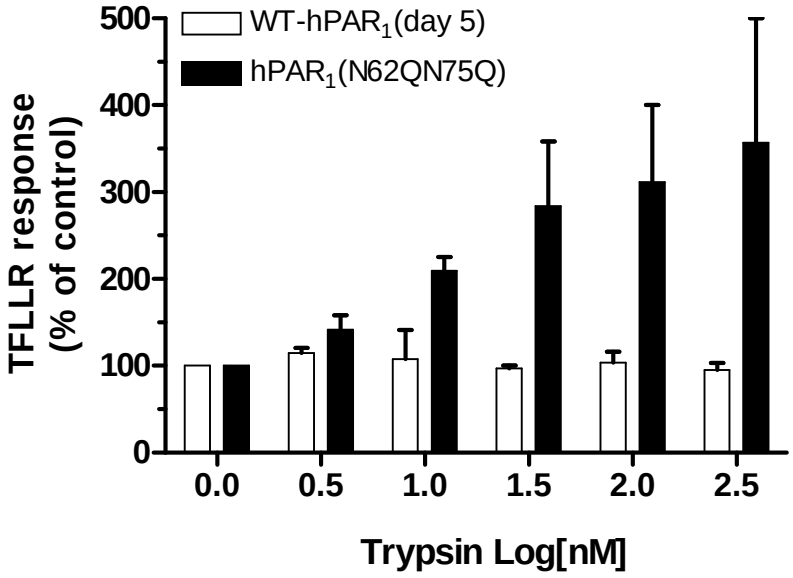

Figure 4.3.1 Analysis of trypsin disarming in wt-hPAR$_1$ and hPAR$_1$(N62QN75Q). 100 μM TFLLR-NH_2 (TF) responses following trypsin then 5 nM thrombin (TH) challenge in wt-hPAR$_1$ and hPAR$_1$(N62QN75Q) transfected KNRK cells. Cells were loaded with Fluo-3 (22 μM) for 25 minutes at RT. Cell loading/viability was assessed by addition of A23187 (calcium ionophore, 2 μM). An increase in fluorescence (E_{530}) monitored by fluorescence spectrophotometry is indicative of calcium mobilisation. The data sets are expressed as mean ± SEM from three separate experiments.

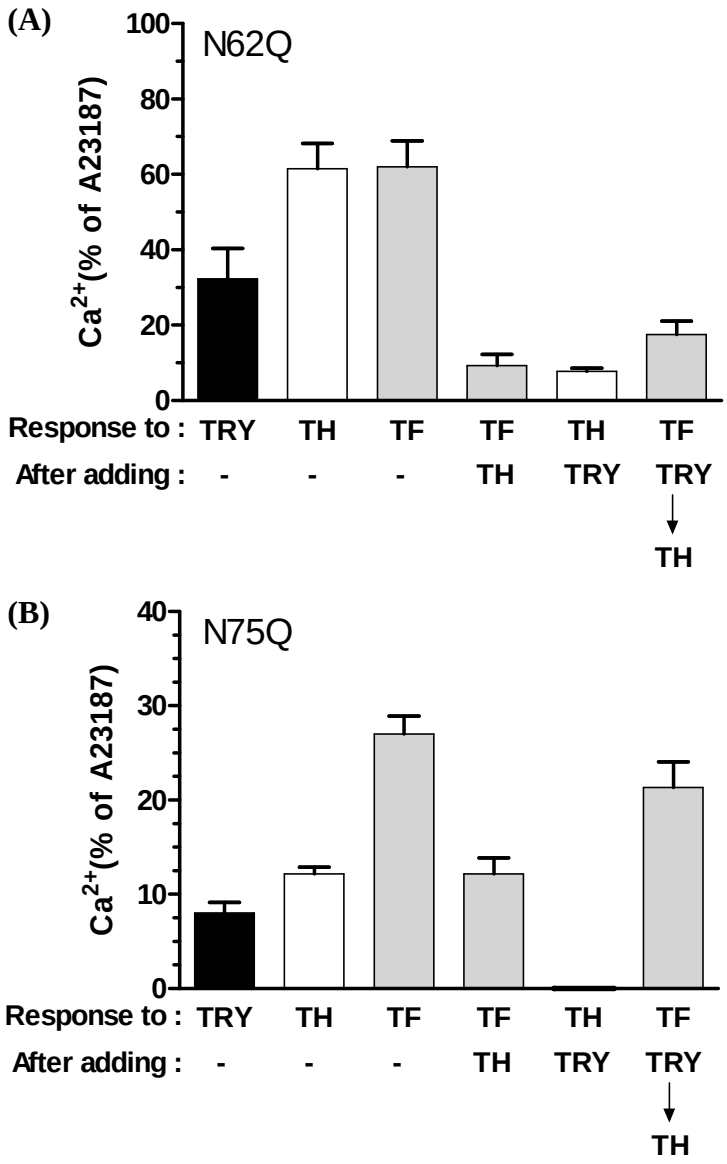

Figure 4.3.2 Analysis of trypsin disarming in hPAR$_1$(N62Q) and hPAR$_1$(N75Q). (A) hPAR$_1$(N62Q) and (B) hPAR$_1$(N75Q) transfected KNRK cells calcium signalling response following the addition of 100 nM trypsin (TRY) 5 nM thrombin (TH) and 100 μM TFLLR-NH_2 (TF). Cells were loaded with Fluo-3 (22 μM) for 25 minutes at RT. Cell loading/viability was assessed by addition of A23187 (calcium ionophore, 2 μM). An increase in fluorescence (E_{530}) monitored by fluorescence spectrophotometry is indicative of calcium mobilization. The data sets are expressed as mean ± SEM from three separate experiments.

4.3.2 Thermolysin, elastase and proteinase 3, but not cathepsin G displayed enhanced ability to disarm $hPAR_1$(N62QN75Q)

We next assessed the ability of several proteinases to activate or disarm wt-$hPAR_1$ and $hPAR_1$(N62QN75Q) using the calcium signalling assay.

For $hPAR_1$(N62QN75Q) and wt-$hPAR_1$ (day5) significant differences ($p< 0.0001$) in responses to 5 nM thrombin following the addition of thermolysin at different concentrations were observed (Figure 4.3.3). The thrombin response curve after adding thermolysin at increasing concentration for $hPAR_1$(N62QN75Q) shifted 30-fold to the left when compared to wt-$hPAR_1$. For $hPAR_1$(N62QN75Q) the calcium signalling response to thrombin started to decrease after application of thermolysin at 3 nM (~80% of control thrombin response). The thrombin triggered calcium response was totally ablated after challenging $hPAR_1$(N62QN75Q) with 300 nM thermolysin (Figure 4.3.3 closed squares). However, for wt-$hPAR_1$ the thrombin triggered calcium responses remained elevated at thermolysin concentrations up to 30 nM. The calcium signalling response to thrombin started to decrease following 100 nM thermolysin addition (~80% of thrombin control). The thrombin triggered calcium response in wt-$hPAR_1$ was totally ablated after addition of 1000 nM thermolysin.

For $hPAR_1$(N62QN75Q) and wt-$hPAR_1$ (day5) significant differences ($p< 0.0001$) in responses to 5 nM thrombin following the addition of elastase at different concentrations were observed (Figure 4.3.4). For wt-$hPAR_1$ no changes were observed in thrombin triggered calcium responses after the addition of 1 nM elastase, and the thrombin triggered calcium response was totally ablated after addition of 15 nM elastase (Figure 4.3.4). The thrombin response curve for $hPAR_1$(N62QN75Q) shifted left half a log when compared to wt-$hPAR_1$. For $hPAR_1$(N62QN75Q) the calcium signalling response to thrombin started to decrease after challenging the cells with 1 nM elastase

(~80% of control thrombin response). The thrombin triggered calcium response was totally ablated after challenging cells with 5 nM elastase (Figure 4.3.4).

For $hPAR_1$(N62QN75Q) and wt-$hPAR_1$ (day5) no significant differences ($p>0.05$) in responses to 5 nM thrombin following the addition of cathepsin G from 10 nM to 300 nM were observed (Figure 4.3.5). The thrombin triggered calcium response was totally ablated after addition of 300 nM cathepsin G for both $hPAR_1$(N62QN75Q) and wt-$hPAR_1$.

For $hPAR_1$(N62QN75Q) and wt-$hPAR_1$ (day5) significant differences ($p< 0.0001$) in responses to 5 nM thrombin following the addition proteinase 3 were observed (Figure 4.3.6). For wt-$hPAR_1$ no changes were observed in the thrombin triggered calcium response following the addition of 1000 nM of proteinase 3. In contrast, significant decreases in the response to thrombin were observed in $hPAR_1$(N62QN75Q) following the addition of proteinase 3 from 1 nM to 1000 nM. The thrombin triggered calcium signal response was totally abolished after the addition of 1000 nM proteinase 3.

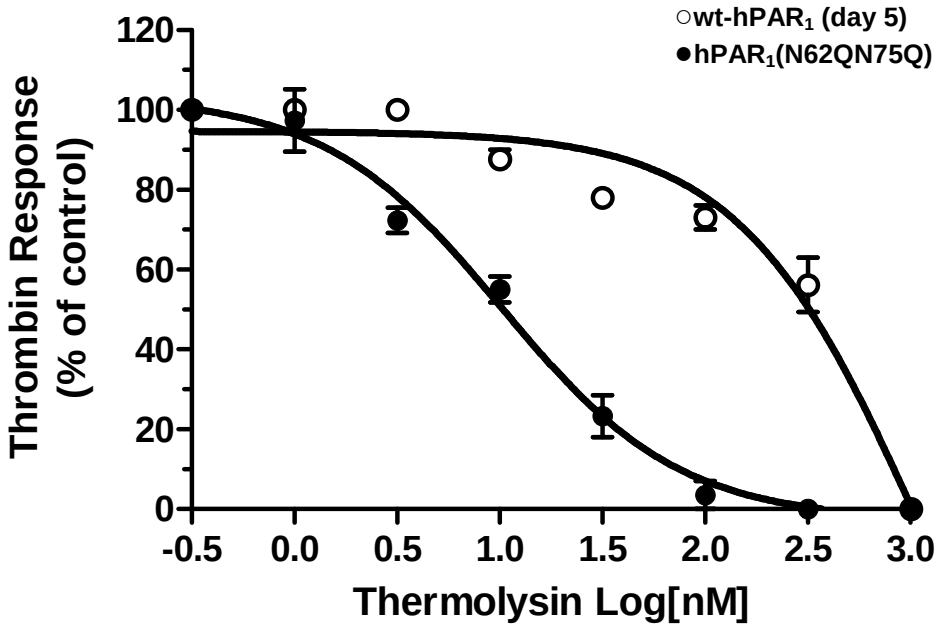

Figure 4.3.3 Analysis of thrombin-induced calcium signalling following thermolysin challenge in wt-hPAR$_1$ (day 5) and the glycosylation mutant hPAR$_1$(N62QN75Q). Cells were loaded with Fluo-3 (22 μM) for 25 minutes at RT before stimulated by the addition of thermolysin, and then further challenged with thrombin (5 nM). Cell loading/viability was assessed by addition of A23187 (calcium ionophore, 2 μM). An increase in fluorescence (E_{530}) monitored by fluorescence spectrophotometry is indicative of calcium mobilisation. Results are expressed as mean ± SEM from at least three independent experiments.

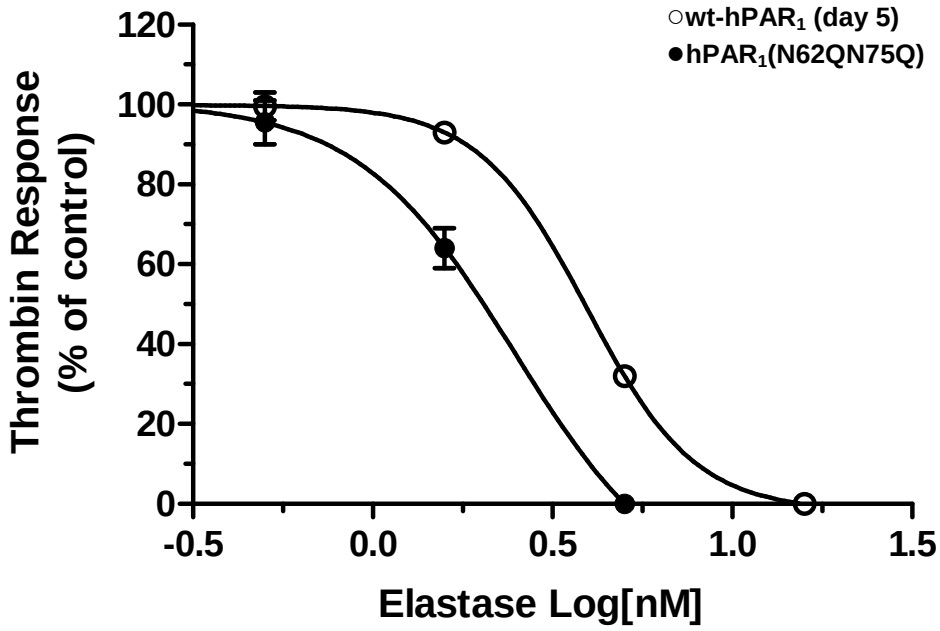

Figure 4.3.4 Analysis of thrombin-induced calcium signalling following elastase challenge in wt-hPAR$_1$ (day 5) and the glycosylation mutant hPAR$_1$(N62QN75Q). Cells were loaded with Fluo-3 (22 μM) for 25 minutes at RT before being challenged by the addition of elastase, and then further challenged with thrombin (5 nM). Cell loading/viability was assessed by addition of A23187 (calcium ionophore, 2 μM). An increase in fluorescence (E_{530}) monitored by fluorescence spectrophotometry is indicative of calcium mobilisation. Results are expressed as mean ± SEM from at least two independent experiments.

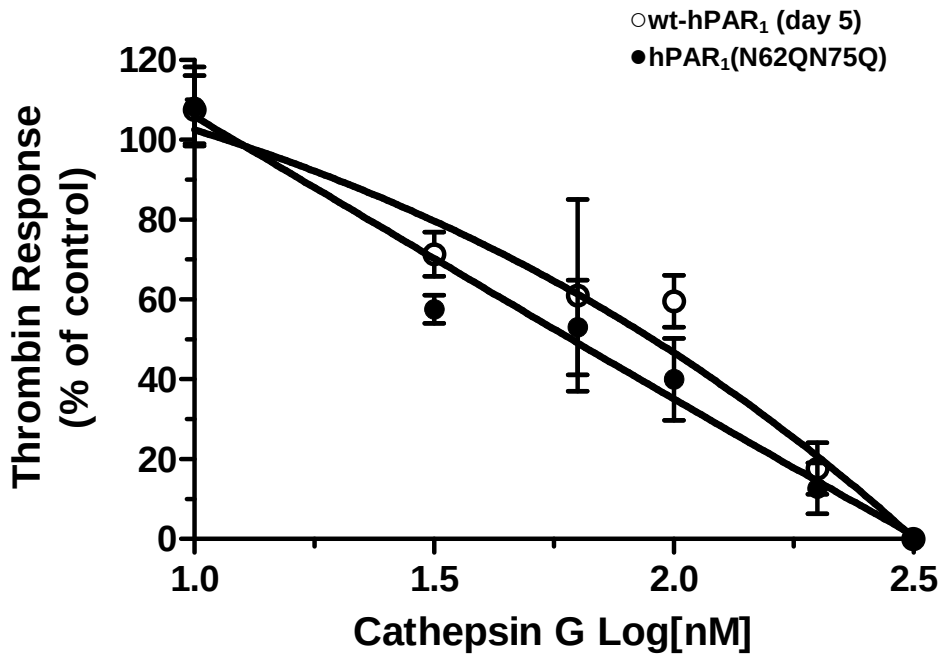

Figure 4.3.5 Analysis of thrombin-induced calcium signalling following cathepsin G challenge in wt-hPAR$_1$ (day 5) and the glycosylation mutant hPAR$_1$(N62QN75Q). Cells were loaded with Fluo-3 (22 μM) for 25 minutes at RT before being challenged by the addition of cathepsin G, and then further challenged with thrombin (5 nM). Cell loading/viability was assessed by addition of A23187 (calcium ionophore, 2 μM). An increase in fluorescence (E_{530}) monitored by fluorescence spectrophotometry is indicative of calcium mobilisation. Results are expressed as mean ± SEM from at least two independent experiments.

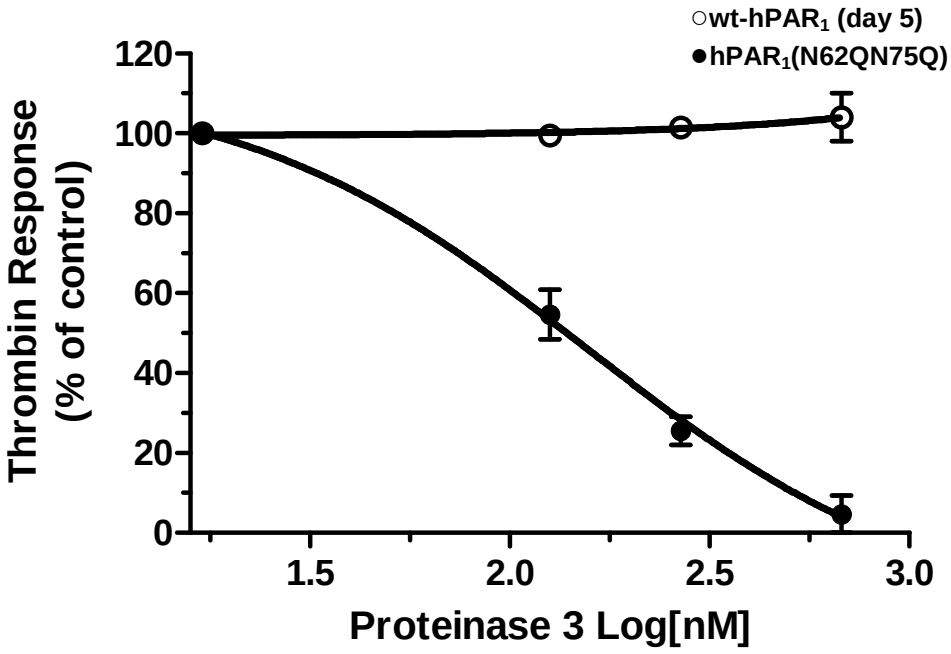

Figure 4.3.6 Analysis of thrombin-induced calcium signalling following proteinase 3 challenge in wt-hPAR$_1$ (day 5) and the glycosylation mutant hPAR$_1$(N62QN75Q). Cells were loaded with Fluo-3 (22 μM) for 25 minutes at RT before being challenged by the addition of proteinase 3 and then further challenged with thrombin (5 nM). Cell loading/viability was assessed by addition of A23187 (calcium ionophore, 2 μM). An increase in fluorescence (E_{530}) monitored by fluorescence spectrophotometry is indicative of calcium mobilisation. Results are expressed as mean ± SEM from at least three independent experiments.

4.3.3 Thermolysin, elastase, cathepsin G and proteinase 3 mainly disarm $hPAR_1(N75Q)$

The ability of thermolysin and three neutrophil serine proteinases (elastase, cathepsin G and proteinase 3) to activate/disarm $hPAR_1(N62Q)$ and $hPAR_1(N75Q)$ was investigated (Figure 4.3.7).

Challenging $hPAR_1(N62Q)$ cells with 5 nM thrombin (TH) or 100 µM TFLLR-NH_2 (TF) resulted in a calcium response of 64.7 ± 7 % of A23187 and 67.8 ± 5 % of A23187 respectively (Figure 4.3.7 (A)). In addition, addition of TF following TH addition resulted in a calcium response of 9 ± 3 % of A23187 (Figure 4.3.7 (A)). Addition of 50 nM thermolysin (THE) had no observable effect on calcium signalling in $hPAR_1(N62Q)$. Addition of TH following THE addition resulted in a calcium response at 53.5 ± 4.6% of A23187 which is comparable to that obtained with TH added alone (64.7 ± 7 % of A23187). Addition of TF following the addition of THE and TH resulted in a similar calcium response to the response obtained with TF following just TH addition (13.6 ± 4 % of A23187 and 9 ± 3 % of A23187 respectively) (Figure 4.3.7 (A)). Addition of 1.5 nM elastase (ELA) had no observable effect on calcium signalling in $hPAR_1(N62Q)$ cells (Figure 4.3.7 (A)). Addition of TH following ELA addition resulted in a calcium response 49 ± 3.5 % of A23187. Addition of TF following the addition of ELA and TH resulted in a similar calcium response to the TF response obtained following just TH addition 12 ± 1 % of A23187 and 9 ± 3 % of A23187 respectively) (Figure 4.3.7 (A)). Addition of 100 nM cathepsin G (CG) had no observable effect on calcium signalling in $hPAR_1(N62Q)$ cells (Figure 4.3.7 (A)). After challenging $hPAR_1(N62Q)$ cells with CG, addition of TH resulted in a small decrease in the calcium response compared to that obtained with TH added alone (39 ± 3.8 % of A23187 and 64.7 ± 7 % of A23187 respectively). Addition of TF following the addition of THE and TH triggered a calcium

response at 16 ± 6 % of A23187 that was slightly larger than that obtained with TF following TH addition (9 ± 3 % of A23187) (Figure 4.3.7 (A)). Addition of 300 nM proteinase 3 (PR3) had no observable effect on calcium signalling in $hPAR_1$(N62Q) cells. Addition of TH following PR3 addition resulted in a calcium response 67 ± 6.7 % of A23187 which is comparable to that obtained when TH was added alone (64.7 ± 7 % of A23187). Addition of TF following the addition of PR3 and TH resulted in a calcium response similar to that obtained with TF following TH addition (11.6 ± 4 % of A23187 and 9 ± 3 % of A23187 respectively) (Figure 4.3.7 (A)).

Challenging $hPAR_1$(N75Q) cells with TH or TF resulted in a calcium response 12 ± 0.7 % of A23187 and 27 ± 2 % of A23187 respectively. In addition, addition of TF following TH addition resulted in a calcium response 13.6 ± 1 % of A23187 (Figure 4.3.7 (B)). No observable calcium response was detected after challenging $hPAR_1$(N75Q) cells with THE. After challenging $hPAR_1$(N75Q) cells with THE, addition of TH resulted in a calcium response which was comparable to that obtained to TH alone (10 ± 1 % of A23187 and 12 ± 0.7 % of A23187 respectively), and finally challenging the cells with TF triggered a calcium response 21 ± 2 % of A23187 (Figure 4.3.7 (B)). No observable calcium response was detected after challenging $hPAR_1$(N75Q) cells with ELA or with TH following the addition of ELA. In addition, the response to TF following ELA and TH addition was the same as that obtained with TF alone (28 ± 1 % of A23187 *vs.* 27 ± 2 % of A23187) (Figure 4.3.7 (B)).

Addition of CG had no observable effect on calcium signalling in $hPAR_1$(N75Q) cells. Challenging cells with TH following the addition of CG resulted in a calcium response 10 ± 1 % of A23187 which was comparable to that obtained with TH alone (12 ± 0.7 % of A23187). Addition of TF following the addition of CG and TH triggered a calcium response which was of similar magnitude to that obtained with TF following TH

addition (17 ± 1 % and 13.6 ± 1 % of A23187 respectively) (Figure 4.3.7 (B)). Addition of PR3 had no observable effect on calcium signalling in $hPAR_1$(N75Q) cells (Figure 4.3.7 (B)). Addition of TH following challenging $hPAR_1$(N75Q) cells with PR3 resulted in a very small decrease in calcium response compared to that obtained with TH alone (10 ± 0.5 % of A23187 and 12 ± 0.7 % of A23187 respectively). Finally challenging the cells with TF following PR3 and TH addition triggered a calcium response 20.5 ± 0.5 % of A23187 (Figure 4.3.7 (B)).

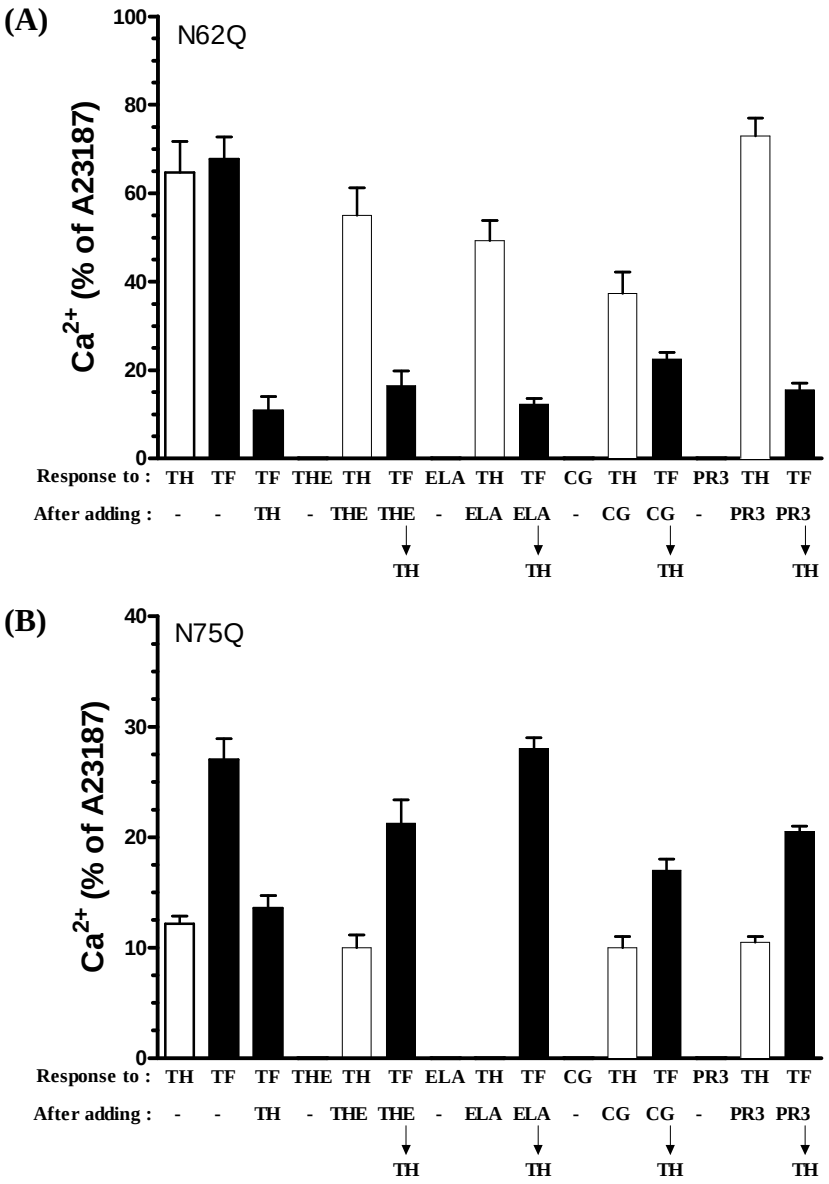

Figure 4.3.7 Analysis of $hPAR_1$(N62Q) and $hPAR_1$(N75Q) calcium signalling following proteinase stimuli. (A) $hPAR_1$(N62Q) and (B) $hPAR_1$(N75Q) cells were loaded with Fluo-3 (22 μM) for 25 minutes at RT before being stimulated by the addition of either 50 nM thermolysin (THE), 1.5 nM elastase (ELA), 100 nM cathepsin G (CG), or 300 nM proteinase 3 (PR3) and then challenged with 5 nM thrombin (TH), followed by 100 μM TFLLR-NH_2 (TF). Cell loading/viability was assessed by addition of A23187 (calcium ionophore, 2μM). An increase in fluorescence (E_{530}) monitored by fluorescence spectrophotometry is indicative of calcium mobilization. Results are expressed as the mean ± SEM of at least three independent experiments.

4.3.4 Molecular evidence that cathepsin G and proteinase 3 are disarming hPAR$_1$(N62QN75Q)

Addition of 100 nM cathepsin G (CG) to hPAR$_1$(N62QN75Q) cells before the addition of 5 nM thrombin (TH) markedly reduced ($p< 0.001$) the response to TH compared with the response obtained with TH added alone (11 ± 2 % of A23187 and 30 ± 5 % of A23187 respectively) (Figure 4.3.8 (A)). In contrast, prior addition of cathepsin G failed to reduce the thrombin calcium signal in CG mutant cells when compared to the control (32.5 ± 8 % of A23187 and 36.5 ± 8 % of A23187 respectively) ($p>0.05$) (Figure 4.3.8 (A)).

No observable calcium response to TH was observed when 300 nM PR3 had been added to the hPAR$_1$(N62QN75Q) cells prior to TH challenge (Figure 4.3.8 (B)). In contrast, prior addition of PR3 failed to reduce the thrombin calcium signal in the PR3 mutant cells, when compared to the response obtained with TH added alone (13 ± 2 % of A23187 and 12.33 ± 2.5 % of A23187 respectively) ($p>0.05$) (Figure 4.3.8 (B)).

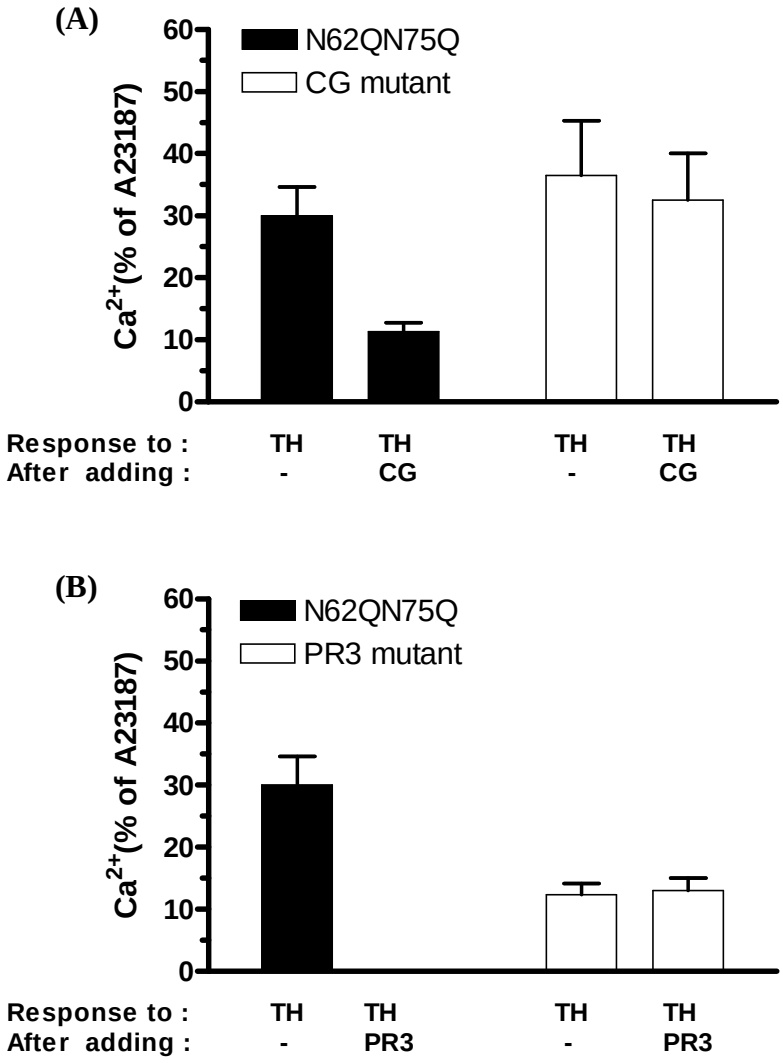

Figure 4.3.8 Molecular evidence that cathepsin G and proteinase 3 are disarming $hPAR_1$(N62QN75Q). (A) CG mutant and (B) PR3 mutant cells were loaded with Fluo-3 (22 μM) for 25 minutes at RT before the addition of test agents. Cell loading/viability was assessed by addition of A23187 (calcium ionophore, 2 μM). An increase in fluorescence (E_{530}) monitored by fluorescence spectrophotometry is indicative of calcium mobilisation. TH, 5nM thrombin; CG, 100 nM cathepsin G; PR3, 300 nM proteinase 3. Results are expressed as the mean ± SEM of at least two independent experiments.

4.4 Discussion

In this chapter, we reported for the first time that glycosylation (especially Asn^{75}) in the N-terminus of $hPAR_1$ downstream of the tethered ligand regulates receptor disarming to trypsin, thermolysin and the neutrophil proteinases elastase and proteinase 3, but not cathepsin G.

Having found that trypsin shows reduced activity towards $hPAR_1$(N62QN75Q) when compared to wt-$hPAR_1$ in Chapter 3, we explored the ability of trypsin to disarm these receptors. Our data revealed that trypsin disarms and activates $hPAR_1$(N62QN75Q) and $hPAR_1$(N75Q), whilst mainly activating wt-$hPAR_1$ and $hPAR_1$(N62Q). The most critical observation which supports this conclusion is that not only did trypsin trigger a calcium response in all PAR_1 types but the response to PAR_1-AP remained largely intact after the addition of trypsin and thrombin in the $hPAR_1$(N62QN75Q) and $hPAR_1$(N75Q) cell lines. Trypsin can activate PAR_1 by cleaving at the activating cleavage site Arg^{41}-Ser^{42} to expose the tethered ligand (Loew *et al.*, 2000; Macfarlane *et al.*, 2001; Sokolova & Reiser, 2007). Moreover, trypsin has also been reported to cleave PAR_1 at residues Arg^{70}-Leu^{71} and Lys^{82}-Gln^{83} which amputates the tethered ligand from receptor (Loew *et al.*, 2000). Furthermore these residues are suggested to be cleaved by trypsin much faster than the residues Arg^{41}-Ser^{42} (Nakayama *et al.*, 2003). Given that these two potential trypsin cleavage sites are located close to Asn^{75}, it is not surprising that in the N62QN75Q and N75Q mutants trypsin can gain easy access to these cleavage sites and therefore disarm these mutant receptors. In contrast, when PAR_1 is fully glycosylated at Asn^{75} these cleavage sites are subsequently shielded by the attached oligosaccharide and thus trypsin disarms wt-$hPAR_1$ less efficiently. Interestingly, Nakayama's previous study reported that 100 nM trypsin cleaved PAR_1 but did not activate it in HUVEC cells, thus suggesting receptor disarming (Nakayama

et al., 2003). We therefore assume that the glycosylation status of PAR_1 in HUVEC cells must be different to our PAR_1-KNRK system. Indeed, Brass and colleagues reported that PAR_1 expressed in HUVECS, platelets, and HEL cells migrated as a homogenous species with an apparent mass of 66 kDa (Brass *et al.*, 1992). This molecular mass is considerably below that reported in other cell systems, including ours, and suggests that PAR_1 is not so heavily glycosylated in these cell types. Therefore we suggest that the Asn^{62} and Asn^{75} might not be fully glycosylated in HUVECs and therefore these potential trypsin cleavage sites around Asn^{75} are more readily available for trypsin cleavage, and subsequent disarms.

Our data also revealed that thermolysin disarms $hPAR_1$(N62QN75Q) with 30 fold better efficiency than wt-$hPAR_1$. One previous study in insect SF9 cells reported that thermolysin may represent an important mechanism of rapid receptor deactivation of the human thrombin receptor (Chen *et al.*, 1996). Furthermore, like us, one previous study for PAR_1 in astrocytes found that treatment with thermolysin generated a thrombin-insensitive receptor, whereas the response to the activating peptide was not affected (Ubl *et al.*, 2000). In the literature, it is well established that the predicted thermolysin cleavage sites in PAR_1 are within the tethered ligand domain (SFLLR) at Phe^{43}-Leu^{44} and Leu^{44}-Leu^{45}, suggesting that thermolysin would be expected to remove the exodomain of PAR_1 and destroy the tethered ligand and thus disarm the receptor (Dery *et al.*, 1998; Hamilton *et al.*, 1999). Interestingly, in our study system, removing both of the glycosylation sequons (Asn^{62} and Asn^{75}) resulted in a receptor that was more efficiently disarmed by thermolysin, whereas removal of glycosylation of Asn^{62} sequon from the receptor had no observable effect on thermolysin disarming. However the N75Q receptor did display increased disarming compared to wt-$hPAR_1$, thus suggesting that this sequon regulates PAR_1 disarming by thermolysin. Therefore, we predict that

apart from the well established cleavage sites, there might be some other thermolysin cleavage sites in the N-terminus of PAR_1 especially in the region of the glycosylation site Asn^{75}. In theory, the bacterial thermolysin cleaves peptide bonds amino-terminally to the hydrophobic residues leucine and isoleucine, with some specificity for phenylalanine and valine (Hamilton *et al.*, 1999). Therefore we suggest that Leu^{71}-Val^{72} in PAR_1 may also be a potential thermolysin cleavage site, and it is very close to Asn^{75} site. When amputating the Asn^{75} glycosylation this potential thermolysin cleavage site (Leu^{71} -Val^{72}) will be more readily available for thermolysin cleavage.

We have shown that the neutrophil proteinases elastase, cathepsin G and proteinase 3 do not activate PAR_1 in our KNRK cell system, but rather disarm the receptor. Interestingly, Molino and colleagues also reported that cathepsin G can block the response of platelets and endothelial cells to thrombin (Molino *et al.*, 1995). In addition, like us, Renesto and co-workers reported that elastase, cathepsin G and proteinase 3 can cleave and inactivate PAR_1 in platelets and human endothelial cells (Renesto *et al.*, 1997). In contrast, Suzuki and colleagues reported that elastase can activate PAR_1 in human lung epithelial cells and also mentioned that proteolytic cleavage of PAR_1 by elastase might activate or inactivate the receptor depending on the site of cleavage (Suzuki *et al.*, 2005). The authors also suggested that the extent of glycosylation of the receptor could influence the site and extent of cleavage of the receptor (Suzuki *et al.*, 2005). In our current study, we note that elastase disarms $hPAR_1$(N62QN75Q) better than wt-$hPAR_1$ at the same concentration, and 1.5 nM elastase disarms $hPAR_1$(N75Q), but not $hPAR_1$(N62Q). Renesto and colleagues' mass spectrometry study indicated that elastase cleaves the N-terminus of $hPAR_1$ at Val^{72}-Ser^{73} and Ile^{74}-Asn^{75} which are located after the tethered ligand (Renesto *et al.*, 1997). Furthermore, Loew *et al.* reported that elastase cleaved the PAR_1 exodomain at Ala^{36}-Thr^{37}, Val^{72}-Ser^{73} and

Ala^{86}-Phe^{87} sites with preferential cleavage at Val^{72}, which would disable the receptor (Loew *et al.*, 2000). Therefore after amputating the Asn^{75} glycosylation, the potential cleavage sites Val^{72}-Ser^{73} might be more easily accessible for elastase cleavage.

Since cathepsin G (CG) has been reported to have both activating and disarming actions on PARs (Molino *et al.*, 1995; Renesto *et al.*, 1997; Sambrano *et al.*, 2000; Ramachandran *et al.*, 2007), we tested the role of N-terminal glycosylation of $hPAR_1$ in regulating this proteinase. We have demonstrated that CG could clearly disarm $hPAR_1$(N62QN75Q) and wt-$hPAR_1$, preventing activation by thrombin, but not by the PAR_1-AP TFLLR-NH_2. In addition, our data also revealed that CG at 100 nM disarms $hPAR_1$(N62Q) and $hPAR_1$(N75Q). Like us others have also reported that CG at 30nM could disarm PAR_1 (Ramachandran *et al.*, 2007). Molino *et al.* reported that in addition to the Arg^{41}-Ser^{42} site, CG cleaves PAR_1 at Phe^{43}-Leu^{44} and Phe^{55}-Trp^{56} removing the tethered ligand and rendering the receptor unresponsive to thrombin (Molino *et al.*, 1995). In 1997 Renesto and colleagues' mass spectrometry study indicated that CG cleaves PAR_1 on platelets and endothelial cells downstream of the thrombin cleavage site at Phe^{55}-Trp^{56} and Tyr^{69}-Arg^{70} (Renesto *et al.*, 1997). Thus we then concluded that CG might have four potential cleavage sites in the N-terminus of $hPAR_1$ (Arg^{41}-Ser^{42}, Phe^{43}-Leu^{44}, Phe^{55}-Trp^{56}, and Tyr^{69}-Arg^{70}). Furthermore, Loew *et al.* kinetic analyses showed that the preferential CG cleavage site for PAR_1 is Phe^{55}-Trp^{56} site (Loew *et al.*, 2000). Moreover, our finding with the CG mutant is in accord with previous report that has demonstrated that Phe^{55}-Trp^{56} is the main region cleaved within the receptor N-terminus by cathepsin G (Molino *et al.*, 1995). Also, we have reported from Chapter 3 that Asn^{62} seems not actually heavily glycosylated in our KNRK system. Therefore we suggest that PAR_1 glycosylation have no observable effect in regulating cathepsin G sensitivity towards PAR_1.

Finally, we assessed proteinase 3 (PR3) inhibition of thrombin-induced Ca^{2+} mobilization in wt-$hPAR_1$, $hPAR_1$(N62QN75Q), $hPAR_1$(N62Q) and $hPAR_1$(N75Q). Our data revealed that 300 nM PR3 disarms $hPAR_1$(N62QN75Q) but not wt-$hPAR_1$, $hPAR_1$(N62Q) or $hPAR_1$(N75Q). It is well estabilished that PR3 has an elastase-like specificity for Ala, Ser, and Val at the P1 site (Rao *et al.*, 1991a). One previous study on human oral epithelial cells also pointed out that PR3 can rapidly cleave PAR_2 between Arg and Ser and relatively inefficiently cleave between Lys and Val (Uehara *et al.*, 2002). Furthermore, PR3 cleaved the peptide corresponding to the N-terminus of PAR_2 at Arg^{36}-Ser^{37} indicating that site of the PAR_2 is structurally accessible by PR3 (Uehara *et al.*, 2002). Interestingly, one previous study on synthetic peptides reported that the cleavage site for PR3 in N-terminus of PAR_1 is Val^{72}-Ser^{73} (Renesto *et al.*, 1997). In addition, Loew and colleagues' kinetic analysis on the N-terminus domain of PAR_1 showed that PR3 early cleavage sites for PAR_1 are Ala^{36}-Thr^{37}, Pro^{48}-Asn^{49}, Val^{72}-Ser^{73}, Ala^{92}-Ser^{93}, and the late cleavage site is Pro^{54}-Phe^{55} (Loew *et al.*, 2000). Furthermore, Sokolova *et al.* suggested in recent reviews that PR3 cleaves human PAR_1 at Ala^{36}-Thr^{37} and Val^{72}-Ser^{73} (Sokolova & Reiser, 2007). Although there are differences, previous studies have agreed that the Val^{72}-Ser^{73} might be the earliest cleavage site for PR3. We therefore altered that site by creating a mutation $A^{72}A^{73}$ in our $hPAR_1$(N62QN75Q) (named PR3 mutant), and indeed the PR3 almost immediately lost the ability to disarm the mutant receptor. As mentioned by Loew *et al.* there exists a late cleavage site between Pro^{54}-Phe^{55}, we therefore suggest that apart from the Val^{72}-Ser^{73} cleavage site there might exist relatively inefficient later cleavage events between Pro^{54}-Phe^{55}, and possibly at Pro^{48}-Asn^{49} (Loew *et al.*, 2000). Thus there might be a possibility that if we expose PAR_1 with PR3 for a greater length of time, PR3 might disarm wt-$hPAR_1$. Indeed, we did notice that this phenomenon happened casually when we

accidently pre-incubated PAR_1 with PR3 for more than 3 min (data not shown). We have shown that in wt-$hPAR_1$ cells, PR3 does not disarm the receptor immediately (within 1 min), however, after the amputation of the glycosylation in Asn^{62} and Asn^{75} PR3 immediately disarmed the glycosylation mutant receptor and inhibited thrombin-induced Ca^{+} mobilization. We therefore suggest that glycosylation at Asn^{62} and Asn^{75} together regulate $hPAR_1$ signalling to proteinase 3.

Interestingly Compton's previous study reported that sialylation regulates $hPAR_2$ signalling to tryptase (Compton *et al.*, 2002b). After removing the sialysation from the receptor, the receptor becomes increasingly sensitive towards tryptase activation. Therefore it will be of great interest to assess whether sialylation plays an important role in regulating $hPAR_1$ signalling to proteinases studied in this chapter in the future work.

5.1 Introduction

According to the derived amino acid sequence, $hPAR_4$ possesses only one putative *N*-linked glycosylation site ($N^{56}D^{57}S^{58}$) which is located on the receptor N-terminus downstream of the tethered ligand (Figure 5.1.1) (Compton, 2003). A previous study has reported that PAR_4 runs higher than its predicted molecular mass when assessed by western blot analysis (Shapiro *et al.*, 2000). Bolton and colleagues have reported that PAR_4 expressed in human eosinophils and mononuclear cells migrates as two bands, one at ~80 kDa and the other one at ~40 kDa; the authors also suggested, but did not prove, that the apparent higher MW may be a result of differential glycosylation (Bolton *et al.*, 2003). During the course of this thesis Leger and co-workers demonstrated that *(i)* wt-PAR_4 migrates with a molecular mass from 32-81 kDa; *(ii)* PNGase-F treated wt-PAR_4 runs with a molecular weight from 32-70 kDa, and *(iii)* the mutant N56S also ran between 32-70 kDa (Leger *et al.*, 2006). In addition, the authors showed that PAR_4 undergoes homologous dimerisation and heterologous dimerisation with PAR_1. Glycosylation was not involved in homologous PAR_4 dimerisation since the glycosylation mutant was also found to dimerise (Leger *et al.*, 2006). Although PAR_4 has been demonstrated to be glycosylated, there currently exists no information on the role of *N*-linked glycosylation or receptor sialylation in regulating PAR_4 signalling. Therefore, in this chapter we sought to 1) establish whether PAR_4 is glycosylated, and 2) explore the role of glycosylation and sialylation in regulating $hPAR_4$ cell surface expression and receptor signalling.

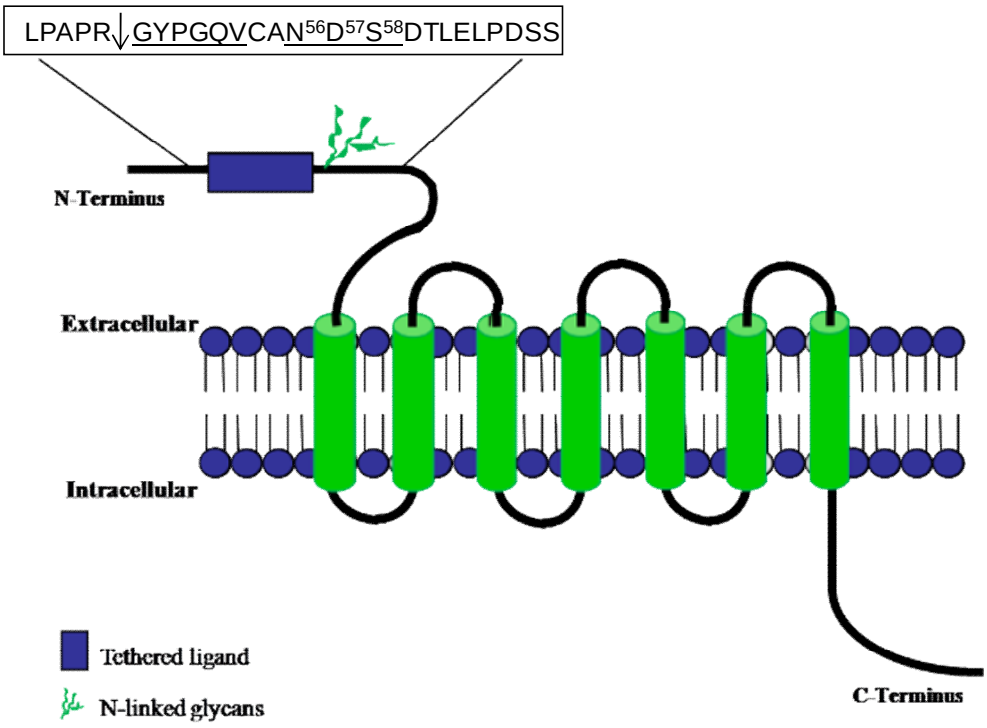

Figure 5.1.1 Representative model of hPAR$_4$ displaying the potential *N*-linked glycosylation site. hPAR$_4$ contains one potential *N*-linked glycosylation sequon ($N^{56}D^{57}S^{58}$), which is located near the cleavage/activation site (R↓G) and tethered ligand (GYPGQV) of the receptor. [Adapted from (Compton, 2003)]

5.2 Materials and Methods

5.2.1 Materials

Monoclonal anti-AU1 antibody was obtained from COVANCE (California, USA). Anti-PAR_4 polyclonal antibody was purchased from Santa Cruz Biotech (Santa Cruz, CA). PNGaseF was purchased from New England Biolabs (Herts, UK.). Phospho-p44/42 MAP kinase (Thr202/Tyr204) antibody, p44/42 MAP kinase antibody, phospho-p38-MAPK antibody and p38-MAPK antibody were purchased from Cell Signaling Technology, Inc. through New England Biolabs (Herts, UK.). Restore^{TM} Western Blot stripping buffer was bought from PIERCE (Northumberland, UK). PCR primers were designed in house and made by MWG Biotech (Milton Keynes, UK).

5.2.2 Generation of $hPAR_4$ Expressing Cell Line

$hPAR_4$ (POMC-AU1-$hPAR_4$-HA.11 in pcDNA3 (Figure 5.2.1)) was supplied by Dr Compton. $hPAR_4$ was transfected into KNRK cells cultured as described in chapter 2 section 2.6.3. Following single cell cloning (as described in chapter 2 section 2.6.4) cells expressing $hPAR_4$ were selected by calcium signalling assay using PAR_4-AP AYPGQV-NH_2 (100 μM), or by FACS using anti-AU1 or anti-PAR_4 antibody.

5.2.3 Generation of wt-$hPAR_4$ and $hPAR_4$(N20Q) Constructs and Expressing Cell Lines

Construction of $hPAR_4$-eYFP (POMC-AU1-$hPAR_4$-HA.11-eYFP) was essentially performed by fusing $hPAR_4$-HA.11 (POMC-AU1-$hPAR_4$-HA.11) and HA.11-eYFP by overlapping PCR. The PCR amplifications were carried out as described in chapter 2 section 2.2.1. Briefly, $hPAR_4$-HA.11 cDNA was generated from $hPAR_4$ (POMC-AU1-

hPAR$_4$-HA.11 in pcDNA3) expression vector using the *Hind*III-POMC forward primer and the HA.11-PAR$_4$ reverse primer (Table 5.2.1), and PCR amplified through 25 cycles of denaturation at 94°C for 30 sec, annealing at 55°C for 30 sec, and extension for 2 min at 68°C. HA.11-eYFP was amplified from pEYFP vector (Clontech) using a HA.11-eYFP forward primer and an eYFP reverse primer (see Table 5.2.1). The reaction was amplified through 35 cycles of denaturation at 94°C for 30 sec, annealing at 55°C for 30 sec, and extension for 2 min at 68°C. HA.11-eYFP was then fused to hPAR$_4$-HA.11 to generate hPAR$_4$-eYFP cDNA by overlapping PCR using the *Hind*III-POMC forward primer and the eYFP reverse primer, amplifying through 25 cycles of denaturation at 94°C for 30 sec, annealing at 55°C for 30 sec, and extension for 2 min and 30 sec at 68°C. A restriction digest reaction was performed on hPAR$_4$-HA.11-eYFP PCR purified product in order to clone into pcDNA3. Briefly, the restriction digest reaction was carried out by incubating 10 µl of DEPC water, 5 µl of POMC-AU1-hPAR$_4$-HA.11-eYFP PCR product, 2 µl of 10×buffer (2), 2 µl of BSA (100 µg/ml), 0.5 µl of *Xho*I (2000 U/µl) and 0.5 µl of *Hind*III (2000 U/µl) at 37°C for overnight. After gel purification, the *Hind*III-POMC-AU1-hPAR$_4$-HA.11-eYFP-*Xho*I cDNA was ligated between the *Hind*III and the *Xho*I sites of the pcDNA3 vector. The wt-hPAR$_4$ (POMC-AU1-hPAR$_4$-HA.11-eYFP in pcDNA3) expression vector was subsequently amplified and purified, and the colonies containing the hPAR$_4$-eYFP insert were selected and sent to MWG biotech (Milton Keynes, UK) for sequencing using MWG T7 and SP6 primers as described in chapter 2 sections 2.4, 2.5.

For site directed mutatgenesis protocols oligonucleotides (Table 5.2.2) were designed to replace the asparagine (N) residue at position 20 in our hPAR$_4$ reading frame with a glutamine (Q) residue to generate hPAR$_4$(N20Q) expression vector (Figure 5.2.1). The site-directed mutagenesis assays were conducted using the QuickChange® site-directed

mutagenesis kit (Stratagene) as described in chapter 2 section 2.2.2. The resulting cDNA constructs were subsequently amplified, screened and purified as described in chapter 2 sections 2.4, 2.5, and then sequenced to confirm the engineered mutations by MWG biotech (Milton Keynes, UK) using the MWG T7 and SP6 primers.

The permanently expressing wt-hPAR$_4$-KNRK (WT) and hPAR$_4$(N20Q)-KNRK (N20Q), wt-hPAR$_4$-Pro5 (Pro5-hPAR$_4$) and wt-hPAR$_4$-Lec2 (Lec2-hPAR$_4$) cell lines were generated and cultured as described in chapter 2 section 2.6. The clone showing the highest level of expression above control EV cells in FACS analysis was selected for future experiments. KNRK cells at 90%-100% confluence and CHO cells at 40% confluence were used for experiments.

Primer	Sequence
HA.11-eYFP forward	5'-CCCTATGATGTTCCCGATTATGCCATGGTGAGCAAGGGC-3'
eYFP reverse	5'-GGGCCCCTCGAGTTACTTGTACAGCTCGTCCAT-3'
HindIII-POMC forward	5'-GATCGAAGCTTAGCATGCCGAGATCGTGCTGC-3'
HA.11-PAR_4 Reverse	5'-GGCATAATCGGGAACATCATAGGG-3'

Table 5.2.1 Primers used in the PCR reactions for the generation of $hPAR_4$-eYFP cDNA.

Primer	Sequence
N20Q forward	5'-GCCAAGTCTGTGCCCAAGACAGTGACACCCTG-3'
N20Q reverse	5'-CAGGGTGTCACTGTCTTGGGCACAGACTTGGC-3'

Table 5.2.2 The oligonucleotides used in the site-directed mutagenesis for the generation of $hPAR_4$(N20Q).

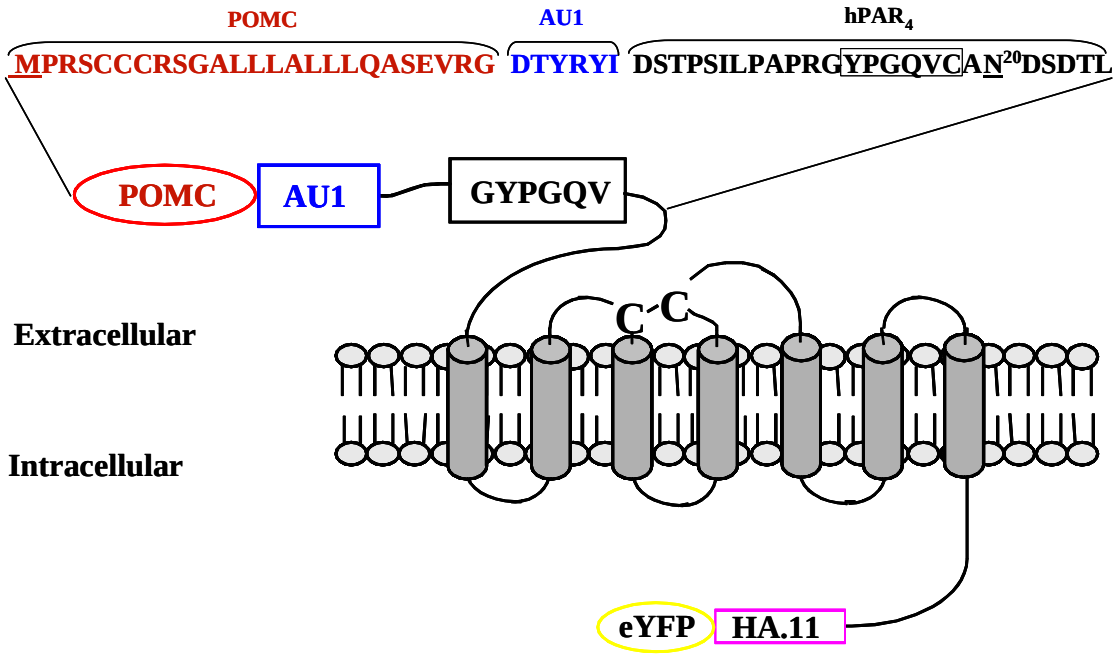

Figure 5.2.1 Representative model of POMC-AU1-hPAR$_4$-HA.11-eYFP in pcDNA3 (named: wt-hPAR$_4$). In our PAR$_4$ model, the potential *N*-linked glycosylation sequon is $N^{20}D^{21}S^{22}$ and is located close to the tethered ligand (GYPGQV). Pro-opiomelanocortin (POMC) signal peptide and AU1 (DTYRYI) epitope tag were fused to the N-terminus of hPAR$_4$. The enhanced yellow fluorescent protein (eYFP) and the haemagglutinin epitope (YPYDVPDYA) were fused to the C-terminal tail of hPAR$_4$. The disulphide bridge is shown by the two cysteines (C-C). The POMC signal peptide enabled efficient expression of PAR$_4$, whilst the AU1 and HA.11epitope tags facilitated isolation and detection of the receptor.

5.2.4 Transient Transfection

Wt-hPAR$_4$ was transfected into 60% confluent parent KNRK, Hela, and COS7 cells in T25 flasks under sterile conditions. The transient transfection was performed using the same transfection method as that described in chapter 2 section 2.6.3, except cells were grown in DMEM complete growth medium for 48-72 h following transfection. Cells were analysed for receptor expression by FACS analysis between 48 and 72 h post-transfection.

5.2.5 Flow Cytometry and Confocal Microscopy Analysis

For the WT and N20Q cell lines, the light emitted by the eYFP (530 nm) fused to the receptor was used to assess receptor global expression. Ten thousand cells were analysed by FACS (chapter 2 section 2.8). Confocal microscopy analysis was performed as described in chapter 2 section 2.9.

5.2.6 Western Blot Analysis

Immunoprecipitation of wt-hPAR$_4$ from KNRK, Pro5 and Lec2 cells and hPAR$_4$(N20Q) from KNRK cells via the HA.11 epitope tag was carried out as described in chapter 2 section 2.10. To assess the degree of *N*-linked glycosylation of hPAR$_4$, immunoprecipitated wt-hPAR$_4$ from KNRK was incubated with 2 µl PNGaseF (500,000 U/ml) at 37 ºC for 1 h. Samples were then separated on a 10% SDS/PAGE gel before transfer to Hybond C PVDF membrane. The membrane was incubated with the murine anti-HA.11 monoclonal antibody [1 µg/ml] in PBS (0.1% Tween-20) 2% non-fat milk at 4^{o}C overnight. The membrane was then incubated with goat anti-mouse HRP [0.25 µg/ml] in PBS (0.1% Tween-20) with 2% non-fat milk for 60 min at RT before analysis using the ECL detection system. Blots were then stripped at RT for 20 min in

Western Blot Stripping Buffer (PIERCE), and then incubated with the anti-eYFP antibody [0.5 μg/ml] in PBS (0.1% Tween-20) 2% non-fat milk at 4^{o}C overnight. Preliminary experiments confirmed that the stripping agent had removed the majority of the primary & secondary antibody. After incubating with goat anti-mouse HRP [0.25 μg/ml] in PBS (0.1% Tween-20) containing 2% non-fat milk for 60 min at RT, the $hPAR_4$ receptor was visualized by using the ECL detection system as described in chapter 2 section 2.11.

5.2.7 Calcium Signalling Assay

The calcium signalling assay was performed essentially as described in chapter 2 section 2.7. Functional $hPAR_4$ activity was assessed by treating cells with the PAR_4-AP AYPGQV-NH_2 (100 μM) and thrombin (5 nM). In order to remove endogenous PAR_1 activity in CHO cells the $hPAR_1$-AP TFLLR-NH_2 (100 μM) was added to the cells prior to the addition of PAR_4-AP.

5.2.8 MAP Kinase Signalling Analysis

WT and N20Q cells were seeded into 6-well plates and grown to over 90% confluence. Cells were then quiesced for 24 h in DMEM serum-free medium (DMEM with 2 mM L-glutamine and 1% penicillin/streptomycin, 100 μM sodium pyruvate). Cells were then challenged with the PAR_4-AP AYPGQV-NH_2 (100 μM) at different time points (5, 10, 20, 30 and 60 min) before the reaction was stopped and cells lysed by replacing the buffer with 0.3 ml of Laemmli's sample buffer [2% SDS, 10% glycerol, 50mM Tris-HCl (pH 6.8), 5 mM EDTA, 0.008% bromophenol blue, 0.5% β-Mercaptotheanol]. The cell lysates were then transferred into 1.5 ml Eppendorf tubes and centrifuged at 13200

g for 10 min at 4°C. The supernatants were then recovered and samples were boiled for 5 min before being resolved on a 10% SDS gel.

Activation of ERK and p38-MAPK was monitored by immunoblot analysis with antibodies for phosphorylated (activated) signalling protein. Immunoblotting with equal amounts of sample protein (25 µl/well) loaded in each well was carried out as described in chapter 2 section 2.11. Briefly, membranes were incubated with anti-phosphorylated antibody [1 µg/ml] in 5% BSA, PBS (0.1% Tween 20) overnight at 4^{o}C, and then incubated with the secondary antibody donkey anti-rabbit IgG HRP-linked antibody [1 µg/ml] for 60 min in PBS (0.1% Tween 20) 2% non-fat milk at RT for 60 min. In all experiments, blots were stripped at 37°C for 2 h in Western Blot Stripping Buffer (PIERCE) after the phosphorylated signalling blot assay and re-probed with antibodies [1 µg/ml] for visualizing the total protein to confirm equal protein loading.

5.3 Results

5.3.1 Generation of Functional Cell Lines for $hPAR_4$

We initially attempted to transfect and express $hPAR_4$ in the KNRK cell line. Functional $hPAR_4$ expressing cells ($hPAR_4$-KNRK) were assessed by *(i)* measuring agonist triggered increases in intracellular calcium levels, and *(ii)* FACS analysis by staining with anti-AU1 FITC antibody. However, the calcium signalling experiments with $hPAR_4$-KNRK cells failed to demonstrate any appreciable activation of PAR_4 following the addition of the PAR_4-AP AYPGQV-NH_2 (100 μM) (data not shown). FACS data from the first round of $hPAR_4$-KNRK single cell cloning also failed to show any differences in fluorescence compared to EV cells (data not shown). Thus, we decided to fuse eYFP protein to the tail of $hPAR_4$ to help us identify positive clones.

5.3.2 Generation of wt-$hPAR_4$ and $hPAR_4$(N20Q) constructs and Expressing Cell Lines

Since PAR_4 was proving problematic to express, we attached enhanced yellow fluorescent protein (eYFP) to the c-terminal tail of the receptor (Figure 5.2.1) in the hope that positive clones would be easier to select by FACS (we have termed the eYFP tagged $hPAR_4$ as wt-$hPAR_4$). The wt-$hPAR_4$ and $hPAR_4$(N20Q) cDNA constructs were successfully generated. Automated DNA sequencing confirmed the presence of the desired mutation (data not shown).

In order to determine the best cell line for expressing $hPAR_4$, we selected Hela, COS7 and KNRK cell lines for transient transfection of wt-$hPAR_4$, and assayed for receptor expression by FACS analysis using eYFP as a fluorescence signal. Unfortunately, wt-$hPAR_4$ transfected Hela cells died of bacterial infection (data not shown). FACs data obtained from wt-$hPAR_4$ transfected COS7 and KNRK (Figure 5.3.1) showed that there

was a bigger rightward shift between the negative control cells and WT transfected cells in the KNRK cell line than in the COS7 cell line. Therefore WT and N20Q permanently expressing KNRK cell lines were successfully generated. Pro5-hPAR$_4$ and Lec2-hPAR$_4$ were also produced in order to study the effect of sialic acid on receptor expression and function.

5.3.3 N20Q Displays Diminished Cell Surface Expression and Partial Cytosolic Retention

Two wt-hPAR$_4$ transfected KNRK cell lines were successfully generated (high-wt & medium-wt) (Figure 5.3.2). The N20Q displayed similar global expression to the medium-wt ($p>0.05$) (Figure 5.3.2 (B) and (C)), and both displayed significantly less expression compared to high-wt [percentage relative to high-wt ± S.E.M: 30.7 ± 1 % (n=6) for medium-wt and 30.4 ± 3 % (n=6) for N20Q respectively].

Analysis of hPAR$_4$ localization by confocal microscopy demonstrated that all PAR$_4$ expressing cell types were expressed on the cell membrane (Figure 5.3.3 (B), (C) and (D)), whilst there was no specific fluorescence (eYFP signalling) observed in EV (Figure 5.3.3 (A)). However, the relative florescence intensity of the receptor at the cell surface appeared to be reduced in N20Q when compared with high-wt and medium-wt. Furthermore, N20Q was also observed in the cytoplasm to a greater degree than that observed in wt-hPAR$_4$ (Figure 5.3.3 compare (B) & (C) with (D)).

(A)

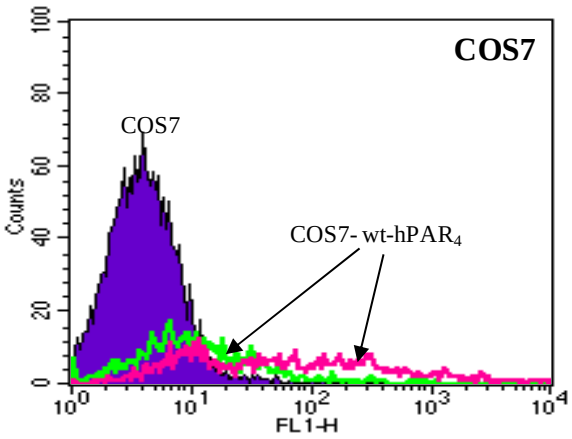

(B)

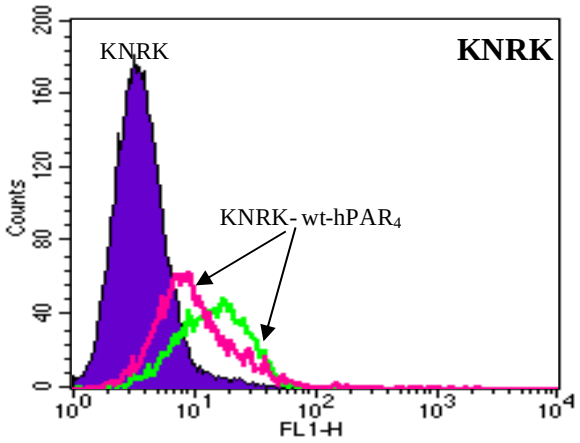

Figure 5.3.1 Flow cytometry analysis of wt-hPAR$_4$ transiently transfected into KNRK and COS7 cells. (A) COS7 and **(B)** KNRK cells were transfected with wt-hPAR$_4$, and then cultured for 72 hours in normal growth medium. Cells were washed, and analyzed for fluorescence (FL1-H) by flow cytometry.

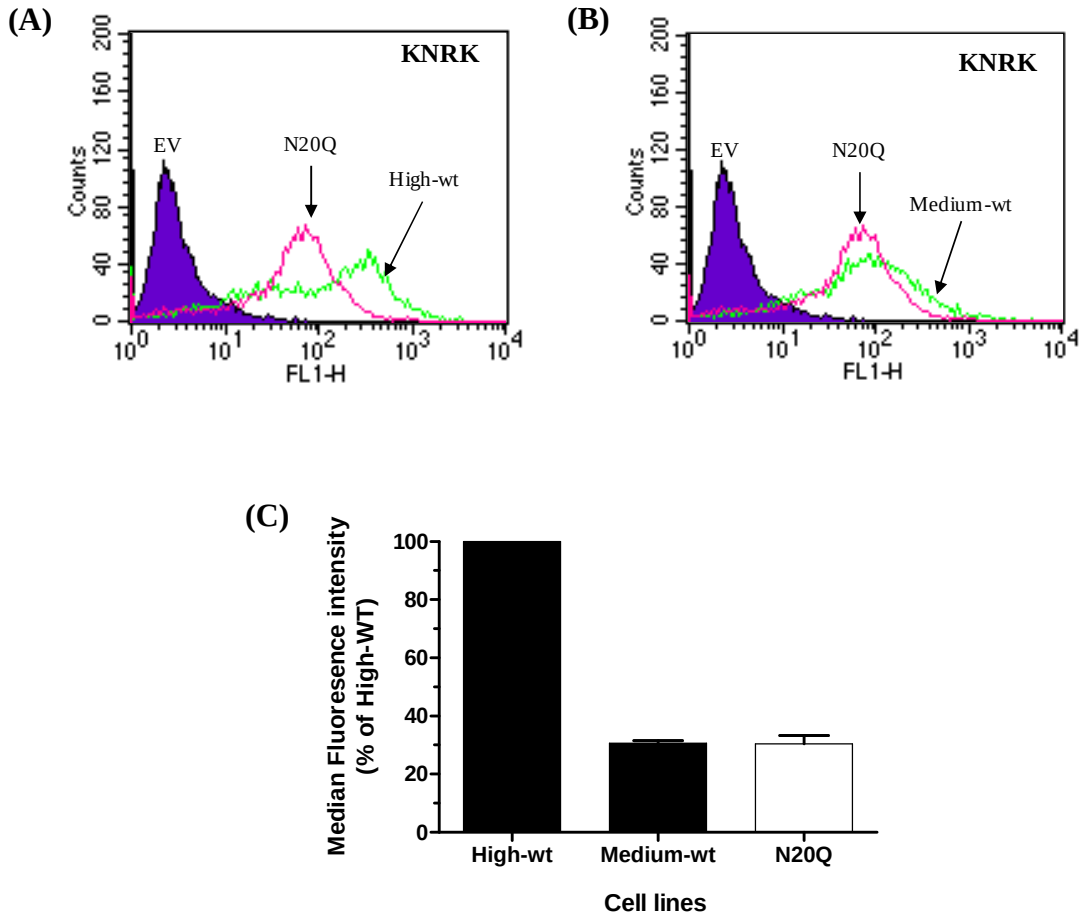

Figure 5.3.2 Flow cytometry analysis for wt-hPAR$_4$ and hPAR$_4$(N20Q) KNRK expressing cell lines. (A): Flow cytometry analysis for EV, high-wt and N20Q. **(B):** Flow cytometry analysis to compare medium-wt and N20Q receptor expression. Cells were washed in PBS, and analyzed for fluorescence (FL1-H) by flow cytometry. The results are representative of three separate experiments. **(C):** Bar graph showing relative receptor expression for N20Q, high-wt and medium-wt cell lines. Results are expressed as the mean ± SEM of six separate experiments.

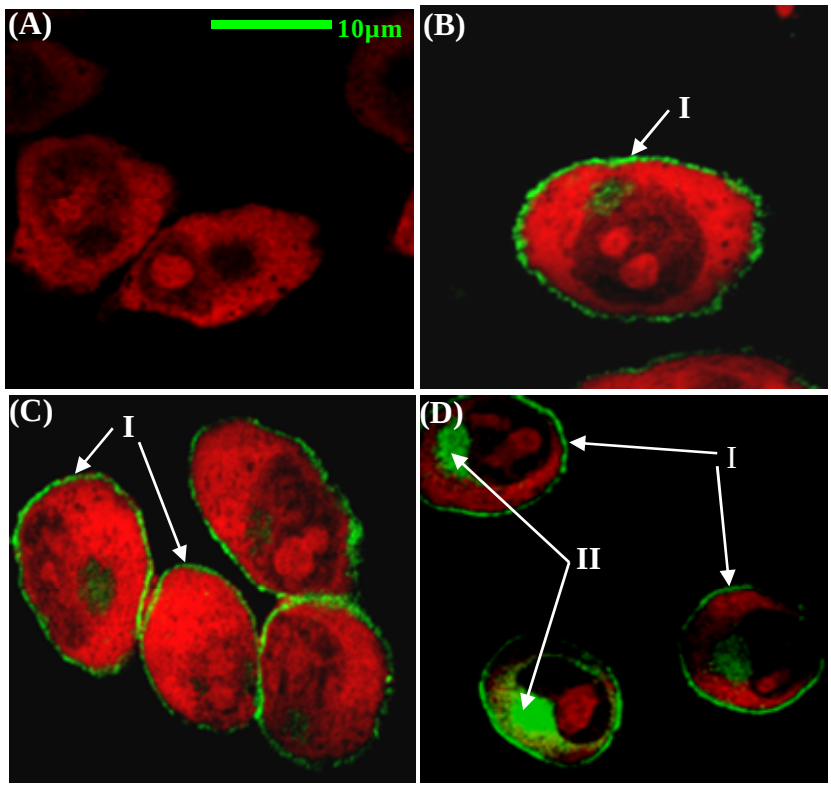

Figure 5.3.3 Removal of the glycosylation sequon in hPAR$_4$ results in partial retention of the receptor within the cytosol. Confocal microscopy images for **(A)** EV, **(B)** High-wt, **(C)** Medium-wt, **(D)** N20Q. Cells were grown on glass coverslips before fixing and permeabilising. Cells were stained with propidium iodide prior to visualising. eYFP is visualised here in green and propidium iodide in red. **I:** Cell surface expression; **II:** internal receptor expression. The results are representative of four separate experiments.

5.3.4 $hPAR_4$ is a Glycosylated Receptor

Western blot analysis of immunoprecipitated wt-$hPAR_4$ using either the HA.11 antibody or the eYFP antibody demonstrated that wt-$hPAR_4$ runs as multiple bands ranging from 35-106 kDa (Figure 5.3.4 (A)). Several bands could be identified ranging from ~35 kDa to ~45 kDa, 2 clear bands at ~65 kDa and ~68 kDa, and 2 bands observed at ~89 kDa and ~106 kDa. The glycosylation mutant $hPAR_4$(N20Q) also ran as multiple bands but only ranging from ~35 kDa to ~85 kDa (Figure 5.3.4 (A)). In addition, there was only one band at ~65 kDa and 2 bands at ~79 kDa and ~85 kDa. When treated with PNGaseF, wt-$hPAR_4$ ran at a lower molecular mass, with bands ranging from 79-85 kDa, compared to untreated wt-$hPAR_4$, but similar to that observed for the $hPAR_4$(N20Q) (Figure 5.3.4 (B)). No bands were detected in EV cell line.

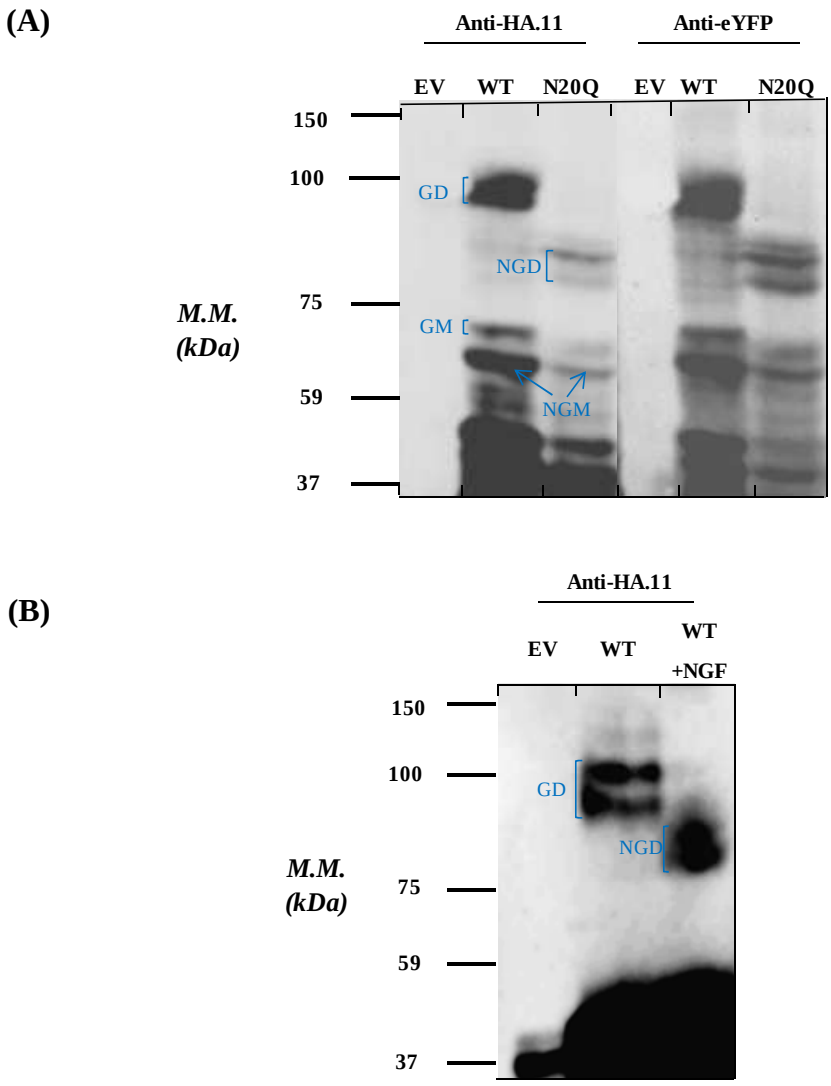

Figure 5.3.4 Western blot analysis of wt-hPAR$_4$ and hPAR$_4$(N20Q) in KNRK cells. **(A):** Blots for EV, WT and N20Q. **(B):** Blots for WT, and PNGaseF (NGF) treated WT. Immunoprecipitated hPAR$_4$ protein was incubated with PNGaseF for 1 hour at 37°C. Immunoprecipitated proteins were resolved by SDS-PAGE before immunoblotting with either the monoclonal HA.11 antibody or the eYFP antibody. EV, protein sample from pcDNA3 transfected KNRK cells; WT, protein sample from wt-hPAR$_4$ transfected KNRK cells; N20Q, protein sample from hPAR$_4$(N20Q) transfected KNRK cells. WT+NGF, protein sample from PNGaseF treated wt-hPAR$_4$ transfected KNRK cells. GD indicates glycosylated dimer; NGD, nonglycosylated dimer; GM, glycosylated monomer; NGM, nonglycosylated or minimally glycosylated monomer. M.M., molecular mass.

5.3.5 $hPAR_4$ Couples Weakly to Calcium in KNRK Cell Line

The functionality of wt-$hPAR_4$ and N20Q was initially assessed by measuring agonist-triggered increases in intracellular calcium levels. The KNRK parent cell line was initially tested for the presence of functional $hPAR_4$ (Figure 5.3.5 (A)). Challenging KNRK parent cells with 100 μM of the selective PAR_4-AP, AYPGQV-NH_2 resulted in no calcium signal (Figure 5.3.5 (A)). However, subsequent treatment with A23187 (2 μM) did induce a robust calcium response. In high-wt cells calcium signal was generated when AYPGQV-NH_2 (100 μM) was added (Figure 5.3.5 (B)). Addition of A23187 (2 μM) following the AYPGQV-NH_2 challenging to high-wt cells also resulted in a robust increase in fluorescence. No calcium signal was observed when challenging medium-wt cells with AYPGQV-NH_2 (100 μM), although subsequent treatment with A23187 (2 μM) did induce a robust calcium response (Figure 5.3.5 (C)). N20Q cells displayed no calcium signal after the addition of AYPGQV-NH_2 (100 μM) (Figure 5.3.5 (D)). Subsequent treatment of N20Q with A23187 (2 μM) did induce a robust calcium response.

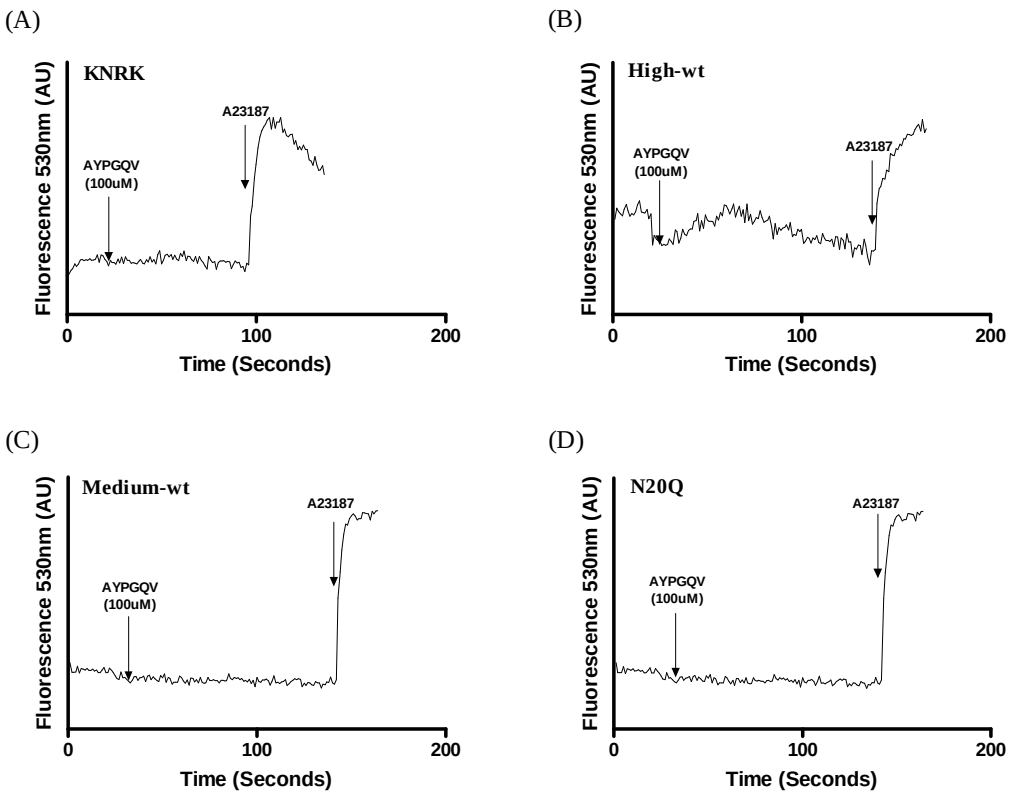

Figure 5.3.5 Representative traces of PAR_4-AP AYPGQV-NH_2 triggered calcium responses in wt-hPAR_4 and hPAR_4(N20Q) transfected KNRK cells. AYPGQV-NH_2 (100 µM) triggered calcium response for **(A):** KNRK, **(B):** High-wt, **(C):** Medium-wt, and **(D):** N20Q. An increase in fluorescence (E_{530}) monitored by fluorescence spectrophotometry is indicative of calcium mobilization. Cells were loaded with Fluo-3 (22 µM) for 25 minutes at RT before functional hPAR_4 activity was assessed by treating cells with the hPAR_4-AP AYPGQV-NH_2. Cell loading/viability was assessed by addition of A23187 (calcium ionophore, 2 µM). Arrows indicate when test agonists were added. Data shown is representative of three independent experiments.

5.3.6 Glycosylation of hPAR$_4$ Inversely Regulates Coupling to ERK and p38 MAPK Signalling Pathways

In order to characterise the effect of *N*-linked glycosylation on PAR$_4$ MAPK signalling, PAR$_4$-AP AYPGQV-NH$_2$ (100 µM) triggered p38 and ERK MAPK activation time courses for WT (high-wt) and N20Q were produced (Figure 5.3.6 and 5.3.7).

Activation of WT and N20Q with AYPGQV-NH$_2$ resulted in the phosphorylation of p38 MAPK but with dramatic differences ($p<0.0001$) in the magnitude of the responses between the two receptors when analysed using a two-way ANOVA table (Figure 5.3.6). AYPGQV-NH$_2$ triggered phosphorylation of p38 MAPK in WT cells with maximal activation observed at 5 min (14 ± 6 fold of control), which declined thereafter but remained elevated up to the 60 min time point tested (Figure 5.3.6). AYPGQV-NH$_2$ also triggered phosphorylation of p38 MAPK in N20Q cells with maximal activation observed at 5 min (2 ± 0.7 fold of control). However the magnitude of response was far smaller than that seen for WT (2 ± 0.7 *vs*. 14 ± 6 fold above control for N20Q and WT respectively). In the AYPGQV-NH$_2$ treated N20Q cells p38 MAPK phosphorylation levels remained elevated up to 30 min post agonist challenge and declined to almost near basal level by the 60 min time point tested (Figure 5.3.6).

The effect of PAR$_4$-AP AYPGQV-NH$_2$ (100 µM) stimulation on the phosphorylation of ERK (p42/44 MAPK) for WT and N20Q cell lines was also investigated (Figure 5.3.7). Activation of WT and N20Q with AYPGQV-NH$_2$ both resulted in the phosphorylation of ERK but with striking differences ($p=0.0016$) in the magnitude of the response when analysed by two-way ANOVA table (Figure 5.3.7). Activation of WT with AYPGQV-NH$_2$ stimulated phosphorylation of ERK (1.3 ± 0.1 fold of control) at 5 min time point,

which fluctuated thereafter but still remained elevated up to the 30 min time point (1.5 ± 0.3 fold of control) (Figure 5.3.7). ERK phosphorylation levels declined to basal levels by the 60 min time point. AYPGQV-NH_2 also triggered phosphorylation of ERK (1.9 ± 0.1 fold of control) at the 5 min time point in N20Q cells, however the ERK phosphorylation levels increased thereafter up to the 60 min time point tested (3 ± 0.6 fold of control) (Figure 5.3.7).

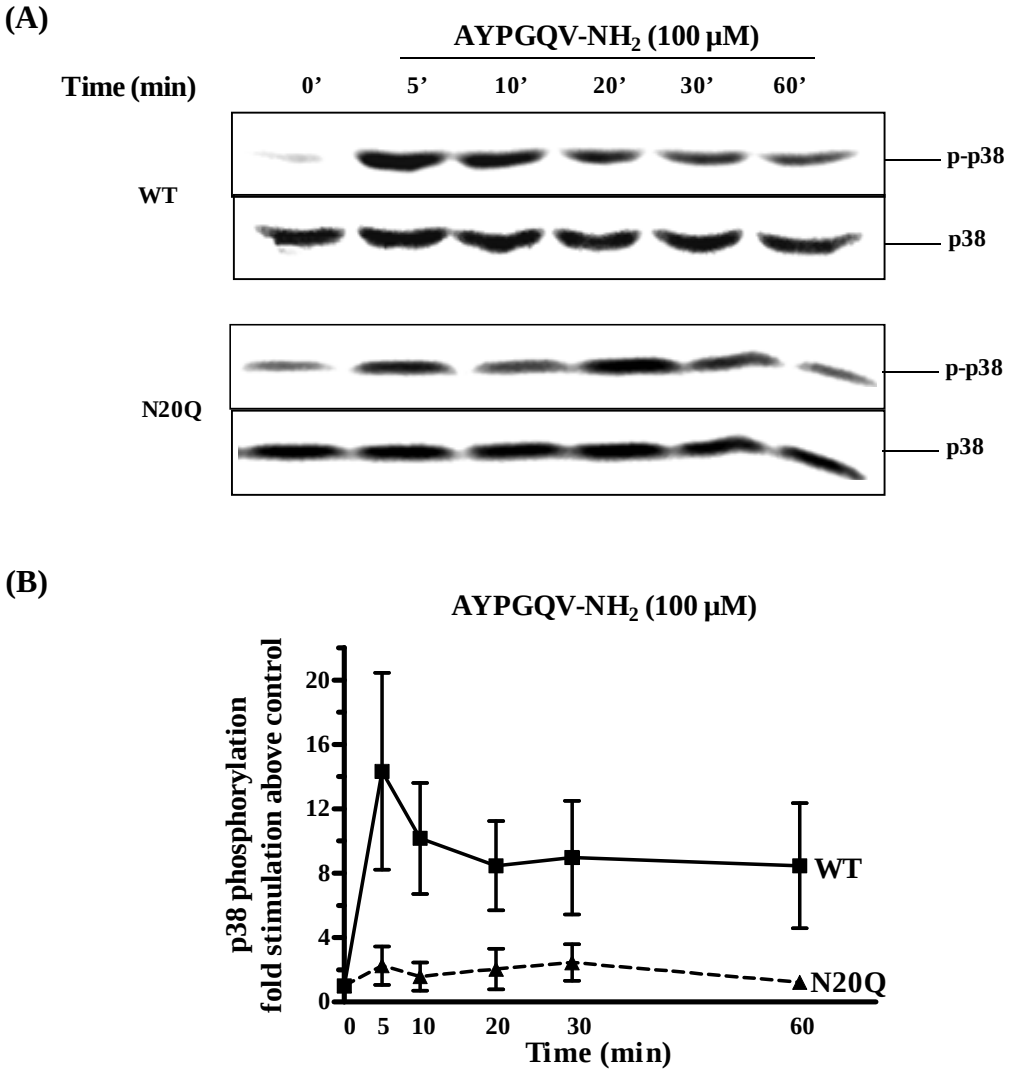

Figure 5.3.6 WT and N20Q mediated phosphorylation of p38 MAPK in KNRK cells. (A): Representative blots of WT and N20Q stimulated phosphorylation of p38 MAPK. Cells were rendered quiescent for 24 hours prior to stimulation with 100 µM AYPGQV-NH_2 for the times indicated. Whole cell lysates were prepared and assayed by western blotting. Blots shown are a representative of three separate experiments. Gels were probed with anti-phosphorylated p38 antibody and then re-probed with anti-total p38 antibody. WT, wt-$hPAR_4$ transfected KNRK cell line; N20Q, $hPAR_4$(N20Q) transfected KNRK cell line; p-p38, phosphorylated p38. **(B):** Blots were quantified by densitometry and expressed as mean ± SEM (fold stimulation).

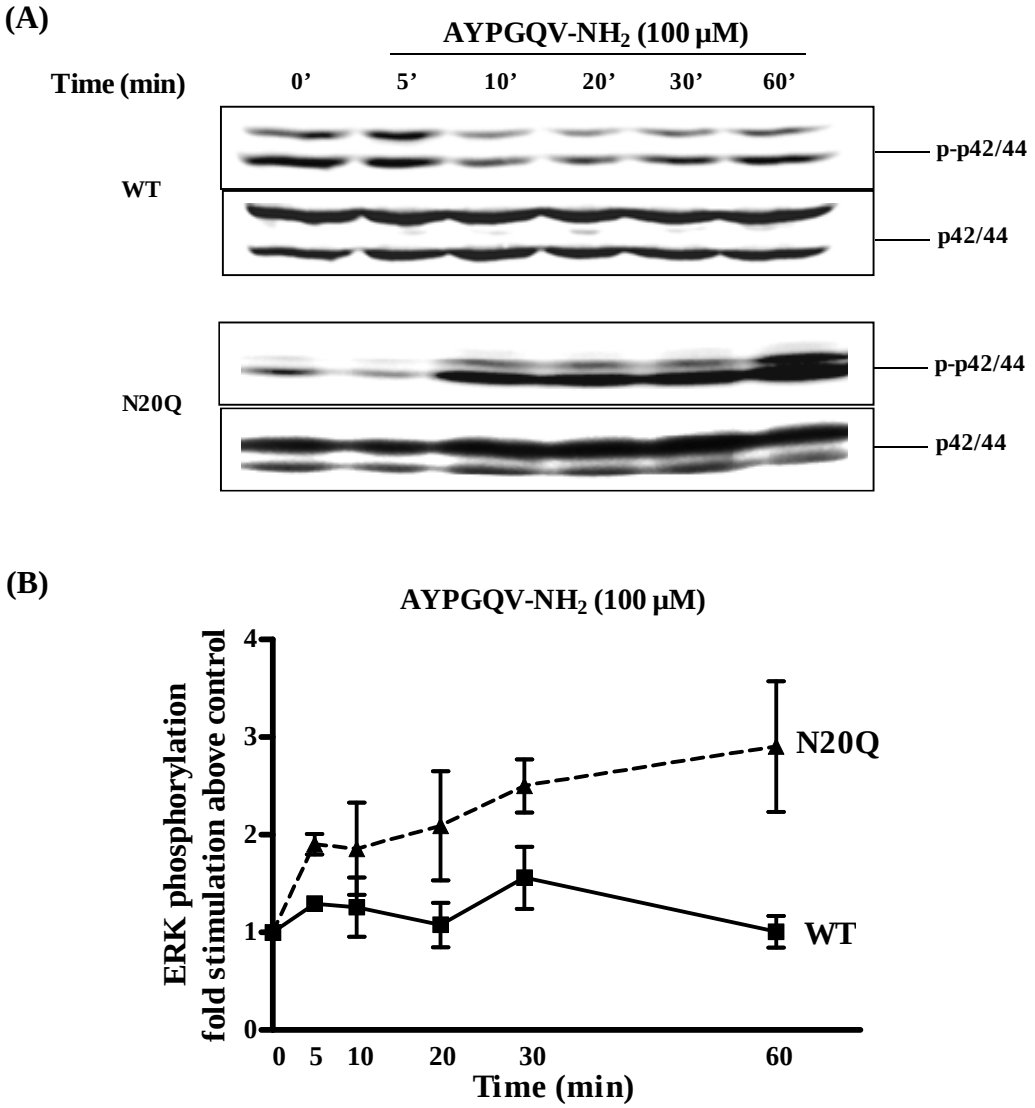

Figure 5.3.7 WT and N20Q mediated phosphorylation of p42/44 MAPK in KNRK cells. (A): Representative blots of WT and N20Q stimulated phosphorylation of p42/44 MAPK. Cells were rendered quiescent for 24 hours prior to stimulation with 100 µM AYPGQV-NH_2 for the times indicated. Whole cell lysates were prepared and assayed by western blotting. Blots shown are a representative of three separate experiments. Gels were probed with anti-phosphorylated p42/44 antibody and then re-probed with anti-total p42/44 antibody. WT, wt-hPAR_4 transfected KNRK cell line; N20Q, hPAR_4(N20Q) transfected KNRK cell line; p-p42/44, phosphorylated p42/44. **(B):** Blots were quantified by densitometry and expressed as mean ± SEM (fold stimulation).

5.3.7 The Effect of Sialylation on hPAR$_4$ Expression and Cellular Distribution

Expression of wt-hPAR$_4$ in Pro5 and Lec2 cell was initially assessed by FACS. Both Pro5-PAR$_4$ (wt-hPAR$_4$ transfected Pro5 cells) and Lec2-PAR$_4$ (wt-hPAR$_4$ transfected Lec2 cells) cell lines show significant rightward shifts in fluorescence when compared to untransfected Pro5 and Lec2 cells respectively (Figure 5.3.8 (A), and (B)). Lec2-PAR$_4$ showed no significant differences in receptor global expression when compared with Pro5-PAR$_4$ ($p=0.3598$) (Figure 5.3.8 (C)).

Analysis of eYFP tagged hPAR$_4$ localization in permeabilized cells by confocal microscopy demonstrated that Pro5-PAR$_4$ was expressed predominantly on the cell surface, although some receptor expression could be detected throughout the cytosol as well (Figure 5.3.9). However, the relative fluorescence intensity of the receptor appeared to be reduced in Lec2-PAR$_4$ when compared with Pro5-PAR$_4$. Furthermore, Lec2-PAR$_4$ was observed increasingly inside the cells compared to Pro5-PAR$_4$ cells (Figure 5.3.9).

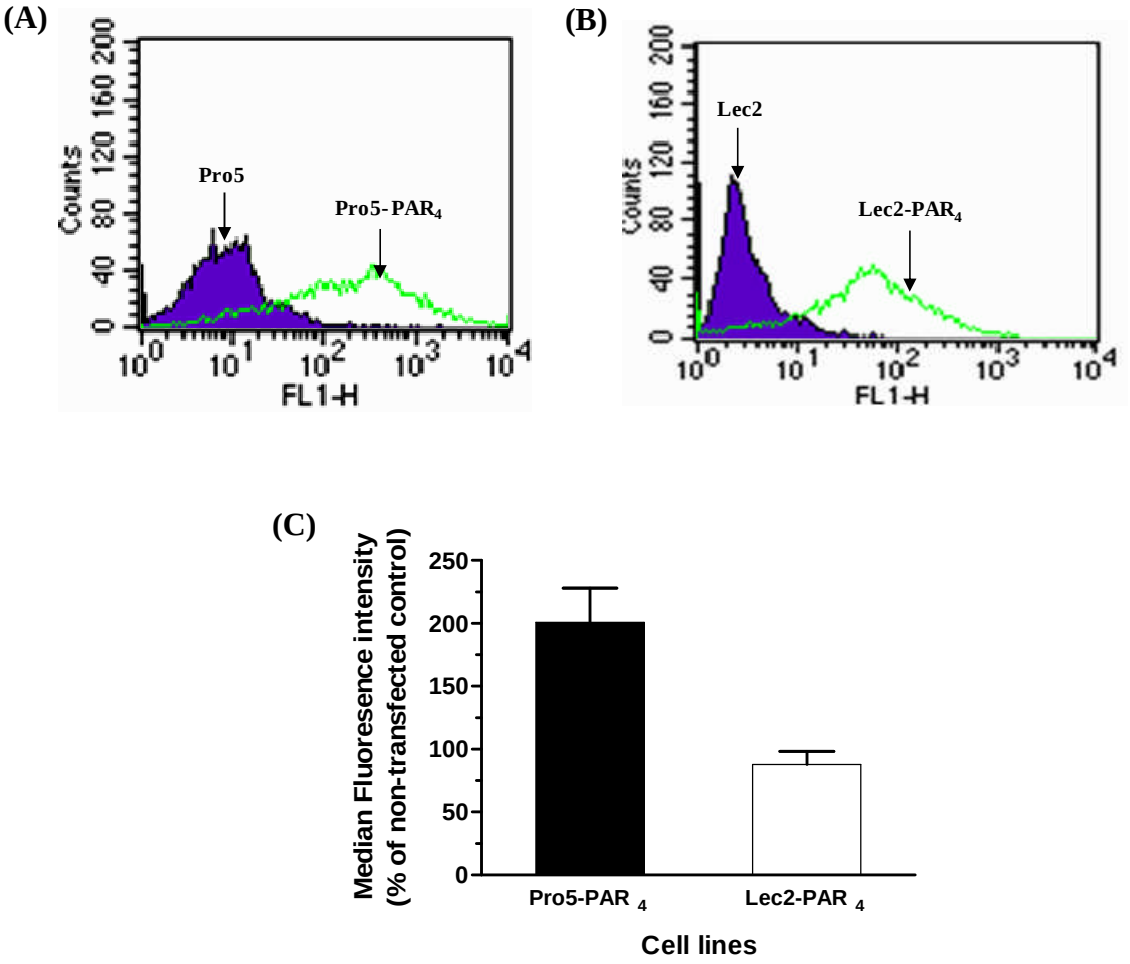

Figure 5.3.8 Flow cytometry analysis for wt-hPAR$_4$ in Pro5 and Lec2 cell lines. Flow cytometry analysis for **(A):** Pro5 and Pro5-PAR$_4$, and **(B):** Lec2 and Lec2- PAR$_4$. Cells were washed in PBS, and analyzed for fluorescence (FL1-H) by flow cytometry. The results are representative of three separate experiments. **(C):** Bar graph showing relative receptor expression between Pro5-PAR$_4$ and Lec2-PAR$_4$ cell lines. Results are expressed as the mean ± SEM of two separate experiments.

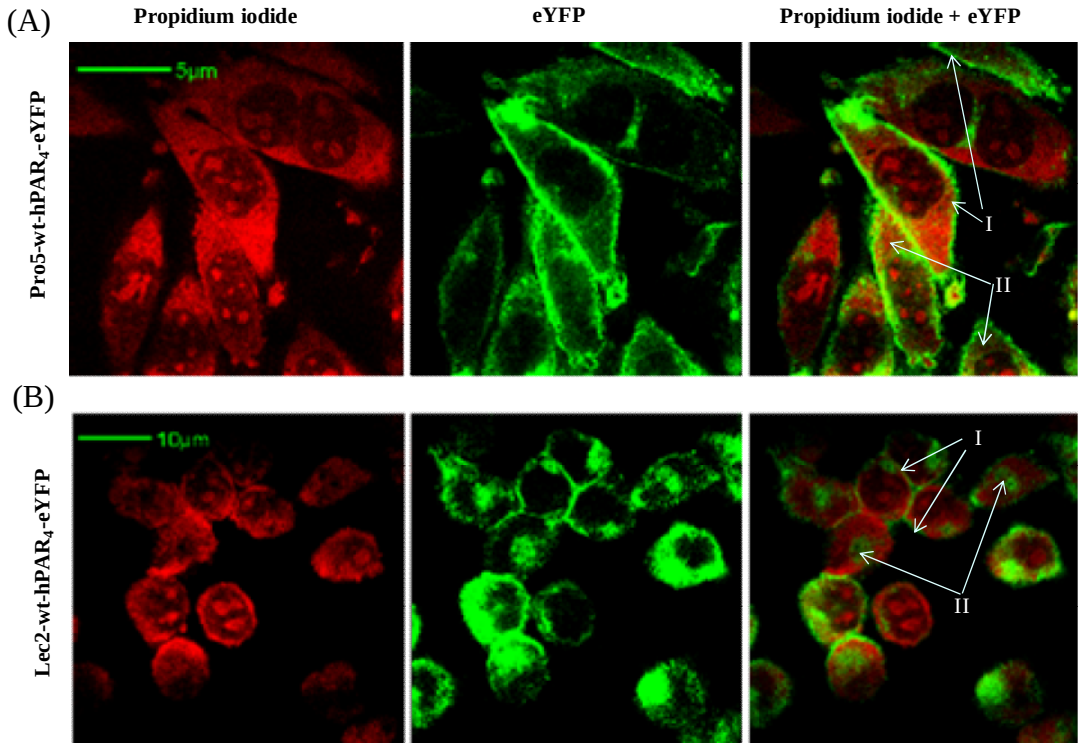

Figure 5.3.9 Confocal microscopy analysis for wt-PAR$_4$ transfected Pro5 and Lec2 cells. Confocal microscopy images for **(A)** Pro5-PAR$_4$ and **(B)** Lec2-PAR$_4$ were produced by growing the cells on coverslips before fixing and permeabilising. Cells were stained with propidium iodide prior to visualising. eYFP is visualised here in green and propidium iodide in red. **I:** Cell surface expression; **II:** internal receptor expression. The results are representative of three separate experiments.

5.3.8 $hPAR_4$ is a Sialylated Receptor

To determine the contribution of sialic acid to the molecular mass of $hPAR_4$, western blot analysis for Pro5-PAR_4 and Lec2-PAR_4 were performed. Results are shown in Figure 5.3.10. Pro5-PAR_4 migrated as several bands observed from 35-106 kDa including several bands ranging from ~35 kDa to ~45 kDa, 2 clear bands at ~65 kDa and ~68 kDa, and multiple bands observed approx. from ~89 kDa to ~106 kDa. Lec2-PAR_4 exhibited a lower molecular mass ranging from approx ~35 kDa to ~94 kDa including several bands at ~35 kDa to ~45 kDa, 2 clear bands at ~65 kDa and ~68 kDa, and multiple bands observed approx. from ~79 kDa up to ~94 kDa. No bands were detected in the non-transfected Lec2 or Pro5 cells.

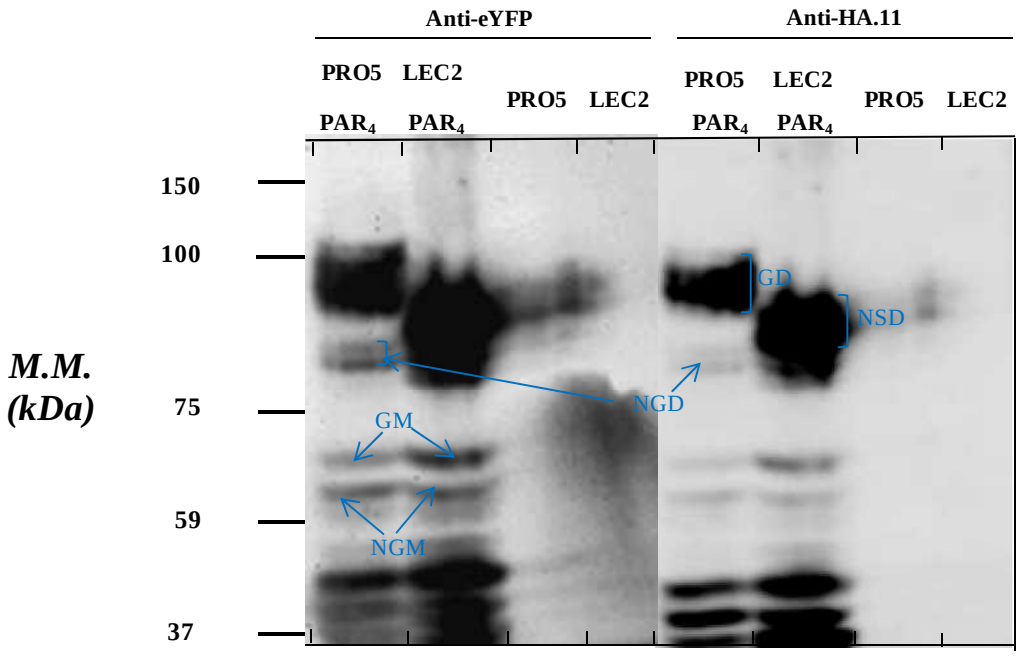

Figure 5.3.10 Western blot analysis of Pro5-PAR$_4$ and Lec2-PAR$_4$. Protein samples were immunoprecipitated by HA.11 immunoprecipitation and were resolved by SDS/PAGE (10% gel) and immunoblotted using either eYFP antibody or a monoclonal HA.11 antibody. GD indicates glycosylated dimmer; NSD, non-sialylated glycosylated dimmer; NGD, nonglycosylated dimmer; GM, glycosylated monomer; NGM, nonglycosylated or minimally glycosylated monomer. M.M., molecular mass. The results are representative of three separate experiments.

5.3.9 The Effect of Sialylation on PAR_4 Calcium Signalling

The functionality of PAR_4 in Pro5 and Lec2 cells was assessed by measuring agonist-triggered increases in intracellular calcium levels (Figure 5.3.11). Pro5-PAR_4 and Lec2-PAR_4 all displayed a rapid and robust increase in fluorescence levels following stimulation with the PAR_4-AP AYPGQV-NH_2 (100 µM) (approximately ~90% and ~60% of A23187 respectively) (Figure 5.3.11 (A), (C)). Challenging Pro5-PAR_4 with TFLLR-NH_2 (100 µM) resulted in a robust increase in fluorescence (approximately ~70% of A23187); further treatment with TFLLR-NH_2 (100 µM) resulted in small increase in fluorescence (approximately under ~5% of A23187). Addition of thrombin (5 nM) following both additions of TFLLR-NH_2 also resulted in a robust increase in fluorescence (approximately ~70% of A23187) (Figure 5.3.11 (B)). Challenging Lec2-PAR_4 with TFLLR-NH_2 (100 µM) resulted in a robust increase in fluorescence (approximately ~50% of A23187); when the cells were stimulated twice with TFLLR-NH_2 (100 µM), no second fluorescence signal was observed following the first application. Subsequent treatment with thrombin (5 nM) resulted in a robust increase in fluorescence (approximately over ~50% of A23187 response) (Figure 5.3.11 (D)).

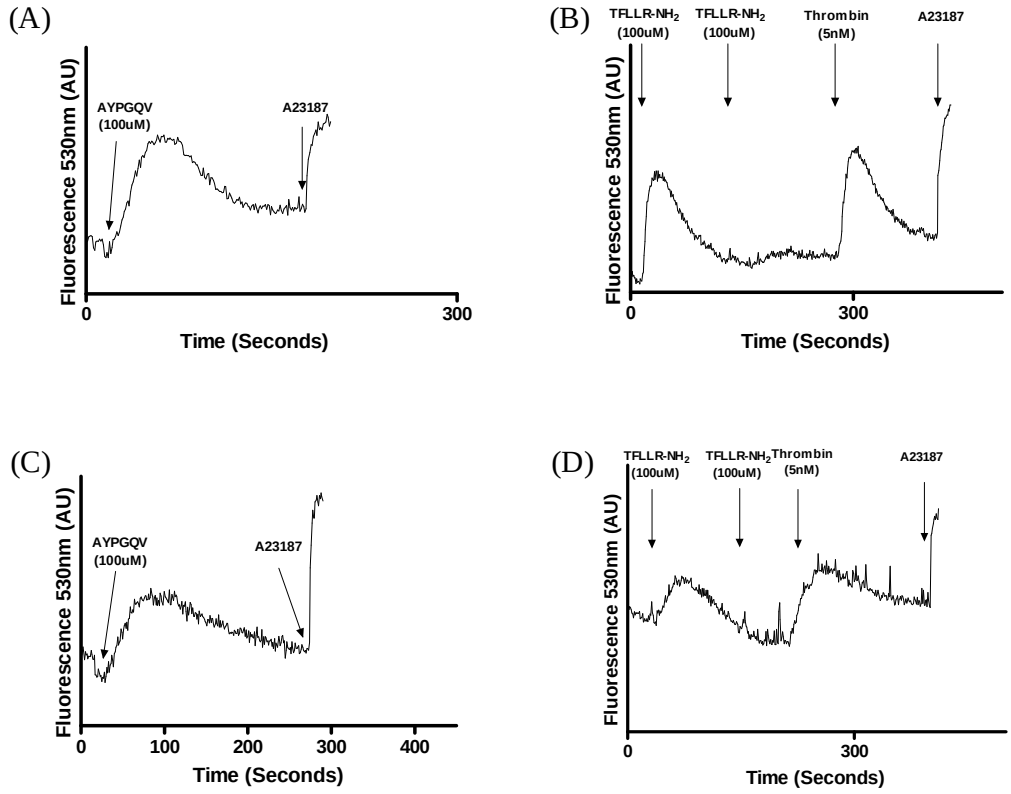

Figure 5.3.11 Representative traces of calcium signalling assay for Pro5-PAR$_4$ and Lec2-PAR$_4$. **(A)** Pro5-PAR$_4$ responses to PAR$_4$-AP AYPGQV-NH$_2$ (100 µM); **(B)** Pro5-PAR$_4$ responses to PAR$_1$-AP TFLLR-NH$_2$ (100 µM) then thrombin (5 nM); **(C)** Lec2-PAR$_4$ responses to PAR$_4$-AP AYPGQV-NH$_2$ (100 µM); **(D)** Lec2-PAR$_4$ responses to PAR$_1$-AP TFLLR-NH$_2$ (100 µM) then thrombin (5 nM). An increase in fluorescence (E_{530}) monitored by fluorescence spectrophotometry is indicative of calcium mobilization. Cells were loaded with Fluo-3 (22 µM) incubating for 25 minutes at RT. Functional hPAR$_4$ activity was assessed by treating cells with the hPAR$_4$-AP AYPGQV-NH$_2$ or thrombin (5 nM). Cell loading/viability was assessed by addition of A23187 (2 µM). Arrows indicate when test agonists were added. Data shown is representative of three independent experiments.

5.4 Discussion

The data presented in this chapter provides convincing evidence that $hPAR_4$ is an *N*-linked glycosylated receptor which is also heavily sialylated. We show that *N*-linked glycosylation and sialylation is required but not essential for $hPAR_4$ cell surface expression. Finally and most importantly, we show for the first time that the signalling pathways activated by a GPCR can be modulated by *N*-linked glycosylation.

Initially, we attempted to express $hPAR_4$ (POMC-AU1-$hPAR_4$–HA.11 in pcDNA3) in the KNRK cell line as we have successfully transfected and expressed $hPAR_1$ in this cell system (Chapter 3). However, we were unable to select the KNRK-$hPAR_4$ expressing cell line efficiently, because *(i)* our anti-AU1 antibody and anti-PAR_4 antibody failed to detect the receptor by FACS analysis, and *(ii)* no calcium signalling response was detected after stimulation with the PAR_4-AP AYPGQV-NH_2 (100 µM) in at least 60 single cell clones (3 repeats of transfection) by calcium signalling assay screening. We then assumed that $hPAR_4$ might not be expressed as well as $hPAR_1$ in KRNK cells, and that we needed a rapid and more efficient method to screen for positive $hPAR_4$ expressing cell lines. We therefore attached enhanced yellow fluorencent protin (eYFP: can be detected easily by FACS analysis when expressed along with the receptor in the cells) to the c-terminal of $hPAR_4$. In order to assess the best cell system for expressing $hPAR_4$, we performed transient transfection of wt-$hPAR_4$ (POMC-AU1-$hPAR_4$–HA.11-eYFP in pcDNA3) into the KNRK, COS-7, and Hela cell lines. Wt-$hPAR_4$ transfected Hela cells died after 24 h of transfection. KNRK and COS-7 cell lines both showed good expression levels of PAR_4. However, the wt-$hPAR_4$ transfected COS7 cells grew slower and displayed more cell death when compared with KNRK transfected wt-$hPAR_4$. We therefore generated high-wt, medium-wt and glycosylation-deficient mutant N20Q cell lines in KNRK cells.

We utilised FACS and confocal microscopy to assess the expression levels and the cellular distribution of wt-hPAR$_4$ and glycosylation-deficient mutant hPAR$_4$(N20Q) in KNRK cell lines. Confocal imaging revealed that both wt-hPAR$_4$ and N20Q were expressed at the cell surface along with some internal localization; however, N20Q displayed dimished cell surface expression and partial cytosolic retention (presumably in golgi apparatus and ER) when compared to wt-hPAR$_4$. Moreover, N20Q still allowed effective cell surface expression which only was slightly reduced compared to medium-wt. The reduced cell surface expression suggests the existence of improper folding of the receptors (Karnik *et al.*, 1988; Karnik & Khorana, 1990). Therefore, glycosylation may play an important role in the correct folding of the receptor and is required but is not essential for cell-surface expression. Interestingly, a previous study using FACS analysis and immunocytochemistry also demonstrated that *N*-linked glycosylation facilitates, but is not essential for, cell-surface expression of hPAR$_2$ (Compton *et al.*, 2002b).

To provide evidence that hPAR$_4$ is *N*-linked glycosylated we treated wt-hPAR$_4$ with PNGaseF. Indeed the drop in MW of PNGaseF treated wt-hPAR$_4$ and non-treated N20Q provided clear evidence that wt-hPAR$_4$ is *N*-linked glycosylated. Since PNGaseF treated wt-hPAR$_4$ displayed a similar molecular weight of 35-85 kDa to that of N20Q, and that wt-hPAR$_4$ ran with a molecular mass from 35-106 kDa, we conclude that approximately ~21 kDa of the molecular mass of hPAR$_4$ can be attributed to *N*-linked glycosylation. The molecular mass of eYFP is predicted to be ~31 kDa according to the amino acid sequence. We predict that the bands around 89-106 kDa may represent a glycosylated dimer of hPAR$_4$; the multiple bands at approx. ~85 kDa and ~79 kDa may represent an unglycosylated dimer of hPAR$_4$; whilst the band at ~68 kDa might be a glycosylated monomer of hPAR$_4$; the band at ~65 kDa might be an unglycosylated monomer of

hPAR$_4$. During the course of this Thesis Leger reported that PAR$_4$ was glycosylated by two approaches (Leger *et al.*, 2006). Firstly, they demonstrated by western blotting that wt-PAR$_4$ expressed in COS7 cells migrated with a molecular mass ranging from 32 kDa to 81 kDa, which included 2 bands at 32-35 kDa, several bands around 60-64 kDa, and a band at 81kDa. Treatment with PNGaseF reduced the molecular weight of wt-PAR$_4$ to 32-70 kDa, which included 2 bands at 32-35 kDa and a band migrated at ~70 kDa. Secondly, they constructed a glycosylation-deficient mutant N56S which migrated with exactly the same pattern as the PNGaseF treated wt-PAR$_4$, and addition of the PNGaseF did not further reduce the molecular mass of the N56S mutant. Thus they, like us, provided convincing evidence that N56 is the sole site of *N*-linked glycosylation in PAR$_4$. The banding pattern of PAR$_4$ was described in detail: bands at 32-35 kDa were predicted to be the nonglycosylated monomer; bands around 60-64 kDa stand for the non-glycosylated dimer; the band at ~70 kDa is the heterogeneously glycosylated PAR$_4$ dimer; the band at ~81kDa is the glycosylated dimer. Interestingly, these findings are in agreement with our PAR$_4$ glycosylation studies. Our PAR$_4$ did display a similar banding pattern to Legers' but the molecular mass of PAR$_4$ is slightly different as we had attached eYFP at the end of PAR$_4$. Furthermore, prior to our study two other groups also predicted that PAR$_4$ is glycosylated as the molecular mass of PAR$_4$ in their western blotting analysis ran higher than the predicted molecular mass of PAR$_4$ (Shapiro *et al.*, 2000; Bolton *et al.*, 2003).

In KNRK cells we only observed a calcium signal in response to the PAR$_4$-AP AYPGQV-NH$_2$ in the High-wt cells. Since the Medium-wt and N20Q both failed to signal to calcium, we conclude that receptor expression and not glycosylation was responsible for the lack of calcium signal. We also conclude that PAR$_4$ does not couple very efficiently to calcium in KNRK cells, unlike our finding in the Pro5 and Lec2 cell

system. Thus, it appears that the cell background may play an important role in the ability of PAR_4 to trigger a calcium signal.

For MAPK signalling experiments, we made some interesting findings. Our data revealed that wt-$hPAR_4$ displayed much greater ability to trigger p38-MAPK phosphorylation after treatment with the PAR_4-AP AYPGQV-NH_2 compared to ERK phosphorylation. One previous study, which is in agreement with our findings, demonstrated that AYPGKF-NH_2 activation of PAR_4 resulted in activation mainly via the p38-MAPK pathway, with a weak activation of ERK in cardiomyocytes (Sabri *et al.*, 2003). Another study also stated that activation of PAR_4 by AYPGKF-NH_2 increased phosphorylation of both ERK1/2 and p38 MAPK in endothelial cells (Syeda *et al.*, 2006). The reduced p38-MAPK activation observed from $hPAR_4$(N20Q) indicated that glycosylation maybe important for PAR_4 triggered p38 MAPK signalling.

The most interesting finding was the ability of $hPAR_4$(N20Q) to signal to ERK, compared to WT that showed little or only modest activation. As mentioned above, it has previously been reported that PAR_4 couples very weakly to ERK in cardiomyocytes (Sabri *et al.*, 2003). However, in HUVEC PAR_4-AP AYPGKF promoted a prolonged activation of ERK1/2 that was evident after 10 min stimulation, a result consistent with our findings in $hPAR_4$(N20Q) (Syeda *et al.*, 2006). A previous study on human vascular smooth muscle cells (SMC), like our findings in $hPAR_4$(N20Q), also show that stimulation of SMC with PAR_4-AP GYPGQV induced a prolonged phosphorylation of ERK1/2 with a maximum at 60 min; in contrast, PAR_1-AP SFLLRN caused a rapid activation of the ERK1/2 with a maximum at 5 min (Bretschneider *et al.*, 2001). Moreover**,** Mazharian *et al.* also demonstrated that in platelet activation of PAR_4 with PAR_4-AP induce ERK and p38 activation which involved in platelet spreading (Mazharian *et al.*, 2007). On the basis of evidence collected from a number of previous

studies, PAR glycosylation appears to be regulated in a cell-specific manner (Compton, 2003). Interestingly, we know from chapter 4 that PAR_1 might not be heavily or fully glycosylated in HUVECS, platelets, and HEL cells. We thus suggest that PAR_4 may also not heavily or fully glycosylated in HUVEC, SMC and platelet cells. Therefore differential glycosylation of PAR_4 may play an important role in the prolonged activation of ERK1/2 signalling observed in different cell system including our $hPAR_4$(N20Q) cells.

We next assessed whether $hPAR_4$ is sialylated and the role of sialylation in regulating $hPAR_4$ expression and calcium signalling. FACS data indicated that Pro5-PAR_4 cells showed higher global expression levels compared to Lec2-PAR_4. Moreover, confocal imaging data revealed that there was more $hPAR_4$ internal localization in Lec2-PAR_4 than in Pro5-PAR_4 cells. Therefore, we could draw a conclusion that Pro5-PAR_4 has higher cell surface expression levels than Lec2-PAR_4 cells. Western blot analysis revealed that Lec2-PAR_4 had a molecular mass that was up to ~12 kDa lower than that observed for Pro5-WT (ranged from ~35 kDa up to ~106 kDa). We suggest that this loss of ~12 kDa is due to the loss of receptor-associated sialic acid, and therefore $hPAR_4$ is sialylated in Pro5 cells. Similarly, Compton's previous study also reported that Pro5-$hPAR_2$ is sialylated, and that sialylation accounted for ~40 kDa, furthermore, sialylation regulates receptor signalling to tryptase (Compton *et al.*, 2002b). Analysis of calcium signalling in Pro5-PAR_4 and Lec2-PAR_4 showed that sialylation has no significant effect on calcium signalling. This shows Lec2-PAR_4 to be sufficiently correctly folded in order to allow receptor activation by AYPGQV-NH_2 and thrombin. The decreased calcium signalling observed from Lec2-PAR_4 cells is unlikely to be due to the removal of sialic acid. Therefore, we suggest that sialytion is required but not essential for efficient cell surface expression. Unfortunately due to time restraints we were unable to

probe the ability of Lec2-PAR_4 to signal to p38 and ERK. Regardless data presented in this chapter provides novel information on the ability of *N*-linked glycosylation to regulate GPCR signalling.

6. GENERAL DISCUSSION

The hypothesis of this thesis was that ***"N-linked glycosylation and sialylation regulate $hPAR_1$ and $hPAR_4$ cell surface expression and signalling".***

The major findings in this research support this hypothesis, and are outlined below:

1) $hPAR_1$ is a heavily glycosylated and sialylated receptor and *N*-linked glycosylation probably occurs at all five consensus sites of $hPAR_1$ in KNRK cells, namely, Asn^{35}, Asn^{62}, Asn^{75}, Asn^{250}, and Asn^{259}. Removal of *N*-linked glycosylation sequons at these positions blocked $hPAR_1$ cell surface expression to varying degrees, and indicated that glycosylation at all sites is required for optimal cell surface expression of $hPAR_1$. With the exception of N62QN75Q no significant changes in receptor sensitivity to thrombin, trypsin and TFLLR-NH_2 were observed when assessed by calcium signalling. Interestingly, N62QN75Q displayed significantly reduced sensitivity to trypsin, but not thrombin and TFLLR-NH_2.
2) Glycosylation in the N-terminus of $hPAR_1$ downstream of the tethered ligand (especially Asn^{75}) regulates receptor disarming to trypsin, thermolysin and the neutrophil proteinases elastase and proteinase 3, but not cathepsin G.
3) $hPAR_4$ is a *N*-linked glycosylated receptor which is also heavily sialylated. Glycosylation is required but not essential for $hPAR_4$ receptor cell surface expression. Signalling pathways activated by $hPAR_4$ can be modulated by *N*-linked glycosylation.

Taken together the findings within this Thesis clearly point out an important role of *N*-linked glycosylation in regulating the cell surface expression and signalling of $hPAR_1$ and $hPAR_4$.

6.1 The effect of *N*-linked glycosylation in regulating PAR cell surface expression

N-linked glycosylation has been shown to be important for a variety of functions including normal protein folding, stability, intracellular trafficking, cell surface expression, secretion and signalling (Helenius, 1994; Taylor & Drickamer, 2003; Helenius & Aebi, 2004). However, the most successfully evidenced function of *N*-linked glycosylation is the promotion of proper folding of newly synthesized polypeptides in the ER (Helenius, 1994). For instance Hawtin and colleagues reported that *N*-linked glycosylation is required for efficient folding of the V_{1a} vasopressin receptor ($V_{1a}R$) (Hawtin *et al.*, 2001). In order to elicit correct intracellular signalling, a GPCR must first go through a series of biosynthetic events aimed at sending the right quantity of properly folded functional receptors to the cell surface (Helenius, 1994; Taylor & Drickamer, 2003). After glycosylation is inhibited, the most commonly observed effect is the generation of misfolded, aggregated proteins which fail to reach a functional state, thus are subsequently degraded inside lysosomes (Ellgaard & Helenius, 2003; Taylor & Drickamer, 2003). Indeed, evidence for that was also shown by our PAR_1 and PAR_4 confocal microscopy images. After the removal of *N*-linked glycosylation in our PAR model, all PAR glycosylation mutant cell types displayed a certain degree of increased cytosolic retention of the receptors, presumably in ER or Golgi apparatus, indicating their poorly folded structure. FACs analysis for PAR_1 provided further evidence for the failure of receptors reach to the cell surface, presumably caused by the removal of *N*-linked glycosylation. Like our findings in PAR_1, studies with N-glycosylation of the AT1 receptor also showed that removal of all N-glycosylation sites resulted in a receptor that was not expressed on the plasma membrane, but instead accumulated in the ER (Deslauriers *et al.*, 1999). Similarly

another group also reported at the same time that *N*-linked glycosylation is required for optimal AT_{1a} angiotensin receptor expression in COS7 cells (Jayadev *et al.*, 1999). Karpa *et al.* also reported that the functional expression of D5 dopamine receptors at the cell surface of HEK293 cells requires the addition of *N*-linked glycosylation, a result consistent with our findings in PAR_1 and PAR_4 (Karpa *et al.*, 1999). Interestingly, our studies on wt-PAR_1 and its glycosylation mutants suggest that *N*-linked glycosylation especially at ECL2 of PAR_1 regulates receptor stability and protects the receptor from degradation. Similarly, Gong *et al.* also reported that *N*-linked glycosylation is important for HERG potassium channel stability (Gong *et al.*, 2002). In addition, it is well known that *N*-glycan carbohydrates stabilize the mature protein, partly by protecting it from degradation by intracellular proteases (Imperiali & O'Connor, 1999; Kundra & Kornfeld, 1999). Furthermore, Deslauriers and colleagues also demonstrated that the *N*-linked glycosylation, especially Asn176 in the second extracellular loop, is important for the AT1 receptor stability and optimal cell surface expression (Deslauriers *et al.*, 1999).

Overall, these findings establish that *N*-linked glycosylation has an important role in PAR expression, and/or stability of the receptor, at the plasma membrane.

6.2 The effect of *N*-linked glycosylation in regulating PAR signalling

Interestingly, Compton *et al.* reported that the extent of PAR glycosylation can have profound effects on the capacity of proteases to activate PAR_2 (Compton *et al.*, 2001). Given that, numerous questions were raised for PAR studies; such as do other proteases signal through these receptors in a similar manner? Are there any other factors, such as post-translational modification of glycosylation, phosphorylation, palmitoylation, acetylation or methylation etc., involved in regulating the function of these receptors?

For the first time we have found that *N*-linked glycosylation of $hPAR_1$ downstream of the tethered ligand (especially Asn^{75}) regulates the capacity of proteinases to disarm PAR_1. It is known that PARs can be activated and attenuated by more than one proteinase (O'Brien *et al.*, 2001). Any proteinase that cleaves the correct peptide bond within the N-terminus of a PAR may be able to expose the tethered ligand domain that binds onto the extracellular loop II of the receptor to initiate signaling (O'Brien *et al.*, 2001). Conversely, proteinases can also disarm the PARs by amputating the tethered ligand domain from the receptor (O'Brien *et al.*, 2001). When PAR_1 is fully glycosylated these cleavage sites are shielded by the attached oligosaccharides and thus proteinases disarm wt-$hPAR_1$ subsequently less efficiently. Therefore after the removal of the glycosylation sequons downstream of the tethered ligand, the potential cleavage sites might be more easily accessible for proteinases cleavage leading to receptor disarming. We thus conclude that *N*-linked glycosylation regulates $hPAR_1$ signalling. Like us, previous studies also reported that glycosylation of notch receptors modulates receptor interaction with different ligands (Moloney *et al.*, 2000; Chen *et al.*, 2001b). In addition, $hPAR_4$ is a singly *N*-linked glycosylated receptor, and this N-glycosylation is located downstream of the tethered ligand. Therefore it will be of great interest to assess whether *N*-linked glycosylation regulates the capacity of proteases to activate/disarm this receptor.

The importance of the *N*-linked glycosylation in $hPAR_4$ was revealed by the signalling response changes seen in the mutant $hPAR_4$(N20Q). We have shown for the first time that MAP Kinase pathways activated by $hPAR_4$ can be modulated by *N*-linked glycosylation. Zhao *et al.* reported that *N*-linked glycosylation of E-cadherin affects cell cycle progression through extracellular signal-regulated protein kinase signaling pathway, a result consistent with our findings PAR_4 (Zhao *et al.*, 2008). In contrast to

our findings with PAR_4, Tansky *et al.* reported removal of both *N*-linked glycosylation sites in the neurokinin 1 receptor (NK1R) did not have a profound effect on the receptors' abilities to activate the MAP kinase families (p42/p44, JNK, and p38) (Tansky *et al.*, 2007). However, our report is the first to show that glycosylation can regulate which MAP Kinase pathway is activated by the receptor. Since little is currently known about PAR_4 in disease, it is unclear what effect these changes in PAR_4 signalling will have.

6.3 *N*-linked glycosylation in PAR related diseases

On the basis of evidence collected from a number of previous studies, PAR glycosylation appears to be regulated in a cell-specific manner (Compton, 2003). An understanding of the regulatory mechanisms of PAR signalling in various tissues and cell types is important for understanding their biological function as well as for providing novel approaches to exploit its activation potential in disease states (Traynelis & Trejo, 2007). The altered receptor pharmacology observed from the removal of *N*-linked glycosylation seen in $hPAR_1$ and $hPAR_4$ glycosylation mutants may play a significant role in diseases and could provide valuable information for the design of new therapeutic agents. The relationships between disease phenotypes and changes in glycosylation have been most intensively studied in the field of cancer biology (Taylor & Drickamer, 2003). The nature of *N*-linked glycans attached to a glycoprotein is determined by the protein and the cell in which it is expressed (Taylor & Drickamer, 2003). The same protein expressed in the same cell type under different growth conditions can be glycosylated in different ways (Taylor & Drickamer, 2003). For example, differential glycosylation is encountered when normal tissue cells are compared with cancer cells derived from these same tissues (Taylor & Drickamer,

2003). In normal endothelial cells for example HUVEC, there is PAR_1 and PAR_2 expressed on the cell surface (O'Brien *et al.*, 2000). The molecular weight of PAR_1 expressed in HUVECS was reported to be ~66kDa (Brass *et al.*, 1992), which is similar to our PAR_1 glycosylation mutant N62QN75Q (removal of glycosylations downstream of the tethered ligand in $hPAR_1$). Thus we suggest that PAR_1 is not heavily glycosylated in normal HUVEC cells. On the other hand, the metastatic potential of cancer cells has found to be correlated extensively with increases in sialylation of cell-surface glycoproteins, and an important cause of this increased sialylation is due to the increased branching of complex *N*-linked oligosaccharides in highly metastatic cells (Taylor & Drickamer, 2003). Thus in cancer cells the glycoprotein would be more heavily glycosylated than in normal tissue cells. We therefore suggest that *N*-linked glycosylation status of PAR_1 in cancer cells may also differ from the normal tissue cells, likely more heavily glycosylated downstream of the tethered ligand of PAR_1. This might be a 'key story' for the developing of angiogenesis. It is well established that proteinases, trypsin-like proteinases in particular, are extremely abundant in the vicinity of tumours (Vergnolle, 2005). In normal HUVEC cells, these proteinases, for example trypsin, will expect to disarm and activate PAR_1 to keep the balance for normal cellular effects. In cancer cells, however, the glycosylation status of PAR_1 may be similar to our wt-$hPAR_1$ expressed in KNRK cells and both heavily glycosylated. Therefore, trypsin can only activate PAR_1. Furthermore, other proteinases (such as proteinse 3, elastase and cathepsin G) disarm PAR_1 in normal cells; however, if present in cancer cells these disarming events may be restricted. Thus the balance between disarming and activating is altered. The mechanisms by which growth factor receptor over-expression induces tumor cell invasion are still not fully understood. However, PAR_1 is now accepted as a potential oncogene and associated with cancer mitogenic and metastatic events.

Activation of PAR_1 leads to cell proliferation and subsequently angiogenesis. Thus inhibition of PAR_1 activation would have beneficial effects against tumour progression in cancer. The fact that some changes in glycosylation on the surface of tumour cells affect the progression of cancer may provide a basis for development of anticancer drugs (Taylor & Drickamer, 2003). Thus *N*-linked glycoylation of PAR_1, especially glycosylation located downstream of the tethered ligand, may be of great potential therapeutic value for cancer treatment.

6.4 Future Work

It is well established that PARs are all *N*-linked glycosylated proteins (Compton, 2003). We previously showed that the non-glycosylated PAR_1 and PAR_4 are inefficiently expressed at the cell surface, and *N*-linked glycosylation regulates receptor signalling. Future study may further address 1) glycosylation status of PAR_1 and PAR_4 in diseases like asthma and cancer, 2) whether glycosylation regulates PAR_1 activation of MAP Kinase signalling, 3) whether sialylation regulates PAR_4 MAP Kinase signalling, 4) whether the positioning of the glycosylation sites within the various extracellular loops of PAR is vital in receptor biosynthesis, 5) whether PAR interacts with elements of the ER-based quality control processes. For example, whether the decreased cell-surface expression of the non-glycosylated receptors are attributed to diminished interactions with molecular chaperones and that mannose trimming of the receptors by ER mannosidase I plays a critical role in receptor cell surface expression.

Reference:

Alm AK, Gagnemo-Persson R, Sorsa T & Sundelin J. (2000). Extrapancreatic trypsin-2 cleaves proteinase-activated receptor-2. *Biochem Biophys Res Commun* **275,** 77-83.

Angata K & Fukuda M. (2003). Polysialyltransferases: major players in polysialic acid synthesis on the neural cell adhesion molecule. *Biochimie* **85,** 195-206.

Apweiler R, Hermjakob H & Sharon N. (1999). On the frequency of protein glycosylation, as deduced from analysis of the SWISS-PROT database. *Biochim Biophys Acta* **1473,** 4-8.

Aragay AM, Collins LR, Post GR, Watson AJ, Feramisco JR, Brown JH & Simon MI. (1995). G12 requirement for thrombin-stimulated gene expression and DNA synthesis in 1321N1 astrocytoma cells. *J Biol Chem* **270,** 20073-20077.

Arora P, Ricks TK & Trejo J. (2007). Protease-activated receptor signalling, endocytic sorting and dysregulation in cancer. *J Cell Sci* **120,** 921-928.

Asfaha S, Brussee V, Chapman K, Zochodne DW & Vergnolle N. (2002). Proteinase-activated receptor-1 agonists attenuate nociception in response to noxious stimuli. *Br J Pharmacol* **135,** 1101-1106.

Asokananthan N, Graham PT, Fink J, Knight DA, Bakker AJ, McWilliam AS, Thompson PJ & Stewart GA. (2002a). Activation of protease-activated receptor (PAR)-1, PAR-2, and PAR-4 stimulates IL-6, IL-8, and prostaglandin E2 release from human respiratory epithelial cells. *J Immunol* **168,** 3577-3585.

Asokananthan N, Graham PT, Stewart DJ, Bakker AJ, Eidne KA, Thompson PJ & Stewart GA. (2002b). House dust mite allergens induce proinflammatory cytokines from respiratory epithelial cells: the cysteine protease allergen, Der p 1, activates protease-activated receptor (PAR)-2 and inactivates PAR-1. *J Immunol* **169,** 4572-4578.

Attramadal H, Arriza JL, Aoki C, Dawson TM, Codina J, Kwatra MM, Snyder SH, Caron MG & Lefkowitz RJ. (1992). Beta-arrestin2, a novel member of the arrestin/beta-arrestin gene family. *J Biol Chem* **267,** 17882-17890.

Babich M, King KL & Nissenson RA. (1990). Thrombin stimulates inositol phosphate production and intracellular free calcium by a pertussis toxin-insensitive mechanism in osteosarcoma cells. *Endocrinology* **126,** 948-954.

Baffy G, Yang L, Raj S, Manning DR & Williamson JR. (1994). G protein coupling to the thrombin receptor in Chinese hamster lung fibroblasts. *J Biol Chem* **269,** 8483-8487.

Baggiolini M, Bretz U, Dewald B & Feigenson ME. (1978). The polymorphonuclear leukocyte. *Agents Actions* **8,** 3-10.

Ballerio R, Brambilla M, Colnago D, Parolari A, Agrifoglio M, Camera M, Tremoli E & Mussoni L. (2007). Distinct roles for PAR1- and PAR2-mediated vasomotor modulation in human arterial and venous conduits. *J Thromb Haemost* **5,** 174-180.

Bar-Shavit R, Maoz M, Yongjun Y, Groysman M, Dekel I & Katzav S. (2002). Signalling pathways induced by protease-activated receptors and integrins in T cells. *Immunology* **105,** 35-46.

Barrett AJ, Rawlings ND & Woessne JF. (1998). *Handbook of Proteolytic Enzymes*. Academic Press, London.

Berger P, Girodet PO, Begueret H, Ousova O, Perng DW, Marthan R, Walls AF & Tunon de Lara JM. (2003). Tryptase-stimulated human airway smooth muscle cells induce cytokine synthesis and mast cell chemotaxis. *FASEB J* **17,** 2139-2141.

Berger P, Perng DW, Thabrew H, Compton SJ, Cairns JA, McEuen AR, Marthan R, Tunon De Lara JM & Walls AF. (2001). Tryptase and agonists of PAR-2 induce the proliferation of human airway smooth muscle cells. *J Appl Physiol* **91,** 1372-1379.

Berger SP, Seelen MA, Hiemstra PS, Gerritsma JS, Heemskerk E, van der Woude FJ & Daha MR. (1996). Proteinase 3, the major autoantigen of Wegener's granulomatosis, enhances IL-8 production by endothelial cells in vitro. *J Am Soc Nephrol* **7,** 694-701.

Bisello A, Greenberg Z, Behar V, Rosenblatt M, Suva LJ & Chorev M. (1996). Role of glycosylation in expression and function of the human parathyroid hormone/parathyroid hormone-related protein receptor. *Biochemistry* **35,** 15890-15895.

Blackhart BD, Emilsson K, Nguyen D, Teng W, Martelli AJ, Nystedt S, Sundelin J & Scarborough RM. (1996). Ligand cross-reactivity within the protease-activated receptor family. *J Biol Chem* **271,** 16466-16471.

Blackhart BD, Ruslim-Litrus L, Lu CC, Alves VL, Teng W, Scarborough RM, Reynolds EE & Oksenberg D. (2000). Extracellular mutations of protease-activated receptor-1 result in differential activation by thrombin and thrombin receptor agonist peptide. *Mol Pharmacol* **58,** 1178-1187.

Bohm SK, Kong W, Bromme D, Smeekens SP, Anderson DC, Connolly A, Kahn M, Nelken NA, Coughlin SR, Payan DG & Bunnett NW. (1996). Molecular cloning, expression and potential functions of the human proteinase-activated receptor-2. *Biochem J* **314 (Pt 3),** 1009-1016.

Boire A, Covic L, Agarwal A, Jacques S, Sherifi S & Kuliopulos A. (2005). PAR1 is a matrix metalloprotease-1 receptor that promotes invasion and tumorigenesis of breast cancer cells. *Cell* **120,** 303-313.

Bolton SJ, McNulty CA, Thomas RJ, Hewitt CR & Wardlaw AJ. (2003). Expression of and functional responses to protease-activated receptors on human eosinophils. *J Leukoc Biol* **74,** 60-68.

Bories D, Raynal MC, Solomon DH, Darzynkiewicz Z & Cayre YE. (1989). Down-regulation of a serine protease, myeloblastin, causes growth arrest and differentiation of promyelocytic leukemia cells. *Cell* **59,** 959-968.

Boven LA, Vergnolle N, Henry SD, Silva C, Imai Y, Holden J, Warren K, Hollenberg MD & Power C. (2003). Up-regulation of proteinase-activated receptor 1 expression in astrocytes during HIV encephalitis. *J Immunol* **170,** 2638-2646.

Bradding P, Walls AF & Holgate ST. (2006). The role of the mast cell in the pathophysiology of asthma. *J Allergy Clin Immunol* **117,** 1277-1284.

Brass LF, Manning DR, Williams AG, Woolkalis MJ & Poncz M. (1991). Receptor and G protein-mediated responses to thrombin in HEL cells. *J Biol Chem* **266,** 958-965.

Brass LF, Vassallo RR, Jr., Belmonte E, Ahuja M, Cichowski K & Hoxie JA. (1992). Structure and function of the human platelet thrombin receptor. Studies using monoclonal antibodies directed against a defined domain within the receptor N terminus. *J Biol Chem* **267,** 13795-13798.

Bretschneider E, Kaufmann R, Braun M, Nowak G, Glusa E & Schror K. (2001). Evidence for functionally active protease-activated receptor-4 (PAR-4) in human vascular smooth muscle cells. *Br J Pharmacol* **132,** 1441-1446.

Bretschneider E, Spanbroek R, Lotzer K, Habenicht AJ & Schror K. (2003). Evidence for functionally active protease-activated receptor-3 (PAR-3) in human vascular smooth muscle cells. *Thromb Haemost* **90,** 704-709.

Burda P & Aebi M. (1998). The ALG10 locus of Saccharomyces cerevisiae encodes the alpha-1,2 glucosyltransferase of the endoplasmic reticulum: the terminal glucose of the lipid-linked oligosaccharide is required for efficient N-linked glycosylation. *Glycobiology* **8,** 455-462.

Burda P, Jakob CA, Beinhauer J, Hegemann JH & Aebi M. (1999). Ordered assembly of the asymmetrically branched lipid-linked oligosaccharide in the endoplasmic reticulum is ensured by the substrate specificity of the individual glycosyltransferases. *Glycobiology* **9,** 617-625.

Buresi MC, Buret AG, Hollenberg MD & MacNaughton WK. (2002). Activation of proteinase-activated receptor 1 stimulates epithelial chloride secretion through a unique MAP kinase- and cyclo-oxygenase-dependent pathway. *FASEB J* **16,** 1515-1525.

Buresi MC, Schleihauf E, Vergnolle N, Buret A, Wallace JL, Hollenberg MD & MacNaughton WK. (2001). Protease-activated receptor-1 stimulates Ca(2+)-

dependent Cl(-) secretion in human intestinal epithelial cells. *Am J Physiol Gastrointest Liver Physiol* **281,** G323-332.

Cabrera-Vera TM, Vanhauwe J, Thomas TO, Medkova M, Preininger A, Mazzoni MR & Hamm HE. (2003). Insights into G protein structure, function, and regulation. *Endocr Rev* **24,** 765-781.

Camerer E, Huang W & Coughlin SR. (2000). Tissue factor- and factor X-dependent activation of protease-activated receptor 2 by factor VIIa. *Proc Natl Acad Sci U S A* **97,** 5255-5260.

Camerer E, Kataoka H, Kahn M, Lease K & Coughlin SR. (2002). Genetic evidence that protease-activated receptors mediate factor Xa signaling in endothelial cells. *J Biol Chem* **277,** 16081-16087.

Campanelli D, Melchior M, Fu Y, Nakata M, Shuman H, Nathan C & Gabay JE. (1990). Cloning of cDNA for proteinase 3: a serine protease, antibiotic, and autoantigen from human neutrophils. *J Exp Med* **172,** 1709-1715.

Cannon JR, Keep RF, Schallert T, Hua Y, Richardson RJ & Xi G. (2006). Protease-activated receptor-1 mediates protection elicited by thrombin preconditioning in a rat 6-hydroxydopamine model of Parkinson's disease. *Brain Res* **1116,** 177-186.

Caughey GH. (2007). Mast cell tryptases and chymases in inflammation and host defense. *Immunol Rev* **217,** 141-154.

Cenac N, Coelho AM, Nguyen C, Compton S, Andrade-Gordon P, MacNaughton WK, Wallace JL, Hollenberg MD, Bunnett NW, Garcia-Villar R, Bueno L & Vergnolle N. (2002). Induction of intestinal inflammation in mouse by activation of proteinase-activated receptor-2. *Am J Pathol* **161,** 1903-1915.

Chambers RC, Dabbagh K, McAnulty RJ, Gray AJ, Blanc-Brude OP & Laurent GJ. (1998). Thrombin stimulates fibroblast procollagen production via proteolytic activation of protease-activated receptor 1. *Biochem J* **333 (Pt 1),** 121-127.

Chen J, Moloney DJ & Stanley P. (2001b). Fringe modulation of Jagged1-induced Notch signaling requires the action of beta 4galactosyltransferase-1. *Proc Natl Acad Sci U S A* **98,** 13716-13721.

Chen X, Earley K, Luo W, Lin SH & Schilling WP. (1996). Functional expression of a human thrombin receptor in Sf9 insect cells: evidence for an active tethered ligand. *Biochem J* **314 (Pt 2),** 603-611.

Chen Z, Gibson TB, Robinson F, Silvestro L, Pearson G, Xu B, Wright A, Vanderbilt C & Cobb MH. (2001). MAP kinases. *Chem Rev* **101,** 2449-2476.

Chiu LL, Perng DW, Yu CH, Su SN & Chow LP. (2007). Mold allergen, pen C 13, induces IL-8 expression in human airway epithelial cells by activating protease-activated receptor 1 and 2. *J Immunol* **178,** 5237-5244.

Cirino G & Vergnolle N. (2006). Proteinase-activated receptors (PARs): crossroads between innate immunity and coagulation. *Curr Opin Pharmacol* **6,** 428-434.

Cocks TM, Fong B, Chow JM, Anderson GP, Frauman AG, Goldie RG, Henry PJ, Carr MJ, Hamilton JR & Moffatt JD. (1999). A protective role for protease-activated receptors in the airways. *Nature* **398,** 156-160.

Cocks TM & Moffatt JD. (2000). Protease-activated receptors: sentries for inflammation? *Trends Pharmacol Sci* **21,** 103-108.

Coeshott C, Ohnemus C, Pilyavskaya A, Ross S, Wieczorek M, Kroona H, Leimer AH & Cheronis J. (1999). Converting enzyme-independent release of tumor necrosis factor alpha and IL-1beta from a stimulated human monocytic cell line in the presence of activated neutrophils or purified proteinase 3. *Proc Natl Acad Sci U S A* **96,** 6261-6266.

Colognato R, Slupsky JR, Jendrach M, Burysek L, Syrovets T & Simmet T. (2003). Differential expression and regulation of protease-activated receptors in human peripheral monocytes and monocyte-derived antigen-presenting cells. *Blood* **102,** 2645-2652.

Compton SJ. (2003). Glycosylation and Proteinase-Activated Receptor Function. *Drug Development Research* **59,** 350-354.

Compton SJ, Cairns JA, Holgate ST & Walls AF. (2000b). Human mast cell tryptase stimulates the release of an IL-8-dependent neutrophil chemotactic activity from human umbilical vein endothelial cells (HUVEC). *Clin Exp Immunol* **121,** 31-36.

Compton SJ, Cairns JA, Palmer KJ, Al-Ani B, Hollenberg MD & Walls AF. (2000a). A polymorphic protease-activated receptor 2 (PAR2) displaying reduced sensitivity to trypsin and differential responses to PAR agonists. *J Biol Chem* **275,** 39207-39212.

Compton SJ, Renaux B, Wijesuriya SJ & Hollenberg MD. (2001). Glycosylation and the activation of proteinase-activated receptor 2 (PAR(2)) by human mast cell tryptase. *Br J Pharmacol* **134,** 705-718.

Compton SJ, Sandhu S, Wijesuriya SJ & Hollenberg MD. (2002b). Glycosylation of human proteinase-activated receptor-2 (hPAR2): role in cell surface expression and signalling. *Biochem J* **368,** 495-505.

Connolly AJ, Ishihara H, Kahn ML, Farese RV, Jr. & Coughlin SR. (1996). Role of the thrombin receptor in development and evidence for a second receptor. *Nature* **381,** 516-519.

Corvera CU, Dery O, McConalogue K, Bohm SK, Khitin LM, Caughey GH, Payan DG & Bunnett NW. (1997). Mast cell tryptase regulates rat colonic myocytes through proteinase-activated receptor 2. *J Clin Invest* **100,** 1383-1393.

Corvera CU, Dery O, McConalogue K, Gamp P, Thoma M, Al-Ani B, Caughey GH, Hollenberg MD & Bunnett NW. (1999). Thrombin and mast cell tryptase regulate guinea-pig myenteric neurons through proteinase-activated receptors-1 and -2. *J Physiol* **517 (Pt 3),** 741-756.

Cottrell GS, Amadesi S, Grady EF & Bunnett NW. (2004). Trypsin IV, a novel agonist of protease-activated receptors 2 and 4. *J Biol Chem* **279,** 13532-13539.

Coughlin SR. (2000). Thrombin signalling and protease-activated receptors. *Nature* **407,** 258-264.

Couvineau A, Fabre C, Gaudin P, Maoret JJ & Laburthe M. (1996). Mutagenesis of N-glycosylation sites in the human vasoactive intestinal peptide 1 receptor. Evidence that asparagine 58 or 69 is crucial for correct delivery of the receptor to plasma membrane. *Biochemistry* **35,** 1745-1752.

Covic L, Gresser AL & Kuliopulos A. (2000). Biphasic kinetics of activation and signaling for PAR1 and PAR4 thrombin receptors in platelets. *Biochemistry* **39,** 5458-5467.

Cumashi A, Ansuini H, Celli N, De Blasi A, O'Brien PJ, Brass LF & Molino M. (2001). Neutrophil proteases can inactivate human PAR3 and abolish the co-receptor function of PAR3 on murine platelets. *Thromb Haemost* **85,** 533-538.

Cunningham MA, Rondeau E, Chen X, Coughlin SR, Holdsworth SR & Tipping PG. (2000). Protease-activated receptor 1 mediates thrombin-dependent, cell-mediated renal inflammation in crescentic glomerulonephritis. *The Journal of experimental medicine* **191,** 455-462.

D'Andrea MR, Derian CK, Leturcq D, Baker SM, Brunmark A, Ling P, Darrow AL, Santulli RJ, Brass LF & Andrade-Gordon P. (1998). Characterization of protease-activated receptor-2 immunoreactivity in normal human tissues. *J Histochem Cytochem* **46,** 157-164.

D'Andrea MR, Rogahn CJ & Andrade-Gordon P. (2000). Localization of protease-activated receptors-1 and -2 in human mast cells: indications for an amplified mast cell degranulation cascade. *Biotech Histochem* **75,** 85-90.

Darmoul D, Gratio V, Devaud H, Lehy T & Laburthe M. (2003). Aberrant expression and activation of the thrombin receptor protease-activated receptor-1 induces cell proliferation and motility in human colon cancer cells. *Am J Pathol* **162,** 1503-1513.

Davidson JS, Flanagan CA, Zhou W, Becker, II, Elario R, Emeran W, Sealfon SC & Millar RP. (1995). Identification of N-glycosylation sites in the gonadotropin-releasing hormone receptor: role in receptor expression but not ligand binding. *Mol Cell Endocrinol* **107,** 241-245.

de Garavilla L, Vergnolle N, Young SH, Ennes H, Steinhoff M, Ossovskaya VS, D'Andrea MR, Mayer EA, Wallace JL, Hollenberg MD, Andrade-Gordon P &

Bunnett NW. (2001). Agonists of proteinase-activated receptor 1 induce plasma extravasation by a neurogenic mechanism. *Br J Pharmacol* **133,** 975-987.

De Kreij A VG, and van den Burg B. . (2000). Substrate specificity in the highly heterogeneous M4 peptidase family is determined by a small subset of amino acids. *J Biol Chem* 31115-31120.

Dery O, Corvera CU, Steinhoff M & Bunnett NW. (1998). Proteinase-activated receptors: novel mechanisms of signaling by serine proteases. *Am J Physiol* **274,** C1429-1452.

Deslauriers B, Ponce C, Lombard C, Larguier R, Bonnafous JC & Marie J. (1999). N-glycosylation requirements for the AT1a angiotensin II receptor delivery to the plasma membrane. *Biochem J* **339 (Pt 2),** 397-405.

Downes GB & Gautam N. (1999). The G protein subunit gene families. *Genomics* **62,** 544-552.

Drake MT, Shenoy SK & Lefkowitz RJ. (2006). Trafficking of G protein-coupled receptors. *Circ Res* **99,** 570-582.

Drickamer METK. (2006). *Introduction to Glycobiology*. OXFORD UNIVERSITY PRESS.

Dulon S, Cande C, Bunnett NW, Hollenberg MD, Chignard M & Pidard D. (2003). Proteinase-activated receptor-2 and human lung epithelial cells: disarming by neutrophil serine proteinases. *Am J Respir Cell Mol Biol* **28,** 339-346.

Elbein AD. (1984). Inhibitors of the biosynthesis and processing of N-linked oligosaccharides. *CRC Crit Rev Biochem* **16,** 21-49.

Ellgaard L & Helenius A. (2003). Quality control in the endoplasmic reticulum. *Nat Rev Mol Cell Biol* **4,** 181-191.

Endo S. (1962). Studies on protease produced by thermophilic bacteria. . *J Ferment Technol* **40,** 346-353.

Fan G, Goldsmith PK, Collins R, Dunn CK, Krapcho KJ, Rogers KV & Spiegel AM. (1997). N-linked glycosylation of the human Ca2+ receptor is essential for its expression at the cell surface. *Endocrinology* **138,** 1916-1922.

Faruqi TR, Weiss EJ, Shapiro MJ, Huang W & Coughlin SR. (2000). Structure-function analysis of protease-activated receptor 4 tethered ligand peptides. Determinants of specificity and utility in assays of receptor function. *J Biol Chem* **275,** 19728-19734.

Faurschou M & Borregaard N. (2003). Neutrophil granules and secretory vesicles in inflammation. *Microbes Infect* **5,** 1317-1327.

Fujiwara M, Jin E, Ghazizadeh M & Kawanami O. (2005). Activation of PAR4 induces a distinct actin fiber formation via p38 MAPK in human lung endothelial cells. *J Histochem Cytochem* **53,** 1121-1129.

Fukushima Y, Oka Y, Saitoh T, Katagiri H, Asano T, Matsuhashi N, Takata K, van Breda E, Yazaki Y & Sugano K. (1995). Structural and functional analysis of the canine histamine H2 receptor by site-directed mutagenesis: N-glycosylation is not vital for its action. *Biochem J* **310 (Pt 2),** 553-558.

Garcia Rodriguez C, Cundell DR, Tuomanen EI, Kolakowski LF, Jr., Gerard C & Gerard NP. (1995). The role of N-glycosylation for functional expression of the human platelet-activating factor receptor. Glycosylation is required for efficient membrane trafficking. *J Biol Chem* **270,** 25178-25184.

Gerszten RE, Chen J, Ishii M, Ishii K, Wang L, Nanevicz T, Turck CW, Vu TK & Coughlin SR. (1994). Specificity of the thrombin receptor for agonist peptide is defined by its extracellular surface. *Nature* **368,** 648-651.

Gether U. (2000). Uncovering molecular mechanisms involved in activation of G protein-coupled receptors. *Endocr Rev* **21,** 90-113.

Glusa E, Saft A, Prasa D & Sturzebecher J. (1997). Trypsin- and SLIGRL-induced vascular relaxation and the inhibition by benzamidine derivatives. *Thromb Haemost* **78,** 1399-1403.

Goffard A, Callens N, Bartosch B, Wychowski C, Cosset FL, Montpellier C & Dubuisson J. (2005). Role of N-linked glycans in the functions of hepatitis C virus envelope glycoproteins. *J Virol* **79,** 8400-8409.

Goke R, Just R, Lankat-Buttgereit B & Goke B. (1994). Glycosylation of the GLP-1 receptor is a prerequisite for regular receptor function. *Peptides* **15,** 675-681.

Gong Q, Anderson CL, January CT & Zhou Z. (2002). Role of glycosylation in cell surface expression and stability of HERG potassium channels. *Am J Physiol Heart Circ Physiol* **283,** H77-84.

Gottschalk A. (1958). Neuraminidase; its substrate and mode of action. *Adv Enzymol Relat Subj Biochem* **20,** 135-146.

Grandaliano G, Monno R, Ranieri E, Gesualdo L, Schena FP, Martino C & Ursi M. (2000). Regenerative and proinflammatory effects of thrombin on human proximal tubular cells. *J Am Soc Nephrol* **11,** 1016-1025.

Grishina Z, Ostrowska E, Halangk W, Sahin-Toth M & Reiser G. (2005). Activity of recombinant trypsin isoforms on human proteinase-activated receptors (PAR): mesotrypsin cannot activate epithelial PAR-1, -2, but weakly activates brain PAR-1. *Br J Pharmacol* **146,** 990-999.

Gui Y, Loutzenhiser R & Hollenberg MD. (2003). Bidirectional regulation of renal hemodynamics by activation of PAR1 and PAR2 in isolated perfused rat kidney. *American journal of physiology* **285,** F95-104.

Hamilton JR, Chow JM & Cocks TM. (1999). Protease-activated receptor-2 turnover stimulated independently of receptor activation in porcine coronary endothelial cells. *Br J Pharmacol* **127,** 617-622.

Hamilton JR & Cocks TM. (2000). Heterogeneous mechanisms of endothelium-dependent relaxation for thrombin and peptide activators of protease-activated receptor-1 in porcine isolated coronary artery. *Br J Pharmacol* **130,** 181-188.

Hamilton JR, Moffatt JD, Frauman AG & Cocks TM. (2001). Protease-activated receptor (PAR) 1 but not PAR2 or PAR4 mediates endothelium-dependent relaxation to thrombin and trypsin in human pulmonary arteries. *J Cardiovasc Pharmacol* **38,** 108-119.

Hamilton JR, Moffatt JD, Tatoulis J & Cocks TM. (2002). Enzymatic activation of endothelial protease-activated receptors is dependent on artery diameter in human and porcine isolated coronary arteries. *Br J Pharmacol* **136,** 492-501.

Hamm HE. (1998). The many faces of G protein signaling. *J Biol Chem* **273,** 669-672.

Hammond C, Braakman I & Helenius A. (1994). Role of N-linked oligosaccharide recognition, glucose trimming, and calnexin in glycoprotein folding and quality control. *Proc Natl Acad Sci U S A* **91,** 913-917.

Hansen KK, Saifeddine M & Hollenberg MD. (2004). Tethered ligand-derived peptides of proteinase-activated receptor 3 (PAR3) activate PAR1 and PAR2 in Jurkat T cells. *Immunology* **112,** 183-190.

Harduin-Lepers A, Vallejo-Ruiz V, Krzewinski-Recchi MA, Samyn-Petit B, Julien S & Delannoy P. (2001). The human sialyltransferase family. *Biochimie* **83,** 727-737.

Hawtin SR, Davies AR, Matthews G & Wheatley M. (2001). Identification of the glycosylation sites utilized on the V1a vasopressin receptor and assessment of their role in receptor signalling and expression. *Biochem J* **357,** 73-81.

He J, Xu J, Castleberry AM, Lau AG & Hall RA. (2002). Glycosylation of beta(1)-adrenergic receptors regulates receptor surface expression and dimerization. *Biochem Biophys Res Commun* **297,** 565-572.

He S, Aslam A, Gaca MD, He Y, Buckley MG, Hollenberg MD & Walls AF. (2004). Inhibitors of tryptase as mast cell-stabilizing agents in the human airways: effects of tryptase and other agonists of proteinase-activated receptor 2 on histamine release. *J Pharmacol Exp Ther* **309,** 119-126.

He S, Gaca MD, McEuen AR & Walls AF. (1999). Inhibitors of chymase as mast cell-stabilizing agents: contribution of chymase in the activation of human mast cells. *J Pharmacol Exp Ther* **291,** 517-523.

He S, Gaca MD & Walls AF. (2001). The activation of synovial mast cells: modulation of histamine release by tryptase and chymase and their inhibitors. *Eur J Pharmacol* **412,** 223-229.

He S, McEuen AR, Blewett SA, Li P, Buckley MG, Leufkens P & Walls AF. (2003). The inhibition of mast cell activation by neutrophil lactoferrin: uptake by mast cells and interaction with tryptase, chymase and cathepsin G. *Biochem Pharmacol* **65,** 1007-1015.

He S & Walls AF. (1998a). The induction of a prolonged increase in microvascular permeability by human mast cell chymase. *Eur J Pharmacol* **352,** 91-98.

Hebert DN, Garman SC & Molinari M. (2005). The glycan code of the endoplasmic reticulum: asparagine-linked carbohydrates as protein maturation and quality-control tags. *Trends Cell Biol* **15,** 364-370.

Helenius A. (1994). How N-linked oligosaccharides affect glycoprotein folding in the endoplasmic reticulum. *Mol Biol Cell* **5,** 253-265.

Helenius A & Aebi M. (2001). Intracellular functions of N-linked glycans. *Science* **291,** 2364-2369.

Helenius A & Aebi M. (2004). Roles of N-linked glycans in the endoplasmic reticulum. *Annu Rev Biochem* **73,** 1019-1049.

Helenius J & Aebi M. (2002). Transmembrane movement of dolichol linked carbohydrates during N-glycoprotein biosynthesis in the endoplasmic reticulum. *Semin Cell Dev Biol* **13,** 171-178.

Hiemstra PS, van Wetering S & Stolk J. (1998). Neutrophil serine proteinases and defensins in chronic obstructive pulmonary disease: effects on pulmonary epithelium. *Eur Respir J* **12,** 1200-1208.

Hirano K. (2007). The roles of proteinase-activated receptors in the vascular physiology and pathophysiology. *Arterioscler Thromb Vasc Biol* **27,** 27-36.

Hirota M, Ohmuraya M & Baba H. (2006). The role of trypsin, trypsin inhibitor, and trypsin receptor in the onset and aggravation of pancreatitis. *J Gastroenterol* **41,** 832-836.

Ho HH, Gilbert MT, Nussenzveig DR & Gershengorn MC. (1999). Glycosylation is important for binding to human calcitonin receptors. *Biochemistry* **38,** 1866-1872.

Hollenberg MD. (1996). Protease-mediated signalling: new paradigms for cell regulation and drug development. *Trends Pharmacol Sci* **17,** 3-6.

Hollenberg MD. (2005a). Physiology and pathophysiology of proteinase-activated receptors (PARs): proteinases as hormone-like signal messengers: PARs and more. *J Pharmacol Sci* **97,** 8-13.

Hollenberg MD & Compton SJ. (2002). International Union of Pharmacology. XXVIII. Proteinase-activated receptors. *Pharmacol Rev* **54,** 203-217.

Hollenberg MD, Saifeddine M, Al-Ani B & Gui Y. (1999). Proteinase-activated receptor 4 (PAR4): action of PAR4-activating peptides in vascular and gastric tissue and lack of cross-reactivity with PAR1 and PAR2. *Can J Physiol Pharmacol* **77,** 458-464.

Hollenberg MD, Saifeddine M, al-Ani B & Kawabata A. (1997). Proteinase-activated receptors: structural requirements for activity, receptor cross-reactivity, and receptor selectivity of receptor-activating peptides. *Can J Physiol Pharmacol* **75,** 832-841.

Hollenberg MD, Saifeddine M, Sandhu S, Houle S & Vergnolle N. (2004). Proteinase-activated receptor-4: evaluation of tethered ligand-derived peptides as probes for receptor function and as inflammatory agonists in vivo. *Br J Pharmacol* **143,** 443-454.

Hossler P, Mulukutla BC & Hu WS. (2007). Systems analysis of N-glycan processing in mammalian cells. *PLoS ONE* **2,** e713.

Houle S, Papez MD, Ferazzini M, Hollenberg MD & Vergnolle N. (2005). Neutrophils and the kallikrein-kinin system in proteinase-activated receptor 4-mediated inflammation in rodents. *Br J Pharmacol* **146,** 670-678.

Howell DC, Goldsack NR, Marshall RP, McAnulty RJ, Starke R, Purdy G, Laurent GJ & Chambers RC. (2001). Direct thrombin inhibition reduces lung collagen, accumulation, and connective tissue growth factor mRNA levels in bleomycin-induced pulmonary fibrosis. *The American journal of pathology* **159,** 1383-1395.

Howell DC, Laurent GJ & Chambers RC. (2002). Role of thrombin and its major cellular receptor, protease-activated receptor-1, in pulmonary fibrosis. *Biochem Soc Trans* **30,** 211-216.

Hung DT, Vu TH, Nelken NA & Coughlin SR. (1992a). Thrombin-induced events in non-platelet cells are mediated by the unique proteolytic mechanism established for the cloned platelet thrombin receptor. *J Cell Biol* **116,** 827-832.

Hung DT, Wong YH, Vu TK & Coughlin SR. (1992b). The cloned platelet thrombin receptor couples to at least two distinct effectors to stimulate phosphoinositide hydrolysis and inhibit adenylyl cyclase. *J Biol Chem* **267,** 20831-20834.

Hung DT, Wong YH, Vu TK & Coughlin SR. (1992b). The cloned platelet thrombin receptor couples to at least two distinct effectors to stimulate phosphoinositide hydrolysis and inhibit adenylyl cyclase. *J Biol Chem* **267,** 20831-20834.

Huntington JA. (2005). Molecular recognition mechanisms of thrombin. *J Thromb Haemost* **3,** 1861-1872.

Hur EM & Kim KT. (2002). G protein-coupled receptor signalling and cross-talk: achieving rapidity and specificity. *Cell Signal* **14,** 397-405.

Imperiali B & O'Connor SE. (1999). Effect of N-linked glycosylation on glycopeptide and glycoprotein structure. *Curr Opin Chem Biol* **3,** 643-649.

Imperiali B & Rickert KW. (1995). Conformational implications of asparagine-linked glycosylation. *Proc Natl Acad Sci U S A* **92,** 97-101.

Innamorati G, Sadeghi H & Birnbaumer M. (1996). A fully active nonglycosylated V2 vasopressin receptor. *Mol Pharmacol* **50,** 467-473.

Ishida Y, Nagai A, Kobayashi S & Kim SU. (2006). Upregulation of protease-activated receptor-1 in astrocytes in Parkinson disease: astrocyte-mediated neuroprotection through increased levels of glutathione peroxidase. *Journal of neuropathology and experimental neurology* **65,** 66-77.

Ishihara H, Connolly AJ, Zeng D, Kahn ML, Zheng YW, Timmons C, Tram T & Coughlin SR. (1997). Protease-activated receptor 3 is a second thrombin receptor in humans. *Nature* **386,** 502-506.

Ishihara H, Zeng D, Connolly AJ, Tam C & Coughlin SR. (1998). Antibodies to protease-activated receptor 3 inhibit activation of mouse platelets by thrombin. *Blood* **91,** 4152-4157.

Ishii K, Gerszten R, Zheng YW, Welsh JB, Turck CW & Coughlin SR. (1995). Determinants of thrombin receptor cleavage. Receptor domains involved, specificity, and role of the P3 aspartate. *J Biol Chem* **270,** 16435-16440.

Janoff A & Scherer J. (1968). Mediators of inflammation in leukocyte lysosomes. IX. Elastinolytic activity in granules of human polymorphonuclear leukocytes. *J Exp Med* **128,** 1137-1155.

Jayadev S, Smith RD, Jagadeesh G, Baukal AJ, Hunyady L & Catt KJ. (1999). N-linked glycosylation is required for optimal AT1a angiotensin receptor expression in COS-7 cells. *Endocrinology* **140,** 2010-2017.

Judex MO & Mueller BM. (2005). Plasminogen activation/plasmin in rheumatoid arthritis: matrix degradation and more. *Am J Pathol* **166,** 645-647.

Kahn ML, Hammes SR, Botka C & Coughlin SR. (1998a). Gene and locus structure and chromosomal localization of the protease-activated receptor gene family. *J Biol Chem* **273,** 23290-23296.

Kahn ML, Nakanishi-Matsui M, Shapiro MJ, Ishihara H & Coughlin SR. (1999). Protease-activated receptors 1 and 4 mediate activation of human platelets by thrombin. *J Clin Invest* **103,** 879-887.

Kahn ML, Zheng YW, Huang W, Bigornia V, Zeng D, Moff S, Farese RV, Jr., Tam C & Coughlin SR. (1998). A dual thrombin receptor system for platelet activation. *Nature* **394,** 690-694.

Kahn ML, Zheng YW, Huang W, Bigornia V, Zeng D, Moff S, Farese RV, Jr., Tam C & Coughlin SR. (1998b). A dual thrombin receptor system for platelet activation. *Nature* **394,** 690-694.

Kanthou C, Kanse SM, Kakkar VV & Benzakour O. (1996). Involvement of pertussis toxin-sensitive and -insensitive G proteins in alpha-thrombin signalling on cultured human vascular smooth muscle cells. *Cell Signal* **8,** 59-66.

Kao RC, Wehner NG, Skubitz KM, Gray BH & Hoidal JR. (1988). Proteinase 3. A distinct human polymorphonuclear leukocyte proteinase that produces emphysema in hamsters. *J Clin Invest* **82,** 1963-1973.

Karnik SS & Khorana HG. (1990). Assembly of functional rhodopsin requires a disulfide bond between cysteine residues 110 and 187. *J Biol Chem* **265,** 17520-17524.

Karnik SS, Sakmar TP, Chen HB & Khorana HG. (1988). Cysteine residues 110 and 187 are essential for the formation of correct structure in bovine rhodopsin. *Proc Natl Acad Sci U S A* **85,** 8459-8463.

Karpa KD, Lidow MS, Pickering MT, Levenson R & Bergson C. (1999). N-linked glycosylation is required for plasma membrane localization of D5, but not D1, dopamine receptors in transfected mammalian cells. *Mol Pharmacol* **56,** 1071-1078.

Kataoka H, Hamilton JR, McKemy DD, Camerer E, Zheng YW, Cheng A, Griffin C & Coughlin SR. (2003). Protease-activated receptors 1 and 4 mediate thrombin signaling in endothelial cells. *Blood* **102,** 3224-3231.

Kaufman CK & Fuchs E. (2000). It's got you covered. NF-kappaB in the epidermis. *J Cell Biol* **149,** 999-1004.

Kaufmann R, Junker U, Nuske K, Westermann M, Henklein P, Scheele J & Junker K. (2002). PAR-1- and PAR-3-type thrombin receptor expression in primary cultures of human renal cell carcinoma cells. *International journal of oncology* **20,** 177-180.

Kaufmann R, Patt S, Zieger M, Kraft R, Tausch S, Henklein P & Nowak G. (2000). The two-receptor system PAR-1/PAR-4 mediates alpha-thrombin-induced [Ca(2+)](i) mobilization in human astrocytoma cells. *J Cancer Res Clin Oncol* **126,** 91-94.

Kaufmann R, Schulze B, Krause G, Mayr LM, Settmacher U & Henklein P. (2005). Proteinase-activated receptors (PARs)--the PAR3 Neo-N-terminal peptide TFRGAP interacts with PAR1. *Regul Pept* **125,** 61-66.

Kaushal S, Ridge KD & Khorana HG. (1994). Structure and function in rhodopsin: the role of asparagine-linked glycosylation. *Proc Natl Acad Sci U S A* **91,** 4024-4028.

Kawabata A, Kuroda R, Kuroki N, Nishikawa H & Kawai K. (2000a). Dual modulation by thrombin of the motility of rat oesophageal muscularis mucosae via two distinct protease-activated receptors (PARs): a novel role for PAR-4 as opposed to PAR-1. *Br J Pharmacol* **131,** 578-584.

Kawabata A, Kuroda R, Minami T, Kataoka K & Taneda M. (1998). Increased vascular permeability by a specific agonist of protease-activated receptor-2 in rat hindpaw. *Br J Pharmacol* **125,** 419-422.

Kawabata A, Morimoto N, Nishikawa H, Kuroda R, Oda Y & Kakehi K. (2000b). Activation of protease-activated receptor-2 (PAR-2) triggers mucin secretion in the rat sublingual gland. *Biochem Biophys Res Commun* **270,** 298-302.

Kawabata A, Nishikawa H, Kuroda R, Kawai K & Hollenberg MD. (2000c). Proteinase-activated receptor-2 (PAR-2): regulation of salivary and pancreatic exocrine secretion in vivo in rats and mice. *Br J Pharmacol* **129,** 1808-1814.

Kawabata A, Nishikawa H, Saitoh H, Nakaya Y, Hiramatsu K, Kubo S, Nishida M, Kawao N, Kuroda R, Sekiguchi F, Kinoshita M, Kakehi K, Arizono N, Yamagishi H & Kawai K. (2004). A protective role of protease-activated receptor 1 in rat gastric mucosa. *Gastroenterology* **126,** 208-219.

Kawabata A, Saifeddine M, Al-Ani B, Leblond L & Hollenberg MD. (1999). Evaluation of proteinase-activated receptor-1 (PAR1) agonists and antagonists using a cultured cell receptor desensitization assay: activation of PAR2 by PAR1-targeted ligands. *J Pharmacol Exp Ther* **288,** 358-370.

Kim S, Foster C, Lecchi A, Quinton TM, Prosser DM, Jin J, Cattaneo M & Kunapuli SP. (2002). Protease-activated receptors 1 and 4 do not stimulate G(i) signaling pathways in the absence of secreted ADP and cause human platelet aggregation independently of G(i) signaling. *Blood* **99,** 3629-3636.

Kimura M, Andersen TT, Fenton JW, 2nd, Bahou WF & Aviv A. (1996). Plasmin-platelet interaction involves cleavage of functional thrombin receptor. *Am J Physiol* **271,** C54-60.

Kimura T, Makino Y, Bathgate R, Ivell R, Nobunaga T, Kubota Y, Kumazawa I, Saji F, Murata Y, Nishihara T, Hashimoto M & Kinoshita M. (1997). The role of N-terminal glycosylation in the human oxytocin receptor. *Mol Hum Reprod* **3,** 957-963.

Knight DA, Lim S, Scaffidi AK, Roche N, Chung KF, Stewart GA & Thompson PJ. (2001). Protease-activated receptors in human airways: upregulation of PAR-2 in respiratory epithelium from patients with asthma. *J Allergy Clin Immunol* **108,** 797-803.

Kohno M & Pouyssegur J. (2003). Pharmacological inhibitors of the ERK signaling pathway: application as anticancer drugs. *Prog Cell Cycle Res* **5,** 219-224.

Kolakowski LF, Jr. (1994). GCRDb: a G-protein-coupled receptor database. *Receptors Channels* **2,** 1-7.

Kornfeld R & Kornfeld S. (1985a). Assembly of asparagine-linked oligosaccharides. *Annu Rev Biochem* **54,** 631-664.

Kornfeld R & Kornfeld S. (1985b). Assembly of Asparagine-Linked Oligosaccharides. *Annu Rev Biochem* **Vol. 54,** Pages 631-664.

Krishnaswamy S, Nesheim ME, Pryzdial EL & Mann KG. (1993). Assembly of prothrombinase complex. *Methods Enzymol* **222,** 260-280.

Krupnick JG & Benovic JL. (1998). The role of receptor kinases and arrestins in G protein-coupled receptor regulation. *Annu Rev Pharmacol Toxicol* **38,** 289-319.

Kube D, Adams L, Perez A & Davis PB. (2001). Terminal sialylation is altered in airway cells with impaired CFTR-mediated chloride transport. *Am J Physiol Lung Cell Mol Physiol* **280,** L482-492.

Kuliopulos A, Covic L, Seeley SK, Sheridan PJ, Helin J & Costello CE. (1999). Plasmin desensitization of the PAR1 thrombin receptor: kinetics, sites of truncation, and implications for thrombolytic therapy. *Biochemistry* **38,** 4572-4585.

Kundra R & Kornfeld S. (1999). Asparagine-linked oligosaccharides protect Lamp-1 and Lamp-2 from intracellular proteolysis. *J Biol Chem* **274,** 31039-31046.

LaMorte VJ, Kennedy ED, Collins LR, Goldstein D, Harootunian AT, Brown JH & Feramisco JR. (1993). A requirement for Ras protein function in thrombin-stimulated mitogenesis in astrocytoma cells. *J Biol Chem* **268,** 19411-19415.

Lan RS, Stewart GA & Henry PJ. (2000). Modulation of airway smooth muscle tone by protease activated receptor-1,-2,-3 and -4 in trachea isolated from influenza A virus-infected mice. *Br J Pharmacol* **129,** 63-70.

Lan RS, Stewart GA & Henry PJ. (2002). Role of protease-activated receptors in airway function: a target for therapeutic intervention? *Pharmacol Ther* **95,** 239-257.

Lee MC & Huang SC. (2007). Proteinase-activated receptor-1 (PAR(1)) and PAR(2) but not PAR(4) mediate contraction in human and guinea-pig gallbladders. *Neurogastroenterol Motil*.

Leger AJ, Jacques SL, Badar J, Kaneider NC, Derian CK, Andrade-Gordon P, Covic L & Kuliopulos A. (2006). Blocking the protease-activated receptor 1-4 heterodimer in platelet-mediated thrombosis. *Circulation* **113,** 1244-1254.

Lehmann F, Tiralongo E & Tiralongo J. (2006). Sialic acid-specific lectins: occurrence, specificity and function. *Cell Mol Life Sci* **63,** 1331-1354.

Lerner DJ, Chen M, Tram T & Coughlin SR. (1996). Agonist recognition by proteinase-activated receptor 2 and thrombin receptor. Importance of extracellular loop interactions for receptor function. *J Biol Chem* **271,** 13943-13947.

Loew D, Perrault C, Morales M, Moog S, Ravanat C, Schuhler S, Arcone R, Pietropaolo C, Cazenave JP, van Dorsselaer A & Lanza F. (2000). Proteolysis of the exodomain of recombinant protease-activated receptors: prediction of receptor activation or inactivation by MALDI mass spectrometry. *Biochemistry* **39,** 10812-10822.

Lohse MJ, Benovic JL, Codina J, Caron MG & Lefkowitz RJ. (1990). beta-Arrestin: a protein that regulates beta-adrenergic receptor function. *Science* **248,** 1547-1550.

Macfarlane SR, Seatter MJ, Kanke T, Hunter GD & Plevin R. (2001). Proteinase-activated receptors. *Pharmacol Rev* **53,** 245-282.

Magazine HI, King JM & Srivastava KD. (1996). Protease activated receptors modulate aortic vascular tone. *Int J Cardiol* **53 Suppl,** S75-80.

Malykh YN, Schauer R & Shaw L. (2001). N-Glycolylneuraminic acid in human tumours. *Biochimie* **83,** 623-634.

Mann KG, Butenas S & Brummel K. (2003). The dynamics of thrombin formation. *Arterioscler Thromb Vasc Biol* **23,** 17-25.

Mari B, Guerin S, Far DF, Breitmayer JP, Belhacene N, Peyron JF, Rossi B & Auberger P. (1996). Thrombin and trypsin-induced Ca(2+) mobilization in human T cell lines through interaction with different protease-activated receptors. *Faseb J* **10,** 309-316.

Mazharian A, Roger S, Berrou E, Adam F, Kauskot A, Nurden P, Jandrot-Perrus M & Bryckaert M. (2007). Protease-activating receptor-4 induces full platelet spreading on a fibrinogen matrix: involvement of ERK2 and p38 and Ca2+ mobilization. *J Biol Chem* **282,** 5478-5487.

McEuen AR, Gaca MD, Buckley MG, He S, Gore MG & Walls AF. (1998). Two distinct forms of human mast cell chymase--differences in affinity for heparin and in distribution in skin, heart, and other tissues. *Eur J Biochem* **256,** 461-470.

McIntosh KA, Plevin R, Ferrell WR & Lockhart JC. (2007). The therapeutic potential of proteinase-activated receptors in arthritis. *Curr Opin Pharmacol* **7,** 334-338.

McNamara CA, Sarembock IJ, Gimple LW, Fenton JW, 2nd, Coughlin SR & Owens GK. (1993). Thrombin stimulates proliferation of cultured rat aortic smooth muscle cells by a proteolytically activated receptor. *J Clin Invest* **91,** 94-98.

Mochizuki K, Kagawa T, Numari A, Harris MJ, Itoh J, Watanabe N, Mine T & Arias IM. (2007). Two N-linked glycans are required to maintain the transport activity of the bile salt export pump (ABCB11) in MDCK II cells. *Am J Physiol Gastrointest Liver Physiol* **292,** G818-828.

Molino M, Barnathan ES, Numerof R, Clark J, Dreyer M, Cumashi A, Hoxie JA, Schechter N, Woolkalis M & Brass LF. (1997). Interactions of mast cell tryptase with thrombin receptors and PAR-2. *J Biol Chem* **272,** 4043-4049.

Molino M, Barnathan ES, Numerof R, Clark J, Dreyer M, Cumashi A, Hoxie JA, Schechter N, Woolkalis M & Brass LF. (1997a). Interactions of mast cell tryptase with thrombin receptors and PAR-2. *J Biol Chem* **272,** 4043-4049.

Molino M, Blanchard N, Belmonte E, Tarver AP, Abrams C, Hoxie JA, Cerletti C & Brass LF. (1995). Proteolysis of the human platelet and endothelial cell thrombin receptor by neutrophil-derived cathepsin G. *J Biol Chem* **270,** 11168-11175.

Molino M, Woolkalis MJ, Reavey-Cantwell J, Pratico D, Andrade-Gordon P, Barnathan ES & Brass LF. (1997b). Endothelial cell thrombin receptors and PAR-2. Two protease-activated receptors located in a single cellular environment. *J Biol Chem* **272,** 11133-11141.

Molla A, Matsumura Y, Yamamoto T, Okamura R & Maeda H. (1987). Pathogenic capacity of proteases from Serratia marcescens and Pseudomonas aeruginosa and their suppression by chicken egg white ovomacroglobulin. *Infect Immun* **55,** 2509-2517.

Moloney DJ, Panin VM, Johnston SH, Chen J, Shao L, Wilson R, Wang Y, Stanley P, Irvine KD, Haltiwanger RS & Vogt TF. (2000). Fringe is a glycosyltransferase that modifies Notch. *Nature* **406,** 369-375.

Momota F, Hirano K, Hirano M, Nishimura J & Kanaide H. (2006). Involvement of Gi/o in the PAR-4-induced NO production in endothelial cells. *Biochem Biophys Res Commun* **342,** 365-371.

Moore CA, Milano SK & Benovic JL. (2007). Regulation of receptor trafficking by GRKs and arrestins. *Annual review of physiology* **69,** 451-482.

Mule F, Baffi MC & Cerra MC. (2002). Dual effect mediated by protease-activated receptors on the mechanical activity of rat colon. *Br J Pharmacol* **136,** 367-374.

Mule F, Pizzuti R, Capparelli A & Vergnolle N. (2004). Evidence for the presence of functional protease activated receptor 4 (PAR4) in the rat colon. *Gut* **53,** 229-234.

Munster-Kuhnel AK, Tiralongo J, Krapp S, Weinhold B, Ritz-Sedlacek V, Jacob U & Gerardy-Schahn R. (2004). Structure and function of vertebrate CMP-sialic acid synthetases. *Glycobiology* **14,** 43R-51R.

Nagata M, Shijubo N, Walls AF, Ichimiya S, Abe S & Sato N. (2003). Chymase-positive mast cells in small sized adenocarcinoma of the lung. *Virchows Arch* **443,** 565-573.

Nagayama Y, Nishihara E, Namba H, Yamashita S & Niwa M. (2000). Identification of the sites of asparagine-linked glycosylation on the human thyrotropin receptor and studies on their role in receptor function and expression. *J Pharmacol Exp Ther* **295,** 404-409.

Nakayama N, Eichhorst ST, Muller M & Krammer PH. (2001). Ethanol-induced apoptosis in hepatoma cells proceeds via intracellular Ca(2+) elevation, activation of TLCK-sensitive proteases, and cytochrome c release. *Exp Cell Res* **269,** 202-213.

Nakayama T, Hirano K, Hirano M, Nishimura J, Kuga H, Nakamura K, Takahashi S & Kanaide H. (2004). Inactivation of protease-activated receptor-1 by proteolytic removal of the ligand region in vascular endothelial cells. *Biochem Pharmacol* **68,** 23-32.

Nakayama T, Hirano K, Shintani Y, Nishimura J, Nakatsuka A, Kuga H, Takahashi S & Kanaide H. (2003). Unproductive cleavage and the inactivation of protease-activated receptor-1 by trypsin in vascular endothelial cells. *Br J Pharmacol* **138,** 121-130.

Nanevicz T, Ishii M, Wang L, Chen M, Chen J, Turck CW, Cohen FE & Coughlin SR. (1995). Mechanisms of thrombin receptor agonist specificity. Chimeric receptors and complementary mutations identify an agonist recognition site. *J Biol Chem* **270,** 21619-21625.

Nanevicz T, Wang L, Chen M, Ishii M & Coughlin SR. (1996). Thrombin receptor activating mutations. Alteration of an extracellular agonist recognition domain causes constitutive signaling. *J Biol Chem* **271,** 702-706.

Nguyen TD, Moody MW, Steinhoff M, Okolo C, Koh DS & Bunnett NW. (1999). Trypsin activates pancreatic duct epithelial cell ion channels through proteinase-activated receptor-2. *J Clin Invest* **103,** 261-269.

Nicole O, Goldshmidt A, Hamill CE, Sorensen SD, Sastre A, Lyuboslavsky P, Hepler JR, McKeon RJ & Traynelis SF. (2005). Activation of protease-activated receptor-1 triggers astrogliosis after brain injury. *J Neurosci* **25,** 4319-4329.

Noorbakhsh F, Vergnolle N, Hollenberg MD & Power C. (2003). Proteinase-activated receptors in the nervous system. *Nat Rev Neurosci* **4,** 981-990.

Nystedt S, Emilsson K, Larsson AK, Strombeck B & Sundelin J. (1995). Molecular cloning and functional expression of the gene encoding the human proteinase-activated receptor 2. *Eur J Biochem* **232,** 84-89.

Nystedt S, Emilsson K, Larsson AK, Strombeck B & Sundelin J. (1995a). Molecular cloning and functional expression of the gene encoding the human proteinase-activated receptor 2. *Eur J Biochem* **232,** 84-89.

Nystedt S, Emilsson K, Wahlestedt C & Sundelin J. (1994). Molecular cloning of a potential proteinase activated receptor. *Proc Natl Acad Sci U S A* **91,** 9208-9212.

Nystedt S, Larsson AK, Aberg H & Sundelin J. (1995b). The mouse proteinase-activated receptor-2 cDNA and gene. Molecular cloning and functional expression. *J Biol Chem* **270,** 5950-5955.

O'Brien PJ, Molino M, Kahn M & Brass LF. (2001). Protease activated receptors: theme and variations. *Oncogene* **20,** 1570-1581.

O'Brien PJ, Prevost N, Molino M, Hollinger MK, Woolkalis MJ, Woulfe DS & Brass LF. (2000). Thrombin responses in human endothelial cells. Contributions from receptors other than PAR1 include the transactivation of PAR2 by thrombin-cleaved PAR1. *J Biol Chem* **275,** 13502-13509.

Offermanns S, Laugwitz KL, Spicher K & Schultz G. (1994). G proteins of the G12 family are activated via thromboxane A2 and thrombin receptors in human platelets. *Proc Natl Acad Sci U S A* **91,** 504-508.

Offermanns S, Toombs CF, Hu YH & Simon MI. (1997). Defective platelet activation in G alpha(q)-deficient mice. *Nature* **389,** 183-186.

Ofosu FA. (2003). Protease activated receptors 1 and 4 govern the responses of human platelets to thrombin. *Transfus Apher Sci* **28,** 265-268.

Ofosu FA, Freedman J, Dewar L, Song Y & Fenton JW, 2nd. (1998). A trypsin-like platelet protease propagates protease-activated receptor-1 cleavage and platelet activation. *Biochem J* **336 (Pt 2),** 283-285.

Ogino Y, Tanaka K & Shimizu N. (1996). Direct evidence for two distinct G proteins coupling with thrombin receptors in human neuroblastoma SH-EP cells. *Eur J Pharmacol* **316,** 105-109.

Oikonomopoulou K, Hansen KK, Saifeddine M, Tea I, Blaber M, Blaber SI, Scarisbrick I, Andrade-Gordon P, Cottrell GS, Bunnett NW, Diamandis EP & Hollenberg MD. (2006a). Proteinase-activated receptors, targets for kallikrein signaling. *J Biol Chem* **281,** 32095-32112.

Oikonomopoulou K, Hansen KK, Saifeddine M, Vergnolle N, Tea I, Diamandis EP & Hollenberg MD. (2006b). Proteinase-mediated cell signalling: targeting proteinase-activated receptors (PARs) by kallikreins and more. *Biol Chem* **387,** 677-685.

Oldham WM & Hamm HE. (2008). Heterotrimeric G protein activation by G-protein-coupled receptors. *Nat Rev Mol Cell Biol* **9,** 60-71.

Olianas MC, Dedoni S & Onali P. (2007). Proteinase-activated receptors 1 and 2 in rat olfactory system: layer-specific regulation of multiple signaling pathways in the main olfactory bulb and induction of neurite retraction in olfactory sensory neurons. *Neuroscience* **146,** 1289-1301.

Opdenakker G, Rudd PM, Ponting CP & Dwek RA. (1993). Concepts and principles of glycobiology. *Faseb J* **7,** 1330-1337.

Ossovskaya VS & Bunnett NW. (2004). Protease-activated receptors: contribution to physiology and disease. *Physiol Rev* **84,** 579-621.

Owen CA & Campbell EJ. (1999). The cell biology of leukocyte-mediated proteolysis. *J Leukoc Biol* **65,** 137-150.

Pang RT, Ng SS, Cheng CH, Holtmann MH, Miller LJ & Chow BK. (1999). Role of N-linked glycosylation on the function and expression of the human secretin receptor. *Endocrinology* **140,** 5102-5111.

Parry MA, Myles T, Tschopp J & Stone SR. (1996). Cleavage of the thrombin receptor: identification of potential activators and inactivators. *Biochem J* **320 (Pt 1),** 335-341.

Paszcuk AF, Quintao NL, Fernandes ES, Juliano L, Chapman K, Andrade-Gordon P, Campos MM, Vergnolle N & Calixto JB. (2008). Mechanisms underlying the nociceptive and inflammatory responses induced by trypsin in the mouse paw. *Eur J Pharmacol* **581,** 204-215.

Payne V & Kam PC. (2004). Mast cell tryptase: a review of its physiology and clinical significance. *Anaesthesia* **59,** 695-703.

Pearson G, Robinson F, Beers Gibson T, Xu BE, Karandikar M, Berman K & Cobb MH. (2001). Mitogen-activated protein (MAP) kinase pathways: regulation and physiological functions. *Endocr Rev* **22,** 153-183.

Pendurthi UR, Ngyuen M, Andrade-Gordon P, Petersen LC & Rao LV. (2002). Plasmin induces Cyr61 gene expression in fibroblasts via protease-activated receptor-1 and p44/42 mitogen-activated protein kinase-dependent signaling pathway. *Arterioscler Thromb Vasc Biol* **22,** 1421-1426.

Peng Q, McEuen AR, Benyon RC & Walls AF. (2003). The heterogeneity of mast cell tryptase from human lung and skin. *Eur J Biochem* **270,** 270-283.

Petrescu AJ, Milac AL, Petrescu SM, Dwek RA & Wormald MR. (2004). Statistical analysis of the protein environment of N-glycosylation sites: implications for occupancy, structure, and folding. *Glycobiology* **14,** 103-114.

Pham CT. (2006). Neutrophil serine proteases: specific regulators of inflammation. *Nat Rev Immunol* **6,** 541-550.

Post GR, Collins LR, Kennedy ED, Moskowitz SA, Aragay AM, Goldstein D & Brown JH. (1996). Coupling of the thrombin receptor to G12 may account for selective effects of thrombin on gene expression and DNA synthesis in 1321N1 astrocytoma cells. *Mol Biol Cell* **7,** 1679-1690.

Quinton TM, Kim S, Derian CK, Jin J & Kunapuli SP. (2004). Plasmin-mediated activation of platelets occurs by cleavage of protease-activated receptor 4. *J Biol Chem* **279,** 18434-18439.

Ramachandran R, Sadofsky LR, Xiao Y, Botham A, Cowen M, Morice AH & Compton SJ. (2007). Inflammatory mediators modulate thrombin and cathepsin-G signaling in human bronchial fibroblasts by inducing expression of proteinase-activated receptor-4. *Am J Physiol Lung Cell Mol Physiol* **292,** L788-798.

Rands E, Candelore MR, Cheung AH, Hill WS, Strader CD & Dixon RA. (1990). Mutational analysis of beta-adrenergic receptor glycosylation. *J Biol Chem* **265,** 10759-10764.

Rao NV, Wehner NG, Marshall BC, Gray WR, Gray BH & Hoidal JR. (1991a). Characterization of proteinase-3 (PR-3), a neutrophil serine proteinase. Structural and functional properties. *J Biol Chem* **266,** 9540-9548.

Rasmussen UB, Vouret-Craviari V, Jallat S, Schlesinger Y, Pages G, Pavirani A, Lecocq JP, Pouyssegur J & Van Obberghen-Schilling E. (1991). cDNA cloning and expression of a hamster alpha-thrombin receptor coupled to Ca2+ mobilization. *FEBS Lett* **288,** 123-128.

Ray K, Clapp P, Goldsmith PK & Spiegel AM. (1998). Identification of the sites of N-linked glycosylation on the human calcium receptor and assessment of their role in cell surface expression and signal transduction. *J Biol Chem* **273,** 34558-34567.

Renesto P, Si-Tahar M, Moniatte M, Balloy V, Van Dorsselaer A, Pidard D & Chignard M. (1997). Specific inhibition of thrombin-induced cell activation by the neutrophil proteinases elastase, cathepsin G, and proteinase 3: evidence for distinct cleavage sites within the aminoterminal domain of the thrombin receptor. *Blood* **89,** 1944-1953.

Ressa DK & Linhardt RJ. (2004). Sialic Acid Donors: Chemical Synthesis and Glycosylation. *Current Organic Synthesis* **1,** 31-46.

Sabri A, Guo J, Elouardighi H, Darrow AL, Andrade-Gordon P & Steinberg SF. (2003). Mechanisms of protease-activated receptor-4 actions in cardiomyocytes. Role of Src tyrosine kinase. *J Biol Chem* **278,** 11714-11720.

Saifeddine M, al-Ani B, Cheng CH, Wang L & Hollenberg MD. (1996). Rat proteinase-activated receptor-2 (PAR-2): cDNA sequence and activity of receptor-derived peptides in gastric and vascular tissue. *Br J Pharmacol* **118,** 521-530.

Salvesen G, Farley D, Shuman J, Przybyla A, Reilly C & Travis J. (1987). Molecular cloning of human cathepsin G: structural similarity to mast cell and cytotoxic T lymphocyte proteinases. *Biochemistry* **26,** 2289-2293.

Sambrano GR, Huang W, Faruqi T, Mahrus S, Craik C & Coughlin SR. (2000). Cathepsin G activates protease-activated receptor-4 in human platelets. *J Biol Chem* **275,** 6819-6823.

Savill JS, Wyllie AH, Henson JE, Walport MJ, Henson PM & Haslett C. (1989). Macrophage phagocytosis of aging neutrophils in inflammation. Programmed cell death in the neutrophil leads to its recognition by macrophages. *J Clin Invest* **83,** 865-875.

Scarborough RM, Naughton MA, Teng W, Hung DT, Rose J, Vu TK, Wheaton VI, Turck CW & Coughlin SR. (1992). Tethered ligand agonist peptides. Structural requirements for thrombin receptor activation reveal mechanism of proteolytic unmasking of agonist function. *J Biol Chem* **267,** 13146-13149.

Schechter I & Berger A. (1967). On the size of the active site in proteases. I. Papain. *Biochem Biophys Res Commun* **27,** 157-162.

Schechter NM, Brass LF, Lavker RM & Jensen PJ. (1998). Reaction of mast cell proteases tryptase and chymase with protease activated receptors (PARs) on keratinocytes and fibroblasts. *J Cell Physiol* **176,** 365-373.

Schmidlin F & Bunnett NW. (2001). Protease-activated receptors: how proteases signal to cells. *Curr Opin Pharmacol* **1,** 575-582.

Schmidt VA, Nierman WC, Maglott DR, Cupit LD, Moskowitz KA, Wainer JA & Bahou WF. (1998). The human proteinase-activated receptor-3 (PAR-3) gene. Identification within a Par gene cluster and characterization in vascular endothelial cells and platelets. *J Biol Chem* **273,** 15061-15068.

Schwartz LB, Lewis RA & Austen KF. (1981). Tryptase from human pulmonary mast cells. Purification and characterization. *J Biol Chem* **256,** 11939-11943.

Seymour ML, Zaidi NF, Hollenberg MD & MacNaughton WK. (2003). PAR1-dependent and independent increases in COX-2 and PGE2 in human colonic myofibroblasts stimulated by thrombin. *Am J Physiol Cell Physiol* **284,** C1185-1192.

Shapiro MJ, Weiss EJ, Faruqi TR & Coughlin SR. (2000). Protease-activated receptors 1 and 4 are shut off with distinct kinetics after activation by thrombin. *J Biol Chem* **275,** 25216-25221.

Shen F, Wang H, Zheng X & Ratnam M. (1997). Expression levels of functional folate receptors alpha and beta are related to the number of N-glycosylated sites. *Biochem J* **327 (Pt 3),** 759-764.

Sheth PD, Pedersen J, Walls AF & McEuen AR. (2003). Inhibition of dipeptidyl peptidase I in the human mast cell line HMC-1: blocked activation of tryptase, but not of the predominant chymotryptic activity. *Biochem Pharmacol* **66,** 2251-2262.

Shimizu S, Gabazza EC, Hayashi T, Ido M, Adachi Y & Suzuki K. (2000). Thrombin stimulates the expression of PDGF in lung epithelial cells. *Am J Physiol Lung Cell Mol Physiol* **279,** L503-510.

Shintani Y, Hirano K, Nakayama T, Nishimura J, Nakano H & Kanaide H. (2001). Mechanism of trypsin-induced contraction in the rat myometrium: the possible involvement of a novel member of protease-activated receptor. *Br J Pharmacol* **133,** 1276-1285.

Shpacovitch V, Feld M, Bunnett NW & Steinhoff M. (2007). Protease-activated receptors: novel PARtners in innate immunity. *Trends Immunol* **28,** 541-550.

Sokolova E & Reiser G. (2007). A novel therapeutic target in various lung diseases: airway proteases and protease-activated receptors. *Pharmacol Ther* **115,** 70-83.

Starkey PM & Barrett AJ. (1976). Human cathepsin G. Catalytic and immunological properties. *Biochem J* **155,** 273-278.

Steinhoff M, Buddenkotte J, Shpacovitch V, Rattenholl A, Moormann C, Vergnolle N, Luger TA & Hollenberg MD. (2005). Proteinase-activated receptors: transducers of proteinase-mediated signaling in inflammation and immune response. *Endocr Rev* **26,** 1-43.

Steinhoff M, Vergnolle N, Young SH, Tognetto M, Amadesi S, Ennes HS, Trevisani M, Hollenberg MD, Wallace JL, Caughey GH, Mitchell SE, Williams LM, Geppetti P, Mayer EA & Bunnett NW. (2000). Agonists of proteinase-activated receptor 2 induce inflammation by a neurogenic mechanism. *Nat Med* **6,** 151-158.

Suidan HS, Bouvier J, Schaerer E, Stone SR, Monard D & Tschopp J. (1994). Granzyme A released upon stimulation of cytotoxic T lymphocytes activates the thrombin receptor on neuronal cells and astrocytes. *Proc Natl Acad Sci U S A* **91,** 8112-8116.

Suzuki T, Moraes TJ, Vachon E, Ginzberg HH, Huang TT, Matthay MA, Hollenberg MD, Marshall J, McCulloch CA, Abreu MT, Chow CW & Downey GP. (2005). Proteinase-activated receptor-1 mediates elastase-induced apoptosis of human lung epithelial cells. *Am J Respir Cell Mol Biol* **33,** 231-247.

Syeda F, Grosjean J, Houliston RA, Keogh RJ, Carter TD, Paleolog E & Wheeler-Jones CP. (2006). Cyclooxygenase-2 induction and prostacyclin release by protease-activated receptors in endothelial cells require cooperation between mitogen-activated protein kinase and NF-kappaB pathways. *J Biol Chem* **281,** 11792-11804.

Tansky MF, Pothoulakis C & Leeman SE. (2007). Functional consequences of alteration of N-linked glycosylation sites on the neurokinin 1 receptor. *Proc Natl Acad Sci U S A* **104,** 10691-10696.

Taylor ME & Drickamer K. (2003). *Introduction to Glycobiology*. Oxford University Press; 2Rev Ed edition (16 Feb 2006).

Tkacz JS & Lampen O. (1975). Tunicamycin inhibition of polyisoprenyl N-acetylglucosaminyl pyrophosphate formation in calf-liver microsomes. *Biochem Biophys Res Commun* **65,** 248-257.

Tordai A, Brass LF & Gelfand EW. (1995). Tunicamycin inhibits the expression of functional thrombin receptors on human T-lymphoblastoid cells. *Biochem Biophys Res Commun* **206,** 857-862.

Tran T & Stewart AG. (2003). Protease-activated receptor (PAR)-independent growth and pro-inflammatory actions of thrombin on human cultured airway smooth muscle. *Br J Pharmacol* **138,** 865-875.

Traynelis SF & Trejo J. (2007). Protease-activated receptor signaling: new roles and regulatory mechanisms. *Curr Opin Hematol* **14,** 230-235.

Trejo J. (2003). Protease-activated receptors: new concepts in regulation of G protein-coupled receptor signaling and trafficking. *J Pharmacol Exp Ther* **307,** 437-442.

Trejo J, Connolly AJ & Coughlin SR. (1996). The cloned thrombin receptor is necessary and sufficient for activation of mitogen-activated protein kinase and mitogenesis in mouse lung fibroblasts. Loss of responses in fibroblasts from receptor knockout mice. *J Biol Chem* **271,** 21536-21541.

Ubl JJ, Grishina ZV, Sukhomlin TK, Welte T, Sedehizade F & Reiser G. (2002). Human bronchial epithelial cells express PAR-2 with different sensitivity to thermolysin. *Am J Physiol Lung Cell Mol Physiol* **282,** L1339-1348.

Ubl JJ, Sergeeva M & Reiser G. (2000). Desensitisation of protease-activated receptor-1 (PAR-1) in rat astrocytes: evidence for a novel mechanism for terminating Ca2+ signalling evoked by the tethered ligand. *J Physiol* **525 Pt 2,** 319-330.

Uehara A, Muramoto K, Takada H & Sugawara S. (2003). Neutrophil serine proteinases activate human nonepithelial cells to produce inflammatory cytokines through protease-activated receptor 2. *J Immunol* **170,** 5690-5696.

Uehara A, Sugawara S, Muramoto K & Takada H. (2002). Activation of human oral epithelial cells by neutrophil proteinase 3 through protease-activated receptor-2. *J Immunol* **169,** 4594-4603.

Unson CG, Cypess AM, Kim HN, Goldsmith PK, Carruthers CJ, Merrifield RB & Sakmar TP. (1995). Characterization of deletion and truncation mutants of the rat glucagon receptor. Seven transmembrane segments are necessary for receptor

transport to the plasma membrane and glucagon binding. *J Biol Chem* **270,** 27720-27727.

van der Geld YM, Limburg PC & Kallenberg CG. (2001). Proteinase 3, Wegener's autoantigen: from gene to antigen. *J Leukoc Biol* **69,** 177-190.

van Koppen CJ & Nathanson NM. (1990). Site-directed mutagenesis of the m2 muscarinic acetylcholine receptor. Analysis of the role of N-glycosylation in receptor expression and function. *J Biol Chem* **265,** 20887-20892.

Vanhauwe JF, Thomas TO, Minshall RD, Tiruppathi C, Li A, Gilchrist A, Yoon EJ, Malik AB & Hamm HE. (2002). Thrombin receptors activate G(o) proteins in endothelial cells to regulate intracellular calcium and cell shape changes. *J Biol Chem* **277,** 34143-34149.

Vaughan PJ, Pike CJ, Cotman CW & Cunningham DD. (1995). Thrombin receptor activation protects neurons and astrocytes from cell death produced by environmental insults. *J Neurosci* **15,** 5389-5401.

Vergnolle N. (1999). Proteinase-activated receptor-2-activating peptides induce leukocyte rolling, adhesion, and extravasation in vivo. *J Immunol* **163,** 5064-5069.

Vergnolle N. (2005). Clinical relevance of proteinase activated receptors (pars) in the gut. *Gut* **54,** 867-874.

Vergnolle N. (2008). Proteinase-activated receptors (PARs) in infection and inflammation in the gut. *Int J Biochem Cell Biol*.

Vergnolle N, Cellars L, Mencarelli A, Rizzo G, Swaminathan S, Beck P, Steinhoff M, Andrade-Gordon P, Bunnett NW, Hollenberg MD, Wallace JL, Cirino G & Fiorucci S. (2004). A role for proteinase-activated receptor-1 in inflammatory bowel diseases. *J Clin Invest* **114,** 1444-1456.

Vergnolle N, Derian CK, D'Andrea MR, Steinhoff M & Andrade-Gordon P. (2002). Characterization of thrombin-induced leukocyte rolling and adherence: a potential proinflammatory role for proteinase-activated receptor-4. *J Immunol* **169,** 1467-1473.

Vergnolle N, Hollenberg MD & Wallace JL. (1999). Pro- and anti-inflammatory actions of thrombin: a distinct role for proteinase-activated receptor-1 (PAR1). *Br J Pharmacol* **126,** 1262-1268.

Voss B, McLaughlin JN, Holinstat M, Zent R & Hamm HE. (2007). PAR1, but not PAR4, activates human platelets through a Gi/o/phosphoinositide-3 kinase signaling axis. *Mol Pharmacol* **71,** 1399-1406.

Vouret-Craviari V, Grall D, Chambard JC, Rasmussen UB, Pouyssegur J & Van Obberghen-Schilling E. (1995). Post-translational and activation-dependent

modifications of the G protein-coupled thrombin receptor. *J Biol Chem* **270,** 8367-8372.

Vu TK, Hung DT, Wheaton VI & Coughlin SR. (1991a). Molecular cloning of a functional thrombin receptor reveals a novel proteolytic mechanism of receptor activation. *Cell* **64,** 1057-1068.

Vu TK, Wheaton VI, Hung DT, Charo I & Coughlin SR. (1991b). Domains specifying thrombin-receptor interaction. *Nature* **353,** 674-677.

Walker TR, Cadwallader KA, MacKinnon A & Chilvers ER. (2005). Thrombin induces DNA synthesis and phosphoinositide hydrolysis in airway smooth muscle by activation of distinct receptors. *Biochem Pharmacol* **70,** 959-967.

Walsh MT, Foley JF & Kinsella BT. (1998). Characterization of the role of N-linked glycosylation on the cell signaling and expression of the human thromboxane A2 receptor alpha and beta isoforms. *J Pharmacol Exp Ther* **286,** 1026-1036.

Wang H, Ubl JJ, Stricker R & Reiser G. (2002). Thrombin (PAR-1)-induced proliferation in astrocytes via MAPK involves multiple signaling pathways. *Am J Physiol Cell Physiol* **283,** C1351-1364.

Wettschureck N & Offermanns S. (2005). Mammalian G proteins and their cell type specific functions. *Physiol Rev* **85,** 1159-1204.

Wheatley M & Hawtin SR. (1999). Glycosylation of G-protein-coupled receptors for hormones central to normal reproductive functioning: its occurrence and role. *Hum Reprod Update* **5,** 356-364.

Wiedow O & Meyer-Hoffert U. (2005). Neutrophil serine proteases: potential key regulators of cell signalling during inflammation. *J Intern Med* **257,** 319-328.

Wiedow O, Muhle K, Streit V & Kameyoshi Y. (1996). Human eosinophils lack human leukocyte elastase. *Biochim Biophys Acta* **1315,** 185-187.

Xu WF, Andersen H, Whitmore TE, Presnell SR, Yee DP, Ching A, Gilbert T, Davie EW & Foster DC. (1998). Cloning and characterization of human protease-activated receptor 4. *Proc Natl Acad Sci U S A* **95,** 6642-6646.

Xu Y, Zacharias U, Peraldi MN, He CJ, Lu C, Sraer JD, Brass LF & Rondeau E. (1995). Constitutive expression and modulation of the functional thrombin receptor in the human kidney. *The American journal of pathology* **146,** 101-110.

Zhao H, Sun L, Wang L, Xu Z, Zhou F, Su J, Jin J, Yang Y, Hu Y & Zha X. (2008). N-glycosylation at Asn residues 554 and 566 of E-cadherin affects cell cycle progression through extracellular signal-regulated protein kinase signaling pathway. *Acta Biochim Biophys Sin (Shanghai)* **40,** 140-148.

APPENDIX A: pcDNA3.1(+/-) Plasmid Map

pcDNA3.1(+/-) Plasmid Map

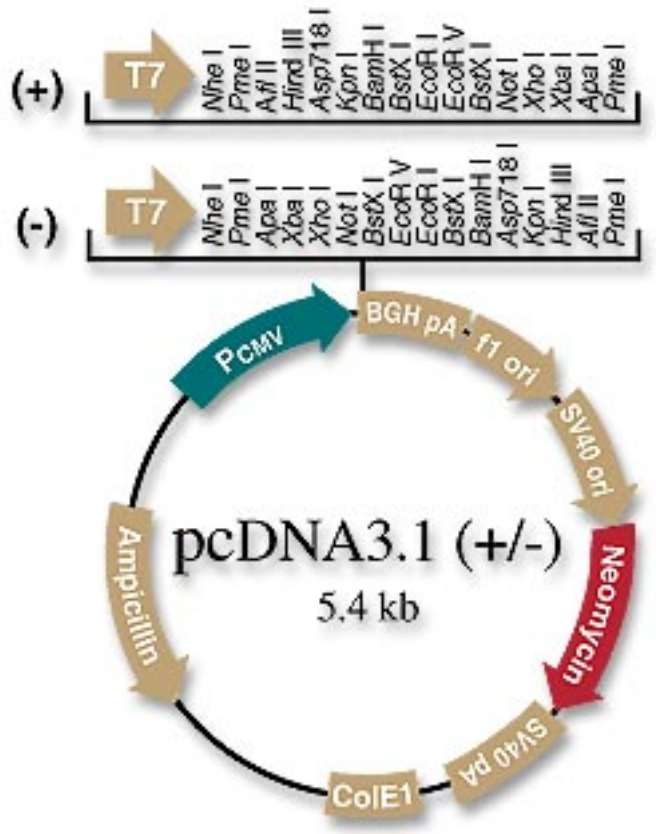

APPENDIX B: pcDNA3 Plasmid Map

pcDNA3 Plasmid Map

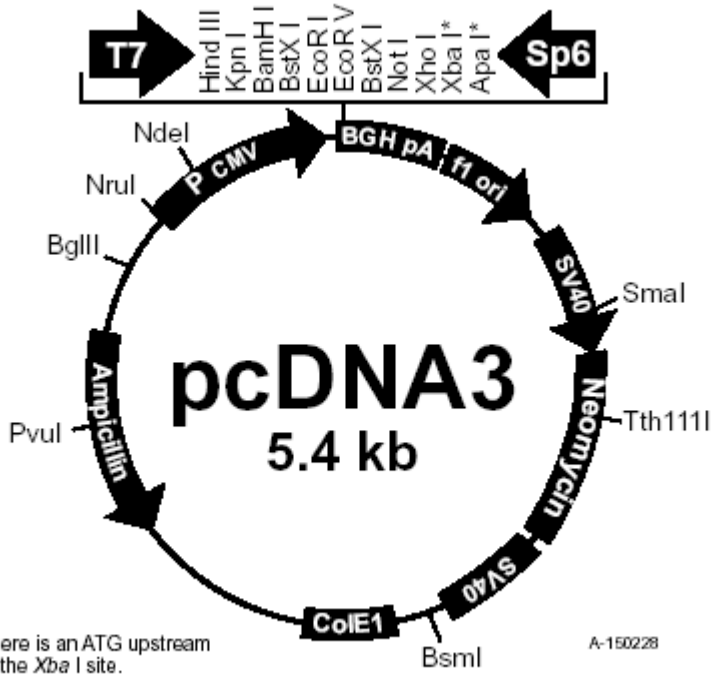

Comments for pcDNA3:
5446 nucleotides
CMV promoter: bases 209-863
T7 promoter: bases 864-882
Polylinker: bases 889-994
Sp6 promoter: bases 999-1016
BGH poly A: bases 1018-1249
SV40 promoter: bases 1790-2115
SV40 origin of replication: bases 1984-2069
Neomycin ORF: bases 2151-2945
SV40 poly A: bases 3000-3372
ColE1 origin: bases 3632-4305
Ampicillin ORF: bases 4450-5310

APPENDIX C: Human proteinase-activated receptor 1(hPAR$_1$)

cDNA/amino acid sequence

```
5′-
Atg ggg ccg cgg cgg ctg ctg ctg gtg gcc gcc tgc ttc agt
 M   G   P   R   R   L   L   L   V   A   A   C   F   S

ctg tgc ggc ccg ctg Ttg tct gcc cgc acc cgg gcc cgc agg
 L   C   G   P   L   L   S   A   R   T   R   A   R   R

cca gaa tca aaa gca aca aat gcc acc tta gat Ccc cgg tca
 P   E   S   K   A   T   N35  A36  T37  L   D   P   R   S

ttt ctt ctc agg aac ccc aat gat aaa tat gaa cca ttt tgg
 F   L   L   R   N   P   N   D   K   Y   E   P   F   W

gag gat gag gag aaa aat gaa agt ggg tta act gaa tac aga
 E   D   E   E   K   N62  E63  S64  G   L   T   E   Y   R

tta gtc tcc atc aat aaa agc agt cct ctt caa aaa caa ctt
 L   V   S   I   N75  K76  S77  S   P   L   Q   K   Q   L

cct gca ttc atc tca gaa gat gcc tcc gga tat ttg acc agc
 P   A   F   I   S   E   D   A   S   G   Y   L   T   S

tcc tgg ctg aca ctc ttt gtc cca tct gtg tac acc gga gtg
 S   W   L   T   L   F   V   P   S   V   Y   T   G   V

ttt gta gtc agc ctc cca cta aac atc atg gcc atc gtt gtg
 F   V   V   S   L   P   L   N   I   M   A   I   V   V

ttc atc ctg aaa atg aag gtc aag aag ccg gcg gtg gtg tac
 F   I   L   K   M   K   V   K   K   P   A   V   V   Y

atg ctg cac ctg gcc acg gca gat gtg ctg ttt gtg tct gtg
 M   L   H   L   A   T   A   D   V   L   F   V   S   V

ctc ccc ttt aag atc agc tat tac ttt tcc ggc agt gat tgg
 L   P   F   K   I   S   Y   Y   F   S   G   S   D   W

cag ttt ggg tct gaa ttg tgt cgc ttc gtc act gca gca ttt
 Q   F   G   S   E   L   C   R   F   V   T   A   A   F

tac tgt aac atg tac gcc tct atc ttg ctc atg aca gtc ata
 Y   C   N   M   Y   A   S   I   L   L   M   T   V   I

agc att gac cgg ttt ctg gct gtg gtg tat ccc atg cag tcc
 S   I   D   R   F   L   A   V   V   Y   P   M   Q   S


ctc tcc tgg cgt act ctg gga agg gct tcc ttc act tgt ctg
 L   S   W   R   T   L   G   R   A   S   F   T   C   L
```

gcc atc tgg gct ttg gcc atc gca ggg gta gtg cct ctc gtc
A I W A L A I A G V V P L V

ctc aag gag caa acc atc cag gtg ccc ggg ctc **aac atc act**
L K E Q T I Q V P G L **N^{250} I^{251} T^{252}**

acc tgt cat gat gtg ctc **aat gaa acc** ctg ctc gaa ggc tac
T C H D V L **N^{259} E^{260} T^{261}** L L E G Y

tat gcc tac tac ttc tca gcc ttc tct gct gtc ttc ttt ttt
Y A Y Y F S A F S A V F F F

gtg ccg ctg atc att tcc acg gtc tgt tat gtg tct atc att
V P L I I S T V C Y V S I I

cga tgt ctt agc tct tcc gca gtt gcc **aac cgc agc** aag aag
R C L S S S A V A **N R S** K K

tcc cgg gct ttg ttc ctg tca gct gct gtt ttc tgc atc ttc
S R A L F L S A A V F C I F

atc att tgc ttc gga ccc aca aac gtc ctc ctg att gcg cat
I I C F G P T N V L L I A H

tac tca ttc ctt tct cac act tcc acc aca gag gct gcc tac
Y S F L S H T S T T E A A Y

ttt gcc tac ctc ctc tgt gtc tgt gtc agc agc ata agc tcg
F A Y L L C V C V S S I S S

tgc atc gac ccc cta att tac tat tac gct tcc tct gag tgc
C I D P L I Y Y Y A S S E C

cag agg tac gtc tac agt atc tta tgc tgc aaa gaa agt tcc
Q R Y V Y S I L C C K E S S

gat ccc agc agt tat **aac agc agt** ggg cag ttg atg gca agt
D P S S Y **N S S** G Q L M A S

aaa atg gat acc tgc tct agt aac ctg **aat aac agc** ata tac
K M D T C S S N L **N N S** I Y

aaa aag ctg tta act tag -3′
K K L L T **Stop**

The amino acids coloured blue are predicted extracellular glycosylation sequons.

APPENDIX D: Representative model of POMC-M1-hPAR$_1$-HA.11-eYFP cDNA

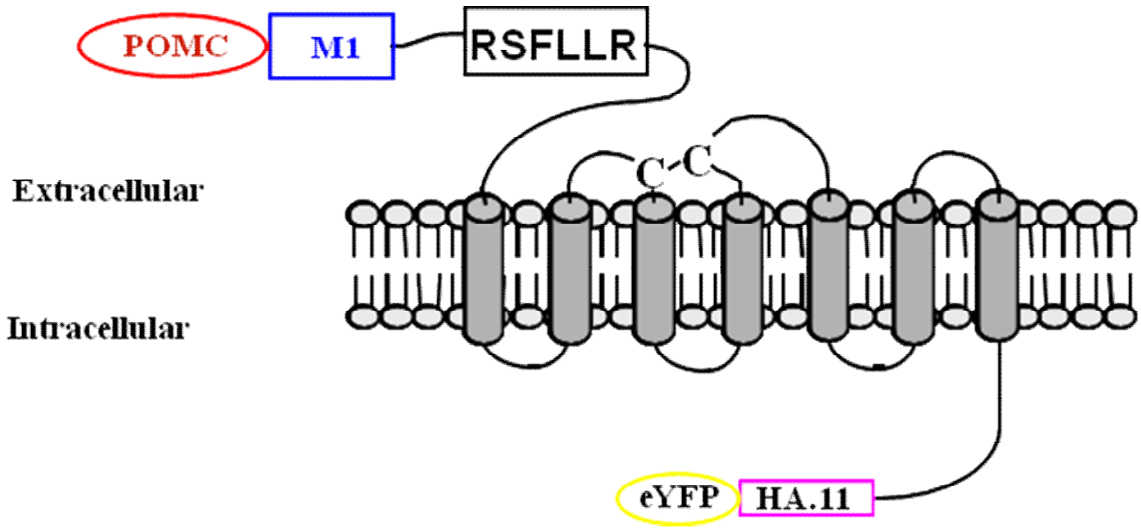

Representative model of POMC-M1-hPAR$_1$-HA.11-eYFP: Pro-opiomelanocortin (POMC) signal peptide and M1 epitope tag were fused to the N-terminus of hPAR$_1$. The enhanced yellow fluorescent protein (eYFP) and the haemagglutinin epitope (YPYDVPDYA) were fused to the C-terminal tail of hPAR$_1$. The disulphide bridge is shown by the two cysteines (C-C). The POMC signal peptide enabled efficient expression of PAR$_1$, whilst the M1 and HA.11epitope tags facilitated isolation and detection of the receptor.

APPENDIX E: hPAR$_4$–eYFP cDNA sequence

*Hind*III-POMC-AU1-hPAR$_4$-HA11-eYFP-stop-*Xho*I-Anchor cDNA sequence

5'-
GATCGAAGCTTAGCATGCCGAGATCGTGCTGCTGCCGCTCGGGGGCCCTGTTGCTGGCCTTACTGCTTC
*Hind*III--POMC
AGGCCTCCATGGAAGTGCGTGGTGACACATACAGATACATAGACAGCACGCCCTCAATCCTGCCTGCCC
AU1
CCCGCGGCTACCCAGGCCAAGTCTGTGCCAATGACAGTGACACCCTGGAGCTCCCGGACAGCTCACGGG
CACTGCTTCTGGGCTGGGTGCCCACCAGGCTGGTGCCCGCCCTCTATGGGCTGGTCCTGGTGGTGGGGC
TGCCGGCCAATGGGCTGGCGCTGTGGGTGCTGGCCACGCAGGCACCTCGGCTGCCCTCCACCATGCTGC
TGATGAACCTCGCGACTGCTGACCTCCTGCTGGCCCTGGCGCTGCCCCCGCGGATCGCCTACCACCTGC
GTGGCCAGCGCTGGCCCTTCGGGGAGGCCGCCTGCCGCCTGGCCACGGCCGCACTCTATGGTCACATGT
ATGGCTCAGTGCTGCTGCTGGCCGCCGTCAGCCTGGATCGCTACCTGGCCCTGGTGCACCCGCTGCGGG
CCCGCGCCCTGCGTGGCCGGCGCCTGGCCCTTGGACTCTGCATGGCTGCTTGGCTCATGGCGGCCGCCC
TGGCACTGCCCCTGACACTGCAGCGGCAGACCTTCCGGCTGGCGCGCTCCGATCGCGTGCTCTGCCATG
ACGCGCTGCCCCTGGACGCACAGGCCTCCCACTGGCAACCGGCCTTCACCTGCCTGGCGCTGTTGGGCT
GTTTCCTGCCCCTGCTGGCCATGCTGCTGTGCTACGGGGCCACCCTGCACACGCTGGCGGCCAGCGGCC
GGCGCTACGGCCACGCGCTGAGGCTGACCGCAGTGGTGCTGGCCTCCGCCGTGGCCTTCTTCGTGCCCA
GCAACCTGCTGCTGCTGCTGCATTACTCGGACCCGAGCCCCAGCGCCTGGGGCAACCTCTATGGTGCCT
ACGTGCCCAGCCTGGCGCTGAGCACCCTCAACAGCTGCGTGGATCCCTTCATCTACTACTACGTGTCGG
CCGAGTTCAGGGACAAGGTGCGGGCAGGGCTCTTCCAACGGTCGCCGGGGGACACCGTGGCCTCCAAGG
CCTCTGCGGAAGGGGGCAGCCGGGGCATGGGCACCCACTCCTCTTTGCTCCAGCCCTATGATGTTCCCG
ATTATGCCATGGTGAGCAAGGGCGAGGAGCTGTTCACCGGGGTGGTGCCCATCCTGGTCGAGCTGGACG
HA11--eYFP
GCGACGTAAACGGCCACAAGTTCAGCGTGTCCGGCGAGGGCGAGGGCGATGCCACCTACGGCAAGCTGA
CCCTGAAGTTCATCTGCACCACCGGCAAGCTGCCCGTGCCCTGGCCCACCCTCGTGACCACCTTCGGCT
ACGGCCTGCAGTGCTTCGCCCGCTACCCCGACCACATGAAGCAGCACGACTTCTTCAAGTCCGCCATGC
CCGAAGGCTACGTCCAGGAGCGCACCATCTTCTTCAAGGACGACGGCAACTACAAGACCCGCGCCGAGG
TGAAGTTCGAGGGCGACACCCTGGTGAACCGCATCGAGCTGAAGGGCATCGACTTCAAGGAGGACGGCA
ACATCCTGGGGCACAAGCTGGAGTACAACTACAACAGCCACAACGTCTATATCATGGCCGACAAGCAGA
AGAACGGCATCAAGGTGAACTTCAAGATCCGCCACAACATCGAGGACGGCAGCGTGCAGCTCGCCGACC
ACTACCAGCAGAACACCCCCATCGGCGACGGCCCCGTGCTGCTGCCCGACAACCACTACCTGAGCTACC
AGTCCGCCCTGAGCAAAGACCCCAACGAGAAGCGCGATCACATGGTCCTGCTGGAGTTCGTGACCGCCG
CCGGGATCACTCTCGGCATGGACGAGCTGTACAAGTAACTCGAGGGGCCC-3'
eYFP-stop-*Xho*I-Anchor

APPENDIX F: Restriction Enzyme Recognition Sites

*Hind*III

*Xho*I

*Bam*HI

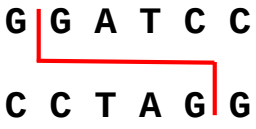

APPENDIX G: DNA and protein standards

1kb Plus DNA ladder

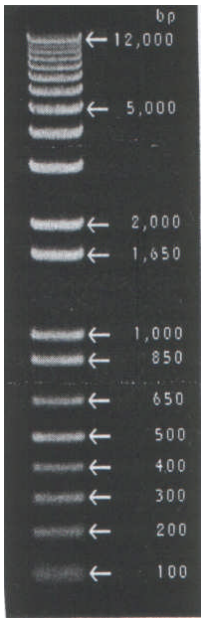

Precision Plus Protein Standard